INTERPLAY BETWEEN EPITHELIAL INNATE SENSING AND MUCOSAL IMMUNITY

By

LISA SCARFE

A thesis submitted to the University of Birmingham for the degree of

DOCTOR OF PHILOSOPHY

Institute of Immunology and Immunotherapy

College of Medical and Dental Sciences

University of Birmingham

UNIVERSITY OF BIRMINGHAM

October 2023

Abstract

Maintenance of intestinal integrity is dependent on crosstalk between epithelial, stromal and immune cells and the gut microbiota. Nod-like receptor (NLR) apoptosis inhibitory proteins (Naips) activate the NLRC4 inflammasome upon recognition of gram-negative bacteria, leading to pyroptosis/apoptosis, intestinal epithelial cell expulsion and release of IL-1β, IL-18 and prostaglandin E_2 (PGE_2). NAIPs also appear to have homeostatic roles within the intestinal epithelium, as our group has previously shown that Naips suppress colonic tumourigenesis but enhance colonic inflammation. We aimed to further understand the role of Naips on the immune compartment in inflammatory disease, using models of colorectal cancer and *Salmonella* infection. Following *Salmonella* infection, mice lacking epithelial Naips ($Naip^{\Delta/\Delta}$) had increased numbers of TCRαβCD8αα and TCRγδ+ intraepithelial lymphocytes, which was not caused by increased bacterial burden. Using colonic organoids, we identified increased IL-15/IL-15R in $Naip^{\Delta/\Delta}$ and altered basal levels of eicosanoids ($PGF_{2\alpha}$ and 17,18-DiHETE) with altered expression of eicosanoid-related genes. However, organoid co-cultures suggested neither explained the increase in intraepithelial lymphocytes, with further work needed to elucidate the mechanism behind this. Following colorectal cancer induction, only slight differences were seen in the tumour infiltrating lymphocytes of $Naip^{\Delta/\Delta}$ mice compared to $Naip^{fl/fl}$, though there was a trend towards decreased conventional CD4+ T cells and an increase in TCRγδ cells. However, $Naip^{\Delta/\Delta}$ cancer-derived organoids increased MHCII expression in response to IFNγ, whereas $Naip^{fl/fl}$ did not. This was not explained by differences in IFNγ signalling or prostaglandin production. Further investigation is needed to determine the exact role of Naips in colorectal cancer and why $Naip^{\Delta/\Delta}$ mice experience increased tumorigenesis.

COVID-19 Mitigation Statement

The COVID-19 pandemic had a significant impact on the research planned for this thesis. Working restrictions due to the pandemic meant that our *Naip*$^{\Delta/\Delta}$ mice could not be rederived as promptly as initially planned, meaning we did not have access to mice until 12-18 months into the 3 year project. As these mice formed the basis of much of the project, and since they were also required to generate new organoid lines, our output was severely limited in that time. These in vivo experiments were also planned to be the initial experiments on which in vitro experiments were to be informed. This put a great delay on the project. Due to the delay, we initiated work with already established tumour organoids, basing experiments on the literature, rather than findings *in vivo*. Thus, by the end there was not sufficient time to work on mechanistic underpinnings of our in vivo findings.

Acknowledgements

Firstly, I'd like to thank the Wellcome Trust for funding this project and to everyone on the MIDAS team – Steve, Graham, Robin, Eva and Vikki – for always making me feel so supported.

A huge thank you to Kendle Maslowski for her supervision and support throughout the project, you've been a fantastic person to work for. Thank you to Alastair Copland for being so incredibly knowledgeable and patient. Thanks to Gillian for teaching me how to be an honest cell farmer and being my lab best friend. Thank you to all members of the Flabbies past and present, in particular David, Sarah and Rebecca, for all your advice and for creating a safe space to grow. I feel so fortunate to have been surrounded by kind and supportive people for the past four years.

The biggest thank you to my wonderful MIDAS cohort – Poppy, Abbey, David, Sofia and Rachel. I literally couldn't have done it without you. Thanks to Tristan, Abbie and Tom for all the support and good times. Thank you to Niamh for helping make Birmingham home. Thank you to Katy, Meg and Chloe for your endless love, support and voicenotes. Thanks to Eve, Jess and Jorge for always being at the other end of the phone.

Most importantly I'd like to thank my mum, dad and sister, Jess. I couldn't have done this without your unwavering love and support and I'm so grateful to have you. Thank you for always supporting me while I go and get those figs.

Abbreviations

AA – Arachidonic Acid

AIM2 – Absent in Melanoma 2

Akt – Ak Strain Transforming (Protein Kinase B)

AMP = Antimicrobial Protein

AOM – Azoxymethane

APCmin – Adenomatous Polyposis Coli mutant

APC - Antigen Presenting Cell

ASC – Apoptosis-Like Speck

Bcl-2 – B Cell Lymphoma 2

BIR - Baculovirus inhibitor-of-apoptosis repeat

BTNL – Butrophylin-Like

cAMP – Cyclic Adenosine monophosphate

CARD - Caspase-Activation and Recruitment Domain

CBP – cAMP Responsive-Element-Binding Protein

Ccnd1 – Cyclin D1

CCR – C-C Chemokine Receptor

CCR9 – Chemokine Receptor 9

CD– Cluster of Differentiation

CFU – Colon Forming Units

CIITA – Class II Transactivator

COX – Cyclooxygenase

cPLA2 – Cytosolic Phospholipase 2

CRC – Colorectal Cancer

CTL – Cytotoxic Lymphocyte

CXCL – Chemokine Ligand

DAMP – Damage Associated Molecular Pattern

DC – Dendritic Cell

DNA - Deoxyribonucleic Acid

DSS – Dextran Sodium Sulfate

EET – Epoxyeicosatrienoic Acids

EGFR – Epidermal Growth Factor Receptor

ELISA – Enzyme-Linked Immunosorbent Assay

EP – Prostaglandin E Receptor

ER – Endoplasmic Reticulum

ERK – Extracellular Signal Related Kinase

EZH2 – Enhancer of Zeste Homolog 2

FAP – Familial Adenomatous Polyposis

FCS – Fetal Calf Serum

FGF – Fibroblast Growth Factor

FMO – Fluorescence Minus One

FoxP3 – Forkhead Box P3

FP – Prostaglandin F Receptor

GALT – Gut Associated Lymphoid Tissue

GARP - Glycoprotein-A Repetitions Predominant

GAS - γ Activated Site

GITR - Glucocorticoid-induced TNFR-related protein

GzmB – Granzyme B

HETE – Hydroxyeicosatetraenoic Acids

HGPD – Hydroxyprostaglandin Dehydrogenase

HLA – Human Leukocyte Antigen

HPETE – Hydroperoxyeicosatetraenoic Acids

IDO - Indoleamine-pyrrole 2,3-dioxygenase

IEC – Intestinal Epithelial Cell

IEL – Intra-Epithelial Lymphocyte

IFN - Interferon

IFNγR – Interferon γ Receptor

Ii – MHC-II–Associated Invariant Chain

IL - Interleukin

ILC – Innate Lymphoid Cell

IP – Intraperitoneal

ISG – Interferon Signature Genes

JAK – Janus Kinase

KGF - Keratinocyte Growth Factor

LC/MS – Liquid Chromatography Mass Spectrometry

LFA-1 – Lymphocyte Function-associated Antigen 1

LOX – Lipoxygenase

LPAM1 - Lymphocyte Peyer's Patch Adhesion Molecule-1

LPS – Lipopolysaccharide

LT – Leukotriene

LXA4 - Lipoxin A4

MAPK – Mitogen Activated Protein Kinases

MARCKS – Myristoylated Alanine-Rich C-Kinase Substrate

MCM5 – Minichromosomal Maintenance Deficient 5

MCP - Monocyte Chemotactic Protein 1

Mdm2 – Murine Double Minute 2

MHC – Major Histocompatibility Complex

MICA - MHC Class I Polypeptide-Related Sequence A

mLN – Mesenteric Lymph Node

mPGES1 - Microsomal prostaglandin E synthase-1

mTOR – Mammalian Target of Rapaycin

MyD88 - Myeloid Differentiation Primary Response Protein

NACHT - NAIP (neuronal apoptosis inhibitory protein), CIITA (MHC class II transcription activator), HET-E (incompatibility locus protein from Podospora anserina) and TP1 (telomerase-associated protein)

NAIP - NLR Family of Apoptosis Inhibitory Proteins

NCR – Natural Cytotoxicity Receptors

NFκB - Nuclear factor kappa-light-chain-enhancer of activated B cells

NK – Natural Killer

NKG2D/A – Natural Killer Group 2 D/A

NLR - Nucleotide-binding and Oligomerization Domain Like Receptor

NLRC4 - NLR family CARD domain-containing protein 4

NLRP1 - Nucleotide-binding domain, Leucine-rich–containing family, Pyrin domain–containing

NOD - Nucleotide-binding and Oligomerization Domain

NS – No Significance

NSAID – Non-Steroidal Anti-Inflammatory Drug

NT – Not Treated

PAMP – Pathogen Associated Molecular Pattern

PD-1 - Programmed Cell Death Protein 1

PD-L1 - Programmed Cell Death Ligand 1

PG – Prostaglandin

PGLYRP2 - Peptidoglycan Recognition Protein 2

PI3K – Phosphoinositide 3-Kinase

PIAS - Protein Inhibitor of Activated STATs

PPAR – Peroxisome Proliferator-Activated Receptor

PRR – Pattern Recognition Receptor

qRT-PCR – quantitative reverse transcriptase polymerase chain reaction

RA – Retinoic Acid

Runx3 – Runt Related Transcription Factor 3

SOCS - Suppressor Of Cytokine Signalling

STAT – Signal Transducer and Activator of Transcription

STm – Salmonella Typhimurium

T3SS – Type 3 Secretion System

T-bet - T-box expressed in T cells

Tcm – T Cntral Memory Cell

TCR – T cell receptor

TGF-β – Transforming Growth Factor β

Th – T helper

ThPOK - T helper-inducing POZ Krueppel factor

Thy1 – Thymus Cell Antigen 1

TIL – Tumour Infiltrating Lymphocyte

TL – Thymus Leukaemia Antigen

TLR – Toll-Like Receptor

TNBS - Trinitrobenzene Sulfonic Acid

TNF – Tumor Necrosis Factor

TRAIL - Tumor necrosis factor-Related Apoptosis-Inducing Ligand

Treg – Regulatory T cells

TXA2 – Thromboxane A2

ULBP - UL16-binding proteins

VEGF – Vascular Endothelial Growth Factor

Wnt - Wingless-Related Integration Site

WT – Wild Type

YFP – Yellow Fluorescent Protein

β2m - β2-Microglobulin

Contents

List of figures

List of tables

1 Introduction

The intestinal tract has the important role of balancing nutrient absorption with protection from pathogens. Gut homeostasis in the face of food particles, the microbiota, and potential pathogens requires delicate cross-talk between various cell types. The intestinal epithelium is integral in achieving this, acting as single-cell physical barrier to pathogens, and producing a mucus layer. Intestinal epithelial cells (IECs) express a variety of Pattern Recognition Receptor (PRRs) which enable them to respond to pathogen and damage associated molecular patterns (PAMPs and DAMPs) and initiate downstream responses and communication with other cells. Understanding these processes can provide insight into the mechanisms which limit infection and drive inflammatory diseases, such as colorectal cancer (CRC). Here, we focus NLR family apoptosis inhibitory proteins (Naips), a PRR found in intestinal epithelial cells, and Naips function in infection and inflammatory diseases of the gut. Part of the following introduction is taken from the review article 'Inflammasome-independent functions of Naips and NLRs in the intestinal epithelium', Scarfe *et al* (2021), which was published as part of this project (Scarfe, Mackie and Maslowski, 2021).

1.1 NLR family apoptosis inhibitory proteins

Naips are intracellular PRRs which sense components of gram-negative bacteria. Like most inflammasome proteins in the NLR family, Naips contain a leucine-rich repeat domain and a NACHT domain, so named as it consists of a Nucleotide Binding Domain, Helical Domain 1, Winged Helix Domain and Helical Domain 2. Notably, NLR proteins are now not thought of as NOD-like receptor proteins but as proteins which contain nucleotide-binding-domain leucine-rich repeat components (Bauer and Rauch, 2020). Naips also contain three N-terminal baculovirus inhibitor of apoptosis protein repeat (BIR) domains at the N-terminus (Bauer and Rauch, 2020). The C57BL/6 genome encodes 4 functional Naip paralogues, for example, Naip1 and 2 bind to the PrgI needle and PrgJ rod subunit of the Type III secretion system (T3SS) of *Salmonella* Typhimurium (STm), respectively,

whereas Naip5 and 6 recognise flagellin (Kofoed and Vance, 2011; Zhao *et al.*, 2011; Yang *et al.*, 2013). Humans express a single NAIP isoform which has been shown to sense both flagellin and *S*Tm T3SS components in macrophages (Zhao *et al.*, 2011; Yang *et al.*, 2013; Kortmann, Brubaker and Monack, 2015; Ruiz *et al.*, 2017). Whilst the majority of literature has characterised Naips in macrophages, they are also highly expressed in other innate immune cells and IECs (Diez *et al.*, 2000; Sellin *et al.*, 2014; Allam *et al.*, 2015). Naips are highly expressed in the colon, with increasing expression levels from the cecum to the distal colon, as we as in innate immune cells such as macrophages, dendritic cells and neutrophils (Diez *et al.*, 2000; Allam *et al.*, 2015). As described by Allam *et al.,* there is some variation in the expression of the different Naip isoforms, with expression of Naip5 and 6 increasing in expression from the ileum to the distal colon, but with expression of Naip1 and 2 remaining relatively consistent in all parts of the colon. Interestingly, Naip2 is expressed at lower levels compared to other isoforms (Allam *et al.*, 2015). Naip5 and 6 are also more highly expressed in splenic innate cells compared to other isoforms (Allam *et al.*, 2015). So far, Naips have not been reported to be expressed in lymphocytes, with the spleen and mesenteric lymph nodes being shown to have overall low Naip expression despite high expression in CD11c+ and CD11b+CD11c- splenocytes (Allam *et al.*, 2015).

1.1.1 The Naip/NLRC4 Inflammasome

Upon ligand binding, Naips oligomerize with Nod-Like Receptor family, CARD-containing 4 (NLRC4) to form the Naip/NLRC4 inflammasome. Like Naip, NLRC4 contains a NACHT domain and a leucine-rich repeat domains, as well as a caspase activation and recruitment (CARD) domain (Bauer and Rauch, 2020). The Naip/NLRC4 inflammasome is one of several canonical inflammasomes identified within IECs, which usually consist of Caspase-1, the adaptor protein apoptosis speck-like protein (ASC), plus an NLR protein (e.g. NLRP1, NLRP3, NLRC4, NLRP6 or NLRP12) or proteins such as Absent in Melanoma 2 (AIM2) (Winsor *et al.*, 2019). Caspase-1 is activated via its CARD domain, which is recruited to CARD domains in other proteins. As NLRC4 contains a CARD domain, it can either directly

recruit pro-Caspase-1 via the association of the two proteins CARD domains, or it can recruit Caspase-1 via the adaptor protein ASC, which also has a CARD domain and allows for more efficient Caspase-1 activation (figure 1.1) (Rauch *et al.*, 2017; Bauer and Rauch, 2020). Association with ASC also allows NLRC4 to activate Caspase-8 (Rauch *et al.*, 2017). Pro-Caspase-1 contains a CARD domain, a large subunit (p20) and a small subunit (p10) (Ball *et al.*, 2020). Upon recruitment the pro-Caspases are cleaved and activated (Winsor *et al.*, 2019). In macrophages, Caspase-1 proteolytically cleaves and activates pro-IL-1β, pro-IL-18 and Gasdermin D, the latter of which forms pores in the plasma membrane of the cell, resulting in pyroptosis and release of IL-1β and IL-18 (Franchi *et al.*, 2006; Miao *et al.*, 2006, 2010; Molofsky *et al.*, 2006; Shi *et al.*, 2015). Caspase-8 activation leads to apoptotic cell death, with IL-1β, IL-18 and other alarmins retained within the cell, resulting in a less inflammatory form of cell death (Van Opdenbosch *et al.*, 2017). This caspase-8 mediated apoptosis can be inhibited by TLR signalling, via expression of c-FLIP; a process that leaves NLRC4-mediated pyroptosis unaffected (Van Opdenbosch *et al.*, 2017). In addition, Caspase-3 has recently been reported to be activated by the Naip/NLRC4 inflammasome. Caspase-3, an executioner caspase, is canonically activated by initiator caspases, such as Caspase-8, resulting in apoptotic cell death (Fattinger *et al.*, 2021). Functioning in parallel to the canonical inflammasome described above, detection of cytosolic lipopolysaccharide (LPS) can activate the non-canonical inflammasome, resulting in activation of Caspase 4/11 (Knodler *et al.*, 2014).

In IECs, pathogen detection by Naips leads to expulsion of the infected cell into the gut lumen and cell death (Sellin *et al.*, 2014). Whilst this causes moderate enteropathy, it acts as a critical first line of defence in limiting bacterial dissemination. This was illustrated by Hausmann *et al*., using wild-type isogenic tagged strains of *S*Tm to determine dissemination to the mesenteric lymph nodes. Increased colony forming units and numbers of tagged *S*Tm were found in *Nlrc4*-/- and IEC-specific Naip knock-out mice (*Naip1-6*$^{IEC\Delta/\Delta}$). However, this effect was lost when using the STm$^{\Delta4}$ strain, which lacks the type three secretion system 1 delivered effector proteins it requires for IEC invasion. The Naip

ligands, flagellin and the T3SS, are required for IEC invasion and are subsequently downregulated to avoid immune detection. Thus, Naips expressed in the IECs, as opposed to the innate immune cells, are vital in the initial detection of *Salmonella* infection (Hausmann *et al.*, 2020). A separate study showed that lack of Caspase-1 caused increased *S*Tm burden and reduced epithelial expulsion, with Caspase-11 only having an effect under inflammatory conditions, generated by pre-treatment with IFNγ, further highlighting the importance of this pathway in early infection (Crowley *et al.*, 2020). In the absence of this mechanism, *S*Tm infected mice suffer excessive IEC loss and collapse of the epithelial barrier at later time points, due to TNF release by bone marrow-derived cells (Fattinger *et al.*, 2021).

Naip-mediated cell death appears to take on both apoptotic and pyroptotic qualities in IECs. Initial experiments using FlaTox, a potent activator of Naip5-6 which delivers flagellin to the cytosol of cells, found that lysis of IECs occurred prior to cell expulsion in a manner similar to pyroptosis (Rauch *et al.*, 2017). This effect was lost if either both Caspase-1 and Caspase-8 or if Caspase-1 alone was ablated (Rauch *et al.*, 2017). However, *S*Tm infection of intestinal organoids has since found that plasma membrane integrity is lost at varying stages, most often after expulsion, as well as Caspase-3 cleavage (Fattinger *et al.*, 2021). Taken together, these results suggest a combination of inflammatory and apoptotic cell death occurs, potentially with the activation of multiple caspases simultaneously and redundancy between the caspases (Rauch *et al.*, 2017; Van Opdenbosch *et al.*, 2017; Fattinger *et al.*, 2021). The resultant gap created by cell expulsion is closed by cells in an actomyosin-dependent manner, allowing the epithelial barrier to be maintained. If actin polymerisation is blocked no expulsion occurs (Rauch *et al.*, 2017; Ventayol *et al.*, 2021). In addition, contractions of IECs occur which densely packs cells at the site of infection. Sub-lytic levels of Gasdermin D-mediated pore formation are thought to lead to ion fluxes which trigger these non-muscle myosin II contractions. This contraction was shown in both mouse and human IEC monolayers, and was lost if Naips, NLRC4, Caspase-1 or Gasdermin D were ablated as well as in the

presence of blebbistatin or Gd3+, which blocks myosin and ion fluxes caused by Gasdermin D pores, respectively (Ventayol *et al.*, 2021).

As well as cell expulsion and death, Naip/NLRC4 activation in IECs results in release of IL-18 and eicosanoids (Moltke *et al.*, 2012; Rauch *et al.*, 2017). Mice treated with potent Naip activator FlaTox suffered fluid loss, vascular leakage, and diarrhoea. *Nlrc4*-/-, *Naip5*-/- and *Caspase-1*-/- mice were protected from this effect (Moltke *et al.*, 2012). This had been suggested to be a result of Caspase-1-mediated Ca^{2+} influx into peritoneal macrophages, resulting in activation of cytosolic phospholipase A_2 ($cPLA_2$), the enzyme upstream of eicosanoid biosynthesis (Moltke *et al.*, 2012). However, intestinal tissue PGE_2 release following FlaTox treatment has since been shown to be comparable between wild-type (WT) mice and mice which exclusively expressed NLRC4 in the IECs, suggesting that eicosanoids release can be mediated by the IECs (Rauch *et al.*, 2017).

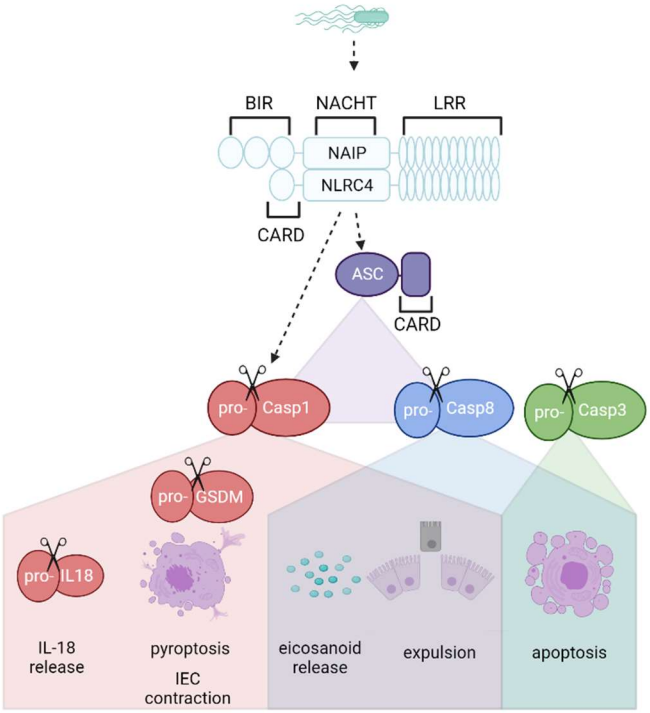

Figure 1.1 – Effects of the Naip/NLRC4 inflammasome in intestinal epithelial cells

Naip isoforms sense components of gram-negative bacteria, such as *Salmonella*, and co-oligomerises with NLRC4, forming an inflammasome. Naip contains a NACHT domain, a leucine-rich repeat (LRR) domain, and three N-terminal baculovirus inhibitor of apoptosis protein repeat (BIR) domains, whereas NLRC4 contains a NACHT and LRR domain along with a caspase activation and recruitment (CARD) domain. NLRC4 then binds pro-Caspase-1 directly via its CARD domain, or binds the adaptor protein apoptosis speck-like protein (ASC), which can also recruits pro-Caspase-1 or pro-Caspase-8 via its CARD domain. The pro-Caspases are then proteolytically cleaved, resulting in their activation. Caspase-1 can then cleave Gasdermin D, leading to pyroptotic death and expulsion of the cell. Caspase-8 can also lead to cell death but this is reported to be more apoptotic (Bauer and Rauch, 2020). Both Caspase-1 and Caspase-8 can trigger eicosanoid release and Caspase-1 also triggers IL-18 release (Rauch *et al.*, 2017). Caspase-3 has also been shown to trigger apoptotic-like cell death downstream of Naips (Fattinger *et al.*, 2021). Figure created in Biorender

1.1.2 Naips as tumour suppressors

Aside from their roles involving the NLRC4 inflammasome, Naips have also been shown to function as tumour suppressors in colorectal cancer. Allam *et al*., found that mice with all Naip isoforms deleted (*Naip1-6* $^{\Delta/\Delta}$) were protected from dextran sulfate sodium (DSS)-induced colitis, but suffered greater tumour burden following treatment with the carcinogen azoxymethane (AOM) alone, and in the AOM/DSS model of colitis-associated cancer. The effect was epithelial NAIPs-mediated, as IEC-specific KO had increased AOM/DSS-induced tumourigenesis whereas knockout in the myeloid compartment had comparable tumour burden as floxed controls (Allam *et al.*, 2015). During DSS-induced colitis, *Naip1-6*$^{\Delta/\Delta}$ mice exhibited reduced pro-inflammatory cytokine transcripts (*Il-1α/β*, *-6*, *-17*, *Cxcl-1*) and increased anti-apoptotic and survival transcripts (*Bcl-2*, *Myc*, *Mdm2*, *Ccnd1* and *Il-22*), suggesting increased repair following damage and limitation of inflammation (Allam *et al.*, 2015). Interestingly, *Naip1-6* $^{\Delta/\Delta}$ mice failed to activate p53 and apoptosis in the early response to carcinogen (AOM). *Naip1-6* $^{\Delta/\Delta}$ mice also had increased STAT3 phosphorylation following AOM exposure compared to *Naip1-6*$^{fl/fl}$ controls, however this was not recapitulated in *Nlrc4-/-* , *Caspase-1/11-/-* or *Asc-/-* mice (Allam *et al.*, 2015). Additionally, production of IL-1β or IL-18 was not affected in *Naip1-6*$^{\Delta/\Delta}$ mice after AOM nor during active colitis or in tumours, further implying that inflammasome activation is not involved the phenotype of *Naip1-6* $^{\Delta/\Delta}$ mice (8). Together, this suggests that the phenotype of *Naip1-6* $^{\Delta/\Delta}$ mice may arise via a mechanism separate to inflammasome activation. Indeed, it would not be expected that known activators of the Naip/NLRC4 inflammasome (i.e. pathogen components) would be present in the context of carcinogen or DSS, though it could be feasible that a component of the microbiota could provide such a signal (Allam *et al.*, 2015). Other studies have reported that *Caspase1-/-* and *Nlrc4-/-* mice also have increased tumour burden following AOM/DSS treatment, but exhibited similar colitis symptoms to WT, in contrast to *Naip1-6* $^{\Delta/\Delta}$ mice (Hu *et al.*, 2010; Allam *et al.*, 2015), suggesting that Naips, NLRC4 and Caspases might not only have differing roles during tumour induction, but also likely involving

multiple different pathways. However, in the absence of side-by-side knock-out experiments of the different inflammasome components (i.e. Naips, NLRC4, ASC, Caspase-1) using corresponding littermate controls, it is difficult to unpick whether the effect on Naips in cancer is driven exclusively by inflammasome or non-inflammasome mechanism or a combination of the two. In addition, due to the difficulty of generating quadruple KO mice, Allam *et al*. deleted the entire *Naip* locus. The possibility of this resulting in off-target effects cannot be excluded, due to the possibility of regulatory elements in the non-coding regions. It is also worth noting that some of the experiments in this study did not use littermate controls (Allam *et al.*, 2015). The role of individual Naips could also be investigated in the future, however this could be hampered by redundancy between paralogues. Naips have also been shown to be downregulated in mouse and human colorectal tumours, which could imply loss of cell types expressing Naips or an active repression of what might be considered an innate tumour suppressor to aid tumour escape (Endo *et al.*, 2004; Allam *et al.*, 2015).

1.1.3 Other NLR family members in colorectal cancer

Many NLRs activate the inflammasome to produce IL-18 and IL-1β and initiate pyroptosis. However, a number of NLR proteins have non-inflammasome functions, including NOD1, NOD2, NLRP10, NLRC3, NLRC5, NLRX1 and CIITA. These NLRs often regulate transcription of the NFκB, MAPK and major histocompatibility complex (MHC) signalling pathways (Meissner *et al.*, 2010; Zhu and Cao, 2017). A number of PRR families have been linked to cancer development, including the NLR family (figure 2). Increased tumorigenesis following AOM/DSS exposure is seen in *Nlrc3-/-*, *Nlrp3-/-*, *Nlrp6-/-*, *Nlrc4-/-*, *Nlrp1-/-*, *Nlrx1-/-* and *Nlrp12-/-* mice (Zhu and Cao, 2017). Many NLR proteins have been linked to cancer development via inflammasome-dependent pathways (Pandey, Shen and Man, 2019), including NLRC4 (Hu *et al.*, 2010) and NLRP1 (Williams *et al.*, 2015). *Caspase-1-/-* and *Asc-/-* mice have also been shown to have increased tumorigenesis following AOM/DSS exposure (Hu *et al.*, 2010; Pandey, Shen and Man, 2019). Loss of IL-18 release is thought to at least partially mediate this,

with *Il18*-/- and *Il18r1*-/- mice also having increased tumorigenesis following AOM/DSS exposure, along with decreased expression of DNA damage repair genes such as *Atm*, *Atr*, *Msh1* and *Parp1* (Pandey, Shen and Man, 2019). In *Caspase-1*-/- mice, administration of recombinant IL-18 reduced signs of inflammation, ulceration and hyperplasia in AOM/DSS treated mice (Zaki *et al.*, 2010; Pandey, Shen and Man, 2019). As NLR proteins are expressed in multiple cell types in the colon, their tumour suppressor effects are sometimes linked to roles in either the haematopoietic or the non-haematopoietic compartment. The susceptibility of *Nlrp6*-/- mice, for example, has been linked to NLRP6 function in haematopoietic cells (Chen *et al.*, 2011) and myofibroblasts (Normand *et al.*, 2011) in separate studies. It has also been reported that *Nlrp6*-/- mice have altered microbiota due to the defective inflammasome, and that this can increase susceptibility to colorectal cancer, although other studies contradict this (Hu *et al.*, 2013; Mamantopoulos *et al.*, 2017; Pandey, Shen and Man, 2019). Clearly the roles of NLR proteins in the gut are complex in both health and disease and so too, are their contributions towards colorectal cancer development.

However, some NLR proteins have non-inflammasome roles in the IECs, which have similarities to Naips in colorectal cancer, as outlined by Allam *et al.*, 2015. For example, NLRX1, which does not form an inflammasome, has tumour suppressor role in IECs (Lei and Maloy, 2016). Tumorigenesis is increased in the AOM/DSS model following either whole-body or IEC-specific *Nlrx1* deletion, and in $Apc^{Min/+}$ mice, which sporadically develop intestinal polyps, with whole-body *Nlrx1* deletion (Koblansky *et al.*, 2016; Lei and Maloy, 2016; Tattoli *et al.*, 2016). Accordingly, these mice recovered faster following DSS treatment, despite comparable inflammation to WT (Tattoli *et al.*, 2016). Tattoli *et al*., concluded this was due to increased TNF signalling (Tattoli *et al.*, 2016), however, Koblansky *et al*., proposed that NLRX1 inhibited MAPK and NFκB signalling, which otherwise would lead to IL-6 release and subsequent STAT3 phosphorylation (Koblansky *et al.*, 2016). In addition, *Nlrp12*-/- mice are more susceptible to colitis and colitis-associated cancer, which has been explained by heightened NFκB and ERK signalling (Zaki *et al.*, 2011; Allen *et al.*, 2012). Absent in melanoma 2 (AIM2) is

reduced in colorectal cancer (Dihlmann *et al.*, 2014), and loss of AIM2 increases tumorigenesis in both the AOM+DSS and $Apc^{Min/-}$ models of colorectal cancer in a inflammasome-independent manner, possibly via PI3K/Akt signalling (Man *et al.*, 2015; Wilson *et al.*, 2015; Chen, Wang and Yu, 2017). A small number of studies have also shown NLRC3 to have tumour suppressive roles in IECs. *Nlrc3*-/- mice are more susceptible to DSS-induced colitis and experienced greater tumorigenesis in both the AOM/DSS and $Apc^{Min/+}$ model. Specific knock out of *Nlrc3* in the IECs also resulted in increased tumorigenesis following AOM/DSS compared to knock out specifically in the myeloid or haematopoietic compartment. This effect appeared to be mediated by the PI3K/mTOR pathway (Karki *et al.*, 2016, 2017). Clearly then NLR proteins are having non-inflammasome-mediated roles in CRC, and these appear to converge on similar signalling pathways, such as PI3K and NFκB (fig.1.2).

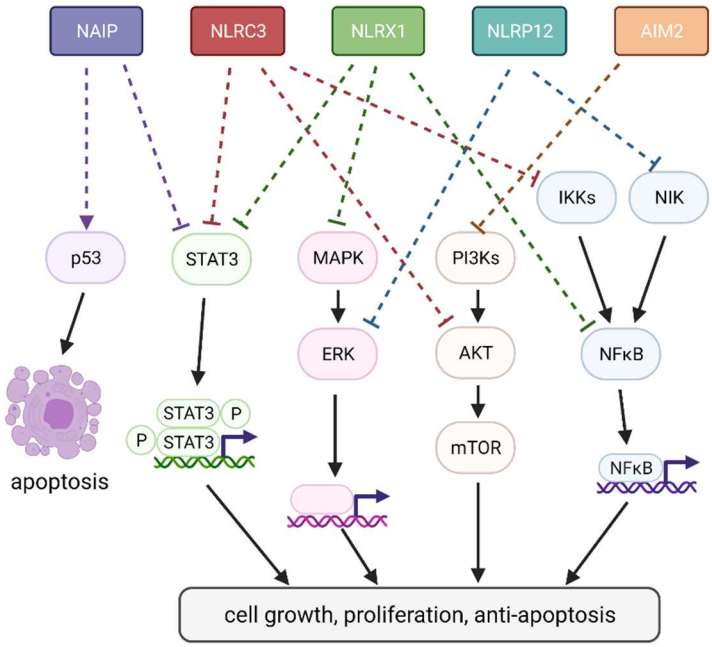

Figure 1.2 – Non-inflammasome roles of NLR proteins in the intestinal epithelium during colorectal cancer

Many NLR proteins including NAIP, NLRC3, NLRX1, NLRP12 and AIM2 act via inflammasome-independent pathways to protect against colorectal cancer. In the absence of Naips, mice experience greater tumorigenesis coupled with increased STAT3 phosphorylation (Allam *et al.*, 2015). Nlrc3-/- mice also have increased STAT3 phosphorylation, as well as increased IκBα and Akt following AOM+DSS treatment (Karki *et al.*, 2016). $Apc^{min/+}$ mice with deletion of NLRX1 have increased NFκB, MAPK and STAT3 activation (Koblansky *et al.*, 2016; Tattoli *et al.*, 2016). Mice lacking NLRP12 have increased tumorigenesis due to NFκB-Induced Kinase (NIK) and ERK signalling (Zaki *et al.*, 2011; Allen *et al.*, 2012). AIM2 protects against tumorigenesis via PI3K signalling (Man *et al.*, 2015; Wilson *et al.*, 2015; Chen, Wang and Yu, 2017). These pathways promote transcription of genes related to cell growth, proliferation, and apoptosis inhibition. Figure created in Biorender.

1.2 Intraepithelial lymphocytes

Intraepithelial lymphocytes (IELs) reside amongst the single cell layer of intestinal epithelial cells (IECs), at a frequency of approximately 1 IEL per 10 IECs (Ma, Qiu and Yang, 2021). These cells do not recirculate but remain within the IECs, where they perform essential functions in response to commensal and invading bacteria, viruses and parasites (Hu, Jia and Edelblum, 2018; Olivares-Villagómez and Van Kaer, 2018). To enable balance between rapid inflammatory response and protection and renewal of the gut barrier, IELs exist in a partially-activated state, with a unique combination of adaptive and innate, cytotoxic and anti-inflammatory characteristics (Hu, Jia and Edelblum, 2018). The majority of IELs possess a TCR and can be split into two main categories – induced and natural (Olivares-Villagómez and Van Kaer, 2018; Ma, Qiu and Yang, 2021). However, some more rare populations have been described which have no TCR, which present a phenotype similar to innate lymphoid cells (ILCs) (Olivares-Villagómez and Van Kaer, 2018; Ma, Qiu and Yang, 2021). Given their diverse nature, different IEL subtypes have been implicated in the response to various pathogens as well as colitis, coeliac disease and colorectal cancer (Inagaki-Ohara *et al.*, 2004; James *et al.*, 2020)

1.2.1 Subtypes of intraepithelial lymphocytes

The IEL compartment comprises a variety of different subtypes, each with distinct markers and properties, but with some common elements. For example, to allow homing to the IECs, IELs express CCR9 and CD103 (also known as integrin αEβ7), which recognise the epithelial layer via CCL25 and E-cadherin, respectively (Olivares-Villagómez and Van Kaer, 2018). Most broadly, IELs can be split into TCR+ and TCR-. TCR+ IELs are known to express activation markers, including CD44 and CD69, as well as markers classically associated with natural killer (NK) cells, including CD16, CD122 and CD161 (Olivares-Villagómez and Van Kaer, 2018). TCR- IELs, on the other hand, are a rare and unusual population, which resemble ILCs. These cells often express an intracellular CD3 chain (iCD3) as well as

CD8αα (Olivares-Villagómez and Van Kaer, 2018; Ma, Qiu and Yang, 2021). Within the TCR+ group, IELs can be divided into induced (or type α) and natural (type β), which are distinguished primarily on their developmental origin and TCR type (Hu, Jia and Edelblum, 2018; Olivares-Villagómez and Van Kaer, 2018). Induced IELs include TCRαβ+CD4+ and TCRαβ+CD8αβ+ cells, which originate in the thymus, undergo positive and negative selection, and subsequently migrate to peripheral lymphoid tissue, before finally locating to the intestinal epithelium (Ma, Qiu and Yang, 2021). They are known to express CD2, CD5, CD28, LFA-1 and thymus cell antigen 1 (Thy1), with some also expressing CD8αα (Ma, Qiu and Yang, 2021). These cells reflect their conventional T cell counterparts, with TCRαβ+CD4+ cells exhibiting T helper cell qualities and TCRαβ+CD8αβ+ cells possessing cytotoxic function (Hu, Jia and Edelblum, 2018). Whereas natural IELs, which include TCRγδ+ and TCRαβ+ CD8αα+ cells, lack CD2, CD5, CD28, Thy1 and LFA-1 (Hu, Jia and Edelblum, 2018). These cells have more tolerogenic tendencies, and known to produce IL-10 and TGF-β (Hu, Jia and Edelblum, 2018).

1.2.1.1 Induced IELs

1.2.1.1.1 *TCRαβ+CD4+*

TCRαβ+CD4+ account for 10-15% of the IEL population in mice and humans (Ma, Qiu and Yang, 2021). In mice, these cells are enriched in the ileum and proximal colon, with numbers dwindling with increasing distance from the cecum (Olivares-Villagómez and Van Kaer, 2018). As these are induced IELs, they are formed from peripheral TCRαβ+CD4+ cells which migrate from the peripheral lymphoid tissue or gut-associated lymphoid tissue (GALT) to the intestinal epithelium (Ma, Qiu and Yang, 2021). During this process, approximately 25-50% of murine TCRαβ+CD4+ will also express CD8αα, with this also observed in humans. This requires T cells to downregulate the CD4 transcription factor ThPOK whilst upregulating Runx3 and T-bet. Cues such as TGF-β, retinoic acid, IFNγ and IL-27 can trigger these transcriptional changes (Konkel *et al.*, 2011; Kaer *et al.*, 2013; Reis *et al.*, 2014). The commensal *bacteria Lactobacillus reuteri* has also been implicated in

TCRαβ+CD4+CD8αα development (Cervantes-Barragan *et al.*, 2017). So far, the exact function of these cells remains unclear. Whilst TCRαβ+CD4+CD8αα are known to have cytolytic activity and granzyme expression (Sasahara *et al.*, 1994; Guy-Grand *et al.*, 1998; Mucida *et al.*, 2013), they have been shown to suppress experimental colitis via IL-10 and possibly acquire FoxP3 expression (Das *et al.*, 2003; Sujino *et al.*, 2016).

1.2.1.1.2 *TCRαβ+CD8αβ+*

The TCRαβ+CD8αβ+ population accounts for 10-15% of murine and 70-80% of human IELs (Olivares-Villagómez and Van Kaer, 2018). These cells began as peripherally activated CD8+T cells that have migrated to the intestinal epithelium. In contrast to their splenic antigen-experienced counterparts, TCRαβ+CD8αβ+ IELs release reduced levels of TNFα and IFNγ, but express granzyme B, CD69, CD103 and β7 integrin constitutively (Olivares-Villagómez and Van Kaer, 2018). Similar to TCRαβ+CD4+ IELs, TCRαβ+CD8αβ+ cells have been shown to also express CD8αα, which increases their activation threshold. Human TCRαβ+CD8αβ+ cells may also express NK cell receptors, such as NKG2D. In coeliac disease, IEC upregulation of IL-15 and NKG2D ligands results in TCRαβ+CD8αβ+ mediated cytolysis of IECs and progression of pathogenesis (Abadie, Discepolo and Jabri, 2012; Jabri and Sollid, 2017).

Table 1.1 - The role of intraepithelial lymphocytes in the gut

Subtype	Origin/Development	Expresses	refs
TCRαβCD4 (Induced)	Antigen-experienced, conventional T cells	CD2, CD5, CD28, LFA-1, Thy1 20-50% also express CD8αα	(Montufar-Solis, Garza and Klein, 2007; Cheroutre, Lambolez and Mucida, 2011)
TCRαβ+CD8αβ+ (Induced)	Antigen-experienced, conventional T cells – mostly effector/memory CD8+ T cells	CD2, CD5, CD28, LFA-1, Thy1, granzyme B, CD69, CD103, β7 intergrin, some express CD8αα	(Abadie, Discepolo and Jabri, 2012; Jabri and Sollid, 2017; Olivares-Villagómez and Kaer, 2018)
TCRαβ+CD8αα+ (Natural)	Homed to intestinal epithelium after thymic development, undergo agonist positive selection	NK cell receptors (Ly49, CD94/NKG2A, CD244, NKG2D), granzyme B CD8αα only once in intestinal epithelium (via TGFβ)	(Konkel *et al.*, 2011; Abadie, Discepolo and Jabri, 2012; Jabri and Sollid, 2017; Olivares-Villagómez and Kaer, 2018)
TCRγδ+ (Natural)	Both thymic and extrathymic origin	IFN-γ, TNF-α, TGF-β, IL-10, IL-13, prothymosin β4, keratinocyte growth factor (KGF), antimicrobial proteins	(Di Marco Barros *et al.*, 2016; Olivares-Villagómez and Kaer, 2018; Ma, Qiu and Yang, 2021)
TCR- ILC1-like	Somewhat dependent on Nfil3 and Tbet but not IL15	Humans – express NKp44 Mice – NKp46 and NK1.1	(Fuchs *et al.*, 2013; Olivares-Villagómez and Kaer, 2018)
TCR- iCD8α	Require IL15, E8I, Notch1, TL antigen	Osteopontin, granzymes, monocyte chemotactic protein 1 (MCP-1), IFN-γ, osteopontin, MHCII.	(Ettersperger *et al.*, 2016; Olivares-Villagómez and Kaer, 2018)
TCR− iCD3+ CD8αα−	Require Notch1 and IL15	Intracellular CD3ε and CD3γ	(Ettersperger *et al.*, 2016; Olivares-Villagómez and Kaer, 2018)

1.2.1.2 Natural IELs

1.2.1.2.1 *TCRγδ+*

TCRγδ+ IELs account for 40-70% of the IEL compartment in mice and 5-20% in humans (Ma, Qiu and Yang, 2021). In humans a Vγ4 subset dominates whereas in mice a Vγ7 subset is most prevalent (Ma, Qiu and Yang, 2021). TCRγδ+ IELs originate in the thymus, although there has been some contention as to whether some may originate extra-thymically, as Vγ7 IELs have been found in athymic mice (Di Marco Barros *et al.*, 2016; Fischer, Golovchenko and Edelblum, 2020). The TCR specificity of these cells is unclear, and they do not appear to be MHC-restricted (Olivares-Villagómez and Van Kaer, 2018). Interaction between γδ IELs and butyrophilin-like (BTNL) molecules influence maturation of the γδ IEL compartment locally in the tissue, measured by IEL number and increased expression of molecules such as CD122 (IL-15Rβ). In the murine gut, BTNL1 and possibly BTNL6 have been shown to specifically promote maturation and expansion of Vγ7+ IELs, which account for the majority of gut resident TCRγδ+ IELs. Despite this, knock-out of *Btnl1* did not result in complete ablation of the Vγ7+ subset (~90% reduction) (Di Marco Barros *et al.*, 2016). Similarly, in humans it has been suggested that BTNL3 and BTNL8 may support Vγ4+ γδ T cells in the gut (Melandri *et al.*, 2018). γδ IELs can display a cytotoxic phenotype, with expression of IFN-γ, TNF-α, IL-17 and IL-22. In mice, IL-17 and IL-22 expressing γδ IELs express the Vγ4 or Vγ6 TCR. Vγ4+ and Vγ6+ T cells usually represent cells which traffic between lymph nodes and tissue, and IL-17-producing γδ T cells have been demonstrated to develop embryonically and reside in the innate lymphoid follicles of the colon (Haas *et al.*, 2012; Muzaki *et al.*, 2017). Thus, these cells may represent an 'induced' population of γδ IELs, rather than a natural population that resided within the intestinal epithelia immediately following thymic development. These IL-17 expressing cells have been shown to infiltrate tumours and can promote tumour progression and metastasis (Suzuki *et al.*, 2020; Reis *et al.*, 2022). Alternatively, γδ IELs have been shown to protect against inflammation and express factors which promote healing such as IL-10, keratinocyte growth factor (KGF) and TGF-β (Olivares-Villagómez and Van Kaer, 2018).

1.2.1.2.2 *TCRαβ+CD8αα+*

The prevalence of TCRαβ+ CD8αα+ cells peaks in early life, and declines with age. As a natural IEL subtype, these cells home immediately to the intestinal epithelium after agonist positive selection in the thymus. These cells appear to have a diverse MHCI restriction, as they strongly reduced in β2-microglobulin-deficient mice but only partially affected by single deletion of classical MHCI molecules, H2-K and H2-D, or non-classical MHCI molecules, such as CD1d, Qa2 or TL. Upon entering the intestinal epithelium, TGF-β provides important signals via Smad3 to induce CD8αα expression. These cells appear to have a regulatory role, expressing TGF-β3, lymphocyte activating 3 (LAG3), and fibrinogen-like protein 2 (Fgl-2). TCRαβ+ CD8αα+ cells have also been shown to protect against colitis via IL-10 release.

1.2.1.2.3 *TCR- IELs*

IELs that do not express a TCR make up a significantly smaller proportion of the IEL compartment. Some innate lymphoid cell-like TCR- IELs exist, which unlike other IELs are not dependent on IL-15 signalling (Olivares-Villagómez and Van Kaer, 2018). However, these cells are reduced by deletion of Nfil3 and Tbet transcription factors (Fuchs *et al.*, 2013). The other TCR- IEL subclass are the iCD8α cells, which are characterised by intracellular expression of CD3ε and CD3γ (Olivares-Villagómez and Van Kaer, 2018). This unusual cell type develops independently of the thymus but does require IL-15 and thymus leukaemia antigen (TL) (discussed below) (Ettersperger *et al.*, 2016). These cells appear to be closer to innate immune cells in function and can present antigen via MHCII (Olivares-Villagómez and Van Kaer, 2018).

1.2.2 The role of CD8αα

A common feature on IELs is the expression of CD8αα, a variation on the classic CD8αβ coreceptor found on conventional T cells (Hu, Jia and Edelblum, 2018). Coreceptors, such as CD4 and CD8, and TCRs normally interact simultaneously with an antigen-presenting MHC molecule, with coreceptors functioning to enhance TCR signalling. This occurs both in conventional thymic selection and activation of mature, conventional T cells. However, whilst CD8αβ enhances binding and signalling via the TCR, CD8αα is thought to decrease antigen sensitivity (Gangadharan and Cheroutre, 2004; Cheroutre and Lambolez, 2008). Unlike CD8αβ, CD8αα expression is not limited to MHCI-restricted T cells, with expression also found on TCRγδ+ and TCRαβ+CD4+ cells (Leishman *et al.*, 2002; Cheroutre and Lambolez, 2008). Once T cells migrate to the gut, regardless of their origin, they tend to induce CD8αα expression (Gangadharan and Cheroutre, 2004). Here, instead of interacting with MHCI, CD8αα preferentially binds thymus leukaemia antigen (TL), which is expressed on all IECs (Leishman *et al.*, 2001). TL is a non-classical MHCI molecule and does not present antigen (Lambolez and Rocha, 2001). When IELs interact with antigen presenting MHCI via their TCR in conjunction with TL, they do not proliferate but produce a high volume of cytokines, such as IFNγ. This is thought to favour renewal of the gut epithelium (Guy-Grand *et al.*, 1998; Lambolez and Rocha, 2001). In contrast, in the absence of TL, IELs would proliferate, produce less cytokines, and kill target cells by self-reactive IELs (Lambolez and Rocha, 2001). Thus, the interaction between CD8αα and TL enables a healthy immune equilibrium to be reached in the gut. CD8αα expression has also been observed on dendritic cells (DCs) and NK cells; in DCs, CD8αα+ confers more efficient cross-presentation and in NK cells it is associated with higher cytotoxicity (Johansson-Lindbom *et al.*, 2003; Hong, Webb and Wilkes, 2007; Geng and Raghavan, 2019).

1.2.3 The role of PRRs and IL-15

A link has been established between PRR signalling, IL-15 and IEL development and maintenance. IL-15 can be produced by haematopoietic and non-haematopoietic cells, including IECs, in response to

infection and tissue damage (Jabri and Abadie, 2015). The majority of IL-15 signalling occurs via trans-presentation, a process first described by Dubois *et al*. (2002), in which IL-15 bound to the IL15 receptor α subunit (referred to here as IL-15/IL-15R) is recognised in a cell contact dependent manner (Dubois *et al.*, 2002). Responding cells recognise this via a receptor consisting of the IL-15 β chain (which also recognises IL-2, also known as CD122) and the common cytokine γ chain (also known as CD132), which also recognises other four α-helix bundle cytokines such as IL-2, IL-7, IL-4, IL-9 and IL-21 (Waldmann, 2006; Rochman, Spolski and Leonard, 2009; Jabri and Abadie, 2015). IL-15 signalling is essential for IEL maintenance, with *IL-15Rα-/-¸IL-2/IL-15Rβ-/-* and *IL-15-/-* mice showing vastly decreased numbers of IELs, particularly TCRγδCD8αα IELs (Suzuki *et al.*, 1997; Lodolce *et al.*, 1998; Kennedy *et al.*, 2000). The significance of IECs in this process is demonstrated by exclusively expressing of IL-15Rα in IECs, which restores the reductions in IELs due to lack of IL-15Rα (Ma *et al.*, 2009). This expression of IL-15 has been linked to innate signalling pathways, with decreased IEL numbers and IL-15 expression in IECs in NOD2, TLR2, TLR4 and MyD88 deficient mice (Kaneko *et al.*, 2004; Yu *et al.*, 2006; Jiang *et al.*, 2013; Qiu *et al.*, 2016). In Nod2-/- and MyD88-/- mice, reintroduction of IL-15 via exogenous IL-15 administration and a transgene, respectively, at least partially restored IEL numbers (Yu *et al.*, 2006; Jiang *et al.*, 2013). In the case of TLR2, IL-15 expression was shown to be mediated via NFκB signalling (Qiu *et al.*, 2016). PRR maintenance of IELs may be driven by recognition of the microbiota, as IEL numbers were restored in mice with depleted gut microbiota following administration of a NOD2 agonist (Jiang *et al.*, 2013). Clearly, IL-15 is central to the crucial role innate signalling pathways hold in IEL maintenance.

1.2.4 IELs in infection

IELs have important roles during infection in the gut, including in response to bacteria, viruses and parasites. Firstly, IELs have cytotoxic effector functions and can therefore induce apoptosis of infected epithelial cells via granzyme, perforin and Fas ligand production (Hu, Jia and Edelblum, 2018). All IELs can induce cytolysis through TCR engagement, but natural IELs can also use natural

killer receptors, such as NKG2D which is upregulated following bacterial infection (Guy-Grand *et al.*, 1996; Bauer *et al.*, 1999). IELs also influence mucus production, with mice lacking γδ IELs experiencing altered mucin expression and glycosylation along with decreased goblet cells (Kober *et al.*, 2014). IELs also secrete anti-microbial peptides which requires epithelial MyD88 signalling (Hu, Jia and Edelblum, 2018).

1.2.4.1 Infection with *Salmonella*

As this project focuses on Naips, which can recognise STm, I briefly describe the role of IELs in STm infection here. Firstly, STm has also been shown to expand the γδ IEL subset (Li *et al.*, 2012). Upon infection γδ IELs also increase their motility between the intercellular space and particularly congregate at the base of the villus, in a TLR/Myd88-dependent manner (Hoytema Van Konijnenburg *et al.*, 2017). In addition, expression of Fas ligand and NKG2D is increased on IELs, along with increased cellular stress ligands (MHC class I polypeptide-related sequence A (MICA) in humans) on epithelial cells which mark them for destruction (Hu, Jia and Edelblum, 2018). CD8αα+ IELs also increase PGLYRP2 expression upon STm infection, which recognises peptidoglycans. If PGLYRP2 is decreased, then susceptibility to infection increases (Lee *et al.*, 2012).

1.3 Inflammatory diseases of the gut

In this project we focused on colorectal cancer (CRC) as well as *Salmonella* infection, and briefly touch upon colitis. Each of these has murine models which are employed to investigate the mechanisms behind the disease and the immune response which takes place. Here we briefly describe each of the diseases, the models used to study them, and explain the current understanding of the immune response mounted.

1.3.1 IBD/Colitis

Inflammatory bowel disease in humans is an umbrella term which covers Crohn's disease and ulcerative colitis. These diseases are characterised by inflammation of the gastrointestinal tract, with

repeated relapse and remission cycles (Lee, Kwon and Cho, 2018). Patients with IBD have increased risk of developing colitis-associated CRC, with 10.8% of patients developing CRC after 40 years of colitis duration (Rutter *et al.*, 2006). One murine model used to study this uses dextran sodium sulfate (DSS) which induces epithelial damage and therefore inflammation (Melgar, Karlsson and Michaëlsson, 2005). This causes similar histological changes and cytokine expression compared to human disease, including TNFα, IFNγ IL-6, IL-8, IL-12, and IL-17 release (Melgar, Karlsson and Michaëlsson, 2005). Other models include administrations of trinitrobenzene sulfonic acid (TNBS), genetic knockout of IL-2 or IL-10, or adoptive cell transfer of CD4+ T cells into immunodeficient mice (Boismenu and Havran, 1994).

1.3.1.1 Immune response to IBD

1.3.1.1.1 *CD8 T cells in colitis*

IBD/colitis is an immune mediated disease and therefore understanding the role the immune system plays during it is pivotal. CD8+ IELs appear to be important during colitis, with adoptive transfer of CD8+ IELs decreasing the susceptibility of *Nod2*-/- mice to colitis in a TNBS model (Jiang *et al.*, 2013). This demonstrates the importance of microbial recognition in this process. Following DSS colitis induction, components of the non-canonical Wnt pathway, such as WNT5A were increased in CD8αα+ IELs, directing them to a more inflammatory phenotype. These cells then expressed NKG2A, CD69, FasL and IFNγ (Zhao *et al.*, 2015).

1.3.1.1.2 *CD4 T cells in colitis*

Th17 cells are one of the major drivers of colitis, with highly elevated levels in the inflamed gut of patients (Zenewicz, Antov and Flavell, 2009). The Th17 cytokines IL-17A, IL-17F and IL-21 are enriched in ulcerative colitis and Crohn's disease, promoting Th1 and Th17 responses (Monteleone *et al.*, 2005; Fina *et al.*, 2008; Lee, Kwon and Cho, 2018). Interestingly, MHCII expression triggered by IFNγ in IECs appears to be protective in colitis, with abrogation of MHCII resulting in elevated innate

immune cells and Th1 cells (Thelemann *et al.*, 2014). The non-classical MHCII molecule CD1d has also been linked to colitis protection, via activation of natural killer T cells (Olszak *et al.*, 2014).

Induction of Tregs is protective in colitis. This was achieved in one study by suppressing IL-17F, which caused expansion of certain commensal bacteria strains (Tang *et al.*, 2018). Mice lacking IL-10, often produced by Tregs, results in intestinal inflammation and is used as a colitis model (Wirtz and Neurath, 2007). One study also showed that IL-10 signalling on Tregs themselves was also shown to be important in suppressing Th17 responses in colitis (Chaudhry *et al.*, 2011).

1.3.1.1.3 *γδ T cells in colitis*

The role of γδ T cells in colitis remains controversial. Increased γδ T cells are present in areas of inflammation and damage in biopsies of IBD patients, regardless of the type of IBD (McVay *et al.*, 1997). Initially, Vδ1 T cells were observed to be elevated in IBD and a major source of IFNγ (McVay *et al.*, 1997). However, later studies suggested that TNF producing Vδ2 were the dominant subtype in IBD (Lo Presti *et al.*, 2019, 2020). γδ+ IELs have been shown to interact with commensal bacteria following DSS-treatment, resulting in increased expression in pro-inflammatory genes such as IL-1β, MIP2, MIP2α, and CXCL9 (Ismail, Behrendt and Hooper, 2009). DSS treatment has also been shown to reduce the percentage of γδ+ IELs in the SI but increase IFNγ, TNFα and IL-17 in those that remain (Pai *et al.*, 2014).

1.3.2 Colorectal cancer

CRC is the second most prevalent cancer in women and third most prevalent in men worldwide (Tariq and Ghias, 2016).CRC can be divided into three subclasses depending on its origin – hereditary, sporadic and colitis-associated (Wang and DuBois, 2010b). Generally, all of these contain activation of the Wnt/β- catenin pathway (Barker *et al.*, 2009). The mechanisms by which CRC can develop are chromosomal instability, CpG island methylator phenotype and microsatellite instability (Tariq and Ghias, 2016). The chromosomal instability pathway is initiated by mutations in the adenomatous

polyposis coli (APC) gene. This occurs in familial adenomatous polyposis (FAP), a hereditary form of CRC (Cherukuri *et al.*, 2014; Leoz *et al.*, 2015). APC normally acts as a negative regulator of Wnt/β-catenin and somatic mutation of the *Apc* gene also occurs in up to 85% of sporadic CRC. CpG island methylator phenotype involves the hypermethylation of tumour suppressor gene promoters, most commonly *MGMT* and *MLH1* (Tariq and Ghias, 2016). Microsatellite instability describes when mutations inactivate DNA mismatch repair genes which normally correct errors in DNA replication (Tariq and Ghias, 2016). Microsatellite instability occurs in around 15% of CRC cases and is associated with better prognosis (Tariq and Ghias, 2016).

Mouse models have been developed to study each of the three subclasses of CRC – hereditary, sporadic and colitis-associated. Familial adenomatous polyposis (FAP) is a hereditary CRC triggered by germline mutations in the adenomatous polyposis coli (APC) gene (Cherukuri *et al.*, 2014; Leoz *et al.*, 2015). It is studied using $Apc^{min/+}$ and $Apc^{\Delta 716/+}$ mice, which have a heterozygous deletion of APC and develop spontaneous SI tumours (Chulada *et al.*, 2000; Corpet and Pierre, 2003). Whilst this is in slight contrast to FAP patients who develop colonic tumours, somatic deletion of APC is also observed in up to 85% of sporadic CRC, highlighting the relevance of this model (Corpet and Pierre, 2003; Cherukuri *et al.*, 2014; Leoz *et al.*, 2015). To model sporadic and colitis-associated cancer, the carcinogen azoxymethane (AOM) is used, which alkylates DNA resulting in K-ras, β-catenin, and more occasionally APC mutations (Corpet and Pierre, 2003; Ishikawa and Herschman, 2010). This is used on its own to model sporadic CRC, or in combination with DSS to model colitis-associated cancer (Ishikawa and Herschman, 2010).

1.3.2.1 The immune response to CRC

1.3.2.1.1 *CD8 T cells in CRC*

Infiltration of CD8+ cytotoxic lymphocytes (CTLs) is an important factor in CRC prognosis, known as an immunoscore (Galon, Fridman and Pagès, 2007). Increased CTLs and increased CTL activation are

particularly associated with microsatellite unstable CRC, which is also associated with improved prognosis (Phillips *et al.*, 2004). Tumours with microsatellite instability had a particularly high prevalence and activation of CD8+ and CD103+ IELs (Dolcetti *et al.*, 1999; Quinn *et al.*, 2003). Intraepithelial TILs have also been linked to longer disease-free survival (Jakubowska *et al.*, 2017). CTLs can directly kill tumour cells via cytolytic components such as perforin, granzymes, granulysin, Fas ligand and tumour necrosis factor α (TNFα) (Russell and Ley, 2002; Golstein and Griffiths, 2018). They also produce IL-2, IL-12 and IFNγ which enhance the cytolytic ability of natural killer (NK) cells and CTLs (Alspach, Lussier and Schreiber, 2019; Bai *et al.*, 2022; Zheng *et al.*, 2023). Intraepithelial lymphocytes have been shown to prevent tumour formation in a cell contact-dependent manner that relied on CD103 and E-Cadherin interactions. In the tumour microenvironment, T cell movement was shown to be restricted and cell-to-cell contact reduced, along with downregulated E-Cadherin by IECs, allowing immune evasion (Christou *et al.*, 2017; Morikawa *et al.*, 2021). Thus CD8+ T cells are pivotal in the immune response to CRC.

1.3.2.1.2 *CD4 T cells in CRC*

Th1 cells enrichment and subsequent IFNγ expression are associated with better prognosis for CRC patients. Th1 cells reduce cancer cell proliferation and angiogenesis whilst also promoting apoptosis and senescence of cancer cells and CD8+ T cells recruitment (Braumüller *et al.*, 2013; Brenner *et al.*, 2020; Bruni, Angell and Galon, 2020; Rentschler *et al.*, 2022). Th22 cells are also associated with good prognosis (Zheng *et al.*, 2023). In contrast, Th17 cells have a more complicated role in CRC. Whilst they can be associated with a poor prognosis due to IL-17 expression (Braumüller *et al.*, 2023), they can also recruit neutrophils and CTLs (Amicarella *et al.*, 2017). One study found that whilst stromal Th17 cells promoted cancer, intraepithelial Th17 cells correlated with greater survival (Amicarella *et al.*, 2017). Other Th17-produced cytokines, such as IL-21 and IL-22 are also enriched in CRC (De Simone *et al.*, 2013). Both IL-17 and FoxP3 expression have been shown to be increased in

microsatellite stable CRC (Gouvello *et al.*, 2008). In concordance with this, one study identified an expanded group of Tregs which expressed RORγT and expressed IL-17, conferring a pro-inflammatory role for these cells (Blatner *et al.*, 2012). Generally, Treg increase during CRC and infiltrate tumours, often developing a highly suppressive phenotype as the disease progresses (Ling *et al.*, 2007; Olguín *et al.*, 2020). In mice, AOM+DSS induced CRC has been shown to increase Treg number, coinciding with expression of CD103, Glycoprotein-A Repetitions Predominant (GARP), CTLA-4, IL-10, express PD-1, Tim3 and CD127 (Pastille *et al.*, 2014; Olguín *et al.*, 2020). Transient ablation of Tregs could suppress tumour size in this model (Pastille *et al.*, 2014). This demonstrates the importance of Tregs in CRC.

1.3.2.1.3 *γδ T cells*

γδ T cells appear to have a complicated role in CRC, with some evidence they can kill tumour cells but other studies demonstrating a protumour effect via IL-17 release (Ma *et al.*, 2020). In humans, γδ T cells can be classified based on their δ chain expression - Vδ1, Vδ2 and Vδ3 (Ma *et al.*, 2020). Vδ1 cells are mostly expressed in the thymus and mucosal tissues, where they express TNF-α and IFN-γ and kill infected and cancerous cells (Todaro *et al.*, 2009; Di Lorenzo, Ravens and Silva-Santos, 2019). Vδ1 IELs which also express NKp46 have been shown to be important in killing of CRC cells (Mikulak *et al.*, 2019). Vδ2 are dispersed in the peripheral blood, are known to recognise tumour cells via phosphor-antigens, resulting in perform, granzyme and IFNγ release and tumour cell death (Gober *et al.*, 2003; Todaro *et al.*, 2009; Li *et al.*, 2020). Finally, Vδ3 are enriched in the liver where they also can induce cell death and release cytokines (Ma *et al.*, 2020). Vγ9Vδ2 are known to be enriched in colon tumours, and a good prognostic marker (Corvaisier *et al.*, 2005; Gentles *et al.*, 2015). In mice, γδ T cells can be divided into IFNγ or IL-17 expressing, with those that express IFNγ also expressing CD27 whereas those that express IL-17 do not (Ribot *et al.*, 2009; Ma *et al.*, 2020). IL-17 expressing γδ

T cells are rare in humans but have been linked to CRC progression (Wu *et al.*, 2014; Razi *et al.*, 2019).

In general, tumours can induce activation of γδ T cells via NK receptors. For example, binding of MHC Class I polypeptide-related sequence A and/or B (MICA/MICB) and UL16-binding proteins (ULBPs) to the receptor NKG2D, results in cytolytic responses such as perforin and granzyme B release (Bauer *et al.*, 1999; Maccalli *et al.*, 2003; Ma *et al.*, 2020). γδ T cells can also recognise TRAIL receptors, which are often overexpressed in tumours, and Fas ligand, which can bind the Fas receptor of tumour cells to induce cell death (Tawfik *et al.*, 2019; Ma *et al.*, 2020). However, IL-17 from γδ T cells can aid cancer, and is shown to promote angiogenesis and promote myeloid-derived suppressor cells by triggering IL-6 release and subsequent STAT3 activation (Wu *et al.*, 2009, 2014; Wakita *et al.*, 2010; Razi *et al.*, 2019).

Specifically in CRC, γδ T cells have been shown to have a protective effect, reducing adenocarcinoma formation in AOM-treated mice (Matsuda, Kudoh and Katayama, 2001). One study found that most γδ T cells in CRC expressed Vδ1 (Meraviglia *et al.*, 2017). Vδ2 T cells have also been shown to kill CRC cells in via antibody-dependent cytotoxicity mediated by FcγRIIIA (CD16) (Varesano, Zocchi and Poggi, 2018). Phospho-antigens are targeted by γδ T cells in CRC, as shown in multiple *ex vivo* experiments (Maeurer *et al.*, 1996; Todaro *et al.*, 2009; Zocchi *et al.*, 2017; Varesano, Zocchi and Poggi, 2018; Mikulak *et al.*, 2019). TCR-mediated killing of tumour cells appeared more important than NKG2D-mediated cytolysis (Todaro *et al.*, 2009). Regarding γδ T cells pro-tumour effects, IL-17 expression has been shown to correlate with CRC tumorigenesis (Grivennikov *et al.*, 2012), and inhibition of IL-17 protects against colitis, CRC and colitis-associated CRC (Wu *et al.*, 2009; Housseau *et al.*, 2016; Kathania *et al.*, 2016). In fact, γδ T cells may be the prime producers of IL-17 in human CRC, with some studies finding that IFN-γ production by γδ T cells may be reduced in CRC compared to healthy tissue (Wu *et al.*, 2014; Meraviglia *et al.*, 2017). Cancerous cells in *Apc* mutant mice have

also been shown to evade γδ+ IELs by downregulating BTNL molecules, which normally interact with the TCR of γδ+ IELs, via β-catenin signalling (Suzuki et al., 2022).

1.3.2.2 The role of IFNγ in CRC

IFNγ is an essential cytokine in the inflammatory response and as such has been implicated in the anti-tumour immune response in a variety of ways (Jorgovanovic *et al.*, 2020). It mainly derives from natural killer (NK) cells, natural killer T (NKT) cells and activated CD4+, CD8+ and γδ T cells (Burke and Young, 2019). Here, I briefly describe the signalling pathways and downstream effects of **I**FNγ signalling, and the consequences this has for the immune compartment and cancer.

1.3.2.2.1 IFNγ signalling

The IFNγ receptor consist of two subunits, IFNGR1 and IFNGR2, which are associated with JAK1 and JAK2 via their intracellular domain. Upon binding of IFNγ to its receptor, JAK1/2 are brought into close proximity, allowing their phosphorylation and activation (fig. 1.3) (Alspach, Lussier and Schreiber, 2019). JAK1/2 then phosphorylates and activates STAT1, which dimerises and translocates to the nucleus. Here it binds the γ activated site (GAS) sequence of DNA, usually alongside co-activators such as p300 , cAMP responsive-element-binding protein (CBP) and minichromosomal maintenance deficient 5 (MCM5) (Platanias, 2005). This drives transcription of IFNγ inducible genes, termed Interferon Signature Genes (ISG), many of which are transcription factors themselves. Inhibition of this pathway is performed by SHP phosphatases (Shp2) or suppressor of cytokine signalling (SOCS) family proteins, which inhibit JAK proteins. Protein Inhibitor of Activated STATs (PIAS) can also negatively regulate this pathway by dephosphorylating STAT1 (Alspach, Lussier and Schreiber, 2019).

Whilst this is the classical pathway of IFNγ signalling, other pathways have been shown to be initiated by IFNγ signalling. Activation of phosphatidylinositol 3-kinase (PI3K) and subsequently Akt and mTOR has also been reported (Jorgovanovic *et al.*, 2020). This pathway may interact with the classical

JAK/STAT pathway, as PI3K can activate protein kinase C-δ (PKC-δ) which phosphorylates STAT1 at serine position 727, enabling full transcriptional activation (Platanias, 2005). One study suggested that whether the JAK/STAT or PI3K/AKT pathway are activated by IFNγ may dependent on concentration, with high IFNγ doses activating JAK/STAT and low doses activating PI3K/Akt in cancer cells (Song *et al.*, 2019).

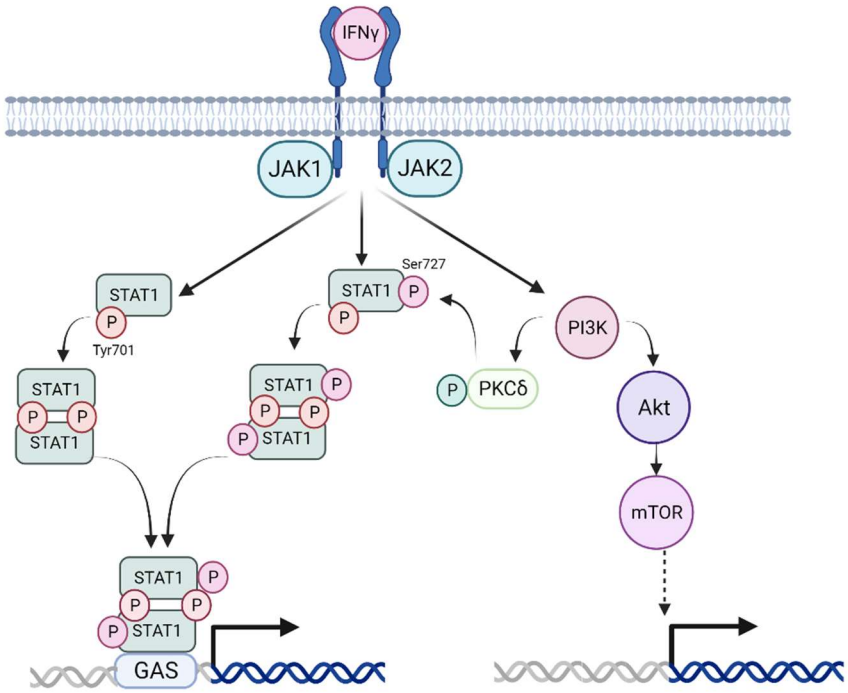

Figure 1.3 – IFNγ signalling pathways

Upon IFNγ binding to its receptor, JAK1 and JAK2 are brought within close proximity, leading to phosphorylation of STAT1 at position Tyr701 (red), triggering STAT1 dimerization and translocation to the nucleus (Alspach, Lussier and Schreiber, 2019). IFNγ signalling can also activate PI3K activity. PI3K can phosphorylate and activate PKCδ, which can then phosphorylate STAT1 at position Ser727 (pink), which enables full transcriptional activation (Platanias, 2005). STAT1 binds the γ activated site (GAS) sequence of DNA to activate transcription of target genes (Platanias, 2005). IFNγ-mediated PI3K activation can also lead to Akt and mTOR signalling, which also leads to transcriptional activation (Jorgovanovic et al., 2020). Figure created in BioRender.

1.3.2.2.2 *The effect of IFNγ on the immune system*

IFNγ can have a wide range of effects on the immune system but is most classically associated with Th1 polarisation and promotion of cytotoxic T cells. Signalling of IFNγ on T cells induces the transcription factor Tbet, which promotes a Th1 phenotype, and inhibits the transcription factor GATA3, thereby inhibiting Th2 and Th17 differentiation (Jenner *et al.*, 2009). Tbet also drives expression of IL-12 receptor and IFNγ, resulting in a positive feedback loop of Th1 differentiation and stabilisation (Szabo *et al.*, 2002). In CD8+ T cells, IFNγ signalling drives proliferation as well as expression of granzyme B and TNF-related apoptosis-inducing ligand (TRAIL) (Whitmire, Tan and Whitton, 2005; Ravichandran *et al.*, 2019). However, there is some evidence that IFNγ can also induce apoptosis of CD4+ T cells and limit proliferation of CD8+ T cells, indicating a level of control over the immune response (Refaeli *et al.*, 2002; Berner *et al.*, 2007). However, Tregs, which also limit immune responses, are antagonised by IFNγ (Caretto *et al.*, 2010; Xin *et al.*, 2014; Olalekan *et al.*, 2015).

Antigen presenting cells (APCs) are also affected by IFNγ. In macrophages, IFNγ signalling drives M1 polarisation and a pro-inflammatory phenotype. Expression of cytokines and chemokine receptors, cellular adhesion proteins and MHCI and II are all increased (Jorgovanovic *et al.*, 2020). IFNγ has also been shown to work synergistically with TLR signalling in macrophages to induce nitric oxide, TNFα and IL-12 production, increasing anti-tumour effectiveness (Müller *et al.*, 2017; Paul *et al.*, 2019). In dendritic cells (DCs) IFNγ signalling drives maturation, along with expression of MHCI and II and costimulatory molecules, such as CD40, CD54, CD80, CD86, and CCR7. It also triggers release of IL-12 family and IL-1β cytokines (Pan *et al.*, 2004; Fang *et al.*, 2018). However, IFNγ also limits DC survival in a dose-dependent manner, allowing antigen presentation and subsequent immune response to be limited (Russell *et al.*, 2009).

1.3.2.2.3 *The effect of IFNγ on cancer cells*

IFNγ can also have a variety of effects on cancer cells themselves. JAK/STAT1 signalling has been shown to activate caspases and initiate caspase-3 and -7 expression, resulting in apoptosis of cancer cells (Hao and Tang, 2018; Song *et al.*, 2019; Jorgovanovic *et al.*, 2020). This has been shown to be particularly relevant in cancer stem cells in CRC, possibly due to the enriched expression of the IFNγ receptor (Ni *et al.*, 2013). IFNγ signalling also inhibits angiogenesis by triggering a change in endothelial cells shape and downregulation of vascular endothelial growth factor A in stromal fibroblasts (Lu *et al.*, 2009; Kammertoens *et al.*, 2017). Metastasis can also be influenced by IFNγ, via increased CXCR4, a chemokine receptor which enables migration, and enhancement of the epithelial-to-mesenchymal transition (H.-C. Chen *et al.*, 2011; Lo *et al.*, 2019).

The effect of IFNγ during cancer also relies on the immune compartment. As well as the previously described effects on immune cells themselves, IFNγ can induce expression of immune checkpoint inhibitors such as PD-L1 and IDO on tumour cells, thus dampening T cell mediated responses and encouraging immune evasion (Jorgovanovic *et al.*, 2020). This confers the importance of IFNγ during immune checkpoint blockade, with expression of an IFNγ signature, including IDO, CXCL10, CXCL9, HLA-DR and STAT1, predicting clinical response (Ayers *et al.*, 2017). In addition, mice with IFNGR-/- tumours were resistant to immune checkpoint therapy (Wang *et al.*, 2019).

1.3.2.3 Role of MHCII in cancer

Induction of MHCII expression is one of the major downstream effects of IFNγ and has a vital role in presenting exogenously derived peptides to CD4+ T cells. Generally, it is expressed constitutively by antigen presenting cells (APCs), such as dendritic cells (DCs) and macrophages, but its expression can be increased in other cell types by IFNγ (Axelrod *et al.*, 2019). This is of interest in cancer as loss of MHCII expression is associated with decreased tumour infiltrating lymphocytes (TILs), increased metastasis, and poorer outcomes (Armstrong *et al.*, 1997; Warabi, Kitagawa and Hirokawa, 2000;

Mortara *et al.*, 2006; Forero *et al.*, 2016; Park *et al.*, 2017; Griffith *et al.*, 2022). MHCII expression can also aid the efficacy of immune checkpoint inhibitor treatment (Johnson *et al.*, 2016; Rodig *et al.*, 2018; Roemer *et al.*, 2018). As such it was of interest to us during this project.

1.3.2.3.1 *MHCII induction by IFNγ*

IFNγ can induce MHCII expression in non-classical APCs, such as the IECs via the transcription factor CIITA. Upon binding of IFNγ to its receptor, as previously described, STAT1 translocates to the nucleus where it binds promoter regions of IFN responsive genes. This interaction stabilised by the transcription factor USF-1. CIITA is one of these IFN responsive genes, once it is expressed it then translocates to the nucleus to act as a scaffold for RFX-family transcription factors mediating MHCII-related gene transcription. MHCII exists as a heterodimer of the α and β chain, and is associated with MHC-II–associated invariant chain (Ii) in the endoplasmic reticulum (ER). Ii sits within the peptide binding pocket so peptide cannot bind while MHCII is in the ER. MHCII then migrates to endosomes, where the acidic environment degrades Ii, allowing MHCII to be loaded with peptides derived from endocytosis. In some cases, MHCII migrates to autophagosomes, enabling the presentation of endogenously derived peptides. Peptide loading stabilises MHCII, allowing it to present the antigen at the cell surface to CD4+ T cells. Interestingly, mutations which favour MHCII-mediated antigen presentation are negatively selected during tumour development. Negative selection was stronger against MHCII-restricted neo-antigens than MHCI-restricted ones, highlighting the importance of CD4-mediatied responses in tumour inhibition (Pyke *et al.*, 2018).

1.3.2.3.2 *Expression of MHCII in cancer*

MHCII expression appears to vary in cancer. In CRC, one study found that, whilst normal colonic IECs did not express MHCII, colonic IECs in 42% of CRC carcinoma and 38% of adenoma patients expressed MHCII. MHCII expression also coincided with increased lymphocyte infiltration, lymphatic invasion and lymph node metastasis (Warabi, Kitagawa and Hirokawa, 2000). Some cancers may also be

resistant to IFNγ induced MHCII expression; a study using CRC patient-derived organoids treated with IFNγ found organoids either responded with strong MHCII upregulation, weak upregulation, or were non-inducible (Pickles *et al.*, 2023). Similar categories of inducibility have been observed in melanoma (Johnson *et al.*, 2016). In CRC organoids, the reduced capacity to express MHCII was shown to be mediated by EZH2 (enhancer of zeste homolog 2) occupancy of the CIITA gene (Pickles *et al.*, 2023). Another mechanism by which MHCII silencing may occur is via methylation of the CIITA gene, which has been reported to prevent HLA expression in CRC (Satoh *et al.*, 2004). In other cancers different mechanisms have been reported. Mutations in promoter regions of CIITA have been reported to drive MHCII expression in some melanoma cell lines (Deffrennes *et al.*, 2001). MAPK activation has also been shown to increase and reduce HLA-DR expression in melanoma and breast cancer, respectively, with these differences possibly due to cell type (Martins *et al.*, 2007; Loi *et al.*, 2016). Particular HLA types could also be relevant in cancer susceptibility, with one study finding that certain HLA genotypes, specifically the DR17 and DR13 alleles, were more prevalent in colitis-associated CRC (Garrity-Park *et al.*, 2009).

1.3.2.3.3 *Effect of MHCII on anti-tumour immune response*

MHCII expression in tumours has been associated with a broad increase in the anti-tumour immune response, including increased CD4+ and CD8+ infiltrating T cells, reduction in lymphatic invasion , greater number of tertiary lymphoid structures (fig.1.4) (Axelrod *et al.*, 2019). Expression of PD-L1, and genes suggesting a Th1 polarisation, such as IFNγ, IL-2, IL-12, were also increased, whereas Th2 associated cytokines, including IL-4, IL-10 and TGFβ were not (Axelrod *et al.*, 2019). In one study looking at colorectal cancer patients, decreased HLA-DR expression coincided with reduced interaction between CD4+ T cells and APCs and decreased co-localisation of CD8+ cytotoxic T cells and tumour cells. Cytotoxic CD8+ cells also appeared to have reduced levels of Ki67 and granzyme B (Griffith *et al.*, 2022). Experiments in mouse models have shown that expression of MHCII or CIITA

increased tumour rejection (Ostrand-Rosenberg, Thakur and Clements, 1990; Meazza *et al.*, 2003; Axelrod *et al.*, 2019), an effect which was abrogated if costimulatory molecules CD80 and CD86 were blocked via antibodies (Baskar *et al.*, 1996). MHCII expressing tumour cells appear to act as APCs when mediating this response, as depletion of macrophages or DCs did not affect rejection of CIITA-expressing tumours (Bou Nasser Eddine *et al.*, 2017). Exactly what peptides MHCII presents in these scenarios remains unclear, as characterisation of peptides bound to MHCII remains challenging and possible neoantigens in different cancer cell lines are variable. MHCII classically presents peptides derived exogenously, and so the loading of endogenous antigens may be dictated by the rate of autophagy in each individual cell line (Axelrod *et al.*, 2019).

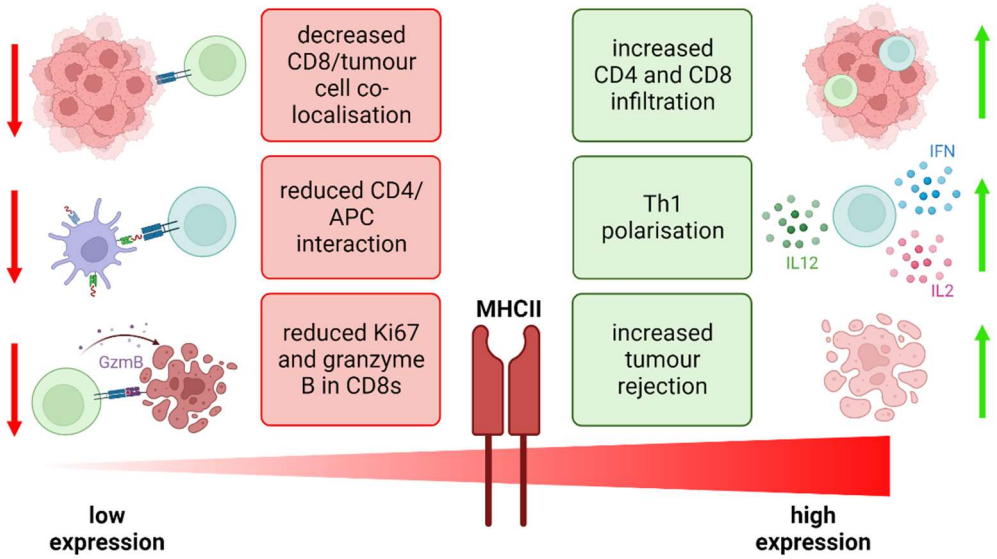

Figure 1.4 – Effects of MHCII expression in cancer

Low expression of MHCII in cancer has been shown to decrease co-localisation of CD8 T cells and tumour cells, reduced interaction between CD4 T cells and APCs, and reduce Ki67 and granzyme B expression by CD8 T cells (Griffith et al., 2022). In contrast, expression of MHCII in cancer is associated with increased infiltration of CD4 and CD8 T cells (Axelrod et al., 2019), increased Th1 polarisation including expression of IFNγ, IL2 and IL12 (Axelrod et al., 2019), and increased tumour rejection (Ostrand-Rosenberg, Thakur and Clements, 1990; Meazza et al., 2003; Axelrod et al., 2019).

1.4 The role of eicosanoids in the gut

Eicosanoids, which include the prostaglandins (PGs), are a family of lipid mediators which have diverse functions in the gut. Whilst many eicosanoids have essential roles in gut maintenance and have been demonstrated to protect against colitis and promote tissue repair, they have also been implicated in the progression of CRC through various mechanisms (Tanaka *et al.*, 2009; Montrose *et al.*, 2010; Wang and DuBois, 2010a). These functions are largely dependent on the cell type expressing and responding to the eicosanoids, the specific eicosanoid and receptor expressed and the spatial and temporal distribution of the eicosanoids. In inflammatory diseases of the gut, such as colitis and CRC, the immune compartment plays a pivotal role in disease prevention and progression and as such eicosanoids can also have a varied impact on immune cell functions. Here, I describe the generation and function of eicosanoids in the gut and how this influences the immune compartment and disease development.

1.4.1 Eicosanoid generation and function

Eicosanoids are all derived from arachidonic acid (AA) (fig. 1.5), which is liberated from the plasma membrane by phospholipases, such as cytosolic phophoslipase2 (cPLA2) (Smyth *et al.*, 2009). AA is subsequently channelled down different enzymatic pathways resulting in different classes of eicosanoids. When metabolised by cyclooxygenases (COXs), AA produces the prostanoid family of mediators, which includes thromboxane A_2 (TXA_2) and the PGs – PGE_2, $PGF_{2\alpha}$, PGD_2 or PGI_2 (Wang and DuBois, 2010a). Initially, COX enzymes produce prostaglandin H_2 (PGH_2), which is subsequently processed by one of many synthases. For example, PGE_2 is generated using one of three PGE_2 synthases (PGESs) - microsomal PGES-1 and -2 and cytosolic PGES (Smyth *et al.*, 2009). Alternatively, AA can be processed via the lipoxygenase pathway to produce the leukotrienes and hydroxyeicosatetraenoic acids (HETEs) (Wang and DuBois, 2010a). The final pathway, the P450

epoxygenase pathway, generates HETEs, epoxyeicosatrienoic acids (EETs) and hydroperoxyeicosatetraenoic acids (HPETEs) (Wang and DuBois, 2010a).

PGE_2 is probably the most studied eicosanoid in inflammation, and the most abundant. COX1, encoded by *Ptgs1*, is constitutively expressed in many cells where it acts to maintain homeostasis. However, it can also be upregulated by IL-3, IL-9 and IL-1 (Cohn *et al.*, 1997). COX2, encoded by *Ptgs2*, is generally only upregulated in response to inflammatory signals, including IL-1α/β, IFN-γ, TNF-α, tumour promoters such as Ras, and hypoxia via HIF-1α (Smyth *et al.*, 2009; Wang and DuBois, 2010b, 2010a). Non-steroidal Anti-Inflammatory Drugs (NSAIDs) inhibit both COX isoforms and as such are known to have detrimental effects on gut repair and maintenance (Wang and DuBois, 2013). As a result, COX2 specific inhibitors (COXIBs) have been developed to circumvent this whilst maintaining inhibition of inflammatory PG production, although these have been noted to have cardiovascular side-effects (Wang and DuBois, 2013). PGE_2 signals via the E series of receptors, EP1-4, as well as via peroxisome proliferator-activated receptors (PPARs) (Wang and DuBois, 2010a). Each of the EP receptors has different function and cellular distribution. Given the short half-life of PGE_2 (less than 15 seconds), receptor localisation is an important factor in determining the PGs effects (Bygdeman, 2003).

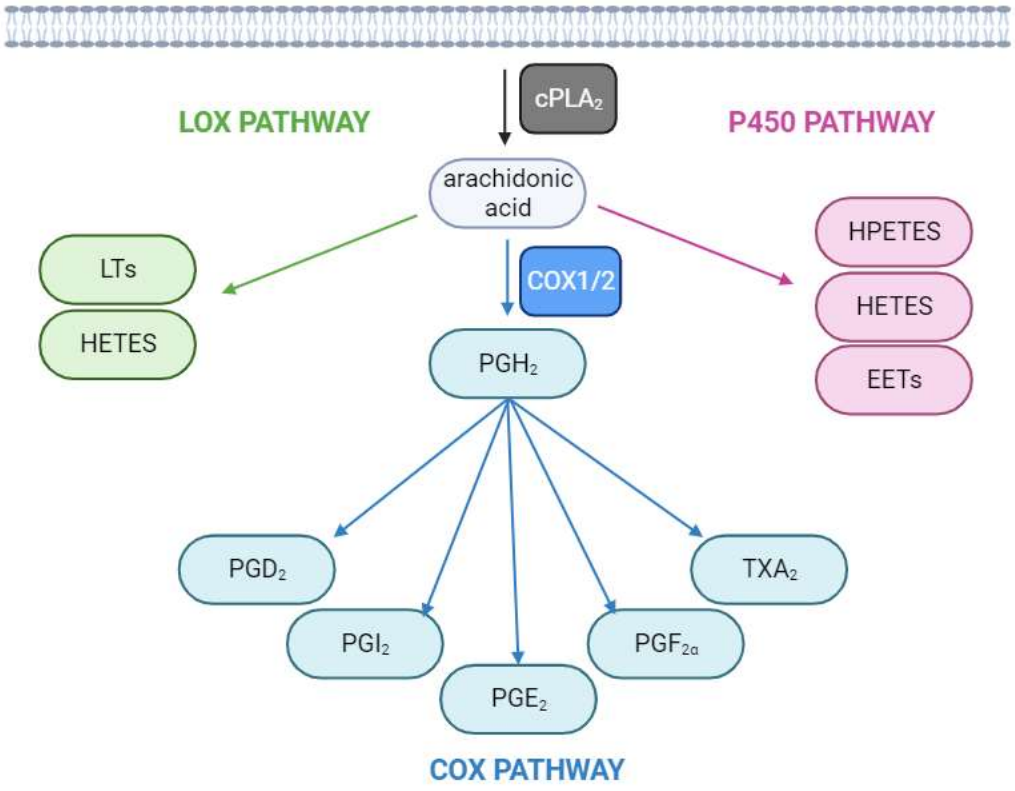

Figure 1.5 – Overview of the main eicosanoid biosynthesis pathways

Eicosanoid synthesis is generally done by one of three pathways – the cyclooxygenase (COX) pathway, the lipoxygenase (LOX) pathway and the p450 epoxygenase pathway. All of these begin with arachidonic acid (AA) being liberated from the plasma membrane by phospholipase A_2. In the COX pathway AA is converted to prostaglandin H_2 (PGH_2) by one of two cyclooxygenase (COX) isoforms. PGH_2 is then converted to a prostaglandin or thromboxane A_2 by synthetases. The LOX pathway generates leukotrienes (LTs) and hydroxyeicosatetraenoic acids (HETEs). The P450 pathway gives rise to HETES, epoxyeicosatrienoic acids (EETs) and hydroperoxyeicosatetraenoic acids (HPETEs) (Smyth *et al.*, 2009; Wang and DuBois, 2010a).

1.4.2 Eicosanoids in gut homeostasis

Prostaglandins have a number of roles in the healthy gut, including promoting mucus, bicarbonate and acid secretion, as well as mucosal blood flow (Halter *et al.*, 2001). The importance of these functions is highlighted by the effects of prolonged NSAID use, which can result in mucosal erosions, ulcerations and perforations (Halter *et al.*, 2001). COX1, the constitutively expressed isoform, is expressed in the colon epithelium and in the lamina propria of both the colon and the SI in humans (Hult *et al.*, 2011). COX2 is expressed in a minority of cells within the crypt epithelium of the colon, as well as a small number of cells in the lamina propria surrounding the crypts in the SI (Hult *et al.*, 2011). However, expression of eicosanoid related enzymes and receptors are altered under inflammatory conditions. COX1 is induced in stem cells of the intestinal crypts following radiation injury; inhibition of COX1 via NSAIDs or genetic knockout reduces the number of stem cells which survive irradiation (Cohn *et al.*, 1997; Houchen, Stenson and Cohn, 2000). This effect may be mediated by EP2 as changes are seen in EP2 expression following radiation injury and *EP2*-/- mice have reduced crypt cell survival (Cohn *et al.*, 1997; Houchen, Stenson and Cohn, 2000). EP2 signalling results in EGFR trans-activation and phosphorylation of Akt by PI3K, resulting in reduced Bax translocation to the mitochondria and reduced apoptosis of crypt cells (Tessner *et al.*, 2004). This is in contrast to physical wound healing, in which Toll-like receptor (TLR) signalling promotes COX2 expression near the crypts. Subsequent PGE_2 signalling via EP4 receptors on epithelial progenitor cells leads to the migration of epithelial cells to close the wound (Miyoshi *et al.*, 2017). Clearly prostaglandins have important functions during maintenance and healing of the gut, but the specific enzymes and cell types involved are varied.

1.4.3 Eicosanoids in colitis

Multiple eicosanoids are known to be enriched during colitis, including PGE_2, PGF2α, PGD2, 12-HETE, 15- HETE and LTB4 (Ferrer and Moreno, 2010). Lipoxin generation may be altered during colitis, and treatment with an LXA4 analogue has reportedly relieved colitis in experimental models (Moreno, 2017). NSAIDs are known to exacerbate colitis symptoms and trigger colitis relapse, highlighting the protective role of prostanoids and as such this is where much research has focused (Montrose *et al.*, 2015; Peng *et al.*, 2017). The dextran sodium sulfate (DSS) model of colitis, in which DSS is administered in the drinking water resulting in damage and inflammation of the colon, has commonly been used to investigate this (Shattuck-Brandt *et al.*, 2000; Ishikawa, Oshima and Herschman, 2011). Consistent with observations in patients, NSAIDs exacerbate DSS-induced colitis, however this is alleviated by PGE_2 (Tanaka *et al.*, 2009). DSS-induced damage and inflammation is also worsened by knockout of $cPLA_2$ or mPGES1 (Montrose *et al.*, 2010).

The protective effects of PGE_2 in colitis are primarily mediated through EP4 signalling. DSS-induced colitis was exacerbated in mice with EP4 knockout or that were administered with an EP4-specific antagonist, in contrast EP4 agonist treatment had the opposite effect (Kabashima *et al.*, 2002; Jiang *et al.*, 2007). EP4 activation led to PI3K/Akt signalling via β-arr1, a scaffold protein which associated with EP4. Knockout of β-arr1 resulted in more severe colitis following DSS treatment, coinciding with decreased Akt phosphorylation (Peng *et al.*, 2017). EP4 localisation is also suggested to change during colitis. In healthy tissue EP4 was expressed exclusively on the apical side of the epithelium but this expression extended to the basolateral side during colitis (Moreno, 2017).

Whilst overall PGs appear protective in colitis, some conflicting evidence exists regarding PGE_2 and COX expression during the disease. It is often reported that PGE_2 levels increase with worsening disease severity, then return to basal levels upon repair (Raab *et al.*, 1995; Wiercińska–Drapało, Flisiak and Prokopowicz, 1999; Brown *et al.*, 2007; Moreno, 2017). Alternatively, PGE_2 has been

reported to decrease during the injury phase before increasing during the repair phase (Melgar *et al.*, 2006; Montrose *et al.*, 2015; Peng *et al.*, 2017). Whilst COX1 expression is reported to remain constant or be reduced, COX2 has been shown to increase in myeloid, endothelial and epithelial cells during the injury phase (Singer *et al.*, 1998; Peng *et al.*, 2017). Deletion of COX2 specifically in epithelial cells had no effect on colitis, whereas endothelial or myeloid specific knockout exacerbated colitis (Ishikawa, Oshima and Herschman, 2011). TLR signalling is suggested to be involved in alterations in COX2 expression. One study found COX2 expression to be increased via TLR4 signalling, however other studies suggest COX2-expressing stromal cells migrate to the crypt base in a TLR/Myd88 dependent manner, as opposed to COX2 expression increasing (Fukata *et al.*, 2006; Brown *et al.*, 2007). This mimics the response seen to physical injury, and could be vital for the effectiveness of PG release considering the short half-life of these molecules (Bygdeman, 2003; Miyoshi *et al.*, 2017). At what stage of disease samples are taken could be vital in understanding some of the discrepancies between studies, with expression of COX1, COX2, EP4 and PGE_2 likely changing throughout the course of disease. The downstream effects of EP4 signalling may also be different in different cell types and disease stages (Dey, Lejeune and Chadee, 2006).

1.4.4 Eicosanoids in colorectal cancer

1.4.4.1 PGE_2 and COX in CRC

PGE_2 is the most abundant eicosanoid found in CRC and the focus of much research (Wang and DuBois, 2013). COX2 is enriched in 90% of carcinomas and 50% of adenomas and generally associated with poorer survival (Ogino *et al.*, 2008; Wang and DuBois, 2013), whereas COX1 expression remains constant in human and murine CRC (Eberhart *et al.*, 1994; Chulada *et al.*, 2000). Deletion of COX2 has been shown to reduce polyp burden and, in some cases, polyp size in *Apc*$^{min/+}$ mice (Chulada *et al.*, 2000; Seno *et al.*, 2002; Cherukuri *et al.*, 2014; Roulis *et al.*, 2020). One study found that no tumours developed following AOM administration in *Ptgs2*-/- mice (Ishikawa and Herschman, 2010). Whilst COX1 is less implicated in CRC, one study found that homozygous or

heterozygous deletion of *Ptsg1* or *2* in *Apc*$^{min/+}$ resulted in a dose-dependent reduction in polyp burden (Chulada *et al.*, 2000). Multiple EP receptors appear to be involved, with genetic deletion of EP2 or administration of an EP1 or EP4 antagonist reducing polyp number in models of FAP (Watanabe *et al.*, 1999; Seno *et al.*, 2002; Wang *et al.*, 2015). Both NSAID and COXIB use reduces CRC risk (Wang and DuBois, 2010b). PGE_2 therefore appears to have a significant role in familial and sporadic CRC.

The effects of PGE_2 in colitis-associated cancer is less clear, presumably due to PGs protective role in colitis and the fact that carcinogenesis is driven by inflammation in this context. Increased COX2 has been observed in patients with colitis-associated cancer (Agoff *et al.*, 2000). In contrast, *Ptgs1*-/- and *Ptgs2*-/- mice had exacerbated colitis but no change in tumorigenesis compared to wild type (Ishikawa and Herschman, 2010). Other studies deduced a TLR4-mediated mechanism for PGE_2 in colitis-associated CRC. When administered DSS, TLR4-/- mice suffer exacerbated colitis and do not upregulate COX2 (Fukata *et al.*, 2006). However, following AOM+DSS treatment, TLR4-/- mice are protected from tumorigenesis. This protection is reversed by PGE_2 treatment during the recovery phase of colitis but not during acute inflammation (Fukata *et al.*, 2007; Hernandez *et al.*, 2010). When PGE_2 was administered, sub-epithelial macrophages upregulated COX2 and epithelial cells upregulated amphiregulin in a TLR4- and COX2- dependent manner. Amphiregulin is an EGFR ligand, leading to epithelial proliferation. This led to the model that TLR4-mediated PGE_2 release was upregulating COX2 in subepithelial macrophages, resulting in further PGE_2 release and subsequent EGFR-driven epithelial cell growth (Fukata *et al.*, 2007; Hernandez *et al.*, 2010). Transactivation of PPARγ by PGE_2 is also controversial in colitis-associated cancer, with one study finding it promotes cancer via PI3K-Akt signalling, but another study finding PPARγ agonist administration following AOM+DSS treatment can reduce tumour burden (Kohno *et al.*, 2005; Wang and DuBois, 2014).

The cell type expressing COX2 appears to be significant in CRC, but also controversial. COX2 is upregulated macrophages, endothelial cells, myofibroblasts of human adenomas and carcinomas, and sometimes in the epithelial cells of carcinomas (Bamba *et al.*, 1999; Hao *et al.*, 1999; Sheehan *et al.*, 1999; Chapple *et al.*, 2000; Adegboyega *et al.*, 2004; Ogino *et al.*, 2008). Polyps of APC mutant mice have increased COX2 expression, possibly specifically in the sub-epithelial macrophages, mirroring human CRC (Hull *et al.*, 1999; Chapple *et al.*, 2000; Kawajiri *et al.*, 2002; Seno *et al.*, 2002). In AOM+DSS treated mice, COX2 is upregulated in stromal fibroblasts, macrophages and endothelial cells (Ishikawa and Herschman, 2010). Whilst the exact mechanism of COX2 upregulation remains to be elucidated, it may involve Tcf/Lef transcription factors activated by β-catenin signalling (Wang *et al.*, 2005). To determine the effect of COX2 in specific cell types, conditional KO mice which lack COX2 in specific cell subsets have been employed alongside CRC models. Only epithelial-specific deletion of COX2 reduced polyp burden in $Apc^{min/+}$ mice, which is perhaps surprising considering epithelial cells only upregulated COX2 once at the carcinoma stage (Adegboyega *et al.*, 2004; Cherukuri *et al.*, 2014). Myeloid-specific COX2 knockout had no effect on burden despite the COX2 upregulation observed in macrophages in $Apc^{min/+}$ mice and in patient adenomas and carcinomas (Hull *et al.*, 1999; Chapple *et al.*, 2000; Cherukuri *et al.*, 2014).However, one study found upregulation of COX2 by macrophages to support tumorigenesis (Ko *et al.*, 2002). Deletion of COX2 in fibroblasts abrogated polyp development in $Apc^{min/+}$ mice, supporting the finding that COX2 is upregulated in the sub-epithelial stromal cells early in CRC development (Shattuck-Brandt *et al.*, 2000; Roulis *et al.*, 2020). It is likely that different cell types are influencing cancer development via PGE_2 at different stages of disease, explaining the discrepancies between these studies. For example, fibroblast-mediated PGE_2 release has been shown to support stem cell expansion and tumour initiation, whereas COX2 has also been linked to angiogenesis which affects larger tumours later in CRC progression (Seno *et al.*, 2002; Cherukuri *et al.*, 2014; Roulis *et al.*, 2020).

1.4.4.2 Supporting cancer stem cells

Cancer stem cells are undifferentiated cells, important in tumour initiation, growth, metastasis and drug resistance (Wang *et al.*, 2015). PGE_2 activation of EP4 has been shown to increase cancer stem cells and liver metastases via MAPK and PI3K/Akt signalling (Wang *et al.*, 2015).This appeared to be COX2 dependent as the tumour-initiating capacity of the cancer cells was reduced upon COXIB administration (Wang *et al.*, 2015). PGE_2 from COX2-expressing fibroblasts has also been shown to support stem cell transformation via EP4-mediated Yap signalling (Roulis *et al.*, 2020). The capacity to form colospheres, a metric of cancer stem cell number, was reduced in SW620 cells by NSAID or COXIB administration. NSAIDs also reduced cancer stem cell markers in murine xenograft cancer model (Moon *et al.*, 2014). However, NSAID inhibition of cancer stem cells could be partly COX-independent, with one study finding NSAIDs induced SMAC-mediated apoptosis of stem cells (Qiu *et al.*, 2010).

1.4.4.3 Supporting growth and inhibiting apoptosis

PGE_2 has been shown to promote CRC growth via its EP2 receptor and β-catenin. Normally, β-catenin undergoes ubiquitin-dependent degradation following its phosphorylation by GSK-3β. However, PGE_2/EP2 signalling activates PI3K/Akt signalling and subsequent phosphorylation of GSK-3β. The Gsα subunit of EP2 binds to axin, causing it to dissociate from GSK-3β. GSK-3β therefore does not phosphorylate β-catenin, allowing it to translocate to the nucleus and activate Tcf- and Lef-dependent transcription and thus driving cancer growth (Castellone *et al.*, 2005). Trans-activation of EGFR by PGE_2 can also activate growth via Extracellular Signal-Related Kinase 2 (Pai *et al.*, 2002). IECs co-cultured with macrophages also increase proliferation and anchorage-dependent growth via COX2-dependent pathways (Ko *et al.*, 2002). COX2 may also inhibit apoptosis; overexpression of COX2 induced Bcl-2 expression and conferred resistance to butyrate-induced apoptosis, with the latter reversed with NSAID treatment (Tsujii and DuBois, 1995). This is consistent with increased Bcl-2

expression and resistance to COXIB-mediated cell death seen in HCA-7 cells administered PGE_2 (Sheng *et al.*, 2001).

1.4.4.4 Effects on angiogenesis

PGE_2 has been demonstrated to promote tumour angiogenesis, an essential factor in tumour growth and metastasis. The increased angiogenesis seen in larger polyps of $Apc^{\Delta 716}$ mice was lost if in combination with *Ptgs2*+/- or *EP2*-/- (Seno *et al.*, 2002). However in *Ptgs2*-/- mice large polyps were completely absent, suggesting the need for COX2-mediated angiogenesis for tumour growth beyond a certain size (Seno *et al.*, 2002; Cherukuri *et al.*, 2014). EP2 and EP4 signalling have both been shown to promote vascular endothelial growth factor (VEGF) and fibroblast growth factor (FGF) in epithelial and endothelial cells, leading to endothelial cell proliferation and survival (Wang and DuBois, 2010a).PGE_2 can also promote endothelial cell migration through the αVβ3 integrin–CDC42 or Rac pathway, and trigger VEGF andCCL2 release by mast cells which further promotes endothelial migration (Wang and DuBois, 2010a). VEGF can also drive COX2 expression, leading to a positive feedback loop that promotes further angiogenesis (Wang and DuBois, 2010a).

1.4.4.5 Other Eicosanoids in cancer

PGI_2 can support CRC progression via PPARδ (Wang and DuBois, 2010a). The leukotriene LTB4 and its receptor CysLT1 are both upregulated during CRC, with CysLT2 expression linked to poor prognosis (Wang and DuBois, 2010a). HETEs signalling via the BLT2 receptor have been linked to tumorigenesis, although this resulted in PGE_2 release. In contrast, PGD_2 may be protective in CRC, with PGD synthase knockout increasing tumour burden in $Apc^{min/+}$ mice (Park *et al.*, 2007). The role of eicosanoids, beyond of PGE_2, is poorly understood and thus an area in need of further research.

1.4.5 Eicosanoids and the immune system

Eicosanoids also have well documented but complicated effects on the immune system, with consequences for diseases of the gut. The effects of PGE_2 are the most widely studied of the eicosanoids, with sometimes contradictory results (Sreeramkumar, Fresno and Cuesta, 2012a; Maseda, Ricciotti and Crofford, 2019). Here, I explore the effects of eicosanoids on immune cells with a focus on T cells (overview in fig. 1.6), as this is where this project has focused. Out of the four EP receptors, T cells only express EP2 and EP4 (Maseda, Ricciotti and Crofford, 2019). Expression of $PGF_{2\alpha}$ receptors have not been observed in T cells (Maseda, Ricciotti and Crofford, 2019). The PGD_2 receptors, DP1 and DP2 (also known as CHTR2), are preferentially expressed on Th2 cells.

1.4.5.1 CD8 T cells and eicosanoids

PGE_2 can influence T cells via effects on antigen presenting cells (APCs). For example, when dendritic cells (DCs) that have matured in the presence of PGE_2 prime CD8+ T cells, it results in lower granzyme B expression and reduced cytolytic ability, although it does not affect proliferation (Watchmaker *et al.*, 2009). Similarly, inhibition of COX led to increased tumour-specific CD8+ T cell responses in a murine plasmacytoma model (Specht *et al.*, 2001). In vitro studies have also demonstrated that PGE_2 can suppress CD8+ T cell survival, type I IFN production and cytotoxicity (Garcia-Peñarrubia, Bankhurst and Koster, 1989). Deletion of COX2 specifically in myeloid cells increased cytolytic function of CD8+ T cells in a murine breast cancer model (Chen *et al.*, 2014). PGD_2 and leukotriene E4 (LTE_4) have been shown to promote recruitment and activation of CD8+ T cells in vitro, with possible implications for eosinophilic asthma (Hilvering *et al.*, 2018).

1.4.5.2 CD4 T cells and eicosanoids

Eicosanoids have been shown to have important functions in the polarisation of Th subsets, however some conflicting results exist as to the exact mechanisms, particularly for PGE_2 (Maseda, Ricciotti and Crofford, 2019). Yao *et al*. found that PGE_2 promoted both Th1 and Th17 cells, with EP4 blockade

causing a decrease in both subsets *in vivo* (Yao *et al.*, 2009). However, another study showed that COX2-mediated PGE_2 increased IL-17 release and the expression of ROR-γt whilst simultaneously decreasing IFNγ and T-bet expression (Napolitani *et al.*, 2009). PGE_2 can upregulate the receptors for IL-1β and IL-23 in T cells via EP2/4 and cAMP, thus inducing Th17 differentiation in the presence of IL-1β and IL-23 (Chizzolini *et al.*, 2008; Boniface *et al.*, 2009). It also reduced IL-10 production, mainly via EP4 (Boniface *et al.*, 2009). Once again, PGE_2 can also mediate its affect via DCs, with PGE_2 treatment of DCs prior to culture with naïve T cells resulting in an increased prevalence of Th1 cells (Lee *et al.*, 2002). In contrast, PGE_2 was also shown to enhance IL-23 release by DCs following stimulation with lipopolysaccharide (LPS), which could lead to Th17 differentiation (Sheibanie *et al.*, 2007; Khayrullina *et al.*, 2008). It has been proposed that these differences in Th17/Th1 induction could be explained by the EP2 and EP4 distributions in murine and human T cells (Maseda, Ricciotti and Crofford, 2019).

PGD_2 and PGI_2, on the other hand, are known to regulate Th2 responses. PGD_2 can trigger IL-4, IL-5 and IL-13 secretion by Th2 cells (Xue, Barrow and Pettipher, 2009; Mitson-Salazar *et al.*, 2016), whereas PGI_2 can inhibit Th2 responses (Zhou *et al.*, 2016). PGI_2 signalling via the IP receptor on Th2 cells resulted in decreased IL-4 and IL-13 expression, and PGI_2 also decreased IFNγ expression in Th1 cells (Takahashi *et al.*, 2002; Lone and Taskén, 2013). PGI_2 has also been proposed to work in conjunction with $PGF_{2\alpha}$ to promote Th17 responses during allergic lung inflammation (Li *et al.*, 2011). The leukotriene LTB_4 has also been shown to promote Th17 responses whilst inhibiting Tregs (Chen *et al.*, 2009). LTB_4 has also been shown to involved in chemotaxis of both CD4+ and CD8+ T cells and adhesion of T cells to epithelial cells via its BTL_1 receptor (Tager *et al.*, 2003; Luster and Tager, 2004).

1.4.5.3 Tregs and eicosanoids

In the case of regulatory T cells (Tregs), once again there is conflicting evidence as to the role of eicosanoids. In human T cells, PGE_2 was shown to promote differentiation of Tregs by inducing FoxP3

expression (Baratelli *et al.*, 2005; English *et al.*, 2009). Human DCs have been shown to more readily promote Treg cells when cultured with PGE_2 in combination with TNFα, IL-1β and IL-6 (Banerjee *et al.*, 2006). Other studies have shown the importance of PGE_2 generated by mPGES1 in Treg generation (Maseda, Banerjee, *et al.*, 2018; Maseda, Johnson, *et al.*, 2018). Deletion of mPGES1 and the subsequent reduction in Tregs was shown to exacerbate colitis (Maseda, Banerjee, *et al.*, 2018). However, other studies have found that PGE_2 can inhibit Treg via EP2 signalling, resulting in decreased GITR, CTLA-4 and IL-10 expression (H. Li *et al.*, 2017). This appeared to depend on Tregs ability to metabolise PGE_2 into 15-keto-PGE_2 via hydroxyprostaglandin dehydrogenase (HGPD), which is enriched in Tregs (Schmidleithner *et al.*, 2019).

1.4.5.4 γδ T cells

There are very few studies investigating the influence of eicosanoids on γδ T cells. PGE_2 and PGI_2, the latter of which functions mainly in the airways, has been shown to promote IL-17 production in γδ T cells via an IL-6 dependent mechanism (Jaffar *et al.*, 2011; Polese *et al.*, 2021). PGE_2 can also inhibit expression of Vγ9Vδ2 TCR, NKG2D and CD16 on γδ T cells (Martinet *et al.*, 2010). Clearly this is an area that requires further research.

1.4.5.5 Other immune cells

Eicosanoids are also reported to have effects on other immune cells. As this thesis focuses on T cells, I shall only briefly describe some of them here. PGE_2 has been shown to decrease expression of NKG2D, CD16 and natural cytotoxicity receptors (NCR: NKp30, NKp44, NKp46) in NK cells via EP2 and EP4 signalling (Martinet *et al.*, 2010). As well as the aforementioned effects on IL-12/IL-23 production, the effect of PGE_2 on DCs can be anti- or pro-inflammatory, depending on what other signals are present during their maturation (Khayrullina *et al.*, 2008). In addition, PGD_2, which can be generated by mast cells, DCs and Th2 cells, can lead to recruitment of eosinophils, basophils and Th2

cells. (Pettipher, Hansel and Armer, 2007). This is only a small sample of the effects eicosanoids can have on the wider immune system, but demonstrates their far reaching effects.

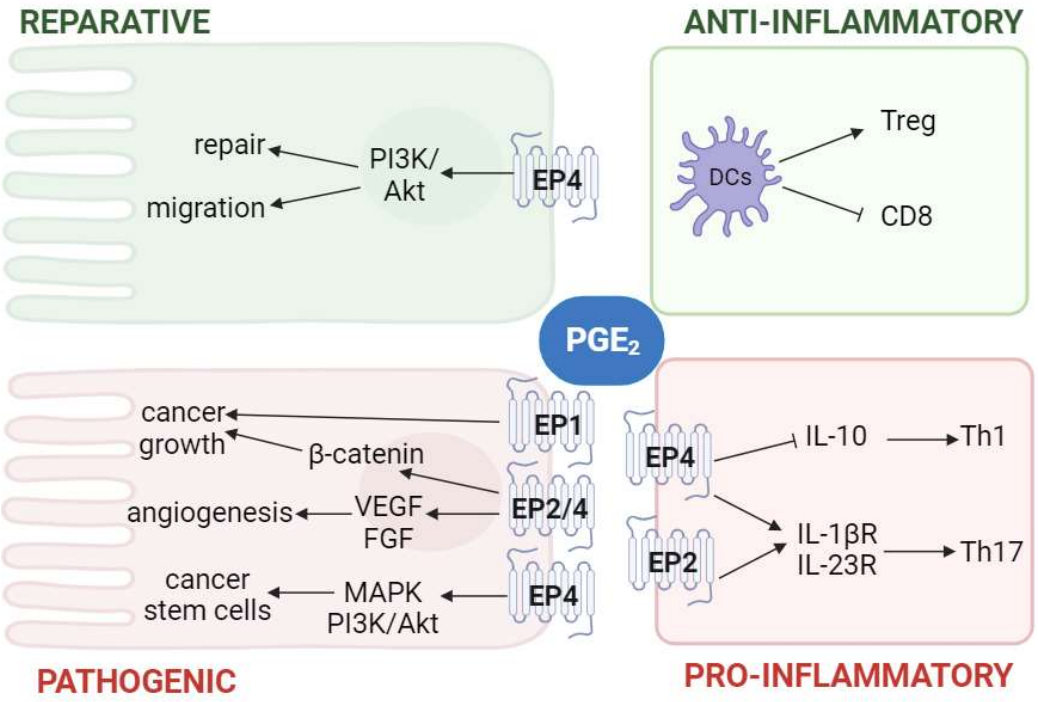

Figure 1.6 – Roles of PGE_2 in inflammation

PGE_2 has a number of anti-inflammatory and pro-inflammatory roles on the intestinal epithelial cells and the immune compartment, with consequences for diseases of the gut. In epithelial cells, PGE_2 can promote CRC via EP1, EP2 and EP4 signalling. This results in cancer growth via β-catenin signalling, angiogenesis via VEGF and FGF expression, and promotion of cancer stem cells through MAPK and Pi3K/Akt pathways (Wang and DuBois, 2010a; Wang *et al.*, 2015). However, it can also signalling via EP4 and PI3K/Akt can also promote repair in colitis (Peng *et al.*, 2017). PGE_2 can also promote Th1 and Th17 responses via EP4 and EP2 which can increase IL-1β and IL-23 receptor expression and reduce IL10 (Lee *et al.*, 2002; Chizzolini *et al.*, 2008; Boniface *et al.*, 2009). However, PGE_2 can influence dendritic cells (DCs) to promote Tregs and inhibit CD8 T cell differentiation (Banerjee *et al.*, 2006; Watchmaker *et al.*, 2009).

1.5 Aims of this thesis

Whilst the epithelial-intrinsic roles of Naips are reasonably well established and described above, the effect of epithelial Naips on the immune compartment remains to be identified. As mice lacking epithelial Naips have previously been shown to have increased tumorigenesis (Allam *et al.*, 2015), understanding the effect Naips have on lymphocytes could be important in understanding this phenotype. Our lab identified changes in eicosanoids in organoids lacking Naips, and as described above these lipid mediators can have a broad range of effects on both immune and epithelial cells.

Our aims for this project were to:

- Identify how epithelial Naips influenced the intraepithelial lymphocyte compartment at baseline and following Salmonella infection.
- Identify alterations in the immune response to colorectal cancer in mice lacking epithelial Naips.
- Understand how Naip knockout affects eicosanoid synthesis and what the implications are for the immune compartment.

2 Materials and Methods

2.1 In vivo studies

2.1.1 Mice

Animal studies were regulated by the Animals (Scientific Procedures) Act 1986 of the United Kingdom and performed under the Personal Project License number I13780903 and the project license number P06118734. Approval was granted by the University of Birmingham's Animal Welfare and Ethical Review Body and all ethical guidelines were adhered to whilst carrying out these studies.

Naip$^{\Delta/\Delta}$ mice were generated at The University of Lausanne as described by Allam *et al.*, 2015. Tissue-specific deletion of *Naip* in the intestinal epithelial cells was achieved using a Villin-Cre driver on a C57BL/6 background (Allam *et al.*, 2015). Mice were housed and bred at the University of Birmingham animal facilities. Heterozygous *Naip*$^{fl/\Delta}$ mice were bred to achieve *Naip*$^{\Delta/\Delta}$ and *Naip*$^{fl/fl}$ littermates which were used in experiments at around 8-10 weeks of age. In all experiments, treatment and genotype groups were littermates and cohoused, unless using STm and not treated groups in which case littermates were kept separate to avoid cross-over of STm. C57BL/6 (Charles River, UK) were also used in some experiments, and were housed at the University of Birmingham. Nr4a3-Timer ("Tocky") (Bending, Martín, *et al.*, 2018; Bending, Paduraru, *et al.*, 2018) crossed with Great-Smart ifng-YFP reporter (Price *et al.*, 2012) on a C57B/6 background, used for analysis of IFNy. In line with UK Home Office regulations, mice were maintained under a controlled 12-hour light/12-hour dark cycle and received food and water ad libitum.

2.1.2 Models of CRC, colitis and STm infection

2.1.2.1 AOM/DSS Colitis-Associated Cancer

Mice were injected i.p. on day 0 with azoxymethane (AOM) (10mg/kg; Sigma-Aldrich). On day 0 dextran sodium sulfate (DSS) (MW 36,000-50,500; APExBIO) was given in the drinking water (3%

wt/vol) for 6-7 days, followed by 14 days of normal water. This treatment was repeated twice, for a total of 3 rounds. Mice were weighed every day during DSS treatment and every other day for the following 7 days. Mice that reached 20% weight loss were sacrificed early and DSS was removed if mice reached 10% weight loss. Mice were sacrificed and colons and mesenteric lymph nodes were excised on day 62. Colons were washed and tumours were counted, measured using a dissecting microscope. Both tumours and surrounding colon tissue which appeared histologically healthy were excised, weighed, and the tumour-infiltrating and IELs were isolated, respectively, for analysis by flow cytometry. In some cases colons were fixed in 4% paraformaldehyde (Merck) for histological analysis.

2.1.2.2 Colitis

Acute colitis was induced using 3% (wt/vol) DSS in the drinking water for 6-7 days. Mice were weighed every day during DSS treatment and every other day for the following 6-7 days. Mice that reached 20% weight loss were sacrificed early and DSS was removed if mice reached 10% weight loss. Mice were sacrificed on day 13 and colons excised and washed. The proximal colon was frozen for ELISA analysis. IELs were isolated from the rest of the colon for flow cytometry analysis.

2.1.2.3 In vivo STm infection

To disrupt the colonic epithelial barrier, mice were administered 3% (wt/vol) DSS in the drinking water for 6-7 days. Mice were weighed every day during DSS treatment and every other day for the following 6-7 days. Mice that reached 20% weight loss were sacrificed early and DSS was removed if mice reached 10% weight loss. On day 12, mice were administered UF20 STm$^{\Delta aroA}$ mCherry :: Amp at a dose of 5x10^{9} CFUs (Hoiseth and Stocker, 1981; Gulig and Doyle, 1993). This bacterial strain has a deletion of the *aroA* gene, meaning it is auxotrophic for aromatic amino acids, thus attenuating it (Hoiseth and Stocker, 1981). STm was grown overnight in LB medium with 1:1000 ampicillin (Thermofisher), shaking at 37˚C. Bacteria were then sub-cultured 1:20 in LB until an OD600 = 0.7 –

0.9, indicating the logarithmic phase growth. Bacteria was then diluted in PBS to a final concentration of $5x10^{10}$, with 100µl administered to each mouse, resulting in a final dosage of $5x10^{9}$ CFUs. In STm dosing experiments, final concentrations of $5x10^{8}$, $5x10^{9}$, and $5x10^{10}$ were used. In some experiments, FTY720 (dose 1mg/kg mouse weight, Sigma-Aldrich), dissolved in water, was administered i.p. on day 12 to block lymph node egress. Mice were sacrificed 24 hours after STm administration, and colons, mesenteric lymph nodes and spleens were excised. Proximal colon, lymph nodes and spleens were used for CFU analysis. For ELISA analysis, some proximal colon was frozen, and some was weighed and resuspended in 100% Matrigel as described by Voabil *et al.*, 2021, topped up with Basic Media (see table 1) and stimulated with αCD3 (2µg/mL, BioLegend) and αCD28 (5µg/mL, BioLegend) antibodies**.** IELs and lymphocytes were isolated from distal colons and lymph nodes, respectively, which were then analysed by flow cytometry.

2.1.3 Lymphocyte Isolation

2.1.3.1 Intra-Epithelial (IEL) Lymphocyte Isolation

Colons and small intestines were opened longitudinally, washed in PBS and chopped into roughly 1cm pieces before digestion in dithiothreitol (DTT) (1mM, Thermofisher) for 40 mins, shaking at 37˚C. DTT acts as a reducing agent, helping to break apart the epithelial layer and thus allowing isolation of the IELs (Trapecar *et al.*, 2017). Samples were centrifuged and the supernatant discarded, before being resuspended in warm RPMI (Gibco) supplemented with 10% FCS (Gibco), 1x penicillin/streptomycin (Invitrogen), 1% L-glutamine (Invitrogen) in a 50ml Falcon. Samples were then shaken vigorously by hand and poured through a 100µM strainer. Colon or small intestine pieces were then resuspended in supplemented RPMI and the process repeated for a total of two shaking steps. The cell strainer was then washed completely with supplemented media and the colon pieces discarded. The flow through was centrifuged and the resulting pellet resuspended in 4ml of 36% percoll (Scientific Laboratory Supplies Ltd) in PBS. This was then carefully layered over 67% percoll in RPMI in a 15ml Falcon tube, and then centrifuged for 30min at 700g with no brake. IELs appear at the

interface between the two percoll layers. The IELs were gently aspirated using a Pasteur pipette, transferred to a 15ml Falcon and washed in supplemented RPMI, ready for downstream analysis.

2.1.3.2 Tumour-Infiltrating Lymphocyte (TIL) Isolation

Tumours were collected in tumour media (TM) consisting of ice-cold advanced DMEM-F12 (Gibco) containing 2% FCS (Gibco), 1x penicillin/streptomycin (Invitrogen), and 50µM β-mercaptoethanol (Merck) and minced into 2-4mm fragment using sterile scissors. Tumour pieces were then washed in TM and pelleted by centrifugation. To digest the tumours, pellets were resuspended in warm digestion buffer (DMEM-F12 (Gibco), 2.5% FCS (Gibco), 1x penicillin/streptomycin (Invitrogen), 0.1mg/ml DNAse (Roche), 1mg/ml Collagenase D (Roche)) and incubated for 30-45 mins at 37˚C, shaking at maximum speed on an orbital shaker. The digestion mixture was then passed through a 70µm cell strainer (BD falcon) and washed in FACS buffer, ready for analysis by flow cytometry.

2.1.3.3 Mesenteric Lymph Node (mLN) Lymphocyte Isolation

Lymph nodes were excised from mice and then mechanically disrupted through a 70µm strainer (BD falcon). Cells were washed with ice-cold PBS and then kept on ice ready for flow cytometry analysis.

2.1.3.4 Splenocyte Isolation

Spleens were excised from C57BL/6 mice and mechanically disrupted through a 70µm strainer (BD falcon). Red blood cells were lysed using ACK lysing buffer (Invitrogen) for 5 mins on ice. Splenocytes were again passed through a 70µm strainer and kept on ice until further use.

2.1.3.5 Epithelial cell isolation

Pieces of colon were washed in PBS with Y-27632 (ROCK inhibitor, 10mM), to preserve epithelial viability, and cut into approximately 1cm pieces. Tissue was then incubated for 20min at 37˚C with constant shaking on an orbital shaker in RPMI (Gibco) containing 2mM EDTA (Merck), 0.5mM DTT (Thermofisher) and Y-27632 (ROCK inhibitor, 10mM). Samples were then collected through a 70µM

filter and washed in excess RPMI with Y-27632 (ROCK inhibitor, 10mM). Cells were then pelleted and frozen at 20˚C for downstream tissue lysis and ELISA analysis.

2.2 Bacterial strains

Salmonella Typhimurium$^{\Delta aroA}$ strain SL3261 (STm$^{\Delta aroA}$, gifted by I. Henderson) or UF20 STm$^{\Delta aroA}$ mCherry :: Amp (gifted by Hidenori Matsui) were grown overnight in plain LB medium and LB containing 1:1000 ampicillin (Thermofisher), respectively, shaking at 37˚C. Overnight cultures were then used for sub-cultures for infection experiments.

2.3 ELISA

For determination of PGE_2 levels, organoid supernatants were collected 24hrs post-infection with STm and a competitive ELISA performed as per the manufacturer's instructions (R&D Systems).

For IFNγ (Invitrogen), IL-17A (Biolegend) and IL-10 (Biolegend) ELISAs frozen pieces of mouse colon were lysed in tissue lysis buffer (150mM NaCl (Sigma), 10mM Tris (Ph7.4, Sigma), 5mM EDTA (Merck), 1mM EGTA (ThermoFisher), 0.1% Nonidet P-40/Triton X (Sigma), cOmplete protease inhibitor cocktaill (Roche, 1:25)) on ice for 30 mins with regular shaking, then centrifuged and the supernatant collected. A BCA assay (Thermo Fisher) was performed on the supernatants to establish protein concentration and 400µg/ml used in the ELISA as per the manufacturer's instructions.

To determine TNFα production, proximal colon was weighed and embedded in 100% Matrigel in a 24 well plate, topped up with basic media (see table 2.1) and stimulated with αCD3 (2µg/mL, BioLegend) and αCD28 (5µg/mL, BioLegend) antibodies. After 24 hours, supernatant was collected and a TNFα ELISA (Invitrogen) was performed as per the manufacturer's instructions.

To determine IL-15/IL-15R expression on intestinal epithelial cells, normal and tumour colonic organoids were collected by dissolving the Matrigel by adding Cell Recovery Solution (Corning) and leaving at 4˚C for 1 hr. Samples were then collected and washed with PBS, centrifuged and the

supernatant discarded. For ex vivo samples, epithelial cells were isolated as described above. Pellets were then lysed in tissue lysis buffer (150mM NaCl (Sigma), 10mM Tris (Ph7.4, Sigma), 5mM EDTA (Merck), 1mM EGTA (ThermoFisher), 0.1% Nonidet P-40/Triton X (Sigma), cOmplete protease inhibitor cocktaill (Roche, 1:25)) on ice for 30 mins with regular shaking, then centrifuged and the supernatant collected. A BCA assay (Thermo Fisher) was performed on the supernatants to establish protein concentration and 350µg/ml used in the IL-15/IL-15R ELISA (Invitrogen) as per the manufacturer's instructions.

2.4 Organoids

2.4.1 Generation and Maintenance

Organoids were generated from *Naip*$^{fl/fl}$ or *Naip*$^{\Delta/\Delta}$ mice (fig. 2.1), using either normal colonic tissue from healthy mice, or using tumours from mice treated with azoxymethane and three rounds of dextran sulfate sodium (3% in drinking water for 7 days, 14 days normal water). Organoids were generated as previously described (Maslowski *et al.*, 2019), but briefly, tumours or healthy colon tissue was excised and washed in cold PBS. For normal tissue, longitudinally opened colon was incubated in 10mL chelation buffer (table 2.1) with 2mM EDTA (Merck) for 40 mins on ice. Then, tubes were shaken vigorously, the chelation buffer removed. Colons were laid out on a petri dish, mucosa side up and epithelial layer physically scraped off using a glass cover slip. Cells collected in PBS and transferred to a 50ml Falcon tube coated in FBS. For tumours organoid isolation, tumours were cut into small 1-2 mm fragments and incubated in digestion buffer for 30 mins, with tubes kept at 37˚C with shaking. For all tissues, supernatant was passed through a 70µM filter and cells were then pelleted and washed with Basic Medium. Cells were then pelleted again and resuspended in Matrigel (Corning) in 24 well plates. Organoids were fed with 500µL Normal Media. For tumour-derived organoids, media was changed to Tumour media once organoids were established, at first with ROCK Inhibitor (Y-27632) (5µM, Sigma). Media was changed every other day and once

established after 1-2 weeks, ROCK Inhibitor was removed from the tumour medium, as constitutive Wnt signalling in tumour cells means no exogenous Wnt ligands need adding for survival.

Organoids were split once a week for maintenance, at a ratio that depended on the current growth and density of the cells. This ratio was typically around 1:10-1:15 for tumour-derived organoids and 1:6 for normal organoids. Cell Recovery Solution (Corning) was used to dissolve the Matrigel for 1hr at 4˚C. All tubes and pipette tips were then coated in FCS, and cells were then transferred to 15ml falcon tubes. Cells were washed with excess Basic Media, centrifuged, supernatant discarded, and pellets resuspended in TrypLE (Gibco) to dissociate organoids to single cells. Tubes were incubated at 37 ˚C in a water bath for 5mins with regular agitation. To further ensure a single cell suspension cells were then manually disrupted using a 10µl pipette tip attached to a 1ml pipette tip coated in FCS and repeated pipetting. TryplE was then washed off with excess Basic Media and cells pelleted. Cells were resuspended in Matrigel and plated in a 24-well plate (50µl per well). Plates were put in an incubator at 37˚C for 5 mins to help set the Matrigel, then the corresponding media added.

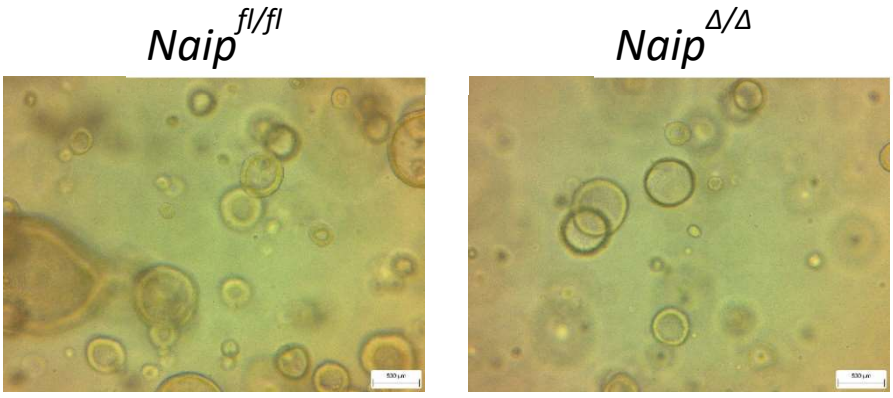

Figure 2.1 - Tumour-derived organoids

Naip$^{fl/fl}$ and *Naip*$^{\Delta/\Delta}$ tumour-derived organoids imaged 4-5 days post split. Bar for scale is 500µM.

2.4.2 Organoid Infection

Bacteria were sub-cultured 1:20 in LB and grown for approximately 1 hour until an OD600 = 0.7 – 0.9 was reached, indicating the logarithmic phase growth. Bacteria were then diluted in PBS to a final concentration of $1x10^8$ CFUs per 5µl (OD600 = 1 = $5x10^8$ CFU/mL). 5µl of the bacterial suspension were then added to the organoid media and incubated for 2hrs. To wash off the infection, media was aspirated and the Matrigel dome washed twice with PBS, before organoids were fed with their corresponding media, with the addition of Gentamycin (1:1000, Thermofisher). After 24hrs cells and supernatants were either collected for downstream assays, or cells were added for co-cultures.

2.4.3 Organoid Co-Cultures

2.4.3.1 RA-Induced Splenocytes

Splenocytes from C57BL/6 were isolated as described above and induced into an IEL-like state in a protocol adapted from Rogoz *et al.*, 2015. On day 0, 6-well plates were pre-coated overnight at 4˚C with αCD3 (2µg/mL, BioLegend) and αCD28 (5µg/mL, BioLegend) antibodies, diluted in PBS. This was then discarded on day 1 and splenocytes diluted in R10 media (RPMI (without glutamine, R&D Systems), 10% FCS (Gibco), 1% penicillin/streptomycin (Invitrogen), 1% Glutamax (Invitrogen), 1% HEPES (Invitrogen), 50µM β-mercaptoethanol (Merck)) at a concentration of $1x10^6$ cells/ml and 2ml added to each well of a 6-well plate. On day 3 retinoic acid (Sigma) was added to the splenocytes at a concentration of 1nM in DMSO. On day 4, splenocytes were washed with R10 media, centrifuged, and resuspended in R20 media containing retinoic acid at 1nM as before, as well as IL-2 (Biolegend) at 10ng/ml. After 2 days stimulation in media with IL-2 and retinoic acid cells were harvested, washed, and counted. To measure cell proliferation, cells were stained with CellTrace Blue (Thermo Fisher) as per the manufacturer's instructions. Briefly, cells were suspended in PBS at a concentration of $1x10^6$ cells/ml, and CellTrace Blue (diluted in DMSO) was added to a final concentration of 5µM. Cells were stained in complete darkness for 20mins and then washed in excess buffer containing at

least 1% FCS. Approximately 500,000 - 1 million splenocytes were then added to the media surrounding organoids in 30% Matrigel domes. 30% Matrigel allowed for entry of splenocytes into the dome. Normal or tumour organoid media was used, depending on the organoids, with an additional 10% FCS, and αCD3 (2µg/mL, BioLegend) to stimulate the T cells. In experiments where RA-induced splenocytes were not being cocultured they were kept in R10 media. Splenocytes were co-cultured with organoids for 48hrs then collected for flow cytometry analysis. Media surrounding the Matrigel was collected in FCS coated 15ml falcon tubes and kept on ice. Matrigel was dissolved using Cell Recovery Solution (Corning) at 4˚C for 1hr. The dissolved Matrigel was then combined with the corresponding media in the 15ml falcon tube to obtain lymphocytes that had remained in the medium or migrated into the Matrigel/organoids, washed with Basic Media and centrifuged. Pellets were then resuspended in TryplE (Gibco) and kept at 37˚C in a water bath for 5 mins with regular agitation. Cells were then manually disrupted using a 10µl pipette tip attached to a 1ml pipette tip coated in FCS and repeated pipetting, to achieve a single cell suspension. TryplE was washed off with excess Basic Media and cells pelleted. The cell pellet was resuspended in FACS buffer ready for staining and downstream analysis.

Table 2.1 - Buffers and Mediums used in organoid generation and maintenance.

Basic Medium	Advanced DMEM F12 (500mL; Life Technologies), Penicillin/Streptomycin (1:100; Invitrogen), Glutamax (1:100; Invitrogen), HEPES (1:100, Invitrogen)
2xN2/B27/NA Medium	N2 (200µL of 100x; Invitrogen), B27 (400µL of 50X; Invitrogen), NA (50µL of 500mM; Sigma) added to 10mL basic medium
Normal Medium	Basic medium + 2xN2/B27/NA (1:1), mNoggin (1:1000, Peprotech), mEGF (1:1000, Peprotech), Rspondin condition medium (1:20, generated in house (adapted from (Fujii *et al.*, 2015) using L cells gifted from the Claire Shannon-Lowe(UoB), A83-01 (1:1000, Tocris), Wnt Fc-fusion protein (0.1nM, Immunoprecise), Y-27632 (ROCK inhibitor, 10mM in PBS, use only for recovering frozen stock, or first establishing, Sigma)
Tumour Medium	Basic medium + 2xN2/B27/NA (1:1), mEGF (1:1000; Peprotech), Y-27632 (ROCK inhibitor, 10mM in PBS, use only for recovering frozen stock, or first establishing, Sigma)
Chelation Buffer	Na2HPO4 (5.6 mmol/L), KH2PO4 (8.0 mmol/L), NaCl (96.2 mmol/L), KCl (1.6 mmol/L), sucrose (43.4 mmol/L), D-sorbitol (54.9 mmol/L) and DL-dithiothreitol (0.5 mmo/L) in distilled water
Digestion Buffer	2.5% FBS (Sigma), Penicillin/Streptomycin (1:100; Invitrogen), collagenase D (400µL; Sigma), Dispase (25U/mL; BD Biosciences) in Advanced DMEM F12 (Life Technologies)

2.4.3.2 Splenocyte Co-cultures

Organoids at 4-5 post-split were either not-treated or infected with STm, as described above, and the media collected and filtered through 0.2µm filters (Thermo Fisher). 1 million splenocytes, isolated as described previously, were added to this organoid-conditioned media and stimulated with αCD3 (2µg/mL, BioLegend) and αCD28 (5µg/mL, BioLegend) antibodies. After 24hrs cells were harvested, washed, and resuspended in FACS buffer.

2.4.3.3 IFNγ stimulation

Organoids were stimulated with recombinant mouse IFNγ (BioTechne) at 10ng/ml by adding to the media surrounding the Matrigel dome. Organoids were then left for 1hr, 24hrs or 48hrs, depending on the experiment, before cells were harvested.

2.4.4 CFU analysis

2.4.4.1 Organoid CFU analysis

Following STm infection of organoids, Matrigel was dissolved using Cell Recovery Solution (Corning) and incubating at 4˚C for 1hr. Cells were then washed with Basic Media, centrifuged and the supernatants discarded. Pellets were resuspended in 100µL Triton X-100 (0.1% in PBS, Sigma) and manually homogenised. This solution was then diluted 1:10 and 1:100 and plated on LB agar plates. For $STm^{\Delta aroA}$ (SL361) LB plates without antibioticswere used, for $STm^{\Delta aroA}$ mCherry LB plates containing 1:1000 Ampicillin were used. Plates were incubated at 37˚C (no CO2) overnight and colonies counted the following day.

2.4.4.2 Ex vivo CFU analysis

Portions of the proximal colon, spleens and mLNs were weighed and subsequently added to 2ml round-bottom tubes containing Triton X-100 (0.1% in PBS, Sigma) and two 5mm stainless steel beads (Qiagen, CAT# 69989). Samples were then homogenised using a TissueLyser II homogeniser (Qiagen, CAT# SM100250-1) at max speed for 3 mins. This was then plated neat onto LB agar plus Ampicillin (1:1000) plates which were incubated at 37˚C (no CO2) overnight and colonies counted the following day. CFUs were calculated per gram of tissue.

2.5 Flow Cytometry Analysis

2.5.1 General staining

For extra-cellular staining, cells were transferred to 96-well round bottom plates and washed in FACS buffer (PBS, 2% FCS (Gibco), 2mM EDTA (Merck), 0.01% sodium azide (Sigma)) and centrifuged for 5

mins at 400g. The supernatant was then discarded, and the cells resuspended in antibody master mix. Antibody master mixes contained eFluor 780 Fixable Viability Dye (1:1000, Invitrogen) and Fc block (1:500, gifted by Prof. Anne Cooke, University of Cambridge) as well as the appropriate antibodies (table 2.2) in FACS buffer. Cells were stained for 30 mins at 4˚C, protected from light, and then washed in FACS buffer and transferred to 5ml polystyrene tubes, ready for analysis on a BD Fortessa X20. For in vivo experiments, 20µl of Molecular Probe Accucheck Counting Beads (Thermo Fisher) were added to tubes prior to acquiring. For single stains, UltraComp eBeads (Invitrogen) and unstained cells were used.

2.5.2 Intracellular staining

For intracellular staining, following extracellular staining, cells were pelleted and resuspended in fixative from the eBioscience Foxp3/Transcription Factor Staining Buffer Set (Invitrogen) for 30 mins at 4˚C, protected from light. The fixative was then washed and discarded, and cells were washed in FACS buffer, and then washed in permeabilization buffer from the Staining Buffer Set. Cells were subsequently resuspended in the relevant antibody master mix made up in in permeabilization buffer and stained for 30-60 mins at 4˚C, protected from light. Cells were then washed in permeabilization buffer, and then in FACS buffer, ready for analysis,

2.5.3 Phospho-flow

To stain phosphorylated proteins, cells were stained for viability, as described above, then transferred to 5ml polystyrene tubes and washed twice with PBS. Cells were resuspended in 1:1 Fixation Buffer (Biolegend) diluted in PBS, comprising ~2% PFA, and incubated at 37˚C from 10 mins. Cells were then centrifuged at 1000xg for 5 mins and fixative discarded, and then washed twice with PBS containing 2% FCS. Cell pellets were then vortexed and resuspended in 1ml TruePhos Fixation Buffer (Biolegend) by adding dropwise with constant vortexing. Samples were then kept overnight at -20˚C. Cells were then centrifuged and fixation buffer discarded and washed a further two times with

PBS containing 2% FCS. Finally, cells were stained with phospho-antibodies (see table 2.2) for 30-45 mins, protected from light, and then washed with PBS containing 2% FCS, ready for flow analysis.

2.5.4 Epithelial flow

For flow analysis of colonic organoids, Matrigel was dissolved using Cell Recovery Solution (Corning) for 1hr at 4˚C. Cell Recovery Solution was then washed off with Basic Media (see table 2.1) containing ROCK Inhibitor (Y-27632) (5µM, Sigma). Cells were then centrifuged, supernatant discarded, and pellets resuspended in 500µl TryplE (Gibco) containing ROCK Inhibitor (Y-27632) (5µM, Sigma) and incubated at 37˚C in a water bath for 5 mins with regular agitation. Cells were then transferred onto ice and a further 500µl of Basic Media plus ROCK inhibitor was added to dilute the TryplE. Cells were then manually disrupted using a 10µl pipette tip attached to a 1ml pipette tip coated in FCS and repeated pipetting, to achieve a single cell suspension. Cells were then washed in excess Basic Media containing ROCK inhibitor. Cells were then kept on ice and during staining ROCK inhibitor was added to FACS buffer at a concentration of 5µM.

2.5.5 Analysis of flow cytometry data

Data were exported from FACSDiva (version 7; BD Biosciences) as flow cytometry standard files (FCS) and analysed with Flow Jo (version 10.7.1, BD Biosciences). Populations were gated first on forward scatter (FSC) and side scatter (SSC) profiles, then doublets were excluded by gating on forward scatter area versus height (FSC-A and FSC-H). Live cells were then gated using APC-Cy7 signal from eFluor-780 Fixable Viability Dye (Invitrogen) against FSC-A. Gating strategies then depended on specific experiments, using antibodies referred to in table 2.2. The absolute number of cell populations was established using AccuCheck Counting Beads (Thermofisher) and the following equation:

$$Number\ of\ counting\ beads\ per\ \mu l\ \times \frac{number\ of\ cells\ counted}{total\ number\ of\ beads\ counted} = absolute\ count\ (\frac{cells}{\mu l})$$

This was then multiplied by the total volume of the sample to calculate the number of cells per colon or small intestine. Fluorescence minus one (FMO) controls were used for gating.

2.5.5.1 Intraepithelial, lamina propria and tumour-infiltrating lymphocyte populations

The standard gating strategy for Intraepithelial/lamina propria lymphocyte populations is shown in figure 2.1. The exact antibodies used in the panel varied depending on if any functional markers were being added to the standard subset-defining panel (table 2.2). The standard gating strategy consisted of selecting live cells, as described above, followed by CD45+CD3+ T cells. T cells were then gated into TCRαβ and TCRγδ. TCRαβ+ cells were then gated on CD4+, to give the TCRαβCD4 population and CD8α+. The latter was then divided into those that were both CD8α+ and CD8β+ (TCRαβCD8αβ) and only CD8α+ (TCRαβCD8αα). TCRγδ cells were then gated on CD8α+ and CD8β+ expression, giving rise to TCRγδCD8αβ and TCRγδCD8αα populations, and on CD4, giving the TCRγδCD4 subset. Of note, TCRγδCD8αβ and TCRγδCD4 were only present and therefore only gated on in tumour samples. Functional markers, such as CD69 and CD103, were gated on against FSC-A within each subset.

For staining of Treg populations within intraepithelial and tumour infiltrating lymphocyte samples, a second panel was used (fig. 2.2). Again, cells were gated on live cells followed by CD45+CD3+. Cells were then gated on CD4 expression, with CD4+ cells then divided into CD25+FoxP3-, CD25-FoxP3+ and CD25+FoxP3+ cells. Each subset was then gated on CTLA4 and PD1.

2.5.5.2 Mesenteric lymph node populations

Mesenteric lymph node samples (gating strategy in fig. 2.3) were initially gated as described above to exclude doublets and then gated on live cells (viability dye negative) and CD3 positive cells. These were divided into CD4+ and CD8α+ cells before gating on functional markers. Gating on single positive and double positive CD69 and CD25 cells was used to assess activation. Gating on CD62L and CD44 was used to distinguish naïve T cells (CD44-CD62L+), effector T cells (C44+CD62L-) and T central memory cells (CD44+CD62L+).

2.5.5.3 RA-induced splenocyte panels

Two panels were used on RA-induced splenocytes. The first involved gating out doublets and selecting live cells as described above. Cells were then gated on CD4 and CD8α and each of these populations gated on LPAM1, CCR9 and CD103. The second panel (fig. 2.4) was similar, but the CD4+ and CD8+ subsets were instead interrogated for CellTrace Blue signal. A gate was drawn after the highest (strongest signal) peak to distinguish between CellTrace Blue Hi and Lo populations.

Table 2.2 - Antibodies used for flow cytometry staining

Target	Clone	Conjugate	Catalogue #	Manufacturer	Dilution	Panel
Live/ Dead	-	Dye – APC Cy7	65-0865-14	Invitrogen	1:1000	All
CD3	17A2	FITC	100203	Biolegend	1:100	IEL/LPL/TIL, CellTrace
CD3	145-2C11	BUV395	563565	BD Biosciences	1:100	mLN
CD3	17A2	AlexaFluor 700	100215	Biolegend	1:100	RA
TCRγδ	GL3	APC	118115	Biolegend	1:100	IEL/LPL/TIL
TCRγδ	GL3	BV421	118119	Biolegend	1:100	CellTrace
TCRβ	H57-597	BV421	109229	Biolegend	1:100	IEL/LPL/TIL
TCRβ	109207	PE	H57-597	Biolegend	1:100	CellTrace
CD45	30-F11	BUV395	564279	BD Biosciences	1:200	IEL/LPL/TIL, RA
CD45	30-F11	FITC	103107	Biolegend	1:200	IEL/LPL/TIL
CD45	30-F11	APC	103111	Biolegend	1:200	CellTrace
CD8β	YTS156.7.7	PE	126607	Biolegend	1:200	IEL/LPL/TIL CellTrace
CD8α	53-6.7	PE Cy7	100721	Biolegend	1:200	IEL/LPL/TIL, CellTrace, RA
CD8α	53-6.7	AlexaFluor 700	100729	Biolegend	1:200	mLN
CD4	RM4-5	BUV737	612844	BD Biosciences	1:200	IEL/LPL/TIL
CD4	GK1.5	BV421	100437	Biolegend	1:200	mLN, RA

Ki67	16A8	APC	652405	Biolegend	1:100	IEL
CD62L	MEL-14	FITC	104405	Biolegend	1:100	mLN
CD44	IM7	PECy7	103029	Biolegend	1:100	mLN
CD69	H1.2F3	APC	104513	Biolegend	1:100	mLN, Treg
CD25	PC61	PE	102007	Biolegend	1:100	mLN
CD103	2E7	BV605	121433	Biolegend	1:100	Treg
CD103	2E7	PE	121405	Biolegend	1:100	RA
CCR9	9B1	FITC	129705	Biolegend	1:100	RA
LPAM1	120607	APC	DATK32	Biolegend	1:100	RA
I-A/I-E	M5/114.15.2	PE Cy7	107629	Biolegend	1:200	IFN
H-2	M1/42	FITC	125507	Biolegend	1:200	IFN
CD80	16-10A1	BV421	104725	Biolegend	1:100	IFN
IFNγR	MOB-47	PE	113603	Biolegend	1:100	IFN
CD1d	1B1	FITC	123507	Biolegend	1:100	IFN
PD-L1	10F.9G2	Dazzle	124324	Biolegend	1:100	IFN
pSTAT1 ser727	A15158B	AlexaFluor 647	686411	Biolegend	1:50	IFN
pSTAT1 Tyr701	58D6	PE	8062S	Cell Signalling	1:50	IFN
pERK	4B11B69	AlexaFluor 647	12-9715-42	Biolegend	1:50	IFN
pAkt	SDRNR	PE	12-9715-42	Invitrogen	1:50	IFN
pmTOR	MRRBY	PE Cy7	25-9718-42	Invitrogen	1:50	IFN

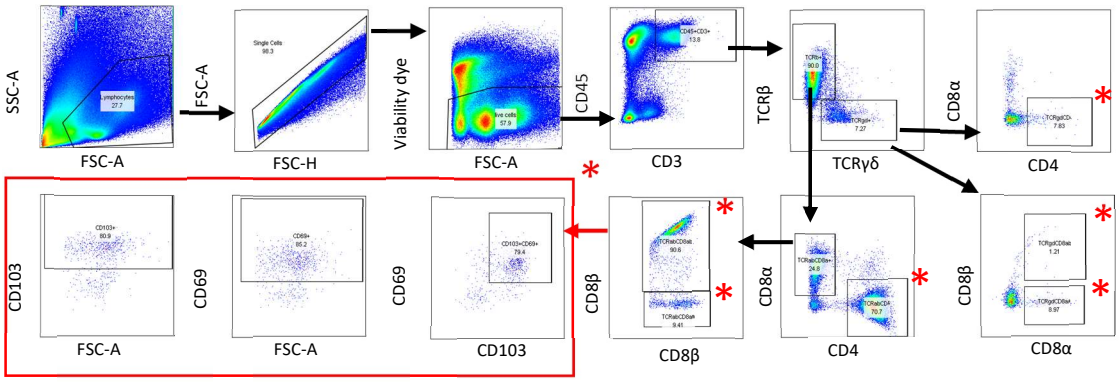

Figure 2.2 – Gating strategy for intraepithelial, lamina propria and tumour infiltrating lymphocytes with example functional markers

Samples from colons, small intestines and tumours were gated based on forward (FSC) and side scatter (SSC) profiles, then doublet gated out. Live cells were gated on negative eFluor-780 Fixable Viability dye staining. T cells were gated on CD45+CD3+ cells followed by TCR type. Individual subsets were then gated based presence of CD8α, CD8β and CD4. If functional markers were also being assessed, these were gated within each subset, as indicated by the red asterisk.

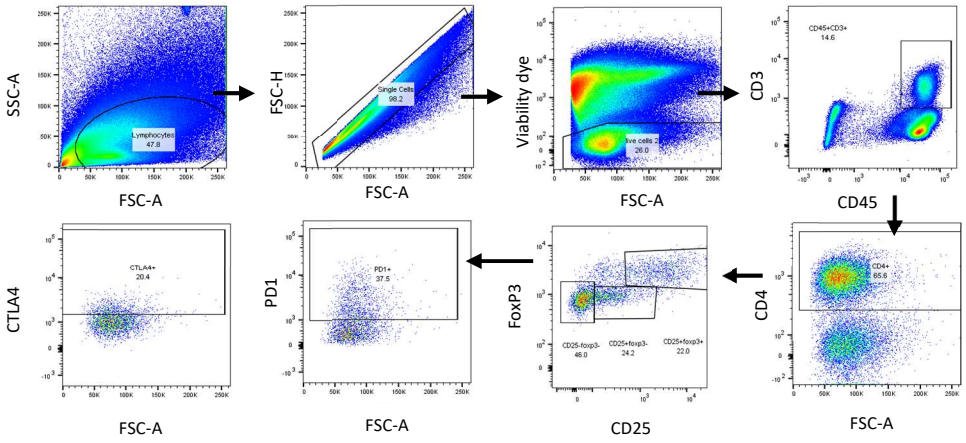

Figure 2.3 - Gating strategy for regulatory T cell populations

Samples from colons and tumours were gated based on forward (FSC) and side scatter (SSC) profiles, then doublet gated out. Live cells were gated on negative eFluor-780 Fixable Viability dye staining. T cells were gated on CD45+CD3+ cells followed by CD4+. CD4 T cells were then gated based on expression of FoxP3 and CD25 and the subsequent populations gated on functional markers CTLA4 and PD1.

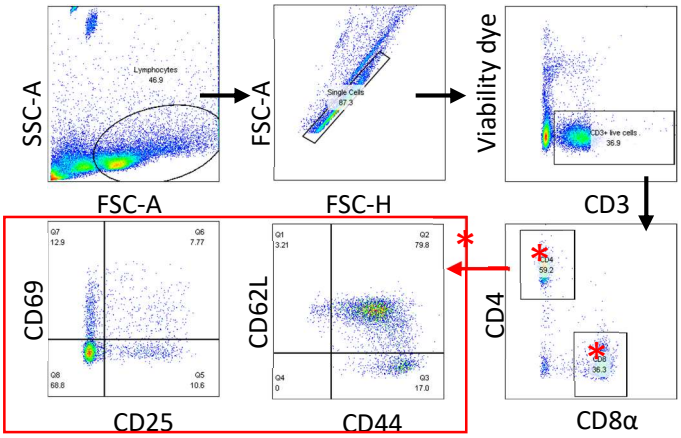

Figure 2.4 – Gating strategy for mesenteric lymph nodes

Mesenteric lymph node samples were gated based on forward (FSC) and side scatter (SSC) profiles, then doublet gated out. Live T cells were gated on negative eFluor-780 Fixable Viability dye staining and positive CD3 staining. T cells were divided into CD4+ and CD8α + groups before beings gated on functional markers. CD62L and CD44 were used to detect resident memory cells and CD25 and CD69 were used to assess activation.

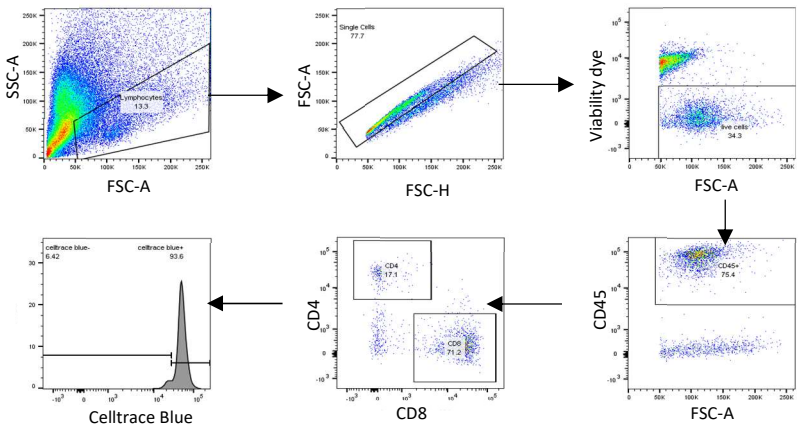

Figure 2.5 – Gating strategy for RA-induced splenocytes

Following co-culture, RA induced splenocytes were gated based on forward (FSC) and side scatter (SSC) profiles, then doublet gated out. Live T cells were gated on negative eFluor-780 Fixable Viability dye staining and epithelial cells gated out using CD45. Cells were then gated on CD4 and CD8α. Within these populations a CellTrace Blue Hi (+) and Lo (-) population was gated.

2.5.6 RNA extraction, RNAseq and qRT-PCR

2.5.6.1 RNA extraction

Organoids were harvested for RNA by addition of 350µL of RNA lysis buffer (Macherey Nagel) to the well, dissolving the Matrigel. This was collected and either stored at -20˚C or RNA isolated immediately. Total RNA was isolated using the Nucleospin RNA II kit (Macherey Nagel) as per the manufacturer instructions. RNA was eluted with 40µL of RNAse-free dH20 and stored at -20˚C short term or -80˚C long term.

2.5.6.2 RNAseq

Using RNA prepared as described above, quality analysis was performed, and libraries were prepared by Genomics Birmingham. Libraries were sequenced using the NextSeq 500 using a Mid 150v2.5 flow cell. Cluster generation and sequencing was performed and FASTQ files generated. FASTQ files were downloaded from the Illumina base space and then uploaded to the BlueBee cloud for subsequent analysis (Lexogen). FASTQ files were merged to generate final FASTQ files which were loaded onto the BlueBee QuantSeq FWD pipeline and aligned to the GRCm38 (mm10) genome. HTSeq-count v0.6.0 was used to generate read counts for mRNA and mapping statistics. Raw read counts in .txt format were used for DESeq2 analysis (Love, Huber and Anders, 2014) in R version 4.0. As described in the appendix (section 8, notes on the code are denoted using a #), by combining the raw read count matrix and a table of the data categories (here called coldata), a DESeq dataset was created. Genes with fewer than 10 reads across all samples were then removed using code described in appendix section 8.1. Log2 fold change estimates were generated using the DESeq algorithm. To generate a PCA plot, the rlog function was used to normalise the data as described in appendix section 8.1.1. In order to generate a list of differentially expressed genes (DEGs) as described in appendix section 8.1.2, log2 fold changes were shrunk using the ashr algorithm (Stephens, 2017). DEGs were selected with an adjusted p value of < 0.05, and gene lists filtered to identify genes with an estimated lfc greater or less than 1.5. Normalised read counts were transformed using the

regularised log (rlog) transformation. Genes were then assigned their ENSEMBL gene IDs and names using the mouse (*Mus musculus*) dataset. From this, KEGG pathway analysis was performed using the clusterProfiler (Yu *et al.*, 2012), DOSE(Yu *et al.*, 2015) , and biomaRt (Durinck *et al.*, 2009) packages. To identify changes in eicosanoid related genes, a gene list was generated from WikiPathways (Martens *et al.*, 2021), combining genes involved in the pathways of eicosanoid metabolisms via cytochrome P450 monooxygenases (WP4349), lipoxygenases (LOX) (WP4348) and cyclooxygenases (COX) (WP4346) in *Mus musculus*. This list was then merged with the list of significantly altered DEGs, so that only genes which were both significantly altered in expression, and which were on the list of eicosanoid-related gene list were kept. From this data set heatmap analysis was performed using the R package pheatmaps (Kolde, 2019) as described in appendix section 8.2. To generate a volcano plot, the original list of significantly altered DEGs was analysed using ggplot2, part of the Tidyverse package (Wickham *et al.*, 2019), as described in appendix section 8.3. Gene name labels and colours were then added to the plot.

2.5.6.3 qRT-PCR

To prepare cDNA, a 5X RT Buffer, Oligo DT, Reverse Transcriptase, dNTPs and RNAsin (all Promega) were used with a Prime Thermal Cycler (45˚C 40mins, 80˚C 10mins, 4˚C hold) (Techne). qPCR was performed using QuantStudio 5 384-well PCR system (CAT# A28140) and SYBR Green (Applied Biosystems). Primers used are described in table 2.3, with m18s used as a housekeeping gene.

Table 2.3 – Primers used for qRT-PCR

Target gene	Primer sequence
mNaip (universal)	F-AACTCAGAGAGATTGAGTTTTCTGGAC, R-CCTGAGAGAACCCAGAGCCTG
Ptgs1	F-GAGCGGGAATAGTAGGCACC , R- ACAAAAGCATGGGCAGTTACG
Ptgs2	F- CCTGGTGAACTACGACTGCT, R- ATTTAGTCGGCCTGGGATGG
cPla2	F- CACTCACCAAGGCCATTATCAT, R- GAGCTGATGTTTGCAGATTGG
mCTIIA	F-AAGCAGGACAGAAGCCTCAGAA , R -GCTTCCTGTGCTTTGAGTCCAT
m18s	F- GATCCATTGGAGGGCAAGTCT, R- CCAAGATCCAACTACGAGCTTTT

2.5.7 Liquid Chromatography/Mass Spectrometry (LC/MS) for Eicosanoids

Following organoid co-culture, as described above, supernatants were collected, filtered through 0.2µm filters, and frozen at -80˚C. Samples were then sent to Prof Valerie O'Donnell and Dr Victoria Tyrrell at The University of Cardiff, where LC/MS was performed, and data analysed.

2.5.8 Statistical Analysis

Data analysis was performed using GraphPad Prism software (version 9.4.1; GraphPad Software Inc., USA). All data are expressed as mean ± standard error of the mean (SEM) unless otherwise stated. Either unpaired t-test, one-way or two-way ANOVA with Tukey's or Sidak's post-test was used. In all cases a p-value of <0.05 was considered statistically significant.

3 The effect of Naips on Eicosanoids

3.1 Introduction

The eicosanoid family includes a broad range of signalling molecules with a variety of functions in health and disease. Prostaglandins, leukotrienes, hydroxyeicosatetraenoic acids (HETEs), epoxyeicosatrienoic acids (EETs), hydroperoxyeicosatetraenoic acids (HPETEs) and thromboxane are all produced from the precursor arachidonic acid (see fig. 1.5) (Wang and DuBois, 2010a). Prostaglandins in particular have been implicated in homeostasis as well as disease of the gut (Dey, Lejeune and Chadee, 2006; Wang and DuBois, 2010a; Kawahara *et al.*, 2015). Colitis is known to be exacerbated by NSAIDs (Montrose *et al.*, 2010; Peng *et al.*, 2017), a class of drug which inhibit the cyclooxygenases which generate prostaglandin precursors, and deletion of enzymes involved in prostaglandin synthesis increases inflammation following DSS treatment (Montrose *et al.*, 2010). There may also be a link between innate signalling and PGE_2 in colitis, as exacerbated disease caused by MyD88 deletion can be alleviated by treatment with PGE_2 (Brown *et al.*, 2007). TLR4 signalling has also been suggested to increase COX2 expression or trigger repositioning of stromal cells expressing COX2 to the intestinal crypt base (Fukata *et al.*, 2006; Brown *et al.*, 2007). Prostaglandins are also implicated in CRC, with COX2 upregulated in 90% of carcinomas and 50% of adenomas and associated with poor survival (Ogino *et al.*, 2008; Wang and DuBois, 2013). PGE_2 has been shown to promote cancer stem vells via MAPK and PI3K/Akt pathways (Qiu *et al.*, 2010; Moon *et al.*, 2014; Wang *et al.*, 2015; Roulis *et al.*, 2020), promote growth and inhibit apoptosis (Tsujii and DuBois, 1995; Sheng *et al.*, 1998; Ko *et al.*, 2002; Pai *et al.*, 2002; Castellone *et al.*, 2005), and support tumour angiogenesis (Seno *et al.*, 2002; Wang and DuBois, 2010a; Cherukuri *et al.*, 2014). Whilst PGE_2 is the most studied of the eicosanoids, others have been implicated in these diseases - $PGF_{2\alpha}$, PGD_2, 12-HETE, 15-HETE and LTB4 have all been found to elevated in colitis (Ferrer and Moreno, 2010). The leukotrienes and PGD_2 have been linked with CRC progression and poor prognosis.

Eicosanoids also have known roles on the immune compartment. PGE_2 has been demonstrated to have concentration-specific effects on T cells, with nanomolar concentrations supporting Th1 and Th17 differentiation and micromolar concentrations suppressing T cell activity (Sreeramkumar, Fresno and Cuesta, 2012b).

Naip knockout mice have previously been shown to be protected from colitis and more susceptible to CRC (Allam *et al.*, 2015) and Naip activation by STm is known to result in PGE_2 release (Rauch *et al.*, 2017). Originally, this effect was ascribed to peritoneal macrophages, and thought to be due to caspase-1 mediated Ca^{2+} influx which activated $cPLA_2$ (Moltke *et al.*, 2012). However, more recently it was shown that Naip-mediated PGE_2 release occurs in the IECs, with intestinal organoids being used to demonstrate this (Rauch *et al.*, 2017). Organoids are a useful tool in studying the epithelial-specific effects of Naip knockout and other conditions. Organoids are established from Lgr5+ stem cells, normally residing at the base of intestinal crypts, which are isolated and then generate epithelial domains resembling the villus, containing all expected differentiated cell types (Sato *et al.*, 2009; Barker *et al.*, 2010). This has proved a useful tool in the study of colorectal cancer, including immune cell cocultures and the generation of patient-derived organoids (Cantrell and Kuo, 2015; Yuki *et al.*, 2020).

While the epithelial-intrinsic functions of Naips are now well described, how the immune compartment is affected by *Naip* epithelial knockout remains to be studied. Naips have been noted to have reduced expression in colorectal tumours in both mice and humans (Endo *et al.*, 2004; Allam *et al.*, 2015). Given the varied literature on eicosanoids role in modulating immune function and intestinal disease outcome, we first hypothesised that changes in eicosanoids due to Naip knockout could be influencing the IELs. Here, we found that tumour-derived $Naip^{\Delta/\Delta}$ organoids have reduced PG expression at baseline as well as in response to STm infection, and therefore aimed to establish what effects this might have on the immune compartment.

In this chapter we aimed to:

- Confirm that STm-induced PGE_2 was reduced by Naip knockout
- Identify any other changes in eicosanoids and genes related to their synthesis
- To assess how altered PG/eicosanoid expression affected T cell responses

3.2 Results

3.2.1 Expression of prostaglandin E_2 and eicosanoid-related genes are reduced in *Naip*$^{\Delta/\Delta}$ tumour-derived organoids

Activation of Naips in IECs has previously been shown to result in PGE_2 release (Rauch *et al.*, 2017). To confirm this was the case in our *Naip*$^{\Delta/\Delta}$ tumour-derived organoids, we analysed the PGE_2 levels of supernatant from *Naip*$^{fl/fl}$ and *Naip*$^{\Delta/\Delta}$ tumour-derived organoids by ELISA (fig 3.1). Note that in this chapter, all organoids used are tumour-derived. To investigate if there were any changes to PGE_2 levels at baseline in the absence of Naips, organoids were either not-treated or infected with STm to activate the Naip pathway. *Naip*$^{fl/fl}$ organoids expressed similar levels of PGE_2 in both non-treated and STm-infected groups, with a modest (non-significant) increase following STm infection. The increase in PGE_2 following STm infection varied between experiments, sometimes showing an increase and sometimes not, resulting in this slight trend. PGE_2 has been reported to be release following Naip activation in the literature (Rauch *et al.*, 2017), so this variability may be due to the ELISA kit itself. In contrast, PGE_2 concentration was greatly diminished in supernatants from *Naip*$^{\Delta/\Delta}$ organoids, regardless of treatment. PGE_2 is one of many eicosanoids, generated by a complicated, multi-enzyme pathway (fig. 1.5) (Smyth *et al.*, 2009). To determine whether this reduction in PGE_2 reflected a reduction in the enzymes responsible for its synthesis, qPCR was performed on the *Naip*$^{fl/fl}$ and *Naip*$^{\Delta/\Delta}$ tumour-derived organoids, which were either not-treated or infected with STm (fig. 3.2). Firstly, knock-out of *Naip* was confirmed using a universal *Naip* primer which recognises all murine *Naip* isoforms (fig 3.2a). *Naip*$^{\Delta/\Delta}$ organoids showed no expression of *Naip*. Next, expression of enzymes involved in eicosanoid synthesis were assessed. These include cyclooxygenase 1 (Cox1) (*Ptgs1*) and cyclooxygenase 2 (Cox2) (*Ptgs2*), which catalyse the conversion of arachidonic acid (AA) to prostaglandin H_2 (PGH_2), prostaglandin E synthetase 1 (*Ptges1*) and 2 (*Ptges2*), which convert PGH_2 to PGE_2, and cytosolic phospholipase A2 (cPLA2, *Pla2g4a*) which performs the initial step of liberating

AA from the plasma membrane (fig 3.2b-e). There were no significant differences in *Pla2g4a* across any conditions, although expression seemed slightly reduced in *Naip*$^{\Delta/\Delta}$ organoids. *Ptgs1*, normally constitutively expressed as seen in *Naip*$^{fl/fl}$ organoids, showed minimal expression in *Naip*$^{\Delta/\Delta}$ organoids. In *Naip*$^{fl/fl}$ organoids *Ptgs1* was upregulated in response to STm infection, but this effect was lost in *Naip*$^{\Delta/\Delta}$ organoids. *Ptgs2*, however, was expressed at a similar level across all conditions, at a relatively high abundance. Both *Ptges1* and *Ptges2* appeared to be upregulated in response to STm in *Naip*$^{fl/fl}$ organoids, although this was not statistically significant. In contrast, in *Naip*$^{\Delta/\Delta}$ organoids both *Ptges1* and *Ptges2* appeared slightly reduced following STm infection. However, only the reduction in *Ptges1* seen in *Naip*$^{\Delta/\Delta}$ STm-treated organoids compared to *Naip*$^{fl/fl}$ STm-treated organoids was statistically significant. Together, this data demonstrates that *Naip*$^{\Delta/\Delta}$ tumour-derived organoids have reduced PGE_2 expression, consistent with previously published literature (Rauch *et al.*, 2017), and fundamental dysregulation of eicosanoid synthesis genes. Whilst there may be some tumour-specific regulation of the eicosanoid pathway, since these experiments were performed in tumour-derived organoids, other data from our lab has shown that *Naip*$^{\Delta/\Delta}$ tumour-derived organoids are unable to express PGE_2 following a range of stimuli which are independent of Naips (data not shown), leading us to hypothesise that Naips could have an as-yet undefined role in regulating gene expression. However, we decided that elucidating this role was outside of the remit of this thesis. Instead, we focused on whether altered PGE_2 production by *Naip*$^{\Delta/\Delta}$ organoids would affect T cell behaviour.

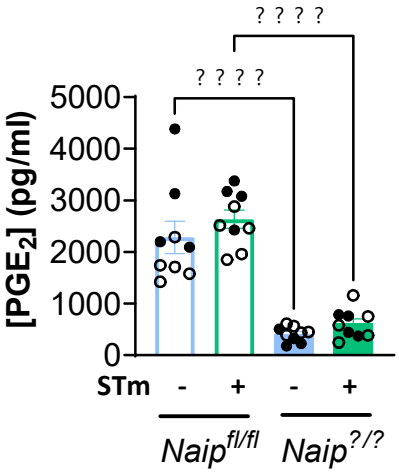

Figure 3.1 - Production of PGE_2 is reduced in tumour-derived $Naip^{\Delta/\Delta}$ organoids

Naip$^{fl/fl}$ and *Naip*$^{\Delta/\Delta}$ tumour-derived organoids were either infected with STm ΔaroA or given PBS as a control. Supernatant was collected after 24hrs and assayed for PGE_2 content by ELISA. Each individual point indicates the average of two technical replicates, derived from an individual well of organoids (i.e., a biological replicate), performed over two independent experiments. Point style indicates which of the two independent experiments it was performed in. One-way ANOVA statistical analysis was performed with Tukey's post-test. ****=P<0.0001.

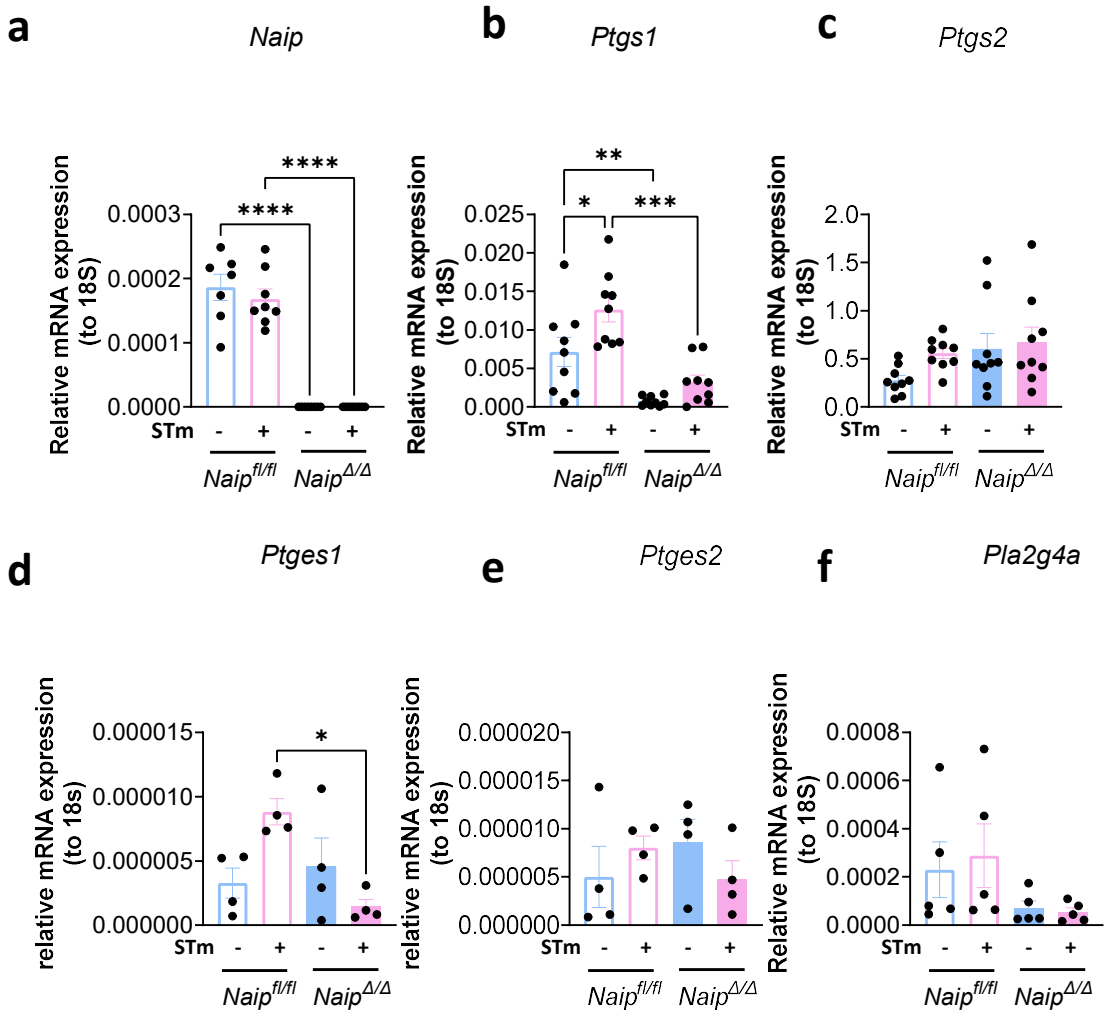

Figure 3.2 - Expression of certain genes related to eicosanoid production are reduced in Naip$^{\Delta/\Delta}$ organoids

Naip$^{fl/fl}$ and *Naip*$^{\Delta/\Delta}$ tumour-derived organoids were infected with STm ΔaroA or PBS control. RNA was extracted from organoids, converted to cDNA, and relative expression of genes determined by qPCR. **a** – Universal *Naip* primer confirmed *Naip* knockout. **b-f** - Expression of eicosanoid biosynthesis genes including those encoding COX1 (*Ptgs1*) (**b**) and COX2 (*Ptgs2*) (**c**), Prostaglandin E synthetase 1 and 2 (*Ptges1* and *Ptges2*) (**d-e**) and cytosolic phospholipase A2 (*Pla2g4a*) (**f**). All expression levels are shown relative to housekeeping gene 18S. Each point indicates the average of two technical replicates, derived from an individual well of organoids (i.e., a biological replicate), performed over multiple independent experiments. One-way ANOVA statistical analysis was performed with Tukey's post-test. * = P<0.05, **=P<0.01, ***=P<0.001, ****=P<0.0001.

3.2.2 Coculture of splenocytes with supernatant from STm infected *Naip*$^{\Delta/\Delta}$ organoids leads to decreased IFNγ expression

To understand the effect of reduced prostaglandin expression on T cells, we cultured splenocytes from Nr4a3-Tocky-*Ifng*-YFP mice with supernatant from *Naip*$^{fl/fl}$ and *Naip*$^{\Delta/\Delta}$ organoids. As Naips respond to STm, and recognition of STm by Naips has previously been reported to result in PGE_2 release (Rauch *et al.*, 2017), the effect of STm infection was also assessed. As shown in fig. 3.4a, *Naip*$^{fl/fl}$ and *Naip*$^{\Delta/\Delta}$ organoids were infected with STm$^{\Delta aroA}$ for 2hrs, and then washed and media replaced, with gentamycin added to kill any extracellular bacteria. At this stage either ibuprofen (Ibu), which inhibits COX enzymes and therefore PGE_2 production, or PGE_2 was added. As *Naip*$^{\Delta/\Delta}$ organoids expressed reduced PGE_2 (fig. 3.1), PGE_2 was added to establish whether this would mimic the untreated *Naip*$^{fl/fl}$ condition, whereas Ibu was added to *Naip*$^{fl/fl}$ to determine if this mimicked the effect of *Naip* knockout. After 24hrs supernatant was collected and used to coculture splenocytes from Nr4a3-Tocky-*Ifng*-YFP mice for 24hrs, in the presence of αCD3 and αCD28 stimulation, before flow cytometry analysis of IFNγ and CD69 expression. In this short time frame (24hrs), we exclusively looked at activation markers rather than polarisation markers, despite the fact PGE_2 has been shown to effect polarisation, as we would not expect changes in polarisation to occur within this timeframe. Nr4a3-Tocky-*Ifng*-YFP mice were utilised primarily for the YFP-*ifng* reporter, although the Tocky TCR activation readout was also measured but showed no changes across different conditions (data not shown). CFUs were comparable between *Naip*$^{fl/fl}$ and *Naip*$^{\Delta/\Delta}$ organoids (fig. 3.3b). In both CD4 and CD8 T cells, reduced IFNγ and CD69 was seen with *Naip*$^{\Delta/\Delta}$ conditioned supernatant compared to *Naip*$^{fl/fl}$, however this was only significant for IFNγ+ CD4 cells (fig. 3.3c). T cells cocultured with *Naip*$^{fl/fl}$ conditioned supernatant had decreased IFNγ and CD69 expression when organoids had been infected with STm, however this decrease was only significant in CD4 IFNγ expression (fig. 3.3c). Our laboratory has recently described a mechanism by which STm infection of epithelium reduces T cells activation (Copland *et al.*, 2023), which this result is in agreement with. This meant STm treatment of

Naip$^{fl/fl}$ reduced IFNγ and CD69 expression to similar levels as *Naip*$^{\Delta/\Delta}$ organoids. There were no further reductions in IFNγ or CD69 expression by cells cultured in STm infected *Naip*$^{\Delta/\Delta}$ organoid conditioned supernatant, and infection in conjunction with PGE_2 did not affect IFNγ or CD69 expression in CD4 or CD8s. However, in *Naip*$^{fl/fl}$ conditioned supernatant, the addition of Ibu during STm infection returned CD69 expression to levels seen in the untreated *Naip*$^{fl/fl}$ group, with a more modest increase in IFNγ. This suggests that the effect of STm on T cells in the context of *Naip*$^{fl/fl}$ organoids is mediated at least partially by prostaglandins. Whereas the discrepancy seen between *Naip*$^{fl/fl}$ and *Naip*$^{\Delta/\Delta}$ organoid treatment groups does not appear to be due to prostaglandins. However, as many of these differences are not statistically significant these trends must be interpreted with caution.

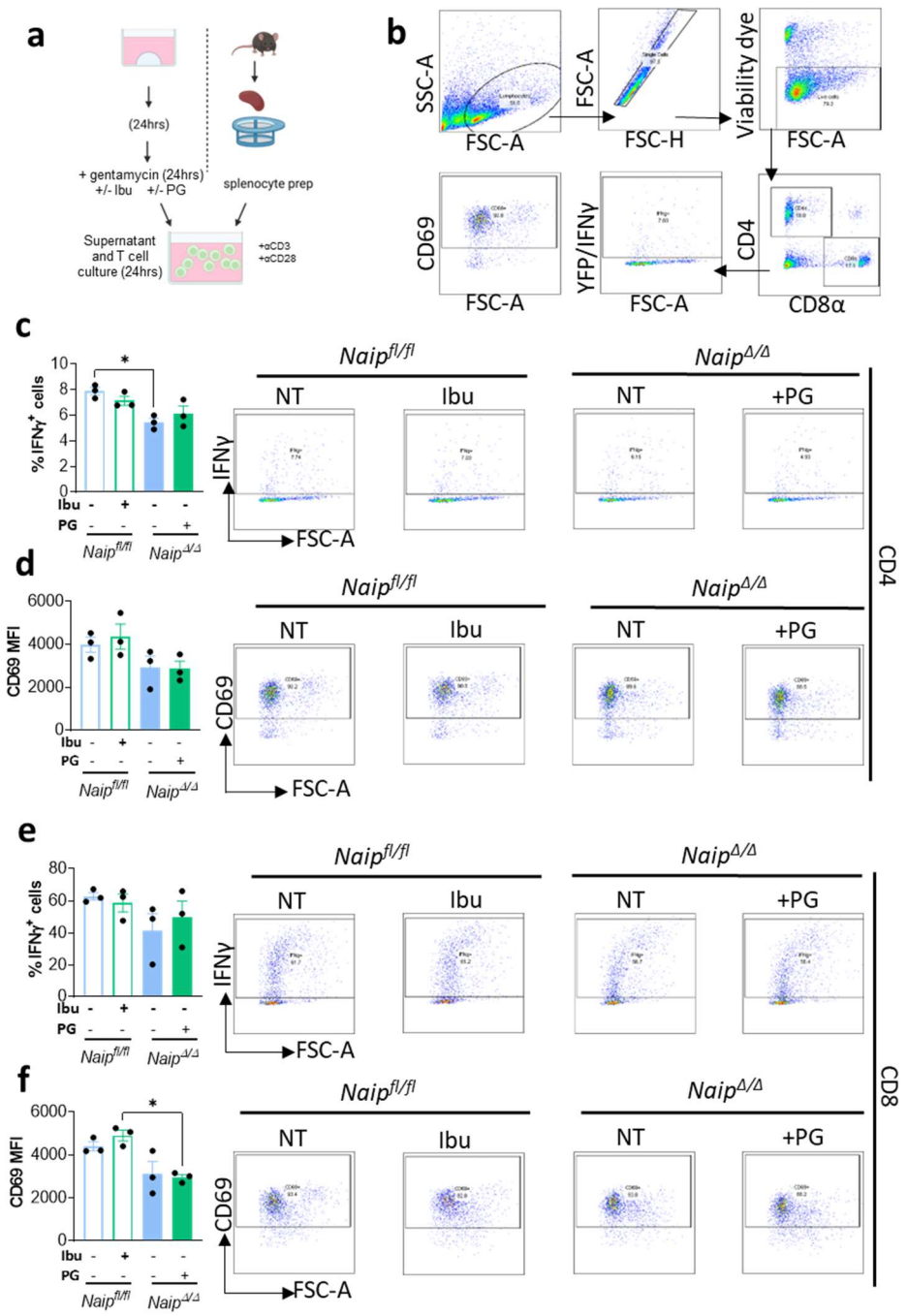

Figure 3.3 - *IFNγ reduced in CD4* T cells *cultured with STm-infected Naip$^{Δ/Δ}$ organoid-conditioned supernatant.*

a- *Naip$^{fl/fl}$* and *Naip$^{Δ/Δ}$* tumour organoids were infected with STm for 2hrs. Media was replaced, gentamycin added plus PGE_2 or ibuprofen (Ibu). After 24hrs, supernatant was used to culture splenocytes from Nr4a3-Tocky-*Ifng*-YFP mice, with αCD3/αCD28 antibodies. IFNγ and CD69 expression analysed by flow cytometry after 24hrs. **b** – Following infection, organoids were homogenised and number of CFUs determined. **c-d** – Percentage of IFNγ+ (**c**) and CD69 MFI (**d**) of CD4 T cells, with example flow plots. **e-f** – Percentage of IFNγ+ (**e**) and CD69 MFI (**f**) of CD8 T cells, with example flow plots. For bar plots, each point is the average of 3 technical repeats, with 3 individual experiments shown (N=3). One-way ANOVA statistical analysis was performed with Tukey's post-test. * = P<0.05, ** = P<0.01, ***=P<0.0001.

3.2.3 Levels of the eicosanoids 17,18-DiHETE and $PGF_{2\alpha}$ are altered in *Naip*$^{\Delta/\Delta}$ organoids

Eicosanoids include a wide range of related molecules, including prostaglandins (Moreno, 2017). Although ELISA had established that PGE_2 release was reduced in *Naip*$^{\Delta/\Delta}$ organoids, there are caveats with this approach, including cross-reactivity with other eicosanoids species (Gandhi *et al.*, 2017). To more accurately determine changes in the whole variety of eicosanoids, liquid chromatography mass spectrometry (LC/MS) was performed on organoid supernatants via collaboration with Valerie O'Donnell's lab at Cardiff University (fig. 3.4). Surprisingly, the only eicosanoids detected in the supernatants were 17,18-DiHETE and $PGF_{2\alpha}$. This was slightly unusual as a larger range are normally detected, though it is not entirely unprecedented (personal communication with Valerie O'Donnell). In conjunction with the O'Donnell lab, we tested different medium conditions, but found this result to be consistent. 17,18-DiHETE was significantly increased in *Naip*$^{\Delta/\Delta}$ organoids whereas $PGF_{2\alpha}$ was completely ablated. 17,18-DiHETE was unaffected by addition of STm or Ibu. In contrast, $PGF_{2\alpha}$ expression was increased in *Naip*$^{fl/fl}$ following STm infection and completely lost following Ibu treatment, confirming the efficacy of Ibu at the concentration used. Interestingly, in the condition in which exogenous PGE_2 was added, no PGE_2 was detected, which may imply that PGE_2 was not stable in our culture medium. Overall, this shows that there are changes in the eicosanoid profile of *Naip*$^{\Delta/\Delta}$ tumour-derived organoids, and suggests the PGE_2 ELISA may have been detecting $PGF_{2\alpha}$ due to cross-reactivity. The increase in 17,18-DiHETE suggests that the cytochrome P450 pathway may be upregulated in *Naip*$^{\Delta/\Delta}$ organoids (Tu *et al.*, 2020), although whether this acts as a compensatory mechanism is unclear.

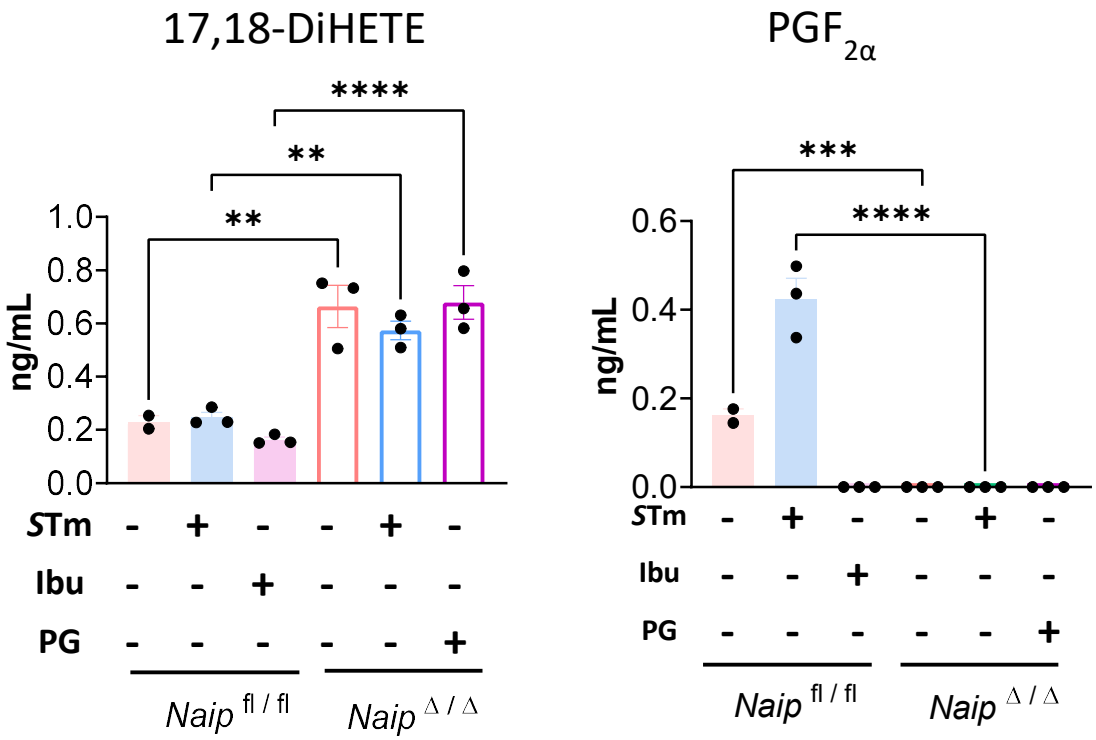

Figure 3.4 - 17,18-DiHETE was increased and $PGF_{2\alpha}$ decreased in the supernatants of $Naip^{\Delta/\Delta}$ tumour-derived organoids

$Naip^{fl/fl}$ and *$Naip^{\Delta/\Delta}$* tumour-derived organoids were infected with STm or not treated for 2hrs. Media was replaced, and gentamycin added to kill remaining extracellular bacteria. For some samples either PGE_2, ibuprofen (Ibu) or LPS was administered. After 24hrs, the organoid-conditioned supernatant was collected, snap frozen, then sent for liquid-chromatography mass spectrometry analysis to determine the eicosanoid content. Only two eicosanoids were identified as being present – 17,18-DiHETE and $PGF_{2\alpha}$. Each individual point indicates a separate well of organoids (i.e. a biological repeat). Representative image shown of 2 individual experiments (N=3). One-way ANOVA statistical analysis was performed with Tukey's post-test. ** = P<0.01, ***=P<0.0001, ****=P<0.00001.

3.2.4 Genes involved in eicosanoid synthesis are altered in *Naip*$^{\Delta/\Delta}$ tumour-derived organoids

Since the LC/MS had shown unexpected changes in eicosanoids, we next performed RNAseq on tumour-derived organoids, to determine any alterations in the wider network of eicosanoid related genes. PCA analysis (fig. 3.5a) showed the two organoid lines varied mostly due to PCA1, which accounted for 99% of the variance. This is perhaps unsurprising given that the two samples were untreated. KEGG pathway analysis highlighted differences in the *Salmonella* infection pathway, as well as cancer associated pathways such as p53 signalling, cell cycle and DNA replication (fig. 3.5b). We next used a volcano plot analysis to identify highly differentially expressed genes (DEGs) out of the 5376 which were significantly altered (fig. 3.5c). Interestingly, both *Marcks* and *Tspan8*, which have been linked to cancer promotion (Zhu *et al.*, 2019; Heo and Lee, 2020; Chiu *et al.*, 2022), was downregulated in *Naip*$^{\Delta/\Delta}$. However, genes related to growth factors such as *Pdgfa* and *Fgfrl1*, encoding platelet derived growth factor and fibroblast growth factor receptor 1, were upregulated. *Tmprss4*, encoding a serine protease which has been associated with poor cancer prognosis, was also increased in *Naip*$^{\Delta/\Delta}$ tumour-derived organoids (de Aberasturi and Calvo, 2015)**.** We next aimed to pull out eicosanoid-related genes, to understand how deletion of Naips altered eicosanoid synthesis. Using a list of eicosanoid related genes generated from WikiPathways (Martens *et al.*, 2021), we identified which of these were significantly altered and generated a heatmap (fig. 3.5d). Genes which were not significantly altered are not shown. This analysis found that *Ptgs1* (COX1) and *Ptgs2* (COX2) were downregulated in *Naip*$^{\Delta/\Delta}$*,* supporting the qPCR data. The only eicosanoid-related genes which were highly downregulated in *Naip*$^{fl/fl}$ were *Pla2g2a* (PLA_2 group IIA) and *Ptgds* (Prostaglandin D_2, synthase, PGDS). *Ptger4*, the gene for PGE_2 receptor EP4, was also slightly downregulated in *Naip*$^{fl/fl}$. Genes in the leukotriene pathway, such as *Lta4h* and *Mgst2*, which encode Leukotriene A4 Hydrolase and Microsomal Glutathione S-Transferase 2, were also reduced in *Naip*$^{\Delta/\Delta}$. Overall, this indicated

that broader changes were taking place in the eicosanoid pathway than we had originally anticipated.

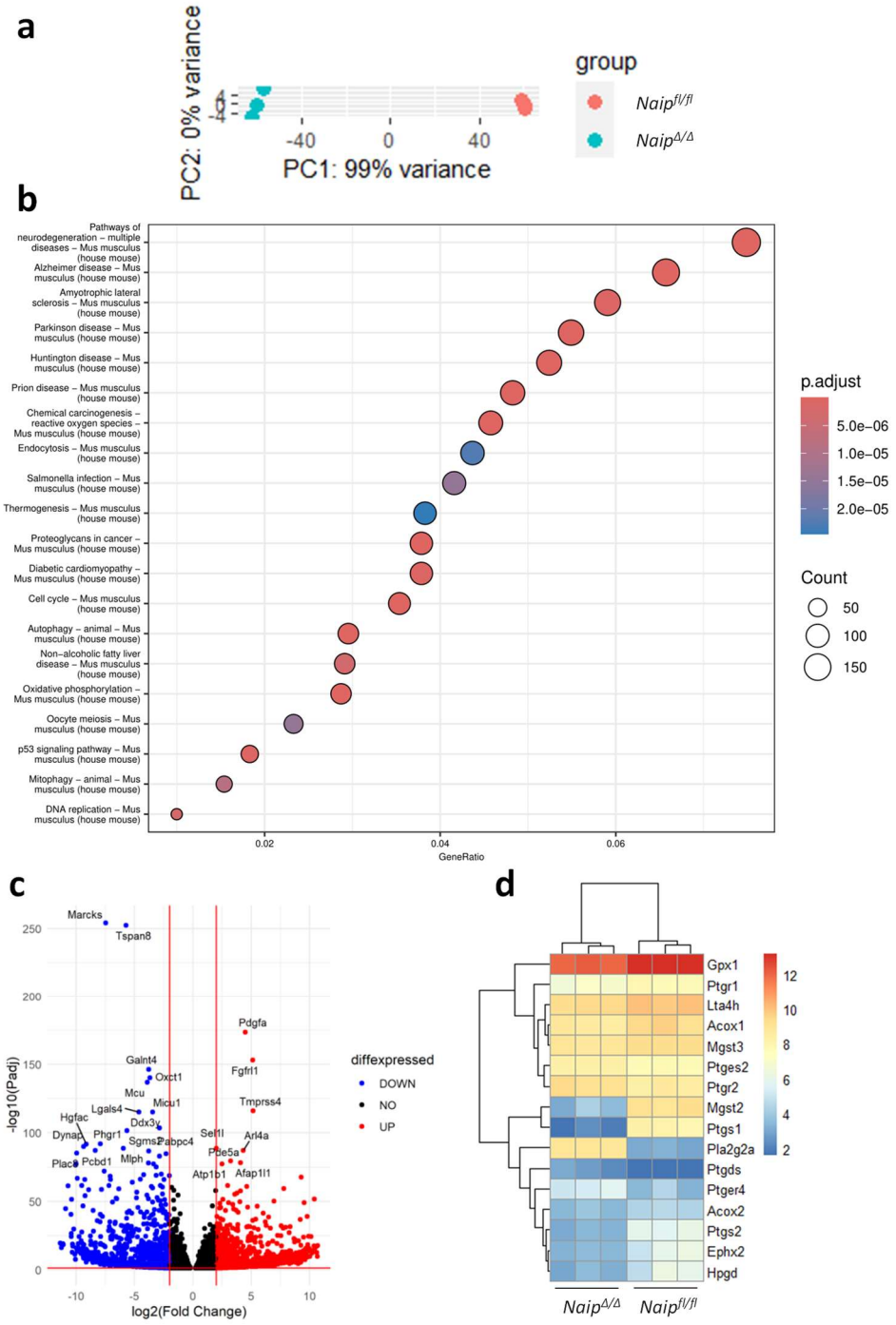

Figure 3.5 - Changes in eicosanoid-related genes in Naip$^{Δ/Δ}$ tumour-derived organoids

RNA was extracted from *Naip$^{fl/fl}$* and *Naip$^{Δ/Δ}$* tumour-derived organoids and RNAseq performed. Data was analysed in R using the DeSeq2 package to identify differentially expressed genes in *Naip$^{Δ/Δ}$* compared to *Naip$^{fl/fl}$*. **a** – PCA plot. **b** – KEGG pathway analysis. Size of each point indicates read count and colour indicates adjusted p value as per the colour key. **c** – Volcano plot indicating differentially expressed genes. **d** – Heatmap of significantly differentially expressed genes relating to eicosanoid biosynthesis. Each column represents a single sample and biological repeat. N=3.

3.3 Discussion

In this chapter, we aimed to identify changes in eicosanoid production in *Naip*$^{\Delta/\Delta}$ organoids, and establish what effects this might have on T cells. Previously, prostaglandins have been shown to have various effects on T cells (Harris *et al.*, 2002; Sreeramkumar, Fresno and Cuesta, 2012b; Lone and Taskén, 2013; Maseda, Ricciotti and Crofford, 2019), and have also been implicated in inflammatory diseases of the gut such as colitis and CRC (Wang and DuBois, 2010a). As *Naip*$^{\Delta/\Delta}$ mice are protected from colitis and have increased tumorigenesis during CRC (Allam *et al.*, 2015), it is possible that any changes in eicosanoids could be influencing this, either through effects on the IECs themselves or via the immune compartment. Here we find that eicosanoid related genes are reduced in *Naip*$^{\Delta/\Delta}$ tumour-derived organoids and that levels of eicosanoids are altered, although the effect was different depending on the assay used. This appeared to reduce IFNγ and CD69 expression in CD4+ splenocytes co-cultured with *Naip*$^{\Delta/\Delta}$ organoids.

3.3.1 The effect of *Naip* knockout on eicosanoid pathways

From qPCR analysis, tumour-derived organoids appeared to have reduced transcriptional expression of certain genes involved with eicosanoid biosynthesis, including *Ptgs1* (COX1), *Ptges1* (Prostaglandin E_2 synthetase 1) and *Pla2g4a* (cPLA2) (fig.3.2). *Ptgs1* (COX1) is generally known as the ubiquitous COX enzyme, whereas Ptgs2 (COX2) is induced during inflammation (Smyth *et al.*, 2009; Wang and DuBois, 2010a, 2010b), supporting the ELISA data (fig. 3.1) showing that *Naip*$^{\Delta/\Delta}$ organoids have reduced PG synthesis at baseline. Both *Ptgs1* and *Ptgs2* were increased in *Naip*$^{fl/fl}$ organoids following STm infection, though perhaps surprisingly this was only significant in *Ptgs1*. This is contrast to studies which have shown *Salmonella* infection to induce *Ptgs2* expression (Eckmann *et al.*, 1997; Bertelsen *et al.*, 2003; Uchiya and Nikai, 2004), but does not increase *Ptgs1* (Bowman and Bost, 2004; Sheppe *et al.*, 2018). Interestingly, there appears to be an altered response to STm in *Naip*$^{fl/fl}$ and *Naip*$^{\Delta/\Delta}$ organoids with regards to *Ptges1* and to a lesser extent *Ptges2* expression. *Naip*$^{fl/fl}$ increased

both enzymes in response to STm whereas *Naip*$^{\Delta/\Delta}$ organoids reduced expression, although only the difference in *Ptges1* was significant. This is perhaps to be expected as Naips recognise STm. However, the mechanism by which *Naip* knockout reduces these transcripts remains to be established. Based on other data from the lab we hypothesised that Naips could function as transcriptional regulators, as had been seen with other NLR family proteins such as NLRC5, which has been shown to translocate to the nucleus following IFNγ stimulation to promote MHCI gene transcription (Meissner *et al.*, 2010). However further research would be needed to validate this theory.

To determine the eicosanoid content of the organoid supernatant more accurately, we also performed LC/MS, as this has been demonstrated to be more sensitive for eicosanoid detection (Gandhi *et al.*, 2017). This found no PGE_2 in either *Naip*$^{fl/fl}$ or *Naip*$^{\Delta/\Delta}$ organoid supernatant but did detect $PGF_{2\alpha}$ in *Naip*$^{fl/fl}$ organoid supernatant, which was increased by STm infection and completely ablated by Ibu treatment. $PGF_{2\alpha}$ was not detected at all in *Naip*$^{\Delta/\Delta}$ organoid supernatant, however, elevated levels of 17,18-DiHETE were observed in *Naip*$^{\Delta/\Delta}$, and this was not altered by STm infection. The LC/MS analysis highlights the potential pitfalls in using ELISA-based assessments of PGs, as here there is significant non-specificity. Infection of human intestinal epithelial cells with *Salmonella* has previously been shown to induce both PGE_2 and $PGF_{2\alpha}$ as well as COX2 expression (Eckmann *et al.*, 1997), supporting the idea that $PGF_{2\alpha}$ could be produced downstream of Naips. One point raised by the LC/MS results is that even in the organoid supernatant which had PGE_2 added there is no PGE_2 present. The PGE_2 is added at the beginning of the 24hr culture, so it likely reflects the very short half-life of PGE_2 or poor stability during the snap-freezing process. PGE_2 is known to have a half-life of less than 15 seconds; it is metabolised to form 15-keto-13,14-dihydro-PGE_2 which then has a half-life of around 8 minutes (Bygdeman, 2003). This is likely to have affected the co-culture experiments which used organoid-conditioned media as opposed to co-cultures with actual organoids. We used supernatants as we were unable to source transwells (these were on back order post-covid) and

previous data from the lab suggested that organoid-conditioned supernatant had the same effect as direct co-culture on T cell activation, at least for the readout of that work (Copland *et al.*, 2023). In future experiments, $PGF_{2\alpha}$ could be added directly to the T cell cultures to determine if that could revert the T cell phenotype.

RNAseq data from tumour-derived organoids overall appeared to support the qPCR data and the observation that tumorigenesis was increased in *Naip*$^{\Delta/\Delta}$ mice (Allam *et al.*, 2015). Firstly, the two genotypes appeared starkly different on the PCA plot, with most of the divergence originating from PCA1. It is perhaps unsurprising that PCA1 accounts for most of the divergence as these organoids were unperturbed and so the difference in genotype accounts for all the differences in gene expression. However, it is interesting that the deletion of Naips causes such a striking difference. KEGG pathways related to cancer progression, such as p53 signalling and the cell cycle were differentially expressed between genotypes, supporting the idea that they would exhibit different tumorigenesis. *Tspan8* and *Marcks* were decreased in *Naip*$^{\Delta/\Delta}$ tumour-derived organoid compared to *Naip*$^{fl/fl}$. Expression of tetraspanin 8, encoded by *Tspan8*, has been linked to progression and metastasis in multiple cancers and shown stemness of cancer cells via sonic hedgehog signalling (Zhu et al., 2019; Heo and Lee, 2020). *Marcks* encodes myristoylated alanine-rich C-kinase substrate (MARCKS), and MARCKS signalling has been shown to contribute to cancer metastasis by promoting cell migration and invasion (Chiu et al., 2022). As *Naip*$^{\Delta/\Delta}$ mice experience worse tumorigenesis it may be surprising that *Tspan8* and *Marcks* are downregulated in *Naip*$^{\Delta/\Delta}$ organoids. However, both lines are tumour-derived organoids and other factors, both epithelial intrinsic and from wider cell types, will factor into tumorigenesis. Certain growth factor-related genes were increased in *Naip*$^{\Delta/\Delta}$ organoids, including *Pdgfra*, activating mutations in which have been linked to gastrointestinal stromal tumours (Heinrich et al., 2003). *Fgfrl1*, which encodes a non-tyrosine kinase signalling molecule, was also upregulated and has been linked to cell proliferation via Akt and MAPK signalling pathways. FGFRL1 also appears to be expressed in various human tumours (Aprajita and Sharma,

2021). *Tmprss4* was also upregulated in *Naip*$^{\Delta/\Delta}$ and has been suggested to be a possible therapeutic target in solid tumours (de Aberasturi and Calvo, 2015). Thus, much of the expression data is consistent with the increased tumorigenesis seen in *Naip*$^{\Delta/\Delta}$ mice. However, this data could be mined further to identify changes in other cancer-related gene pathways, for example the Wnt/β- catenin pathway.

When specifically investigating eicosanoid related genes, the RNAseq analysis supported our qPCR data that *Ptgs1 (*COX1) was downregulated in *Naip*$^{\Delta/\Delta}$ organoids. Interestingly, changes were seen in some leukotriene related genes, such as *Lta4h* and *Mgst2*, but no leukotrienes were detected in the LC/MS. The fact that *Ptger4*, encoding EP4, was downregulated in *Naip*$^{fl/fl}$ organoids is particularly interesting, as EP receptor distribution is a pivotal factor in mediating PGE_2 response. EP4 has also been shown to support cancer stem cells via MAPK and PI3K signalling as well as promote repair during colitis via the PI3K/Akt pathway (Kabashima et al., 2002; Jiang et al., 2007; Wang et al., 2015; Peng et al., 2017). This would be consistent with *Naip*$^{\Delta/\Delta}$ mice being protected from colitis but experiencing worse tumorigenesis. *Ephx2* was also downregulated in *Naip*$^{\Delta/\Delta}$, and this gene has previously been shown to inhibit colon cancer progression by driving breakdown of fatty acids (Zhou et al., 2022). Overall, this data support the idea that changes *Naip*$^{\Delta/\Delta}$ organoids have altered eicosanoid synthesis and that this may be contributing to differences in tumorigenesis observed in *Naip*$^{\Delta/\Delta}$ mice.

3.3.2 The effect of eicosanoids and *Naip* knockout on T cells

To determine how altered eicosanoid production due to *Naip* knockout might affect the immune compartment, splenocytes were prepared from Tocky-*Ifng* reporter mice and cultured in organoid-conditioned supernatant. We observed that IFNγ and CD69 was generally reduced in T cells co-cultured with *Naip*$^{\Delta/\Delta}$ tumour-derived organoids, but that this difference was only statistically significant in the case of IFNγ expression in CD4+ cells. This effect was not reversed by the addition of

PGE_2, however, as we later found that $PGF_{2\alpha}$ and not PGE_2 were affected, and that PGE_2 is not stable for long periods. Previous literature has shown that PGE_2 can induce IFNγ production during Th17 polarisation (Maseda, Johnson, *et al.*, 2018). However, there is some discrepancy in the literature regarding the role of PGE_2 on the IL-17/IFNγ axis. Some studies identified PGE_2 as increasing IL-17 at the expense of IFNγ and Th1 responses (Fabricius *et al.*, 2009; Napolitani *et al.*, 2009), but others have shown it promotes Th1 function and expansion (Yao *et al.*, 2013). This could be due to differences in using murine or human models, differences in receptor expression or in PG concentration (Maseda, Ricciotti and Crofford, 2019). However overall, these studies support the idea that differences in PG production by $Naip^{\Delta/\Delta}$ organoids could affect the activation of CD4+ T cells, but the exact effects require further elucidation.

We also investigated how the change in eicosanoids might interplay with STm infection in organoids, and how this might affect T cells. IECs are known to produce PGE_2 in response to STm infection via NAIP activation (Eckmann *et al.*, 1997; Rauch *et al.*, 2017), and *Salmonella* is known to induce COX2 expression in macrophages (Uchiya and Nikai, 2004). We found that STm infection of $Naip^{fl/fl}$ organoids prior to co-culture resulted in reduced CD69 and IFNγ in CD4 and CD8 T cells, although this was only statistically significant in IFNγ expression of CD4 cells, despite an almost 50% reduction in CD8 T cells. This took IFNγ and CD69 expression levels to a similar level as T cells co-cultured with untreated or STm infected $Naip^{\Delta/\Delta}$ organoids. Interestingly, addition of Ibu to STm-treated $Naip^{fl/fl}$ organoids increased CD69 and, to a lesser extent, IFNγ expression in CD4 and CD8 T cells, suggesting that PG produced in response to STm is causing reduction of CD69 and IFNγ in T cells. However, as $Naip^{\Delta/\Delta}$ organoids also have reduced PGs but still have low CD69 and IFNγ perhaps other factors are contributing to the effect seen in $Naip^{\Delta/\Delta}$ organoids. However, we later found, using an LC/MS-based approach, that the PG species produced by our organoids was $PGF_{2\alpha}$ and not PGE_2. Therefore, repeating these experiments with $PGF_{2\alpha}$ could clarify this result. This was planned but time did not permit. In addition, PGE_2 could not be detected even when spiked into the culture, which could

either mean it is rapidly degraded and therefore has minimal opportunity to act on the T cell cultures, or that it is degraded over the freeze-thaw process before extraction for LC/MS analysis, or that the PGE_2 stock itself was degraded (this was not measured directly). This data is in contrast to Bowman and Bost's study which found that inhibiting COX2 activity during *Salmonella* infection lead to enhancement of the Th1 response, including IFNγ expression, however this study used macrophages and dendritic cells which may account for these differences (Bowman and Bost, 2009). With regards to $PGF_{2\alpha}$ and 17,18-DiHETE which were found to be altered in our LC/MS data, little, to nothing, is known regarding their effects on T cell activation.

3.3.3 The effect of eicosanoids on *Naip*$^{\Delta/\Delta}$ mice during CRC and colitis

How an alteration in eicosanoids in *Naip*$^{\Delta/\Delta}$ mice would affect colitis and colorectal cancer development is unclear, and an area of future research. Firstly, it would be interesting to ascertain the eicosanoid content of *ex vivo* samples from *Naip*$^{\Delta/\Delta}$ mice and to determine expression of eicosanoid related genes from mouse samples. Counter-intuitively, PGE_2 is generally considered pathogenic in CRC (Wang and DuBois, 2010a), but *Naip*$^{\Delta/\Delta}$ mice which appear to have reduced PGs suffer from increased tumorigenesis. PGE_2 can promote cancer stem cells via MAPK and PI3K/Akt pathways (Qiu *et al.*, 2010; Moon *et al.*, 2014; Wang *et al.*, 2015; Roulis *et al.*, 2020), encourage growth and inhibit apoptosis of cancer cells (Tsujii and DuBois, 1995; Sheng *et al.*, 1998; Ko *et al.*, 2002; Pai *et al.*, 2002; Castellone *et al.*, 2005), and support tumour angiogenesis (Seno *et al.*, 2002; Wang and DuBois, 2010a; Cherukuri *et al.*, 2014). $PGF_{2\alpha}$ has also been implicated in CRC, albeit with a smaller number of studies. Qualtrough *et al*. found that colorectal tumours produced $PGF_{2\alpha}$ and the prostaglandin-F receptor (FP) which recognises it (Qualtrough *et al.*, 2007). $PGF_{2\alpha}$ could also induce cell motility and promote carcinoma-derived cells to invade a reconstituted basement membrane (Qualtrough *et al.*, 2007). Metabolites generated due to oxidative stress from $PGF_{2\alpha}$ are also present in the urine of mice and humans with CRC (Zhang *et al.*, 2017; Miyazaki *et al.*, 2021), and in patients with Crohn's disease (Cracowski *et al.*, 2002). $PGF_{2\alpha}$ levels are also increased in colons of mice with a

Citrobacter rodentium induced model of colitis (Chhonker *et al.*, 2021). Little data is available on the effect of 17,18-DiHETE during CRC and colitis. Clearly eicosanoids can have a wide range of roles in these diseases, but how this relates to the effect of *Naip* knockout remains unclear.

3.3.4 Limitations

Experiments from this chapter were performed prior to the generation of normal organoids, meaning that all these results are from tumour-derived organoids. This adds another layer to interpreting these results. Co-culture with tumour conditioned media compared to normal organoid conditioned media may affect T cells, as tumour cells would be releasing different metabolites, such as lactate, succinate and 2-hydroxyglutarate (Mackie *et al.*, 2021). In the future, it would be interesting to repeat these experiments with normal colonic organoids. In addition, LC/MS was performed after the co-culture experiments, meaning we had already used PGE_2 to add to the organoids and it would only later become apparent that in fact $PGF_{2\alpha}$ appeared to be reduced in the $Naip^{\Delta/\Delta}$ organoid supernatants. We would address this by repeating with $PGF_{2\alpha}$ if we took this forward; we could still use Ibu as this still blocks $PGF_{2\alpha}$ production, as seen in fig. 3.5.

3.3.5 Conclusions

In this chapter we identified changes in the eicosanoid biosynthesis pathways of $Naip^{\Delta/\Delta}$ tumour-derived organoids which coincided with changes in eicosanoid distribution. Coculture with $Naip^{\Delta/\Delta}$ tumour-derived organoids appeared to reduce the IFNγ expression of CD4 T cells. However, whether this was due to changes in eicosanoid expression remains unclear, particularly as these experiments used exogenous PGE_2 instead of $PGF_{2\alpha}$. Further work would be needed to identify the effects of altered eicosanoid expression on the immune compartment, and determine how this influences CRC and colitis progression in $Naip^{\Delta/\Delta}$ mice. Indeed, it must be confirmed if this effect on eicosanoids is seen in normal organoids or mice. The mechanism behind altered eicosanoid expression will also be an interesting area of further research.

4 The Role of Naips in Colorectal Cancer

4.1 Introduction

Naips have been previously shown to be protective in colorectal cancer, with mice lacking NAIPs in the IECs experiencing worse tumorigenesis following AOM+DSS or just AOM treatment (Allam *et al.*, 2015). *Naip1-6*$^{IEC\Delta/\Delta}$ mice (referred to from here as *Naip*$^{\Delta/\Delta}$) also had increased STAT3 phosphorylation compared to *Naip*$^{fl/fl}$ following AOM+DSS treatment but this was not recapitulated in *Nlrc4*-/-, *Caspase-1/11*-/- or *Asc*-/- mice and did not coincide with changes in IL-1β or IL-18, suggesting that NAIPs role in CRC development may be independent of the inflammasome (Allam *et al.*, 2015). However, NAIP is not the only member of the NLR family to be linked to CRC suppression. For example, knockout mice for NLRC3, NLRP3, NLRP6, NLRC4, NLRP1, NLRX1 and NLRP12 have been observed to have increased tumorigenesis following AOM+DSS treatment (Zhu and Cao, 2017). Many of the effects of NLR family proteins occur via inflammasome-dependent pathways. To a certain degree the effect of NLRs in CRC can be attributed to IL-18, with *Il18*-/- and *Il18r1*-/- mice experiencing increased tumorigenesis (Pandey, Shen and Man, 2019). However, in some cases, as with *Naip*$^{\Delta/\Delta}$ mice, NLRs affect CRC via inflammasome-independent mechanisms. Deletion of NLRX1, which does not form an inflammasome, specifically in the IECs leads to increase tumorigenesis in both the AOM+DSS and *Apc*$^{Min/+}$ models of CRC, with different studies concluding this was due to increased TNF and NFκB signalling (Koblansky *et al.*, 2016; Tattoli *et al.*, 2016). *Nlrc3*-/- mice also have increased tumorigenesis in the AOM+DSS and *Apc*$^{Min/+}$ models of CRC, which appeared to be mediated by PI3K/mTOR signalling (Karki *et al.*, 2016, 2017). Whilst many of the epithelial cell intrinsic effects of *Naip* knockout during CRC have been established, such as upregulation of *Bcl2*, *Myc* and *Ccnd1* and increased STAT3 phosphorylation (Allam *et al.*, 2015), the effect on the immune response remains to be established. We therefore aimed in this chapter to distinguish any changes in the immune compartment between *Naip*$^{fl/fl}$ and *Naip*$^{\Delta/\Delta}$ mice during CRC.

To understand how epithelial Naips influence the immune compartment in this context, we also assessed expression of markers which could modulate the immune response in *Naip*$^{\Delta/\Delta}$ mice. IFNγ is known to have broad effects on the immune system and an important role in CRC, we therefore focused on markers affected by IFNγ signalling. One of these markers was MHCII, which is known to be beneficial to anti-tumour immune responses, and a loss of which results in reduced immune infiltration (Warabi, Kitagawa and Hirokawa, 2000; Sconocchia *et al.*, 2014; Axelrod *et al.*, 2019; Griffith *et al.*, 2022). Here, we show that in tumour-derived organoids *Naip* knockout results in increased MHCII expression. NLRC4 inflammasome activation and subsequent IL-18 release has been shown to lead to MHCII expression in IECs in vivo (Van Der Kraak *et al.*, 2021). Gasdermin D activation, downstream of Caspase-3/7, has also been shown to drive MHCII expression in IECs in response to dietary antigens (He *et al.*, 2023). We therefore aimed to identify the mechanism behind altered MHCII expression in response to IFNγ and how this can be reconciled with the increased tumorigenesis observed in *Naip*$^{\Delta/\Delta}$ mice.

In this chapter I aimed to:

- Identify changes in the immune compartment of *Naip*$^{\Delta/\Delta}$ mice during AOM+DSS induced CRC
- Assess expression of immune modulating molecules in IECs lacking NAIP
- Understand how expression of these molecules was altered in *Naip*$^{\Delta/\Delta}$

4.2 Results

4.2.1 *Naip*$^{\Delta/\Delta}$ mice have increased tumorigenesis and a greater increase in TCRγδ+ and TCRγδCD4 cells compared to *Naip*$^{fl/fl}$

Previously, *Naip*$^{\Delta/\Delta}$ mice have been shown to have increased tumorigenesis in the AOM+DSS model (Allam *et al.*, 2015). However, it remained to be established whether the immune response to CRC was different in *Naip*$^{\Delta/\Delta}$ mice, and if so, what effect that had on cancer development. We therefore investigated the tumour infiltrating lymphocytes (TILs) in *Naip*$^{fl/fl}$ and *Naip*$^{\Delta/\Delta}$ mice and compared these with the intraepithelial lymphocytes (IELs) in the surrounding healthy tissue. To induce CRC, mice were injected with azoxymethane (AOM) IP to cause DNA damage, followed by three rounds of DSS (3% in drinking water) which causes colonic inflammation that drives carcinogenesis (fig. 4.1a-b). As seen previously, *Naip*$^{\Delta/\Delta}$ mice had significantly increased tumour weight, along with a trend towards increased tumour burden and volume (fig. 4.1c) (Allam *et al.*, 2015). Tumours as wells as 'normal' colonic tissue was then dissected and enzymatically digested to analyse the TIL and IEL compartments. TILs and IELs were gated to distinguish different subsets (fig. 4.1d), in keeping with the IEL subsets investigated in the final chapter of this thesis. These included TCRαβCD4, TCRαβCD8αα, TCRαβCD8αβ, TCRγδ+ and TCRγδCD8αα as investigated in the next chapter, as well as TCRγδCD8αβ and TCRγδCD4 which we had not observed when IELs were isolated from healthy mice but appeared in tumour-induced mice as clear populations (fig. 4.1e). When compared to healthy tissue, TILs were enriched for TCRαβCD4, TCRαβCD8αβ, TCRγδ+ and TCRγδCD4. Strikingly, there were virtually no TCRγδCD4 cells in healthy tissue, but a definite population in TILs. In contrast, TCRαβCD8αα and TCRγδCD8αα cells were reduced in tumours compared to healthy tissue. In *Naip*$^{\Delta/\Delta}$ compared to *Naip*$^{fl/fl}$ tumours, there appeared to be a greater increase in TCRγδ+ and TCRγδCD4 cells, whereas the increase in TCRαβCD4 seen from healthy to tumour tissue was reduced in *Naip*$^{\Delta/\Delta}$.

We next investigated CD103 (fig. 4.2a) and CD69 (fig. 4.2b) expression in these populations, to assess tissue residency. CD103 was decreased in TILs compared to IELs in TCRαβCD8αβ, TCRγδ+ and TCRγδCD4 for both genotypes. In *Naip*$^{\Delta/\Delta}$ mice, CD103 was reduced in TCRγδCD8αβ TILs compared to IELs, and increased in TCRαβCD4 and TCRαβCD8αα TILs compared to IELs, whereas in *Naip*$^{fl/fl}$ mice CD103 expression remained mostly unchanged in these subsets from IELs to TILs. CD69 expression was reduced in TCRαβCD8αβ, TCRγδ+ and TCRγδCD8αβ TILs compared to IELs in healthy tissue. No striking differences were observed between *Naip*$^{fl/fl}$ and *Naip*$^{\Delta/\Delta}$. Double positive CD103+CD69+ TCRαβCD8αα, TCRαβCD8αβ, TCRγδ+, TCRγδCD4 and TCRγδCD8αβ were reduced in TILs compared to IELs in both genotypes (fig. 4.3). However, no differences between *Naip*$^{fl/fl}$ and *Naip*$^{\Delta/\Delta}$ were seen in CD103+CD69+ expression.

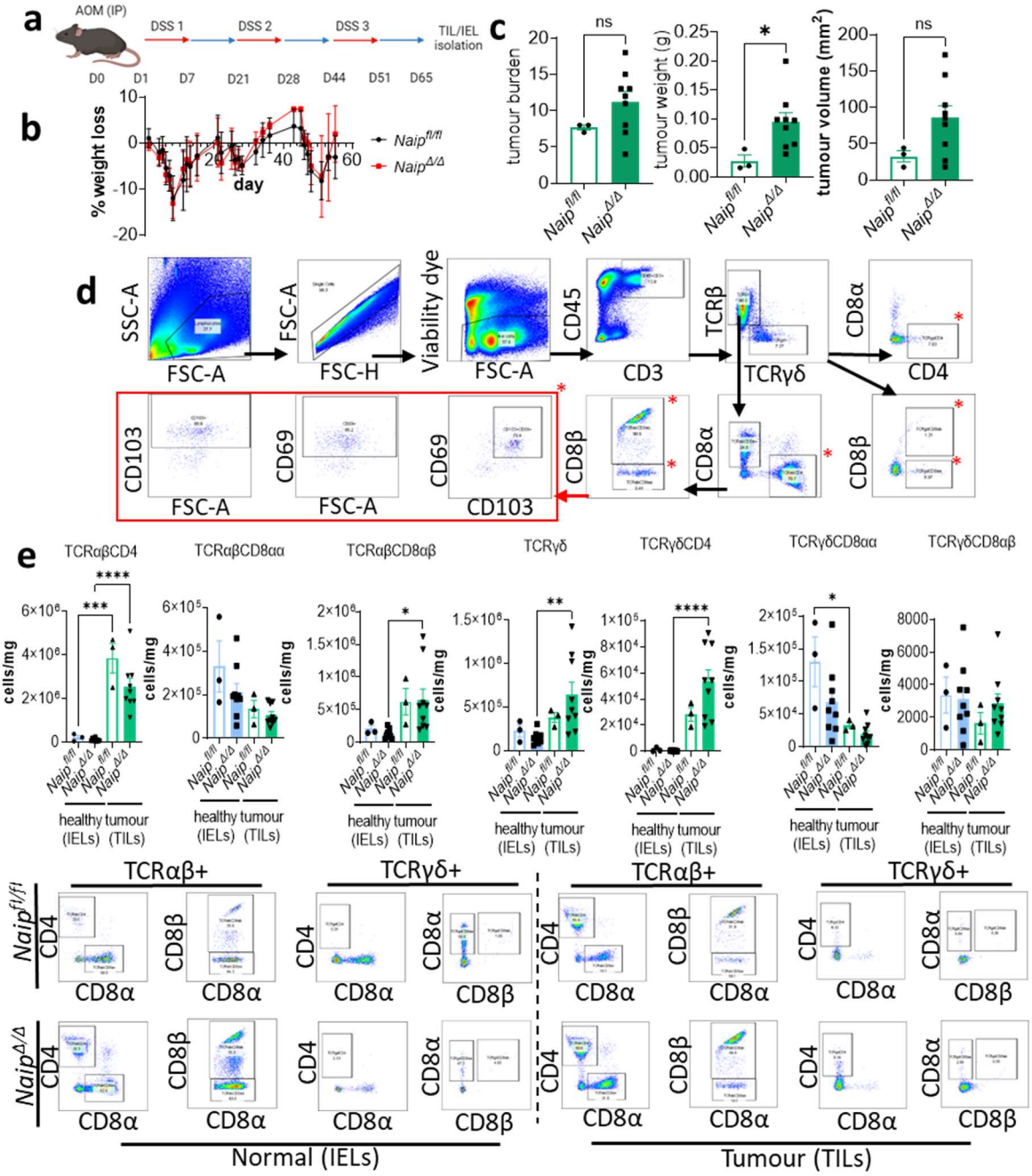

Figure 4.1 - Naip$^{\Delta/\Delta}$ mice have increased tumorigenesis but no changes in number TILs

a - *Naip$^{fl/fl}$* and *Naip$^{\Delta/\Delta}$* mice were injected with azoxymethane (AOM) IP (1mg/kg), followed by three rounds of DSS (3%) in the drinking water for 7 days followed by 14 days of normal drinking water to induce colorectal cancer. Made in Biorender. **b** – Weight loss over the course of the experiment, point indicate mean ± s.e.m. Two-way ANOVA performed with Sidak's post-test. **c** – Tumour burden, weight and volume. Each point indicates a separate mouse, bars indicate mean ± s.e.m. Unpaired t-test performed, *=P<0.05. **d** – Gating strategy for TILs and IELs. Gates with red asterisks were then gated as shown in the red box. **e** – Number of IELs and TILs per mg of tissue for each subset with representative flow plots. Each point indicates an individual mouse, bars indicate mean ± s.e.m. *Naip$^{fl/fl}$* N=3, *Naip$^{\Delta/\Delta}$* N=9, one independent experiment. One-way ANOVA performed with Tukey's post-test. *=P<0.05, **=P<0.01, ***=P<0.001, ****=P<0.0001.

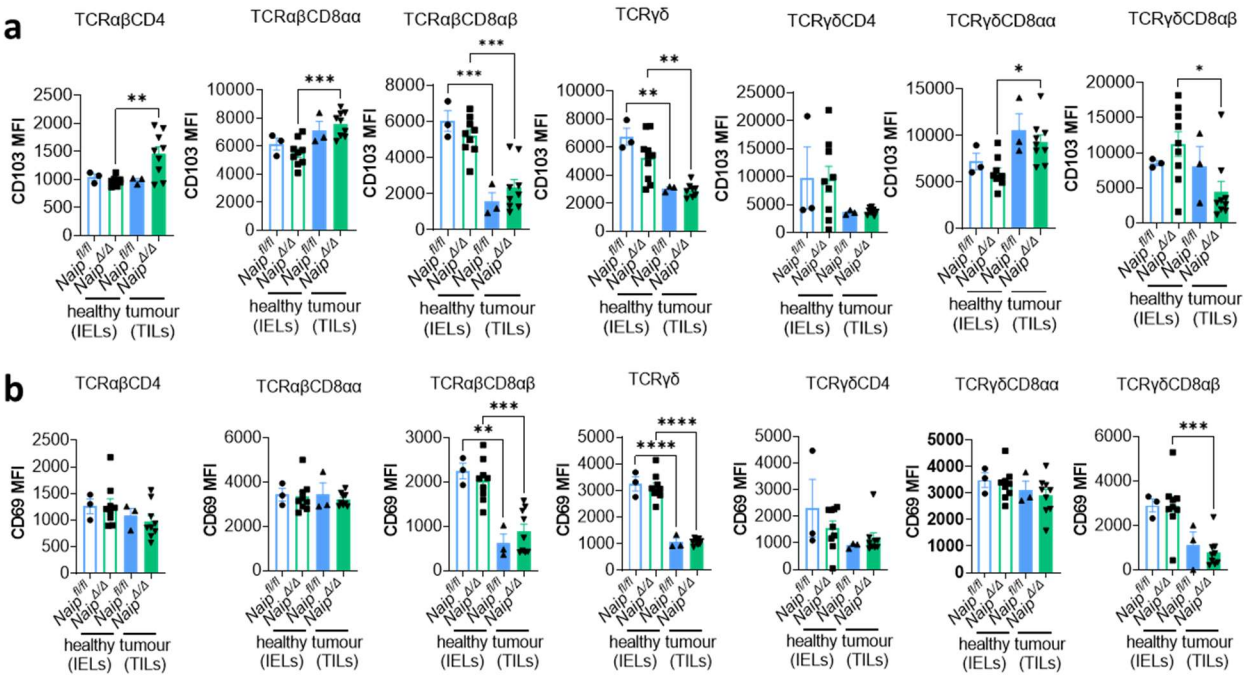

Figure 4.2 - Increase in CD103 expression in TCRαβCD4 and TCRαβCD8αα in Naip$^{Δ/Δ}$ tumours

Naip$^{fl/fl}$ and *Naip$^{Δ/Δ}$* mice were injected with azoxymethane (AOM) IP (1mg/kg), followed by three rounds of DSS (3%) in the drinking water for 7 days followed by 7 days of normal drinking water to induce colorectal cancer. Colon tumours were excised alongside healthy tissue, and the TILs and IELs isolated, respectively. **a** – MFI of CD103 in TIL and IEL subset in colon tumours and healthy tissue. **b** - MFI of CD69 in TIL and IEL subset in colon tumours and healthy tissue. Each individual point indicates a separate mouse, bars indicate mean ± s.e.m. *Naip$^{fl/fl}$* N=3, *Naip$^{Δ/Δ}$* N=9, one independent experiment. One-way ANOVA performed with Tukey's post-test. *=P<0.05, **=P<0.01, ***=P<0.001, ****=P<0.0001.

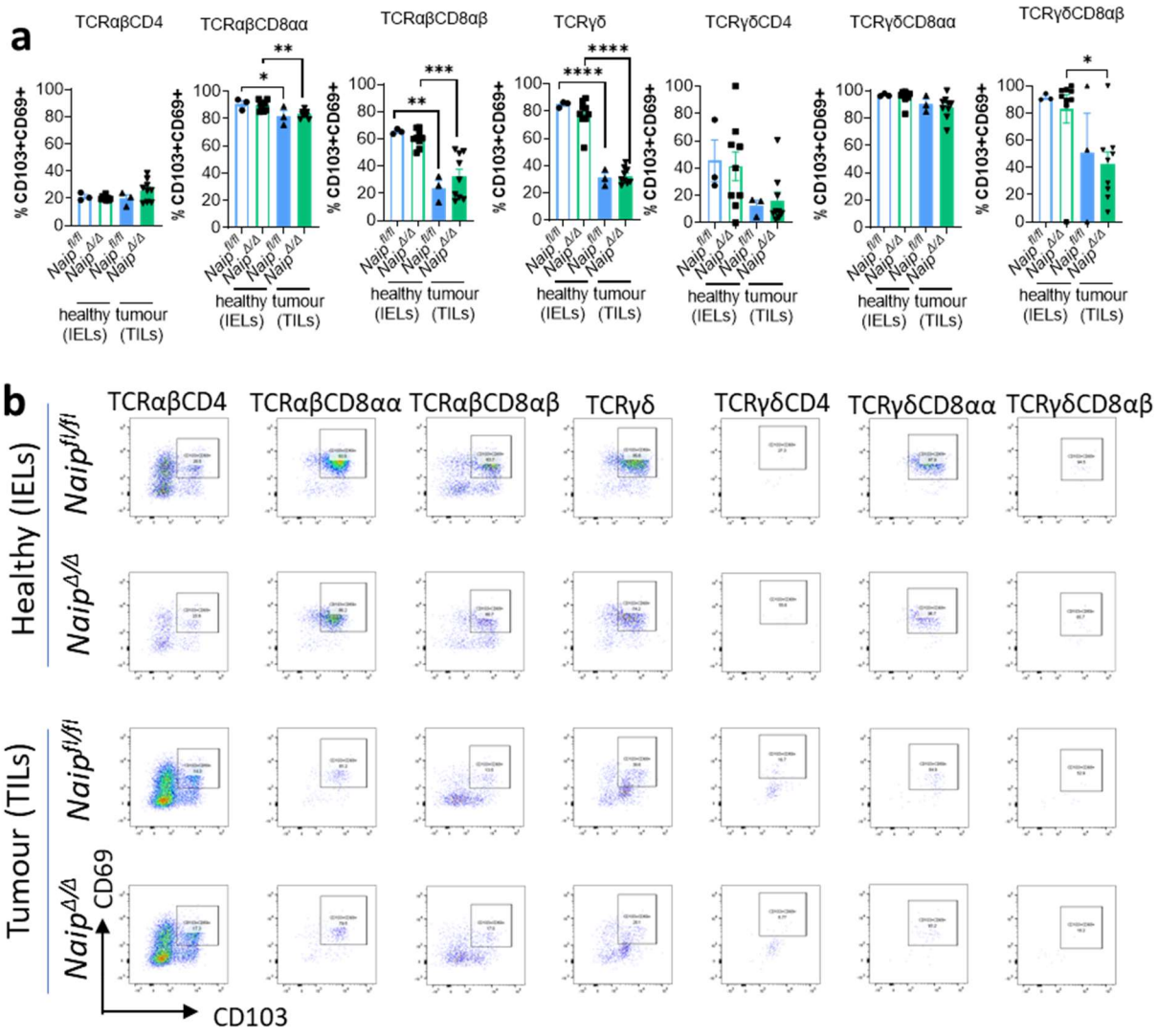

Figure 4.3 – CD103+CD69+ cells are reduced in colorectal tumours compared to healthy tissue

Naip$^{fl/fl}$ and *Naip*$^{\Delta/\Delta}$ mice were injected with azoxymethane (AOM) IP (1mg/kg), followed by three rounds of DSS (3%) in the drinking water for 7 days followed by 7 days of normal drinking water to induce colorectal cancer. Colon tumours were excused alongside healthy tissue, and the TILs and IELs isolated, respectively. **a** –Percentage of CD103+CD69+ cells in TIL and IEL subset in colon tumours and healthy tissue. Each individual point indicates a separate mouse, bars indicate mean ± s.e.m. *Naip*$^{fl/fl}$ N=3, *Naip*$^{\Delta/\Delta}$ N=9, one independent experiment. One-way ANOVA performed with Tukey's post-test. *=P<0.05, **=P<0.01, ***=P<0.001, ****=P<0.0001. **b** – Representative flow plots of CD103+CD69+ cells for each T cell subset.

4.2.2 No difference in Tregs in tumours of *Naip*$^{\Delta/\Delta}$ mice compared to *Naip*$^{fl/fl}$

As *Naip*$^{\Delta/\Delta}$ mice have increased tumorigenesis, we next assessed Treg populations as these are commonly associated with tumour progression and poor prognosis (Olguín et al., 2020). To investigate this, TILs and IELs from healthy tissue were stained for CD4, CD25 and FoxP3 (fig. 4.4). As seen in fig. 4.1e, TCRαβCD4s were enriched in tumours, and this was true for Tregs (CD25+FoxP3+), activated T cells (CD25+FoxP3-) and un-activated CD4 T cells (CD25-FoxP3-) (fig. 4.4c). Of the CD4+ cells, activated T cells appeared to represent a larger proportion in *Naip*$^{\Delta/\Delta}$ mice than in *Naip*$^{fl/fl}$ mice (fig. 4.4d). Next, expression of PD1 and CTLA4 was assessed in these cells (fig. 4.5). No significant changes were seen in PD1 expression in Tregs, activated T cells or un-activated CD4 T cells when comparing IELs and TILs from *Naip*$^{fl/fl}$ and *Naip*$^{\Delta/\Delta}$ mice. CTLA4 expression increased in Tregs from tumours compared to healthy tissue in *Naip*$^{fl/fl}$ mice, whereas in Tregs *Naip*$^{\Delta/\Delta}$ mice it did not. CTLA4 expression in activated CD4 T cells was reduced in tumours compared to healthy tissue in both genotypes. In un-activated CD4s, CTLA4 was reduced in healthy tissue of *Naip*$^{\Delta/\Delta}$ mice compared to healthy tissue of *Naip*$^{fl/fl}$. When considering double positive CTLA4+PD1+ cells, no significant changes were observed. However, there was a trend for increased CTLA4+PD1+ expression in both Tregs and activated CD4s in tumours of both genotypes.

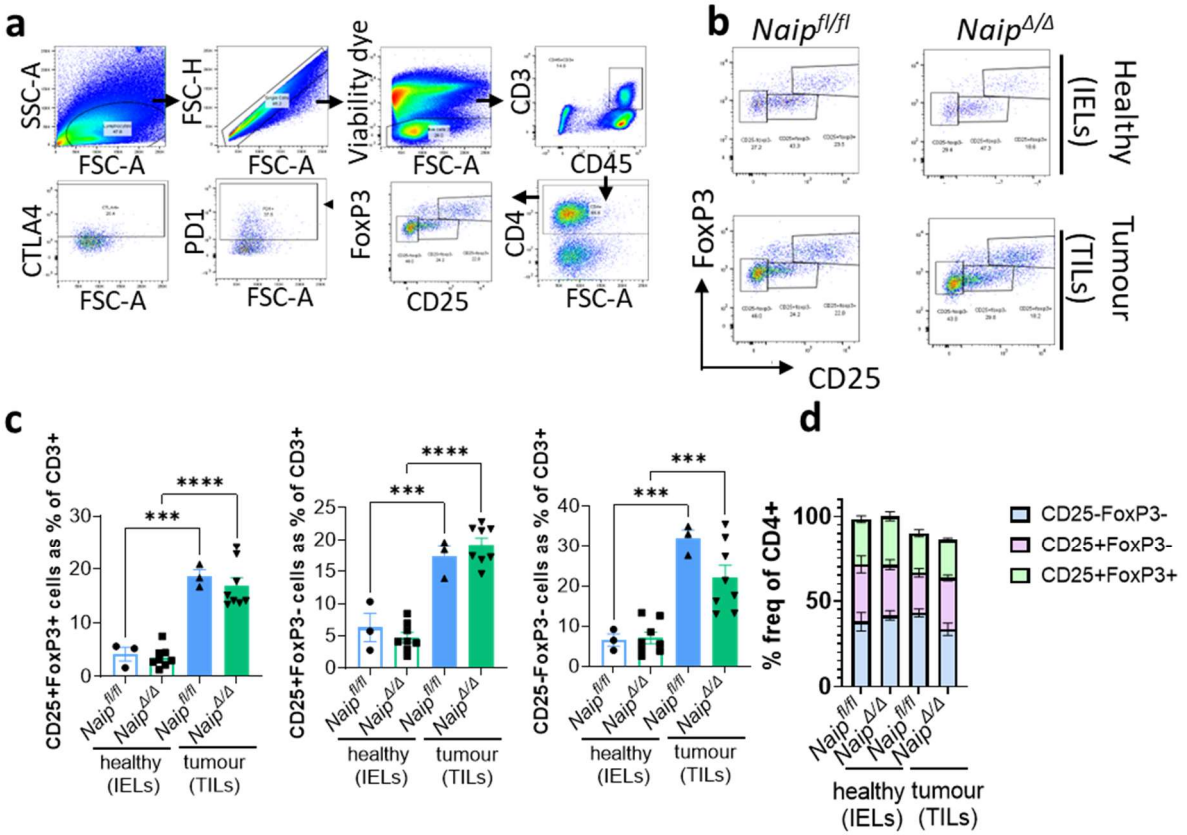

Figure 4.4 - No change in Treg numbers in tumours of Naip$^{\Delta/\Delta}$ mice compared to Naip$^{fl/fl}$

Naip$^{fl/fl}$ and *Naip$^{\Delta/\Delta}$* mice were injected with azoxymethane (AOM) IP (1mg/kg), followed by three rounds of DSS (3%) in the drinking water for 7 days followed by 7 days of normal drinking water to induce colorectal cancer. Colon tumours were excused alongside healthy tissue, and the TILs and IELs isolated, respectively. **a** – Gating strategy for identifying Tregs (CD25+FoxP3+), activated T cells (CD25+FoxP3-) and un-activated CD4 T cells (CD25-FoxP3-). **b** – Representative flow plots of healthy IELs and TILs in *Naip$^{fl/fl}$* and *Naip$^{\Delta/\Delta}$*. Each individual point indicates a separate mouse, bars indicate mean ± s.e.m. **c** – Percentage of CD3+ cells of Tregs, activated T cells and un-activated T cells. **d** – Frequency of each CD4+ population presented as a percentage of CD4+ total. Bars indicate mean ± s.e.m. *Naip$^{fl/fl}$* N=3, *Naip$^{\Delta/\Delta}$* N=9, one independent experiment. One-way ANOVA performed with Tukey's post-test. ***=P<0.001, ****=P<0.0001

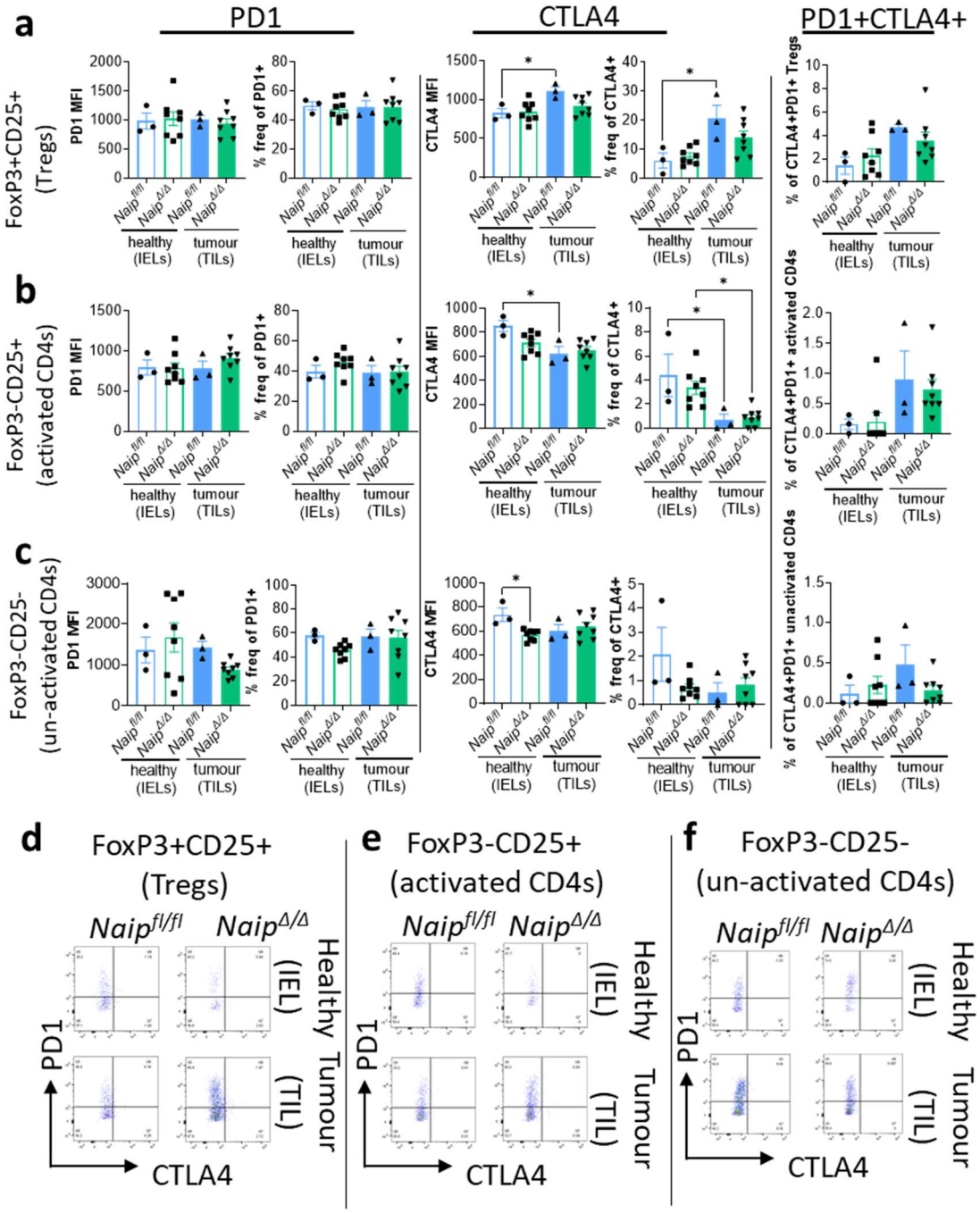

Figure 4.5 –CTLA4 expression altered in CD4 T cells from tumours compared to healthy tissue

Naip$^{fl/fl}$ and *Naip*$^{\Delta/\Delta}$ mice were injected with azoxymethane (AOM) IP (1mg/kg), followed by three rounds of DSS (3%) in the drinking water (7 days DSS followed by 7 days normal water). Tumours and healthy tissue were excised, and TILs and IELs isolated. Tregs (CD25+FoxP3+), activated T cells (CD25+FoxP3-) and un-activated T cells (CD25-FoxP3-) by flow cytometry. (**a-c)** MFI and percentage of PD1+, CTLA4+ and PD1+CTLA4+ Tregs (CD25+FoxP3+) (**a**), activated T cells (CD25+FoxP3-) (**b**) and un-activated T cells (CD25-FoxP3-) (**c**). (d-e) – Representative plots for Tregs (CD25+FoxP3+) (**d**), activated T cells (CD25+FoxP3-) (**e**) and un-activated T cells (CD25-FoxP3-) (**f**). Each point indicates a separate mouse, bars indicate mean ± s.e.m. *Naip*$^{fl/fl}$ N=3, *Naip*$^{\Delta/\Delta}$ N=9, one independent experiment. One-way ANOVA performed with Tukey's post-test. *=P<0.05.

4.2.3 Tumour-derived *Naip*$^{\Delta/\Delta}$ organoids have altered expression of MHCII, CD1d and IFNγ receptor

As we see only small differences in TILs in *Naip*$^{\Delta/\Delta}$ mice compared to *Naip*$^{fl/fl}$ despite the difference in tumorigenesis, we next aimed to investigate what markers the TILs might be encountering in the tumours of *Naip*$^{\Delta/\Delta}$ mice and how these might impact the immune response. To do this we move to *in vitro* experiments using tumour-derived organoids. We investigated markers which could be expressed by IECs and could influence T cell responses at baseline and in response to IFNγ stimulation. As well as having a wide arrange of effects on T cells, IFNγ is also known to have an impact in CRC (Jorgovanovic *et al.*, 2020), hence why we investigated this condition. Tumour-derived organoids were stimulated with IFNγ for 48hrs and expression of MHCI, CD80, CD1d, MHCII and PD1, which have all been reported to be upregulated by IFNγ, as well as the IFNγ receptor (IFNγR) was assessed by flow cytometry. MHCI and MHCII have important roles in presenting antigen to CD8 and CD4 T cells, respectively (Zhou, 2009; Thelemann *et al.*, 2014). CD1d is an alternative MHCI molecule and can interact with γδ T cells and natural killer T cells (Colgan *et al.*, 1996; Macho-Fernandez and Brigl, 2015). CD80 is a co-stimulatory molecule which aids activation of T cells, and promotes immune surveillance in CRC (Sheng *et al.*, 2013; Marchiori *et al.*, 2019). PDL1 acts to limit T cell activation, with particular relevance in cancer (Qian *et al.*, 2018). Finally, IFNγR responds to IFNγ, and can therefore inform us of the ability of the organoids to respond to the IFNγ stimulation. Strikingly, *Naip*$^{fl/fl}$ tumour-derived organoids did not upregulate MHCII in response to IFNγ, whereas *Naip*$^{\Delta/\Delta}$ tumour-derived organoids did (fig. 4.6d). However, no change was seen in MHCI, CD80 or CD1d expression (fig. 4.6). CD1d was reduced in *Naip*$^{\Delta/\Delta}$ at baseline (fig. 4.6c). PDL1 was strongly induced following IFNγ stimulation in both genotypes, indicating both genotypes have the capacity to respond to IFNγ. IFNγR was also reduced in *Naip*$^{\Delta/\Delta}$ at baseline but both genotypes downregulated it in response to IFNγ stimulation (fig. 4.6f); this likely reflects internalisation after signalling is engaged (Blouin and Lamaze, 2013). Together, this suggests some alterations in the markers which could

affect T cells, with the most striking being MHCII. Hence, we decided to investigate this change in MHCII further.

4.2.4 Tumour-derived *Naip*$^{\Delta/\Delta}$ organoids have increased MHCII expression in response to IFNγ stimulation compared to *Naip*$^{fl/fl}$

The drastic difference in MHCII induction in response to IFNγ is particularly interesting in the context of cancer, as loss of MHCII expression is associated with reduced TIL infiltration, increased metastasis and poor prognosis (Armstrong *et al.*, 1997; Warabi, Kitagawa and Hirokawa, 2000; Mortara *et al.*, 2006; Forero *et al.*, 2016; Park *et al.*, 2017; Griffith *et al.*, 2022). To determine whether changes in MHCII expression in *Naip*$^{\Delta/\Delta}$ organoids was specific to tumour organoids, we repeated the IFNγ stimulation on tumour-derived and normal organoids, which are generated from healthy mouse colons (fig. 4.7). In normal organoids, both genotypes increased MHCII expression in response to IFNγ (fig. 4.7b). We next looked at class II transactivator (CIITA) RNA expression in the tumour organoid lines, as CIITA is a transcription factor which is upregulated in response to IFNγ and subsequently drives MHCII gene expression (Jorgovanovic *et al.*, 2020). The phenotype observed in tumour-derived organoids appeared to be maintained at the transcriptional level, with CIITA being upregulated in response to IFNγ stimulation in *Naip*$^{\Delta/\Delta}$ tumour-derived organoids but not in *Naip*$^{fl/fl}$ (fig. 4.8). However, it must be noted that this increase was not significant. The loss of MHCII expression in response to IFNγ during cancer is not uncommon; colonic IECs in only 42% of CRC carcinoma and 38% of adenoma patients expressed MHCII (Warabi, Kitagawa and Hirokawa, 2000). This adaptation allows tumours to avoid immune recognition (Axelrod *et al.*, 2019). However, as *Naip*$^{\Delta/\Delta}$ mice have increased tumorigenesis this increase in MHCII is counterintuitive and may reflect altered pathways due to Naip knockout.

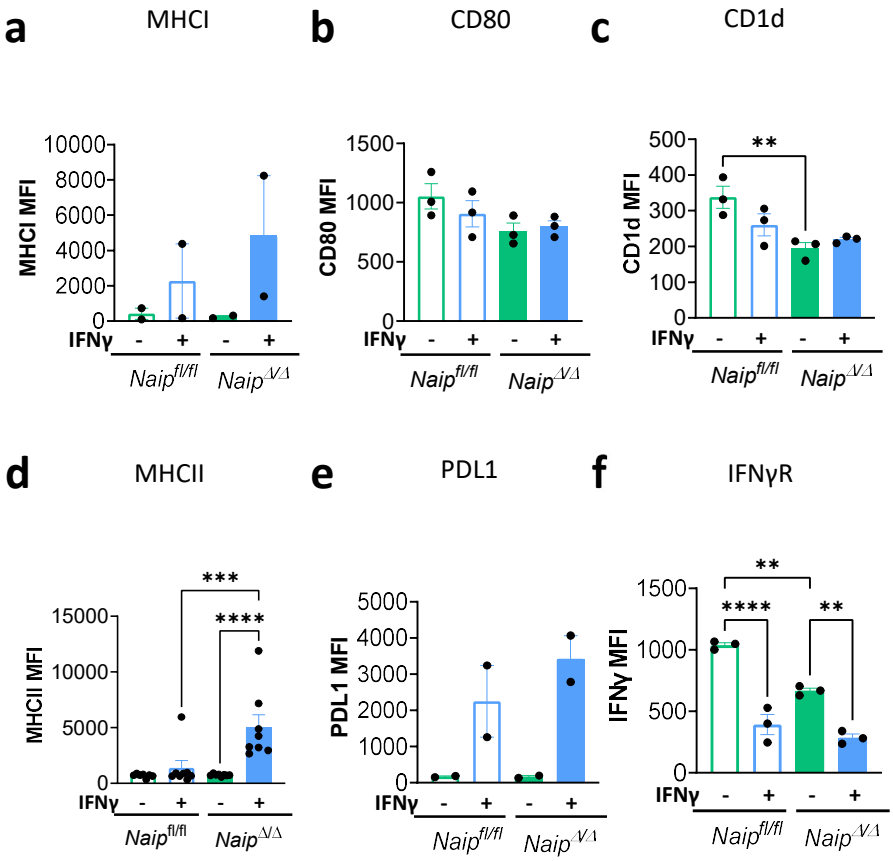

Figure 4.6 – Changes in epithelial cell markers in response to IFNγ stimulation

Naip$^{fl/fl}$ and *Naip*$^{\Delta/\Delta}$ tumour-derived organoids were either not treated or stimulated with IFNγ (10ng/ml) for 48hrs then analysed for expression of markers of interest by flow cytometry. **a** – MFI of MHCI. **b** – MFI of CD80. **c** – MFI of CD1d. **d** – MFI of MHCII. **e** – MFI of PDL1. **f** – MFI of IFNγR. Each individual point is a well of organoids analysed in an independent experiment, bars indicate mean ± s.e.m. N=2-8. One-way ANOVA performed with Tukey's post-test. **=P<0.01, ***=P<0.001, ****=P<0.0001.

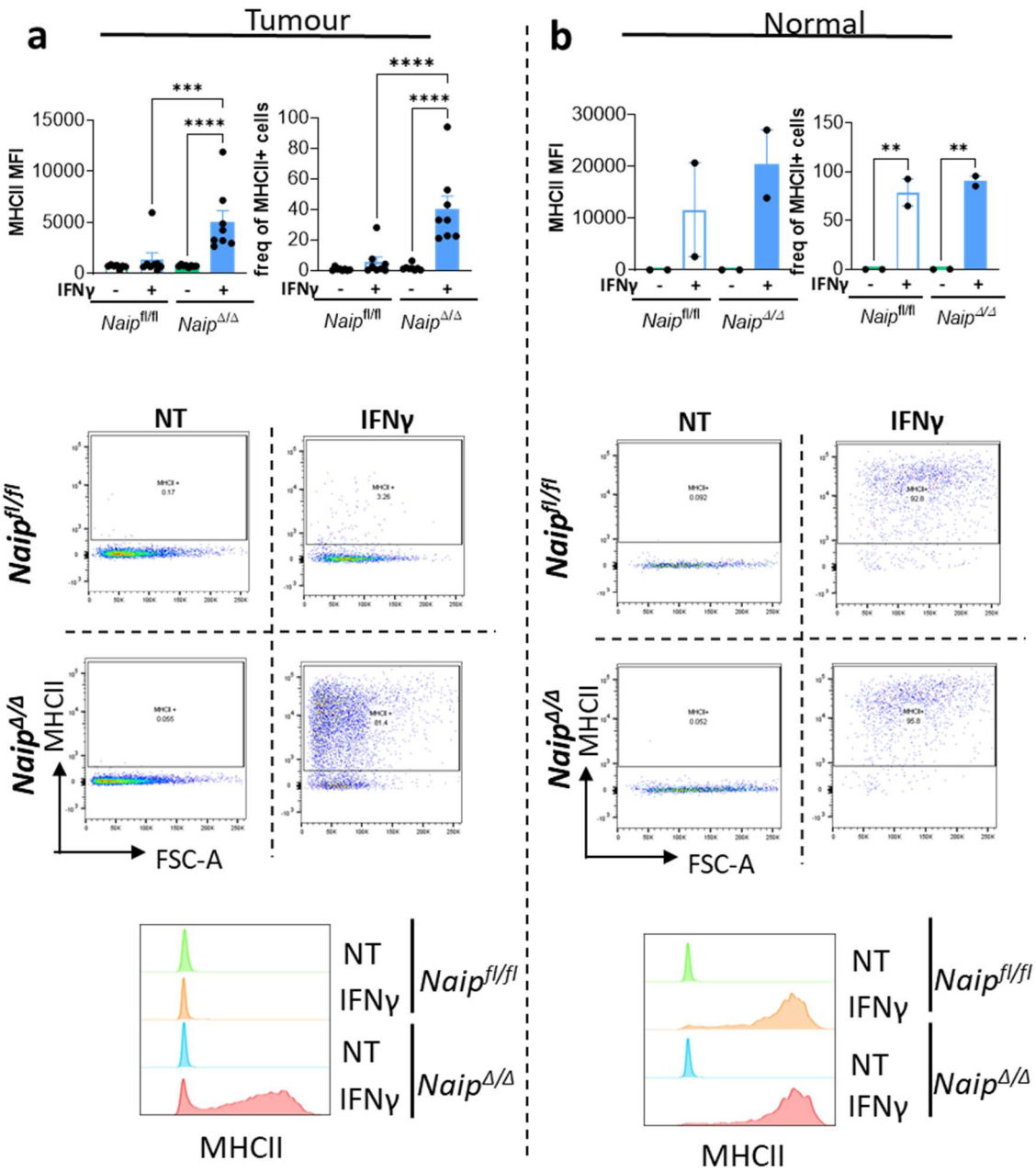

Figure 4.7 – Naip$^{\Delta/\Delta}$* tumour-derived organoids have increased MHCII upregulation compared to *Naip$^{fl/fl}$

(**a-b**) Tumour-derived (**a**) and normal (**b**) *Naip$^{fl/fl}$* and *Naip$^{\Delta/\Delta}$* organoids were stimulated with IFNγ (10ng/ml) for 48hrs then analysed by flow cytometry for MHCII expression. Bar plots show MFI and percentage of MHCII+ cells. Each individual point indicates a separate well of organoids (i.e. a biological replicate), performed over 4 independent experiments. N=8. Bars indicate mean ± s.e.m. One-way ANOVA performed with Tukey's post-test. **=P<0.01, ****=P<0.0001. Representative flow plots and histograms shown for each treatment group.

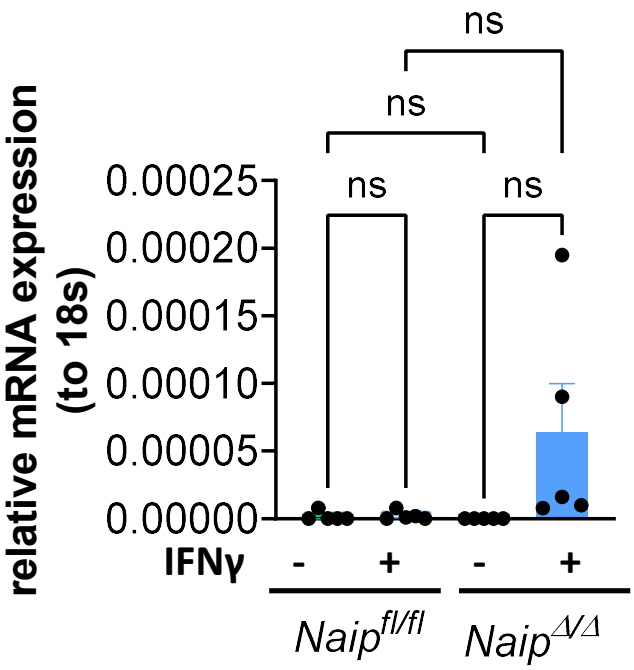

Figure 4.8 - Trend towards increased CIITA expression in Naip$^{\Delta/\Delta}$ tumour-derived organoids following IFNγ expression

Naip$^{fl/fl}$ and *Naip$^{\Delta/\Delta}$* tumour-derived organoids were stimulated with IFNγ (10ng/ml) for 48hrs then RNA collected and RTqPCR performed. Expression of CIITA relative to housekeeping gene 18s shown. Each individual point indicates a separate well of organoids (i.e. a biological replicate), performed over 2 independent experiments. N=5. Bars indicate mean ± s.e.m. One-way ANOVA performed with Tukey's post-test.

4.2.5 Signalling downstream of the IFNγ receptor appears unchanged between *Naip*$^{fl/fl}$ and *Naip*$^{\Delta/\Delta}$ tumour-derived organoids

As the IFNγR is expressed in *Naip*$^{fl/fl}$ tumour-derived organoids, but CIITA is not, we therefore hypothesised that there may be alteration in IFNγ signalling. To investigate IFNγ downstream of IFNγR, phosphorylation of STAT1, mTOR, Akt and ERK was assessed. STAT1 phosphorylation occurs in the classical pathway of IFNγ signalling but an alternative pathway involving Akt and mTOR phosphorylation has also been reported and may interact with the STAT1 pathway (Jorgovanovic *et al.*, 2020). When in their active phosphorylated form, ERK1/2 have also been shown to phosphorylate CIITA resulting in increased MHCII expression (Morgan *et al.*, 2015). Tumour-derived and normal organoids were stimulated with IFNγ for 1, 4 or 24hrs and phosphorylation of STAT1 at tyrosine position 701 (Tyr701) and serine position 727 (Ser727) was assessed. STAT1 is phosphorylated at Tyr701 by JAK1/2 in the initial steps of IFNγ signalling, but phosphorylation at Ser727, whist not required for translocation of STAT1 to the nucleus, is essential for full transcriptional activation (Platanias, 2005). No significant changes were observed between *Naip*$^{fl/fl}$ and *Naip*$^{\Delta/\Delta}$ in both tumour-derived (fig. 4.9a) and normal organoids (fig. 4.9b). Expression between tumour-derived and normal organoids were also comparable. Interestingly, when assessing mTOR, Akt, and ERK phosphorylation in tumour-derived organoids (fig. 4.10a-c), no change was seen in response to 1hr IFNγ stimulation in either *Naip*$^{fl/fl}$ and *Naip*$^{\Delta/\Delta}$. No significant changes were seen between *Naip*$^{fl/fl}$ and *Naip*$^{\Delta/\Delta}$, although a trend towards decreased p-ERK was observed in *Naip*$^{\Delta/\Delta}$ (fig. 4.10c). In contrast, normal *Naip*$^{fl/fl}$ organoids had distinct increase in mTOR, Akt, and ERK phosphorylation in response to IFNγ, whereas *Naip*$^{\Delta/\Delta}$ organoids did not. Phosphorylation of the signalling molecules also appeared reduced overall in *Naip*$^{\Delta/\Delta}$ organoids. However, this experiment was N=1 so some caution can be applied in the interpretation of this. From these experiments, we determined that in the tumour organoids, where we observed an alteration in MHCII expression, the components of IFNγ we investigated appear intact. In keeping with this, other IFN-stimulated markers such as PDL1 were strongly induced in both

genotypes. This indicates that the MHCII repression in *Naip*$^{fl/fl}$ may instead be a result of specific transcriptional (or translational) repression or DNA methylation status. We therefore considered how this change in MHCII expression could be reconciled with the increased tumorigenesis in *Naip*$^{\Delta/\Delta}$ mice.

4.2.6 Differences in response to IFNγ in *Naip*$^{\Delta/\Delta}$ tumour-derived organoids are not due to differences in prostaglandin expression

Previously, we had established that tumour-derived *Naip*$^{\Delta/\Delta}$ organoids had alterations in prostaglandin expression. We next investigated whether this could explain the differences seen in response to IFNγ stimulation by stimulating *Naip*$^{fl/fl}$ organoids with Ibu to reduce prostaglandin expression. Addition of Ibu and thus reduced $PGF_{2\alpha}$ (fig. 3.5) did not change the expression of MHCII, CD80, CD1d or IFNγR in comparison to IFNγ stimulation alone (fig. 4.11). We therefore concluded that altered eicosanoid production was not responsible for these changes.

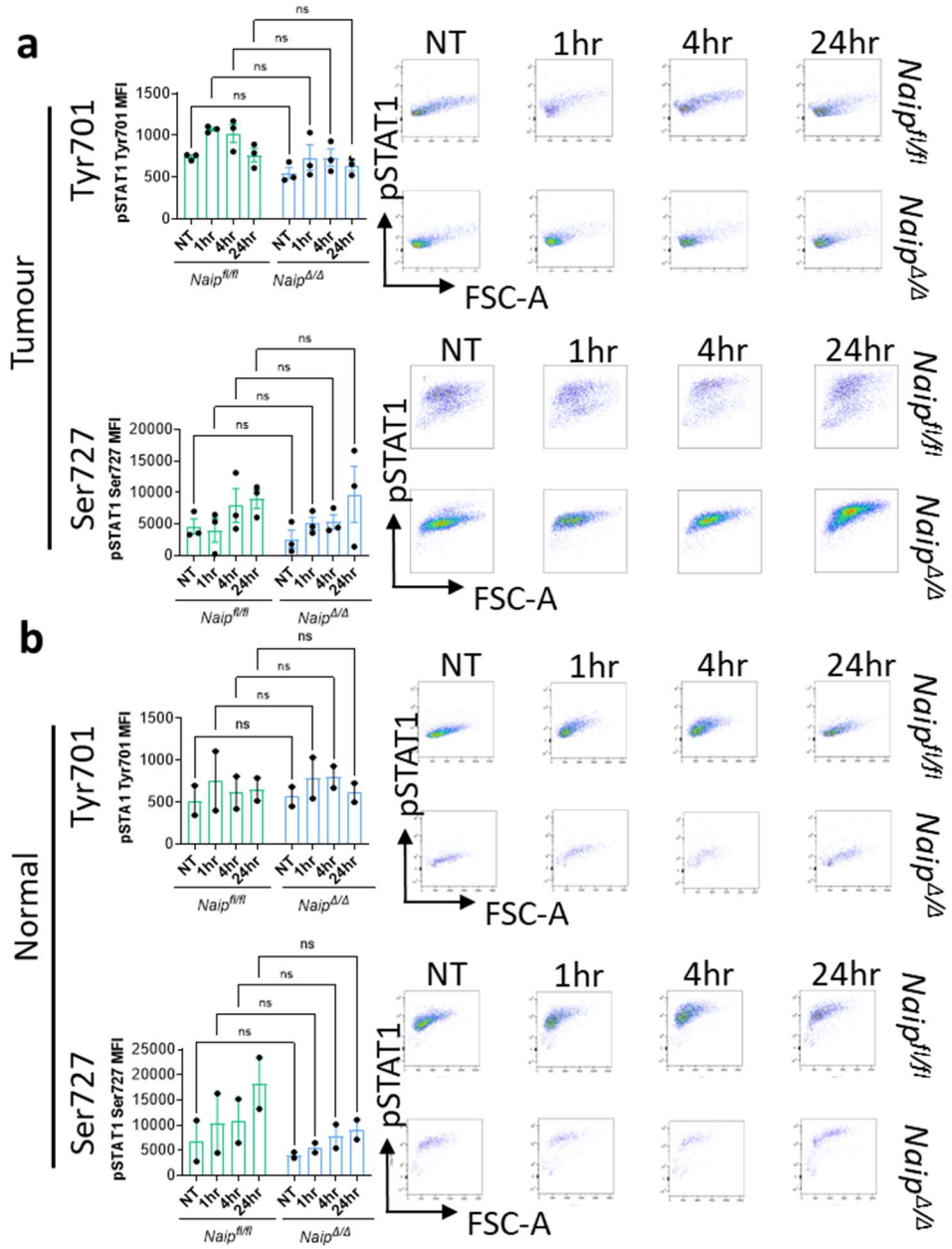

Figure 4.9 – No changes in pSTAT1 signalling downstream of IFNγ in Naip$^{fl/fl}$ and Naip$^{Δ/Δ}$ tumour-derived and normal organoids

Tumour-derived (a) and normal (b) *Naip$^{fl/fl}$* and *Naip$^{Δ/Δ}$* organoids were either not treated (NT) or stimulated with IFNγ (10ng/ml) for 1, 4 or 24hrs then analysed by flow cytometry for phosphorylation of STAT1 at the Tyr701 and Ser727 site. Bar graphs show MFI, with each individual point showing a well of organoids analysed in an independent experiment. N=2-3. Bars indicate mean ± s.e.m. Two-way ANOVA performed with Sidak's multiple comparisons test. Representative flow plots for each treatment shown.

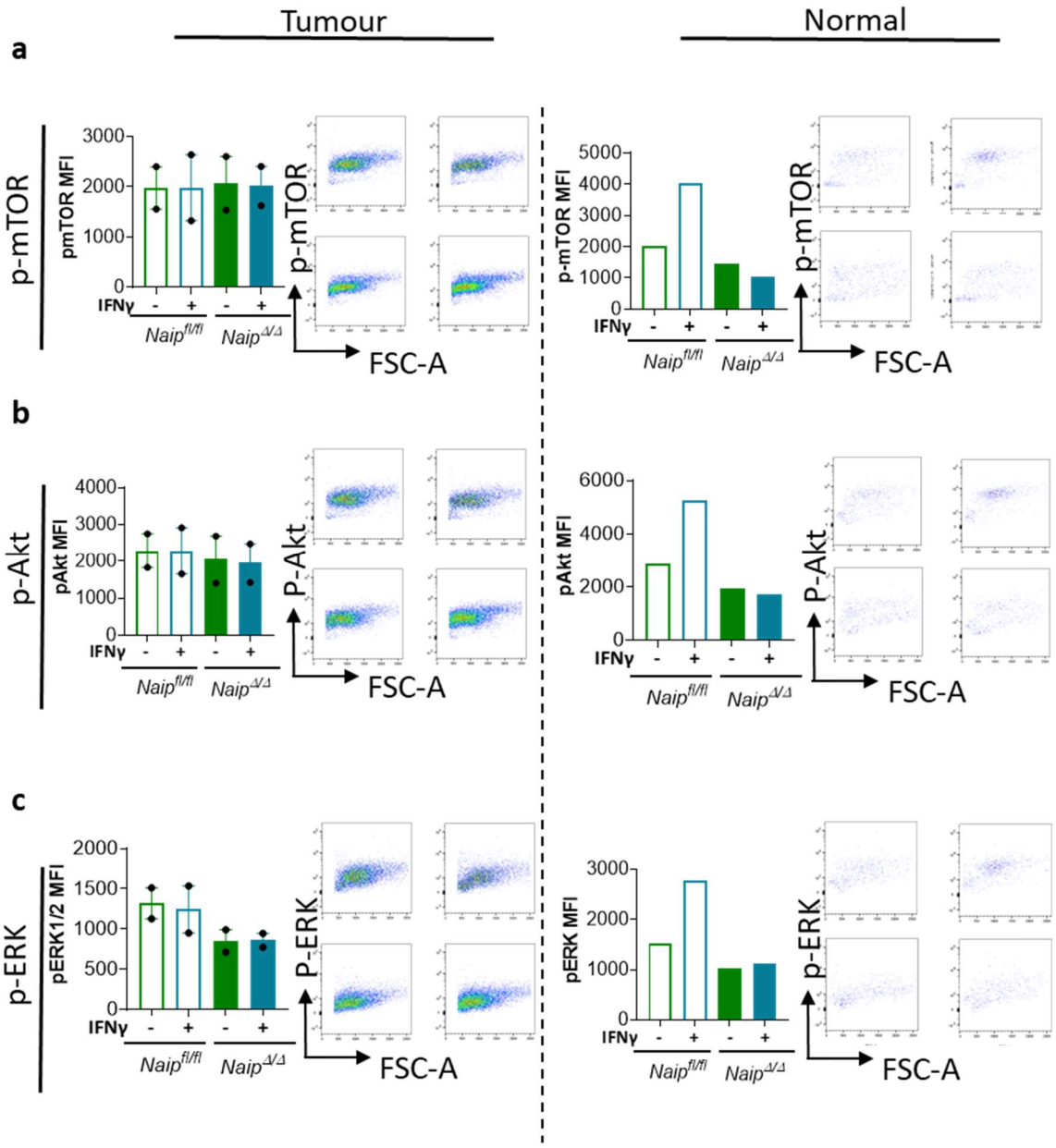

Figure 4.10 - No significant differences in signalling downstream of IFNγ in tumour-derived organoids

Naip$^{fl/fl}$ and *Naip*$^{\Delta/\Delta}$ tumour-derived and normal organoids were either not treated or stimulated with IFNγ (10ng/ml) for 48hrs then analysed for phosphorylation of signalling molecules downstream of IFNγ signalling. **a** – MFI of phosphorylated mTOR with representative flow plots. **b** – MFI of phosphorylated Akt with representative flow plots. **c** - MFI of phosphorylated ERK with representative flow plots. For tumour-derived organoid graphs each individual point is a well of organoids analysed in an independent experiment, bars indicate mean ± s.e.m. N=2. One-way ANOVA performed with Tukey's post-test. For normal organoid graphs N=1.

4.2.7 Coculture with *Naip*$^{\Delta/\Delta}$ organoids reduces IFNγ and CD69 expression in T cells

Whilst *Naip*$^{\Delta/\Delta}$ organoids appeared to have increased MHCII in response to IFNγ, we had not yet assessed the levels of IFNγ production in *Naip*$^{\Delta/\Delta}$ tumours. Nor have we measured T cell functionality, for example tumour killing capacity. However, in the previous chapter I explored CD4 and CD8 T cell activation, measured by IFNγ and CD69 expression, when co-cultured with *Naip*$^{fl/fl}$ and *Naip*$^{\Delta/\Delta}$ tumour organoid conditioned medium (fig. 3.4). Here, I found that both CD4 and CD8 T cells cultured in *Naip*$^{\Delta/\Delta}$ organoid conditioned medium had reduced IFNγ and CD69 expression compared to T cells cultured in *Naip*$^{fl/fl}$ conditioned medium, although this was only statistically significant for CD4 IFNγ expression. This could suggest that *Naip*$^{\Delta/\Delta}$ tumours are producing less IFNγ and therefore even though Naip$^{\Delta/\Delta}$ tumours retain IFN-induced MHCII capacity, it may be that the tumour environment does not support IFNγ production by T cells. It should be noted though that other immune cells populations (e.g. NK cells and macrophages) can be a source of IFNγ (Munder *et al.*, 1998), so expression of IFNγ and MHCII needs to be observed in ex vivo tissues, preferably by IHC methods to enable tissue localisation to be observed.

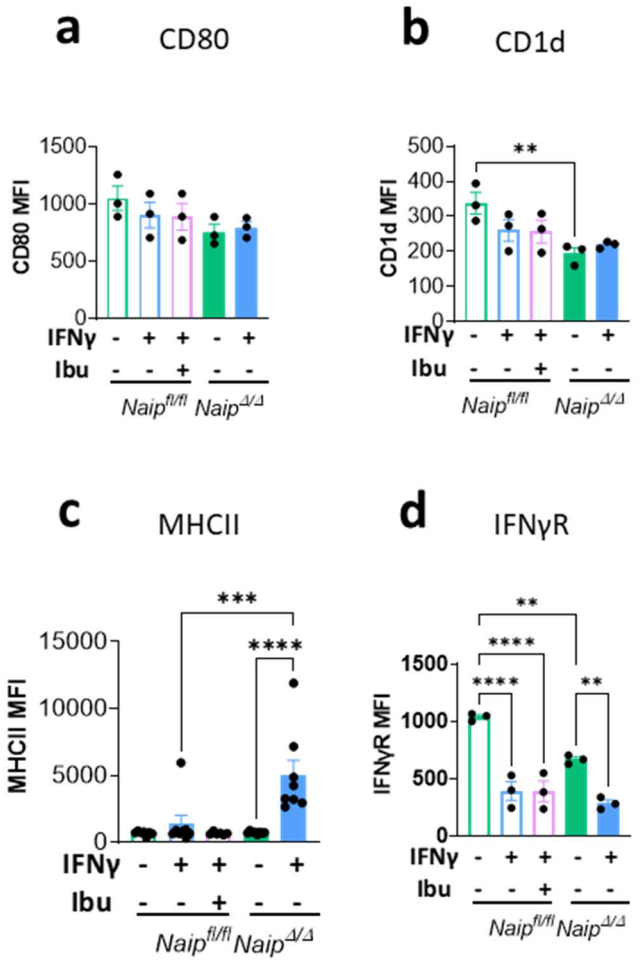

Figure 4.11 - Differences in response to IFNγ in Naip$^{Δ/Δ}$ tumour-derived organoids are not due to differences in prostaglandin expression.

Naip$^{fl/fl}$ and *Naip*$^{Δ/Δ}$ tumour-derived organoids were either not treated or stimulated with IFNγ (10ng/nl). Some conditions were administered IFNγ in combination with Ibu. After 48hrs organoids were analysed for expression of markers of interest by flow cytometry. **a** – MFI of CD80. **b** – MFI of CD1d. **c** – MFI of MHCII. **d** – MFI of IFNγR. Each individual point is a well of organoids (i.e. a biological replicate). For MHCII these were analysed over 4 independent experiments, N=8. For CD80, CD1d and IFNγR these were each analysed in an independent experiment, N=3. Bars indicate mean ± s.e.m. One-way ANOVA performed with Tukey's post-test. **=P<0.01, ***=P<0.001, ****=P<0.0001.

4.3 Discussion

In this chapter we aimed to identify changes to the immune compartment in *Naip*$^{\Delta/\Delta}$ mice during CRC. To achieve this, we focused on the TILs and IELs from tumour and normal tissue in the same mice, looking at overall numbers of different subsets, CD103 and CD69 expression, and at Tregs. We also identified an altered response to IFNγ in *Naip*$^{\Delta/\Delta}$ tumour-derived organoids, which could have implications for the immune response. However, we were left with unanswered questions regarding the mechanism of this altered response, and its relevance to tumours in *Naip*$^{\Delta/\Delta}$ mice.

4.3.1 Few changes between *Naip*$^{fl/fl}$ and *Naip*$^{\Delta/\Delta}$ mice TILs

Naip$^{\Delta/\Delta}$ mice have previously been shown to have increased tumorigenesis, and this was shown to coincide with increased expression of genes related to proliferation, such as *Bcl2*, *Myc* and *Ccnd1*, as well as increased STAT3 phosphorylation (Allam *et al.*, 2015). We aimed to establish if any changes were also occurring in the immune response. We had previously assayed the IELs (described in the next chapter of this thesis), due to their proximity to Naip expressing epithelial cells and given their integral role in gut maintenance and response to infection (Hu and Edelblum, 2017; Olivares-Villagómez and Van Kaer, 2018). However, these cells have also been implicated in CRC, for example by reducing tumour cell viability through cell-contact, CD103-dependent mechanisms (Morikawa *et al.*, 2021), with increased CD8+ IELs linked to better survival in human CRC (Chiba *et al.*, 2004). We therefore investigated the IELs in healthy sections of tissue alongside the TILs, gating on IEL subsets to compare the prevalence of immune cells between genotypes and disease states

Consistent with what has previously been described by Allam *et al*., *Naip*$^{\Delta/\Delta}$ mice had a significant increase in tumour weight, with a strong trend towards increased tumour burden and volume (fig. 4.1). In both genotypes, we observed an increase in TCRαβCD4s and TCRαβCD8αβs. CD4 and CD8 T cells have also been shown to infiltrate tumours previously, with CD8 infiltration linked to better outcomes, and CD4+ Tregs contributing to suppression of the anti-tumour response (Yu and Fu,

2006). Interestingly, *Naip*$^{\Delta/\Delta}$ mice had increased total TCRγδ+ cells in tumours when compared to *Naip*$^{fl/fl}$. This is despite a decrease in TCRγδCD8αα cells and appeared to be mainly driven by an increase in TCRγδCD4 cells. Some previous data has shown a decrease in γδ T cells following AOM+DSS treatment (Dasgupta *et al.*, 2021). The TCRγδCD4 population was not seen in the IELs of healthy tissue, and is generally considered to account for <1% of the TCRγδ+ population (Garcillán *et al.*, 2015). Previously TCRγδCD4 have been found to be low in healthy and tumour tissue (Szeponik *et al.*, 2020), and generally little has been published on them. Some changes in TILs versus IELs could be due to the lightly different digestion steps used, and in future it would be interesting to use the same digestion protocol as the TIL isolation may also be isolation lamina propria lymphocytes and peripheral lymphocytes that have migrated to the tumour. γδ T cells have been ascribed both anti-tumour and pro-tumorigenic effects, with TCR usage suggested to distinguish the two groups. T cells using Vγ4/Vγ6 have been suggested to infiltrate tumours and be pro-tumorigenic whereas Vγ1/Vγ7 are reported to be resident and anti-tumorigenic (Reis *et al.*, 2022). In tumours of AOM+DSS treated mice, Reis *et al*., found clonal expansion mostly of the Vγ6 subset with some expansion of Vγ1 cells, at the expense of the Vγ7 subset (Reis *et al.*, 2022). These Vγ6 cells were found to express PD-1 and IL-17, whereas the Vγ1 and Vγ7 cells isolated from tumours mainly expressed IFNγ but not PD-1 (Reis *et al.*, 2022). This was similar to results found in ACP mutant mice (Reis *et al.*, 2022). IL17 expression by Vγ6 cells appeared to have a pro-tumorigenic role, as deletion of Rorγt and therefore IL-17 production, in T cells resulted in smaller tumours (Reis *et al.*, 2022). It would be interesting to establish whether this effect was also seen in *Naip*$^{\Delta/\Delta}$ mice. Since Naip$^{\Delta/\Delta}$ mice experience increased tumorigenesis following AOM+DSS treatment, and considering the Vγ6 subset are proposed to be pro-tumorigenic, it is likely that tumours of *Naip*$^{\Delta/\Delta}$ mice have similar if not greater expansion of Vγ6 cells and this may account for the increase in γδ T cells compared to *Naip*$^{fl/fl}$. Loss of γδ T cells has been shown to increase polyp formation and histological inflammation following AOM+DSS (Dasgupta *et al.*, 2021). TCRγδ+ cells have also been shown to directly kill cancer cells (Todaro *et al.*,

2009; Tawfik *et al.*, 2019). However, other studies in various cancer types have suggest TCRγδ+ may promote tumours via IL-17 production (Fabre *et al.*, 2016). In CRC, one mouse study suggested TCRγδ and Th17 mediated IL-17 were redundant (Housseau *et al.*, 2016), but a study in humans suggested TCRγδ were the primary IL-17 source (Wu *et al.*, 2014). It would therefore be interesting to assess the IL-17 production by these cells in our model and determine the role these TCRγδ+ cells are having in *Naip*$^{\Delta/\Delta}$ mice.

We next assessed CD103 and CD69 expression in the TILs and IELs, finding that CD103 expression was increased in TCRαβCD4 and TCRαβCD8αα TILs of *Naip*$^{\Delta/\Delta}$ mice. However, there were no changes in the frequency of CD103+CD69+ between *Naip*$^{fl/fl}$ and *Naip*$^{\Delta/\Delta}$ mice, although CD103+CD69+ cells were reduced in tumours compared to healthy tissue in the case of TCRαβCD8αα, TCRαβCD8αβ and TCRγδ+ cells. CD103 interactions with E-cadherin has previously been shown to allow for IEL-mediated killing of small intestinal tumour cells, with *CD103*-/- mice having increased numbers of SI tumours (Morikawa *et al.*, 2021). Deletion of CD103 is known to affect IEL localisation to the gut, with CD103 deletion reducing the number of TCRαβCD8+ cells (Schön *et al.*, 1999) and retention of TCRγδ+ IELs (Edelblum *et al.*, 2012). In our data, CD103 expression was altered in tumour tissue versus healthy tissue differently in different T cell subsets, this did not necessarily correlate with changes seen in TIL number in specific subsets. CD103+ TILs have been associated with increased survival in various cancers including colorectal cancer (Webb *et al.*, 2014; Djenidi *et al.*, 2015; Wang *et al.*, 2016; Hu *et al.*, 2019; Talhouni *et al.*, 2023). CD69 is also reduced in certain TIL subsets which is consistent with other studies (Girardin *et al.*, 2013). CD103 and CD69 are markers sometimes associated with tissue resident memory cells (T_{rm}) (Dumauthioz, Labiano and Romero, 2018), however other papers have used CD103 and CD39 as markers for T_{rm} cells, finding that CD8+CD103+CD39+ cells predicted survival in certain CRC types (Talhouni *et al.*, 2023). CD39 would therefore be an interesting marker to investigate if this experiment was repeated.

Since *Naip*$^{\Delta/\Delta}$ mice have increased tumorigenesis we next investigated the Tregs of *Naip*$^{fl/fl}$ and *Naip*$^{\Delta/\Delta}$ mice treated with AOM+DSS. There was an increase in Tregs in both genotypes which coincided with the previously seen increase in TCRαβCD4 in TILs compared to normal tissue. This is consistent with previous findings that CRC patients have increased Tregs as the disease advances (Ling *et al.*, 2007). However, there were no changes between *Naip*$^{fl/fl}$ and *Naip*$^{\Delta/\Delta}$ mice. This is perhaps surprising given that *Naip*$^{\Delta/\Delta}$ mice have increased tumorigenesis and Tregs are associated with tumour progression (Aristin Revilla, Kranenburg and Coffer, 2022).

4.3.2 Changes in response to IFNγ signalling in *Naip*$^{\Delta/\Delta}$ tumour-derived organoids

We next investigated expression of markers which could modulate the immune response during CRC. Strikingly, we found that *Naip*$^{fl/fl}$ tumour-derived organoids did not upregulate MHCII in response to IFNγ whereas *Naip*$^{\Delta/\Delta}$ organoids did. MHCII expression is known to be relevant in anti-tumour responses, with reduced MHCII leading to reduced immune infiltration (Warabi, Kitagawa and Hirokawa, 2000; Sconocchia *et al.*, 2014; Axelrod *et al.*, 2019; Griffith *et al.*, 2022). In humans, antigen expression by HLA class II molecules is associated with favourable outcomes (Sconocchia *et al.*, 2014). Interestingly, activation of the NLRC4 inflammasome has previously been shown to regulate MHCII expression in IECs via IFNγ (Van Der Kraak *et al.*, 2021). Caspase-3/7 mediated cleavage and inactivation of gasdermin D has also been shown to promote MHCII expression in IECs in response to dietary antigens (He *et al.*, 2023). This study by He *et al*. highlighted that caspases appear to have non-redundant functions as a result of alternative substrate cleavage sites. This supported the idea gasdermin D and the caspases have divergent roles, although whether the non-canonical cleavage of gasdermin D completely abrogates its pyroptotic activity is still debated (He *et al.*, 2023). However, both genotypes of normal organoids upregulated MHCII. This is perhaps unsurprising, as expression of HLA class II molecules can be variable in CRC, with one study finding expression in 23% of human tumours, and only two of four CRC lines tested increasing expression in response to IFNγ (Sconocchia *et al.*, 2014). We decided to investigate if this reflected altered IFNγ

signalling in *Naip*$^{\Delta/\Delta}$ tumour-derived organoids compared to *Naip*$^{fl/fl}$. Levels of CIITA, which drives MHCII transcription downstream of IFNγ (Steimle *et al.*, 1994), were not induced in *Naip*$^{fl/fl}$ tumour-derived organoids, but were slightly increased in *Naip*$^{\Delta/\Delta}$ tumour-derived organoids following IFNγ stimulation, which would be expected given MHCII is increased in these cells. However, levels of STAT1 phosphorylation appeared comparable between genotypes. We therefore looked at an alternative signalling pathway downstream of IFNγ involving Akt and mTOR (Jorgovanovic *et al.*, 2020). ERK has also been shown to regulate CIITA during IFNγ-mediated MHCII expression, so levels of ERK were also assessed (Morgan *et al.*, 2015). No significant changes were seen in mTOR, Akt or ERK in either genotype of tumour-derived organoids. It has been reported that IFNγ concentration can affect which pathways are activated, so possibly this concentration does not activate Akt/mTOR or ERK as strongly (Song *et al.*, 2019). However, in normal organoids, a response to IFNγ stimulation was seen in *Naip*$^{fl/fl}$, but not *Naip*$^{\Delta/\Delta}$. Possibly this is due to low viability of the normal organoids, which died quickly upon being dissociated into single-cell suspension. As this was repeated only once, it is difficult to be certain. Overall, we concluded that signalling is intact in the *Naip*$^{fl/fl}$ tumour organoids, which is supported by the upregulation of PDL1 in response to IFNγ (fig 4.6), suggesting the suppression of MHCII is due to tumour-intrinsic transcriptional repression.

We also identified other markers which would be affected by IFNγ stimulation and tested their expression in tumour-derived organoids. CD1d, a non-classical MHCI molecule, was not upregulated by IFNγ in either genotype which has previously been reported to be in intestinal epithelial cells (Colgan *et al.*, 1996). Interestingly, IFNγR expression was reduced at baseline in *Naip*$^{fl/fl}$ compared to *Naip*$^{\Delta/\Delta}$, which is counter intuitive to the fact *Naip*$^{\Delta/\Delta}$ organoids were more responsive to IFNγ in the case of MHCII. This could possibly be explained by this internalisation of the receptor (Zanin *et al.*, 2021).

It was surprising that few changes were seen in TILs of *Naip*$^{\Delta/\Delta}$ mice and MHCII upregulation in response to IFNγ remained intact in *Naip*$^{\Delta/\Delta}$ organoids, yet *Naip*$^{\Delta/\Delta}$ mice still had increased tumorigenesis. We therefore investigated whether there may be alterations in IFNγ expression in *Naip*$^{\Delta/\Delta}$ tumours. Due to a limited number of tumours, we were unable to perform IFNγ ELISA on in vivo samples. We therefore performed co-cultures of splenocytes from *Ifng*-Tocky reporter mice with supernatant from tumour-derived organoids. We observed that CD4 T cells cultured with supernatant from *Naip*$^{\Delta/\Delta}$ organoids had reduced IFNγ expression. This suggests that whilst *Naip*$^{\Delta/\Delta}$ tumours may still respond to IFNγ by upregulating MHCII, this may be counteracted by an overall reduction in IFNγ in the tumour. Therefore, the net effect of IFNγ/MHCII signalling on the immune compartment in *Naip*$^{\Delta/\Delta}$ tumours may be comparable to *Naip*$^{fl/fl}$ tumours that have lower MHCII induction but possibly higher IFNγ expression. This may explain why *Naip*$^{\Delta/\Delta}$ mice have increased tumorigenesis despite increased signalling that would suggest increased immune activation.

4.3.3 Limitations

One major limitation of this in vivo work is a limited number of mice in the *Naip*$^{fl/fl}$ group. *Naip*$^{fl/fl}$ mice were more susceptible to weight loss during the first round of DSS treatment than their *Naip*$^{\Delta/\Delta}$ littermates, meaning more were sacrificed due to the 20% weight loss limit. Tumour induction was also variable. Tumorigenesis in this model depends on the three rounds of DSS driving inflammation, however susceptibility to DSS-induced inflammation can be affected by the microbiota and is therefore facility-dependent (Brinkman *et al.*, 2013; Li *et al.*, 2018; Khan *et al.*, 2022). As this model takes almost 9 weeks to carry out, whilst mice were also being used for other experiments, this severely limited the number of times we could perform the protocol. Ideally, in future work we would be able to repeat these experiments multiple times.

4.3.4 Conclusions

To conclude, we confirmed that *Naip*$^{\Delta/\Delta}$ mice have increased tumorigenesis compared to *Naip*$^{fl/fl}$, and that changes occur in lymphocyte populations from healthy to tumour tissue. In tumours of *Naip*$^{\Delta/\Delta}$ mice there was a slightly larger increases in TCRγδ+ and TCRγδCD4 cells compared to *Naip*$^{fl/fl}$, and so these γδ T cell functions in the *Naip*$^{\Delta/\Delta}$ mice may warrant further investigation. Despite the differences in tumorigenesis, no changes were seen in the Treg compartment between *Naip*$^{\Delta/\Delta}$ and *Naip*$^{fl/fl}$ mice. However, there were alterations in CD1d and IFNγR at baseline and in MHCII in response to IFNγ in tumour-derived *Naip*$^{\Delta/\Delta}$ organoids, which could affect the T cell responses during CRC. No changes were observed in IFNγ signalling, and the mechanism by which NAIP deletion results in increased MHCII upregulation remains to be elucidated. However, since CD4 T cells cultured with supernatant from *Naip*$^{\Delta/\Delta}$ organoids express decreased IFNγ, it may be that *Naip*$^{\Delta/\Delta}$ tumours have less IFNγ signalling and therefore the effect of increased MHCII on the immune compartment is negligible, allowing for the increased tumorigenesis phenotype.

5 The effect of Naips on the IEL compartment during infection

5.1 Introduction

Much research has focused on the response of Naips to STm, both in IECs and macrophages, and the dynamics of inflammasome activation and IEC expulsion (Rauch *et al.*, 2017). Briefly, activation of epithelial Naips by STm results in NLRC4 inflammasome formation and resultant caspase 1 and 8 activation, resulting in IL18 and PGE_2 release, alongside cleavage of gasdermin D and subsequent expulsion of the infected cell, allowing for limitation of bacterial dissemination (Rauch *et al.*, 2017). In the absence of Naips, STm infection results in increased bacterial burden and eventual epithelial barrier collapse, driven by bone marrow-cell derived TNFα release (Fattinger *et al.*, 2021) Whilst inflammasome activation is known to result in IL-18 and PGE_2 release (Rauch *et al.*, 2017), which will have effects on the immune compartment and aid in bacterial clearance, the exact effects Naips exert on immune cells remains to be studied in detail, but as implied by Fattinger *et al*. (2021), there were consequences of the increased bacterial burden on immune infiltrates in mice lacking Naips. Aside from Naips role in pathogen recognition, Naips have been demonstrated to exacerbate inflammation during colitis, yet reduce tumorigenesis (Allam *et al.*, 2015), as discussed in the previous chapter.

A growing body of evidence suggests that intraepithelial lymphocytes (IELs) have important protective and pathogenic roles during infection and disease of the gut. In response to bacteria, IELs have been shown to regulate mucus and antimicrobial peptide production and kill infected cells (Hu, Jia and Edelblum, 2018). Certain IEL subsets, in particular those which are TCRγδ+, have a protective effect in colitis (Inagaki-Ohara *et al.*, 2004). The survival and maintenance of these cells is dependent on IL-15 expression, particularly by IECs which present IL-15 on its receptor to be recognised in a cell-contact dependent manner (Dubois *et al.*, 2002). IL-15 expression has been shown to be driven by PRRs such as TLR4, TLR2 and NOD2 via downstream MyD88 signalling (Kaneko *et al.*, 2004; Yu *et al.*,

2006; Ma *et al.*, 2009; Jiang *et al.*, 2013; Qiu *et al.*, 2016). PRRs can also affect the IEL compartment during infection, with TLR9 shown to influence IELs in response to STm infection. TLR9-/- mice had increased TCRγδ+ IELs and expression of CD69 on TCRγδ+ and CD8αβ+ IELs (Li *et al.*, 2017). This exemplifies the role innate signalling pathways can have on the IEL compartment, with downstream consequences for infection and inflammation. It is also noteworthy that Naips are expressed in IECs as well as some innate immune cells (Allam *et al.*, 2015), and as a result are in prime position to influence the IELs which patrol the epithelial layer. We therefore questioned what effect NAIPs may be having on the IEL compartment, and how this might impact the response to DSS, which induces colitis, and STm. To address this, we utilised *Naip1-6*$^{IEC\Delta/\Delta}$ mice (referred to from here as *Naip*$^{\Delta/\Delta}$) in which all Naip isoforms are deleted in the IECs only, using a Villin-Cre driver, herein called *Naip*$^{\Delta/\Delta}$. Here we focus mainly on the colon as this area of the gut has the highest NAIP expression and the DSS model primarily causes inflammation in the colon (Yazbeck *et al.*, 2011; Chassaing *et al.*, 2014).

In this chapter we aimed to:

- Investigate whether the IEL compartment was altered in *Naip*$^{\Delta/\Delta}$ mice at baseline.
- Investigate whether the IEL compartment was altered in *Naip*$^{\Delta/\Delta}$ mice following DSS treatment or STm infection.
- Understand the mechanism by which any changes in IEL numbers occur.

5.2 Results

5.2.1 No changes in IEL numbers in naïve *Naip*$^{\Delta/\Delta}$ mice

Given the proximity of NAIP-containing epithelial cells to the IEL compartment, I assessed if there were any changes in IELs in unperturbed *Naip*$^{\Delta/\Delta}$ mice. Due to the scarcity of certain populations, we focused on TCR+ IELs, dividing the IELs into TCRαβCD4, TCRαβCD8αα, TCRαβCD8αβ, all TCRγδ+ and TCRγδCD8αα (fig. 5.1a). The number of each subgroup was calculated as the per colon or small intestine (fig. 5.1b-c). Overall, *Naip*$^{\Delta/\Delta}$ mice had no significant changes in any IEL subsets in the colon or SI. A trend towards decreased TCRγδ+ cells was observed, but this was mainly driven by three particularly high *Naip*$^{fl/fl}$ mice.

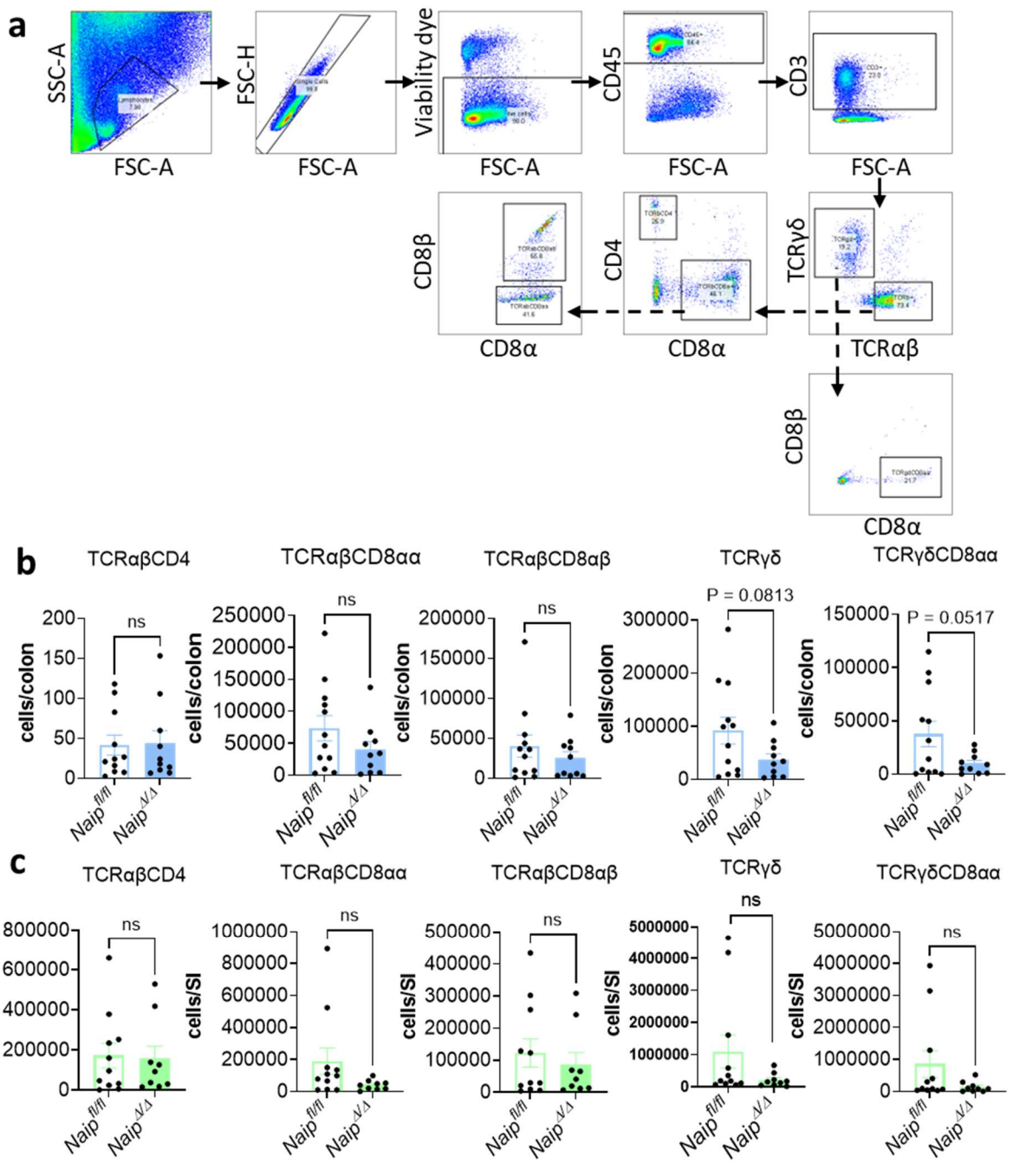

Figure 5.1 - Trend towards decreased TCRγδCD8αα IELs in colons of naive Naip$^{Δ/Δ}$ mice

IELs were isolated from the colons and small intestines (SI) of *Naip*$^{fl/fl}$ and *Naip*$^{Δ/Δ}$ mice and analysed by flow cytometry to determine the numbers of different IEL subsets. **a** – Gating strategy to identify different IEL subsets. Cells were gated for lymphocytes, followed by single cells, live cells, CD45+ and CD3+. Cells were then split between TCRαβ+ and TCRγδ+. TCRαβ+ cells were then gated to determine the CD4+, CD8αα+ and CD8αβ+ groups, whereas TCRγδ+ cells were gated on the total population and CD8αα. **b** – number of cells of each IEL subset in the whole colon of *Naip*$^{fl/fl}$ and *Naip*$^{Δ/Δ}$ mice. **c** - number of cells of each IEL subset in the whole small intestine (SI) of *Naip*$^{fl/fl}$ and *Naip*$^{Δ/Δ}$ mice. Each individual point indicates a separate mouse. *Naip*$^{fl/fl}$ N=12, *Naip*$^{Δ/Δ}$ N=10, four independent experiments. One-way ANOVA statistical analysis was performed with Tukey's post-test. * = P<0.05, **=P<0.001

5.2.2 No changes in colonic IELs following disruption of the epithelial barrier with DSS

Considering that Naip expression is increased in the colon compared to the SI, going forward we focused on the colonic IELs. As no change had been observed in naïve mice, and *Naip*$^{\Delta/\Delta}$ mice have been shown to be protected from colitis (Allam *et al.*, 2015), the effect of DSS administration on colonic IELs in *Naip*$^{\Delta/\Delta}$ mice was investigated. Mice were administered 3% DSS in drinking water for 7 days followed by 7 days of normal water, to enable reparation of the epithelial barrier (fig. 5.2a). Throughout the experiment, no significant differences in weight loss were seen between *Naip*$^{fl/fl}$ and *Naip*$^{\Delta/\Delta}$ mice, though, consistent with previous data, there was a trend for lower weight loss in *Naip*$^{\Delta/\Delta}$ mice (fig. 5.2b). At day 14 mice were sacrificed and colons excised. To compare the IEL numbers seen in DSS-treated mice with baseline, some untreated *Naip*$^{fl/fl}$ mice were also sacrificed. Colon length was comparable between *Naip*$^{fl/fl}$ and *Naip*$^{\Delta/\Delta}$ DSS-treated mice, however when compared to untreated Naip$^{fl/fl}$ mice DSS-treated *Naip*$^{fl/fl}$ mice experienced statistically significant colon shortening but *Naip*$^{\Delta/\Delta}$ did not (fig. 5.2b), though the shortening was mild (approximately 0.5cm). In the IELs, there was a strong trend towards increased IEL numbers upon DSS treatment in all subgroups, with numbers in *Naip*$^{\Delta/\Delta}$ appearing slightly higher than *Naip*$^{fl/fl}$ (fig. 5.2d-e). However, none of these changes were significant, except when comparing non-treated *Naip*$^{fl/fl}$ with DSS-treated *Naip*$^{\Delta/\Delta}$.

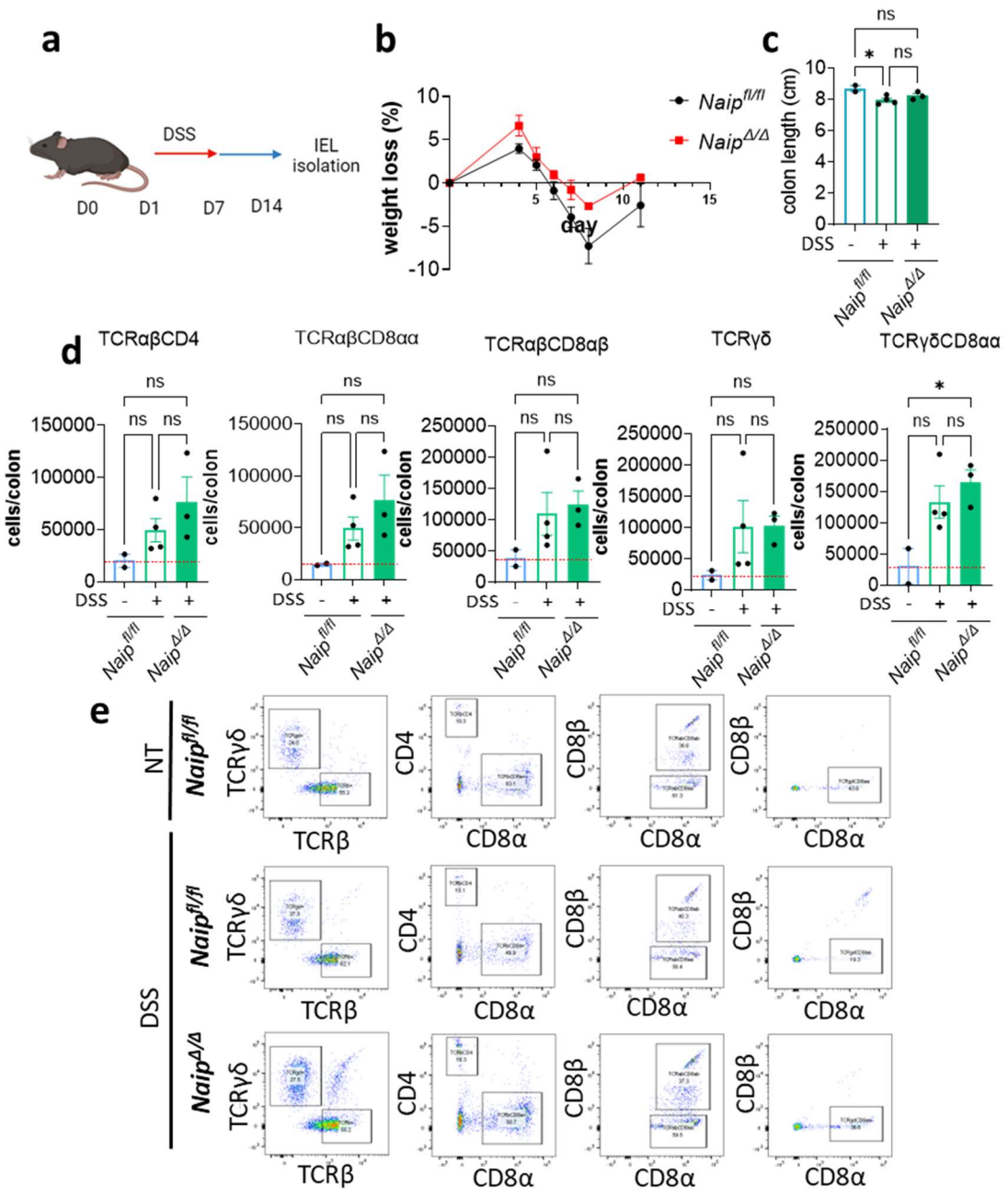

Figure 5.2 - DSS-treated mice have increased colonic IELs but no difference between Naip$^{fl/fl}$ and Naip$^{\Delta/\Delta}$ mice

a - Mice were administered one round of DSS in drinking water for 6 days then returned to normal water for 7 days then sacrificed and colonic IELs isolated. Some *Naip*$^{fl/fl}$ were not treated to determine baseline IEL number. Figure made in Biorender. **b** – Weight loss during DSS treatment. **c** – colon length of *Naip*$^{fl/fl}$ and *Naip*$^{\Delta/\Delta}$ mice following DSS treatment and control *Naip*$^{fl/fl}$ (**d**-**e**) – Number of cells per colon of untreated *Naip*$^{fl/fl}$ mice and DSS-treated *Naip*$^{fl/fl}$ and *Naip*$^{\Delta/\Delta}$ mice (**d**) and corresponding flow plots (**e**) of indicated IEL populations. For (**b**) and (**d**), each individual point indicates a separate mouse. Dotted line indicated average IEL number in naïve mice. Bars indicate mean ± s.e.m. untreated *Naip*$^{fl/fl}$ N=2, treated *Naip*$^{fl/fl}$ N=4, *Naip*$^{\Delta/\Delta}$=3, one independent experiment. For (**b**) two-way ANOVA performed with Sidak's post-test. For (**d**) one-way ANOVA statistical analysis was performed with Tukey's post-test. * = P<0.05.

5.2.3 Increased TCRαβCD8αα and TCRγδ colonic IELs in *Naip*$^{\Delta/\Delta}$ mice following STm infection

The effect of Naip knockout on IELs during STm infection was next investigated. Mice were treated with DSS as before to disrupt the epithelial barrier, before infection with STm$^{\Delta aroA}$ (fig. 5.3a) (Gillis *et al.*, 2018). Contrary to previous data, weight loss was greater in *Naip*$^{\Delta/\Delta}$ mice at the beginning of the experiment, but less than *Naip*$^{fl/fl}$ towards the end (fig. 5.3b). *Naip*$^{fl/fl}$ had slightly shortened colon lengths compared to *Naip*$^{\Delta/,\Delta}$ but this was not significant (fig. 5.4c). A trend for increased IELs in *Naip*$^{\Delta/\Delta}$ in all subsets was observed, but this increase was significant in TCRαβCD8αα, TCRγδ+ and TCRγδCD8αα subsets (fig 5.3d-e). To see if this change extended beyond the IEL compartment, activation markers CD25 and CD69 on total CD4+ and CD8+ T cells in the mesenteric lymph nodes (mLNs) were also investigated. No changes were observed between *Naip*$^{fl/fl}$ and *Naip*$^{\Delta/\Delta}$ in expression of CD69 or CD25 in CD4 (fig. 5.4a-c) or CD8 (fig. 5.5a-c) T cells. Equally no changes were apparent in the frequency of naïve (CD44-CD62L+), T central memory (Tcm; CD44+CD62L+) and effector (CD44+CD62L-) CD4+ T cells (fig. 5.4d). However, a significant increase in effector CD8 T cells was seen in *Naip*$^{\Delta/\Delta}$ mice (fig. 5.5d).

5.2.4 IL-17 expression is increased following DSS treatment

Next, we investigated whether the changes in IELs seen following DSS and DSS+STm treatment was concurrent with changes in the cytokine profile. Following treatment with either DSS or DSS+STm, pieces of colon were homogenised and levels of IFNγ, IL-17 and IL-10 determined by ELISA. Following DSS treatment (fig. 5.6a), there was a trend for increased IFNγ and a significant increase in IL-17 in both *Naip*$^{fl/fl}$ and *Naip*$^{\Delta/\Delta}$. However, IL-17 was increased most significantly in *Naip*$^{fl/fl}$. Following DSS+STm treatment (fig. 5.6b), IFNγ expression seemed comparable between *Naip*$^{fl/fl}$ and *Naip*$^{\Delta/\Delta}$ mice and to untreated mice. Whereas IL-17 expression mirrored DSS-treated mice, with an increase

in both genotypes but particularly in *Naip*$^{fl/fl}$, although in DSS+STm treated mice these changes were not significant. Meanwhile IL-10 expression was comparable between all treatment groups.

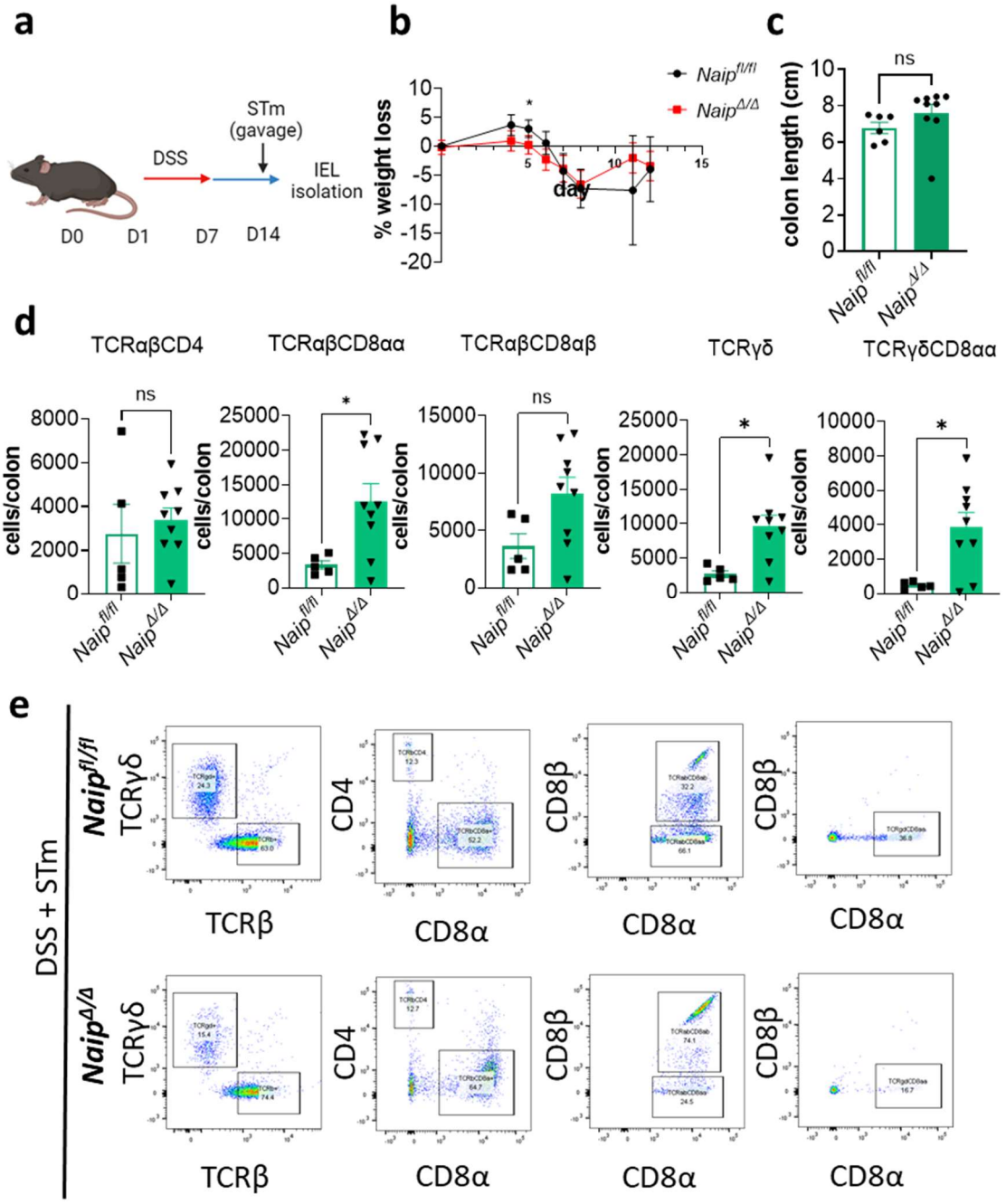

Figure 5.3 - Certain IEL subsets are increased in colons of Naip$^{\Delta/\Delta}$ mice following DSS+STm treatment

a - Mice were administered one round of DSS in drinking water for 6 days then returned to normal water for 7 days. On day 13 mice were administered STm$^{\Delta aroA}$ via oral gavage. 24hrs later mice were sacrificed and colonic IELs isolated. Firgure made in biorender. **b** – Weight loss during DSS treatment. **c** – colon length of *Naip$^{fl/fl}$* and *Naip$^{\Delta/\Delta}$* mice. (**d-e**) – Number of cells per colon of DSS+STm treated *Naip$^{fl/fl}$* and *Naip$^{\Delta/\Delta}$* mice (**d**) and corresponding flow plots (**e**). For (**b**) and (**d**), each individual point indicates a separate mouse. Bars indicate mean ± s.e.m. *Naip$^{fl/fl}$* N=6, *Naip$^{\Delta/\Delta}$* N=9, three independent experiments. For (**b**) two-way ANOVA performed, with Sidak's post test. For (**d**) one-way ANOVA statistical analysis was performed with Tukey's post-test. * = P<0.05

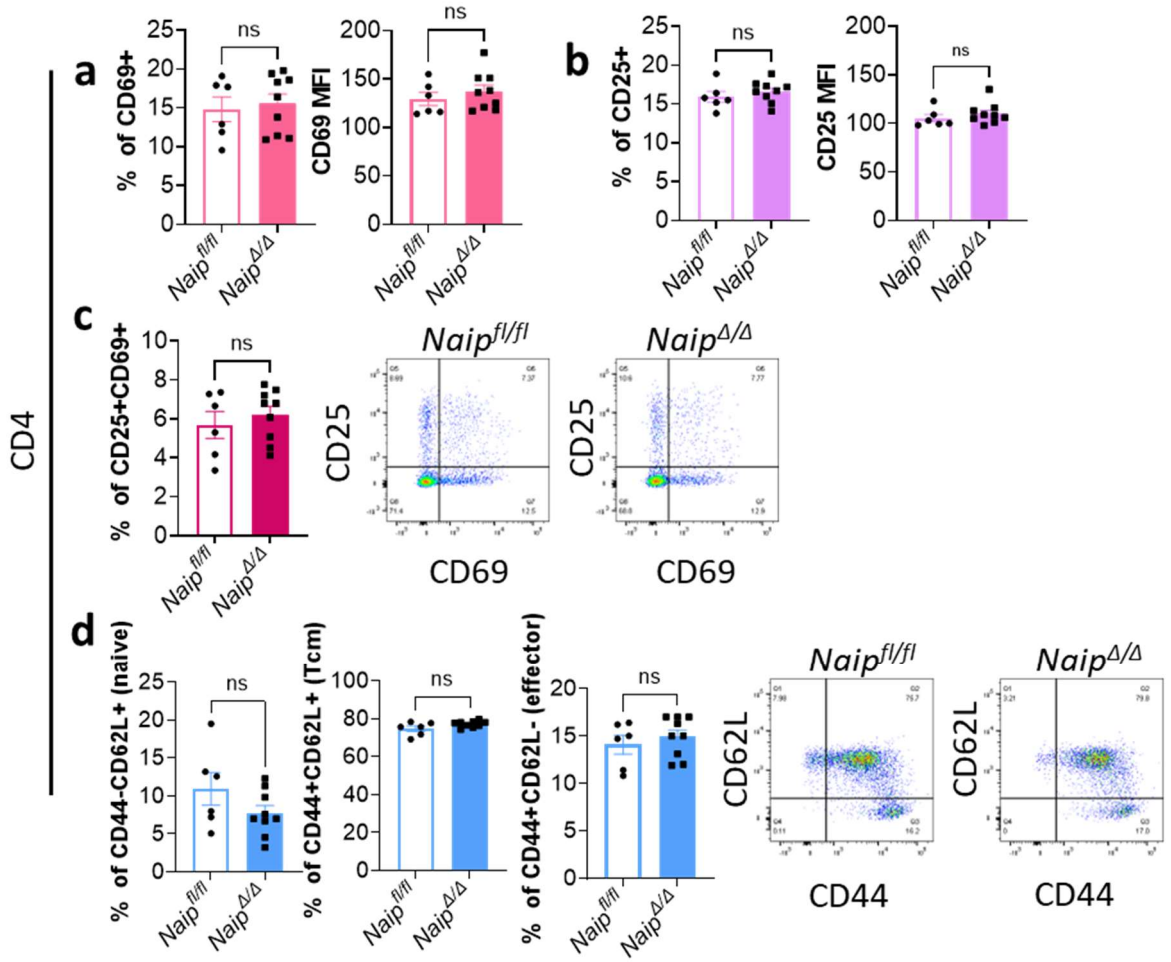

Figure 5.4 - No changes in activation markers or proportion of memory cells in CD4+ T cells from mLNs following DSS+STm treatment

Naip$^{fl/fl}$ and *Naip*$^{\Delta/\Delta}$ mice were administered one round of DSS in drinking water for 6 days then returned to normal water for 7 days. On day 13 mice were administered STm$^{\Delta aroA}$ via oral gavage. 24hrs later mice were sacrificed and mLNs excised and analysed by flow cytometry. (**a-e**) CD4+ T cells. **a** – Percentage of CD69+ CD4 T cells and CD69 MFI of CD4 T cells. **b** - Percentage of CD25+ CD4 T cells and CD25 MFI of CD4 T cells. **c** – Percentage of CD25+CD69+ double-positive CD4 T cells with example flow plots. (**d)** – Percentage of CD44-CD62L+ (naïve), CD44+C62L+ (Tcm) and CD44+CD62L- (effector) CD4 T cells with example flow plots. For bar plots, each individual point indicates a separate mouse. Bars indicate mean ± s.e.m. *Naip*$^{fl/fl}$ N=6, *Naip*$^{\Delta/\Delta}$ N=9 three independent experiments. One-way ANOVA statistical analysis was performed with Tukey's post-test. * = P<0.05.

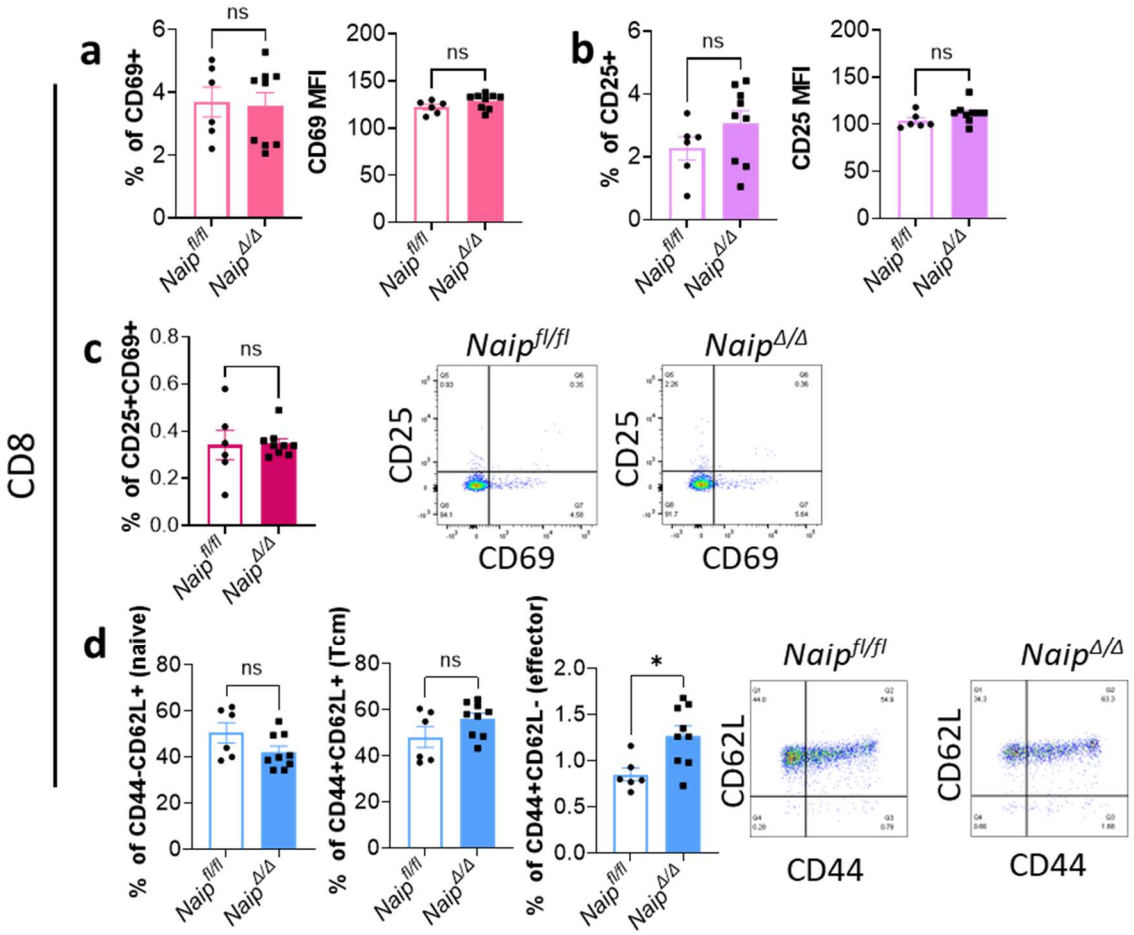

Figure 5.5 - No changes in activation markers or proportion of memory cells in CD8+ T cells from mLNs following DSS+STm treatment

Naip$^{fl/fl}$ and *Naip*$^{\Delta/\Delta}$ mice were administered one round of DSS in drinking water for 6 days then returned to normal water for 7 days. On day 13 mice were administered STm$^{\Delta aroA}$ via oral gavage. 24hrs later mice were sacrificed and mLNs excised and analysed by flow cytometry. (**a-e**) CD8+ T cells. **a** – Percentage of CD69+ CD8 T cells and CD69 MFI of CD8 T cells. **b** - Percentage of CD25+ CD8 T cells and CD25 MFI of CD8 T cells. **c** – Percentage of CD25+CD69+ double-positive CD8 T cells with example flow plots. (**d)** – Percentage of CD44-CD62L+ (naïve), CD44+C62L+ (Tcm) and CD44+CD62L- (effector) CD8 T cells with example flow plots. For bar plots, each individual point indicates a separate mouse. Bars indicate mean ± s.e.m. *Naip*$^{fl/fl}$ N=6, *Naip*$^{\Delta/\Delta}$ N=9 three independent experiments. One-way ANOVA statistical analysis was performed with Tukey's post-test. * = P<0.05.

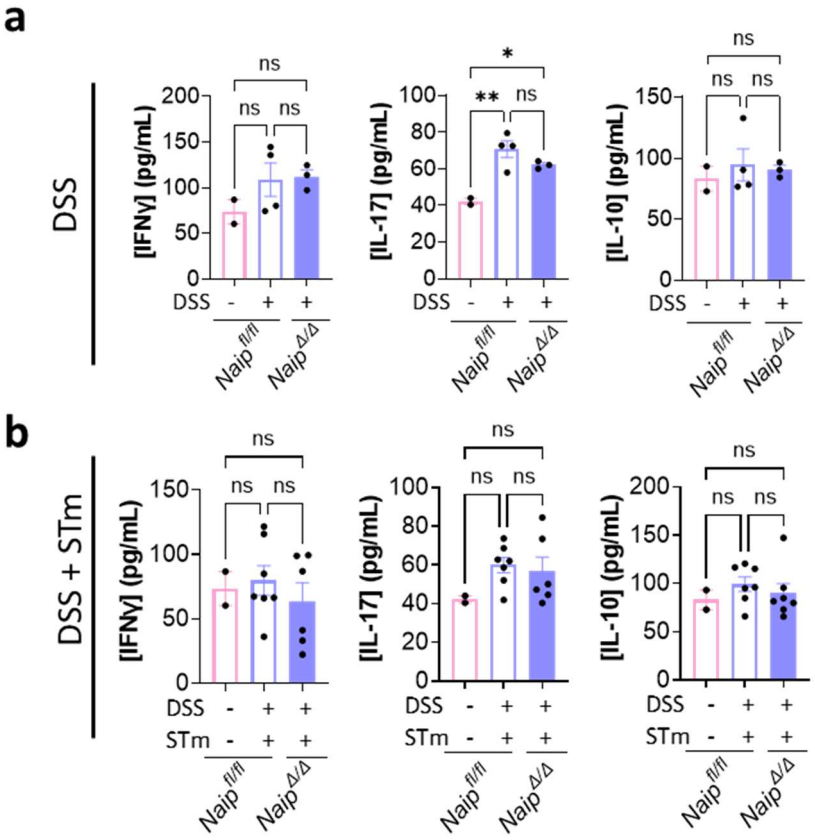

Figure 5.6 - Increased IL-17 expression following DSS treatment in both Naip$^{fl/fl}$ and Naip$^{\Delta/\Delta}$ mice

(**a-b**) - Sections of colons from untreated *Naip$^{fl/fl}$* mice, and *Naip$^{fl/fl}$* and *Naip$^{\Delta/\Delta}$* mice treated with either DSS (**a**) or DSS+STm (**b**) were excised and homogenised and assayed for IFNγ, IL-17, and IL-10. Each individual point indicates a separate mouse. Bars indicate mean ± s.e.m. *Naip$^{fl/fl}$* untreated N=2, *Naip$^{fl/fl}$* DSS-treated N=7, *Naip$^{\Delta/\Delta}$* DSS-treated N=7, one independent experiment. One-way ANOVA statistical analysis was performed with Tukey's post-test. * = P<0.05, **=P<0.01.

5.2.5 Increases in colonic IELs seen in *Naip*$^{\Delta/\Delta}$ mice following DSS+STm treatment may be due to increased proliferation

If IELs are increased in *Naip*$^{\Delta/\Delta}$ mice following DSS+STm treatment, it is possible that this is due to an influx of cells egressing from the lymph nodes, or alternatively the IELs are proliferating in situ. To test this, I administered mice with a drug, FTY720, which blocks lymph node egress (Zhi *et al.*, 2011), concurrently with STm infection. IELs were isolated 24hrs later and additionally stained for Ki67 (fig. 5.7a). During this experiment weight loss was comparable between *Naip*$^{fl/fl}$ and *Naip*$^{\Delta/\Delta}$ mice (fig. 5.7b). IEL numbers were calculated as percentage change between untreated and FTY720-treated for each genotype, with untreated set at 100%. For *Naip*$^{fl/fl}$, IEL numbers decreased when FTY720 was administered, suggesting that in *Naip*$^{fl/fl}$ mice cells emigrate from the lymph nodes to the IEL compartment following DSS+STm treatment. However, in *Naip*$^{\Delta/\Delta}$ mice no changes were seen in IEL number upon FTY720 treatment, although there was quite a range, suggesting that lymph node egress is not the primary cause of IEL expansion in these mice (fig. 5.7c-d). Next, expression of Ki67 was established in these cells, however no differences were seen between *Naip*$^{fl/fl}$ and *Naip*$^{\Delta/\Delta}$ mice or FTY720 treated and untreated. However, Ki67 levels were high in all cells, with all subgroups except TCRαβCD4 at nearly 100% Ki67+ (fig. 5.8.a-c), thus this method may not be optimal. The suitability of Ki67 as a marker of proliferation has previously been called into question, with evidence that Ki67 levels remain high for several days following division (Di Rosa, Cossarizza and Hayday, 2021). Di Rosa *et al*. suggested Ki-67/DNA dual staining as an effective replacement (Di Rosa, Cossarizza and Hayday, 2021).

As before, activation markers in the mLNs were also assessed (fig. 5.9-10). In CD4s, reductions in the percentage of CD69+ and CD25+CD69+ cells were seen in *Naip*$^{fl/fl}$ mice upon treatment with FTY720, though this trend was not significant. CD69, a classic marker of lymph node activation, may be reduced due to proliferation and subsequent dilution of the marker, which normally occurs once cells have left the lymph node (Cibrián and Sánchez-Madrid, 2017). However, this reduction in CD69 was

abrogated in *Naip*$^{\Delta/\Delta}$ mice. The percentage and MFI of CD25+ CD4+ cells remained unchanged by genotype and FTY720 treatment. There was also no change in the distribution of naïve (CD44-CD62L+), Tcm (CD44+CD62L+) and effector (CD44+CD62L-) CD4+ T cells (fig. 5.9d). In CD8s, there was a decrease in the percentage of CD69+ cells following FTY720 treatment in both genotypes (fig. 5.10a). We observed a modest reduction in the percentage of CD25+ and CD25+CD69+ cells in *Naip*$^{fl/fl}$ mice following FTY720 treatment. In contrast to *Naip*$^{\Delta/\Delta}$ mice the percentage of CD25+ and CD25+CD69+ was consistent regardless of FTY720 treatment, but was lower than untreated *Naip*$^{fl/fl}$ mice (fig. 5.10b-c). In CD8s there were no significant changes in the frequencies of naïve (CD44-CD62L+), Tcm (CD44+CD62L+) and effector (CD44+CD62L-) cells regardless of FTY720 treatment or genotype. However, in *Naip*$^{fl/fl}$ mice there was a small trend towards increased naive cells and decreased effector cells with FTY720 treatment (fig. 5.10d).

We therefore conclude that blocking lymph node egress does not convincingly reduce the IEL in *Naip*$^{\Delta/\Delta}$ mice, whereas it does in *Naip*$^{fl/fl}$. The Ki67 data does not give a clear answer to whether IELs in *Naip*$^{\Delta/\Delta}$ mice are proliferating more, but the IELs appear to be proliferating in both genotypes.

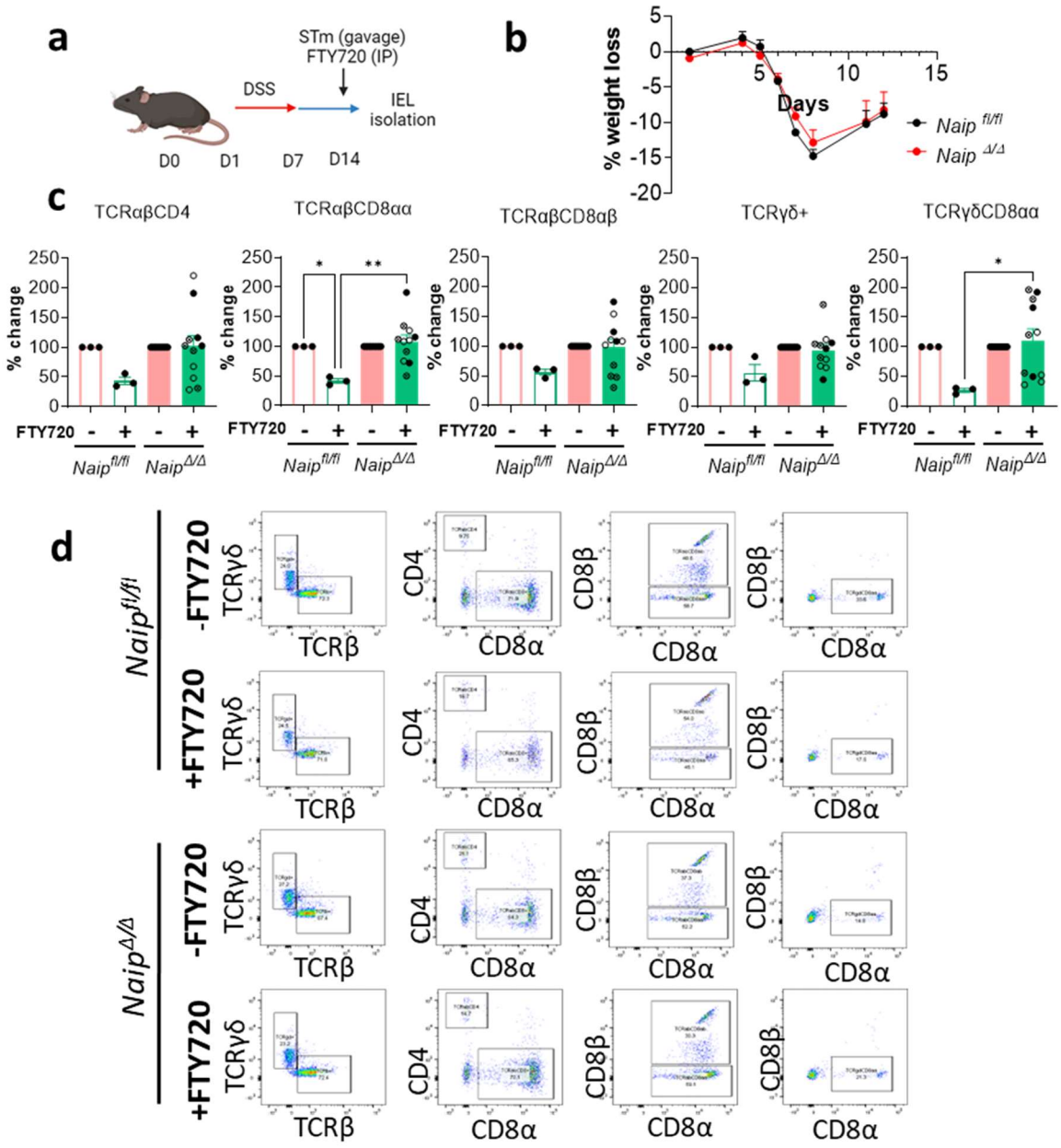

Figure 5.7 - Blocking lymph node egress does not affect colonic IEL numbers in Naip$^{\Delta/\Delta}$ mice following DSS+STm

(**a**) *Naip*$^{fl/fl}$ and *Naip*$^{\Delta/\Delta}$ mice were administered one round of DSS in drinking water for 6 days then returned to normal water for 7 days. On day 13 mice were administered STm$^{\Delta aroA}$ via oral gavage and some were administered the drug FTY720 IP (1mg/kg) to block lymph node egress. 24hrs later mice were sacrificed, colons excised and IELs isolated. Figure made in Biorender. **b** – Weight loss during DSS treatment. **c** - IEL subsets as percentage change from untreated (-FTY720) for each genotype. Each individual point indicates a separate mouse. The two styles of points indicate the two independent experiments. Bars indicate mean ± s.e.m. *Naip*$^{fl/fl}$ N=3, *Naip*$^{\Delta/\Delta}$ -FTY720, N=9, *Naip*$^{\Delta/\Delta}$ +FTY720 N=11, three independent experiments. One-way ANOVA statistical analysis was performed with Tukey's post-test. * = P<0.05, **=P<0.01. **d** – Example flow plots for each IEL subset.

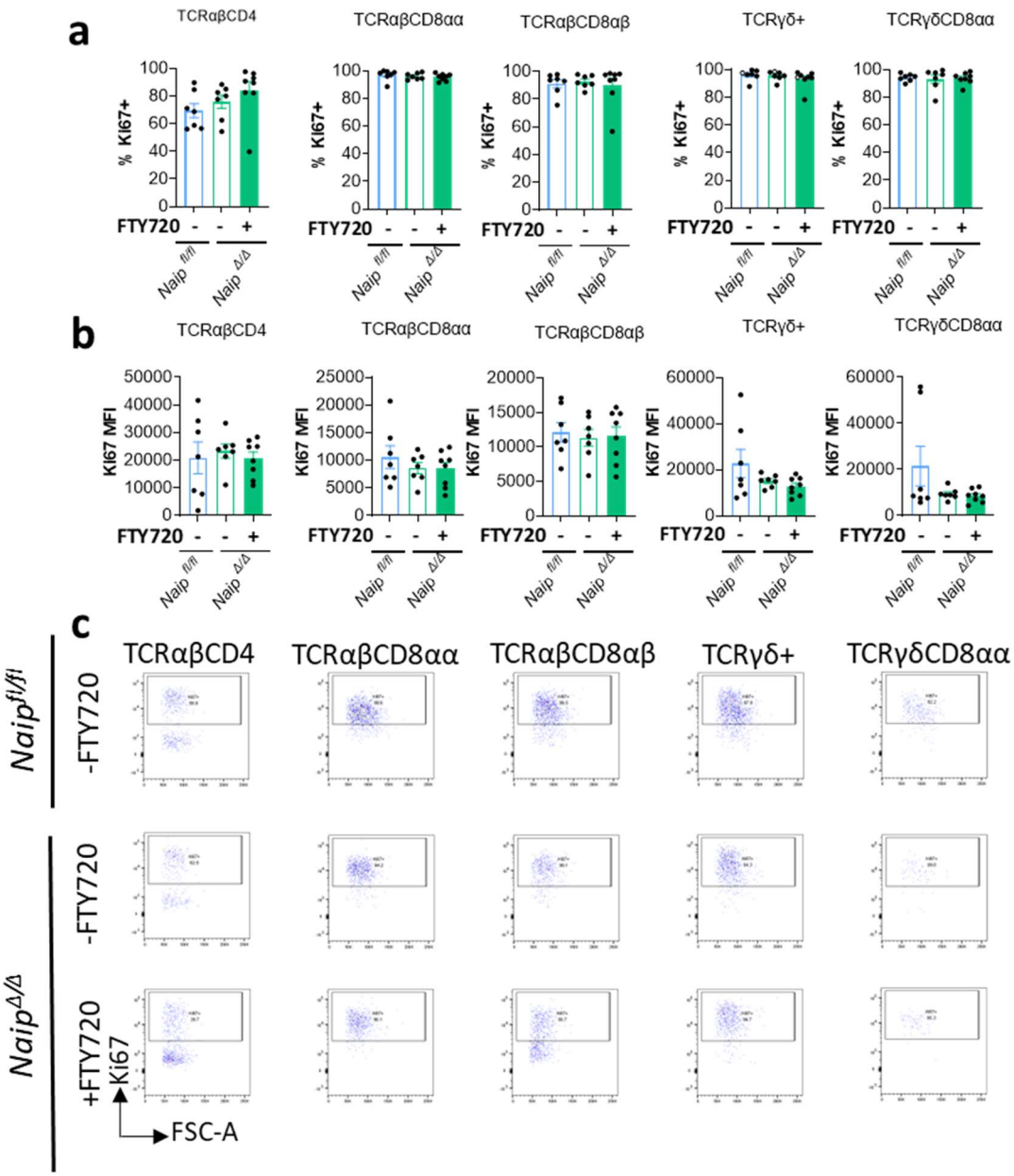

Figure 5.8 – No differences in Ki67 in colonic IELs in Naip$^{fl/fl}$ and Naip$^{Δ/Δ}$ mice following DSS+STm treatment

Naip$^{fl/fl}$ and *Naip$^{Δ/Δ}$* mice were administered one round of DSS in drinking water for 6 days then returned to normal water for 7 days. On day 13 mice were administered STm^{ΔaroA} via oral gavage and some were administered the drug FTY720 IP (1mg/kg) to block lymph node egress. 24hrs later mice were sacrificed, colons excised and IELs isolated. (**a-b**) – Ki67 staining as a percentage of Ki67+ cells (**a**) and Ki67 MFI (**b**) for each IEL subset. Each individual point indicates a separate mouse. Bars indicate mean ± s.e.m. *Naip$^{fl/fl}$* -FTY720 N=7, *Naip$^{Δ/Δ}$* -FTY720 N=7, *Naip$^{Δ/Δ}$*+FTY720 N=8, two independent experiments. One-way ANOVA statistical analysis was performed with Tukey's post-test. **c** – Example flow plots and histograms of Ki67 expression for each IEL subset

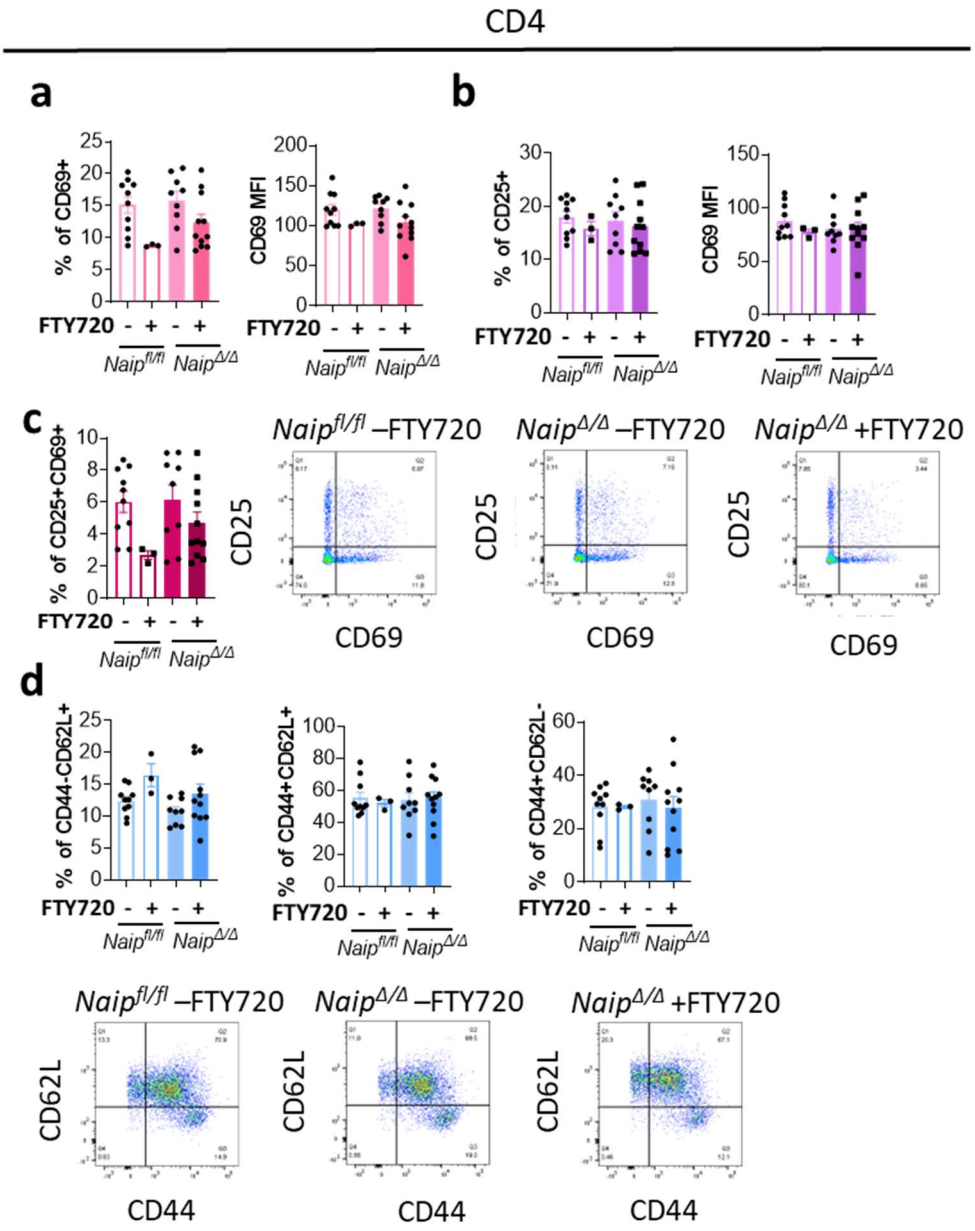

Figure 5.9– No changes in activation markers or proportion of memory cells in CD4+ T cells from mLNs following DSS + STm ± FTY720 treatment

Naip$^{fl/fl}$ and *Naip*$^{\Delta/\Delta}$ mice were administered one round of DSS in drinking water for 6-7 days then returned to normal water for 7 days. On day 13 mice were administered STm$^{\Delta aroA}$ via oral gavage and some were administered the drug FTY720 IP (1mg/kg) to block lymph node egress. 24hrs later mice were sacrificed and mLNs excised and analysed by flow cytometry. (**a-d**) CD4+ T cells. **a** – Percentage of CD69+ CD4 T cells and CD69 MFI of CD4 T cells. **b** - Percentage of CD25+ CD4 T cells and CD25 MFI of CD4 T cells. **c** – Percentage of CD25+CD69+ double-positive CD4+ T cells, with example flow plots. (**d**) – Percentage of CD44-CD62L+ (naïve), CD44+C62L+ (Tcm) and CD44+CD62L- (effector) CD4+ T cells with example flow plots. For bar plots, each individual point indicates a separate mouse. Bars indicate mean ± s.e.m. *Naip*$^{fl/fl}$ -FTY720 N=10, *Naip*$^{fl/fl}$ +FTY720 N=3, *Naip*$^{\Delta/\Delta}$ -FTY720, N=9, *Naip*$^{\Delta/\Delta}$ +FTY720 N=11, two independent experiments. One-way ANOVA statistical analysis was performed with Tukey's post-test.

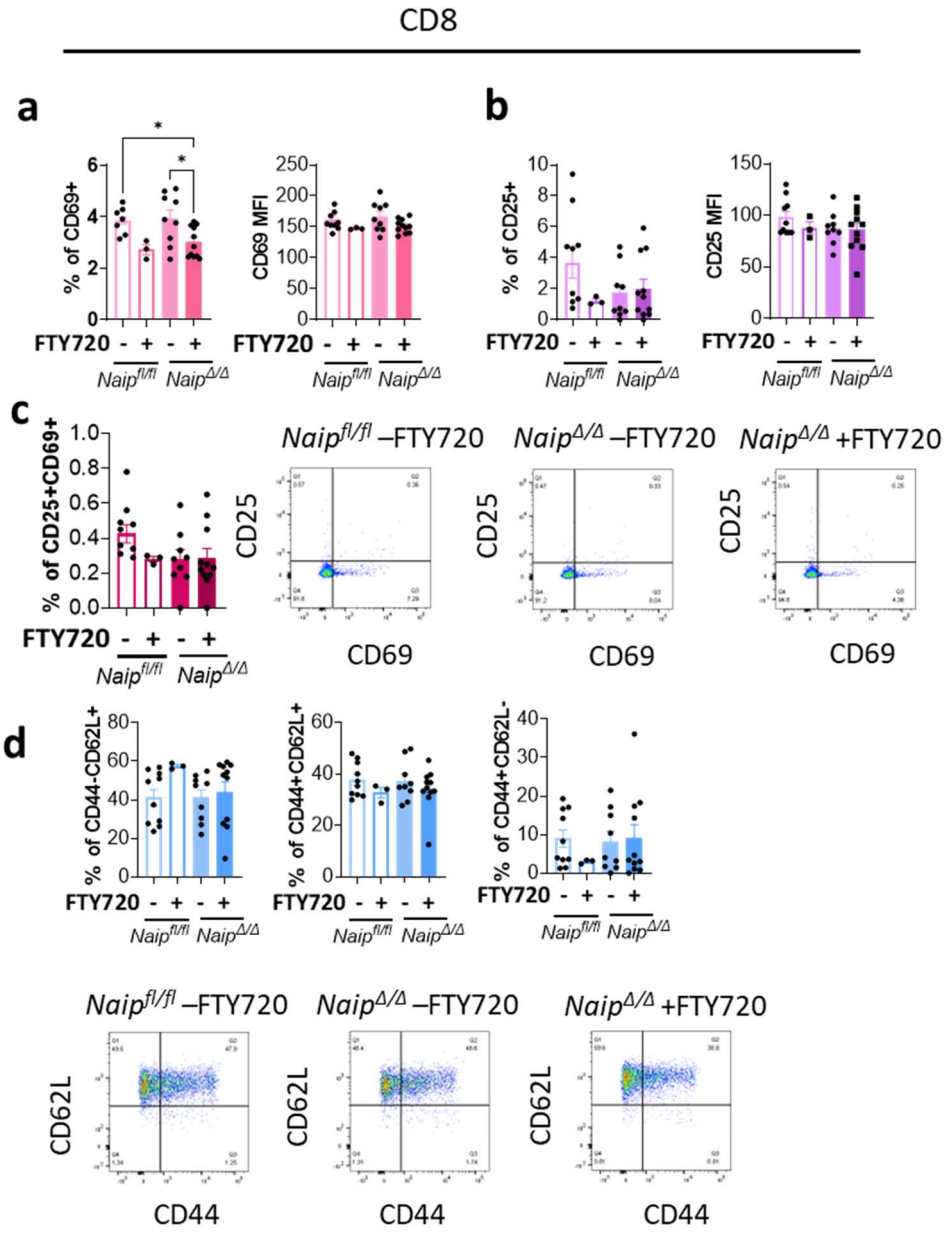

Figure 5.10 - Decreased CD69 expression in mLN CD8 T cells following FTY720 treatment in DSS + STm-treated $Naip^{\Delta/\Delta}$ mice

$Naip^{fl/fl}$ and *$Naip^{\Delta/\Delta}$* mice were administered one round of DSS in drinking water for 6-7 days then returned to normal water for 7 days. On day 13 mice were administered $STm^{\Delta aroA}$ via oral gavage and some were administered the drug FTY720 IP (1mg/kg) to block lymph node egress. 24hrs later mice were sacrificed and mLNs excised and analysed by flow cytometry. (**a-d**) CD8+ T cells. **a** – Percentage of CD69+ CD8 T cells and CD69 MFI of CD8+ T cells. **b** - Percentage of CD25+ CD8 cells and CD25 MFI of CD8+ T cells. **c** – Percentage of CD25+CD69+ double-positive CD8+ T cells, with example flow plots. (**d**) – Percentage of CD44-CD62L+ (naïve), CD44+C62L+ (Tcm) and CD44+CD62L- (effector) CD8 T cells with example flow plots. For bar plots, each individual point indicates a separate mouse. Bars indicate mean ± s.e.m. *$Naip^{fl/fl}$* -FTY720 N=10, *$Naip^{fl/fl}$* +FTY720 N=3, *$Naip^{\Delta/\Delta}$* -FTY720, N=9, *$Naip^{\Delta/\Delta}$* +FTY720 N=11, two independent experiments. One-way ANOVA statistical analysis was performed with Tukey's post-test.

5.2.6 No significant changes in TNFα between *Naip*$^{fl/fl}$ and *Naip*$^{Δ/Δ}$

It has been shown previously that *Naip*$^{Δ/Δ}$ mice experience epithelial barrier collapse following STm infection in a TNF-dependent manner (Fattinger *et al.*, 2021). To investigate whether we could see any changes in TNF in our setting, and whether blocking lymph node egress alters TNF in the colon, we took pieces of colon from mice treated with DSS+STm ±FTY720 suspended in Matrigel (Voabil *et al.*, 2021), then stimulated with αCD3 and αCD28 antibodies to activate T cells within the tissue. After 24hrs, TNFα ELISA was performed on the supernatant. This revealed no significant differences in the TNFα production (fig. 5.11). A modest increase in TNFα was observed in untreated *Naip*$^{Δ/Δ}$ mice compared to *Naip*$^{fl/fl}$, and this was reduced non-significantly in FTY720 treated *Naip*$^{Δ/Δ}$ mice. This perhaps suggests that T cells migrating from the lymph nodes are responsible for the TNFα release, but as this was not statistically significant and done only once, it must be interpreted with caution. However, with time and mouse numbers permitting this would be worth repeating along with the *Naip*$^{fl/fl}$ +FTY720 treatment group.

5.2.7 Increased IELs in *Naip*$^{Δ/Δ}$ is not due to an increase in bacterial burden

Previously it has been shown that *Naip*$^{Δ/Δ}$ mice experience increased bacterial burden following STm infection, thought to be due to lack of expulsion of infected IECs (Rauch *et al.*, 2017). To test this in our model, following DSS+STm treatment and injection with FTY720 mice were sacrificed and pieces of colon, spleen and mLN were homogenised, plated on LB agar overnight, and the number of CFUs per gram of tissue calculated (fig. 5.12). Contrary to previous literature, no statistically significant increase in number of CFUs was observed, though in some individual experiments a trend was observed. Following FTY720 treatment there was a significant increase in CFUs in the colon in *Naip*$^{fl/fl}$ mice, perhaps indicating that reduced IEL numbers are impacting on STm removal.

To further test whether STm dose correlates with IEL numbers, the DSS+STm protocol was repeated on C57BL/6 mice with a range of STm doses – $5x10^8$, $5x10^9$ and $5x10^{10}$ CFUs - as well as some mice

which were treated with DSS only or no treatment (fig. 5.13a). The mice receiving the lowest dose, $1x10^8$ CFU STm has no (or very few) detectable CFUs in the colon, and the $1x10^9$ CFU input (which is the dose used in all previous experiments) had higher retrievable CFU than then highest dose of $1x10^{10}$ CFU, which was unexpected (fig. 5.13b). Looking at numbers of each IEL subset showed no major increase in IEL numbers above that seen in DSS treatment alone. However, in the TCRαβCD8αα, TCRαβCD8αβ, TCRγδ+ and TCRγδ CD8αα subgroups there was a similar increase in IELs in the DSS-only group (fig. 5.13c-d). This suggests that bacterial burden may not be the driving force behind IEL increase in *Naip*$^{\Delta/\Delta}$ mice.

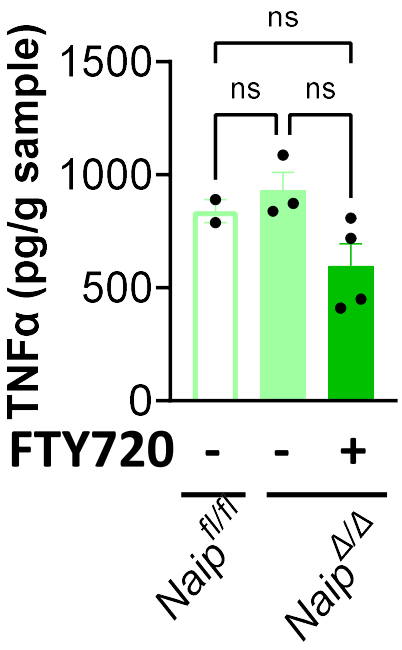

Figure 5.11 – No significant changes in TNFα between Naip$^{fl/fl}$ and Naip$^{\Delta/\Delta}$

Naip$^{fl/fl}$ and *Naip*$^{\Delta/\Delta}$ mice were administered one round of DSS in drinking water for 6 days then returned to normal water for 7 days. On day 13 mice were administered STm$^{\Delta aroA}$ via oral gavage and some were administered the drug FTY720 IP (1mg/kg) to block lymph node egress. 24hrs later mice were sacrificed, and colon excised. Pieces of the colon were suspended in Matrigel and Basic Media, stimulated with αCD3 and αCD28 antibodies and 24hrs later media was collected and a TNFα ELISA performed. Each point represents an individual mouse. Bars indicate mean ± s.e.m. *Naip*$^{fl/fl}$ N=2, *Naip*$^{\Delta/\Delta}$ -FTY720, N=3, *Naip*$^{\Delta/\Delta}$ +FTY720 N=4, one independent experiment. One-way ANOVA statistical analysis was performed with Tukey's post-test.

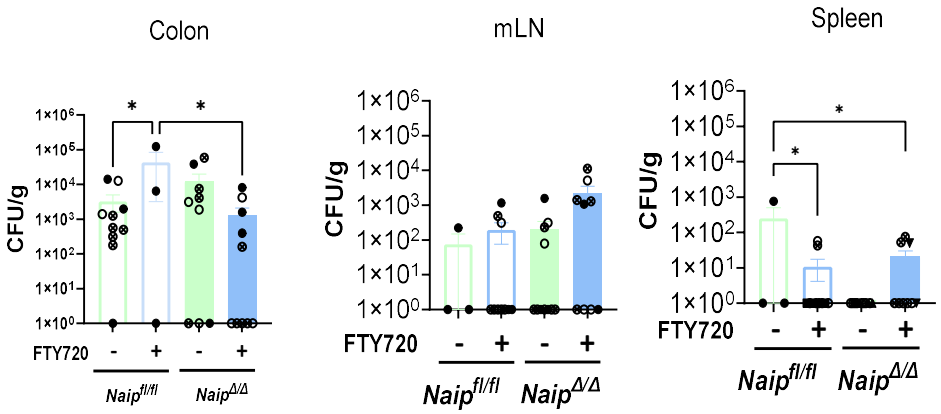

Figure 5.12 - No changes in the CFUs of Naip$^{fl/fl}$ and Naip$^{\Delta/\Delta}$ organs

Naip$^{fl/fl}$ and *Naip*$^{\Delta/\Delta}$ mice were administered one round of DSS in drinking water for 6 days then returned to normal water for 7 days. On day 13 mice were administered STm$^{\Delta aroA}$ via oral gavage and some were administered the drug FTY720 IP (1mg/kg) to block lymph node egress. 24hrs later mice were sacrificed. Pieces of colon, spleen and mLN were homogenised, plated on LB and CFUs were calculated. Each point represents an individual mouse over three separate experiments. The three styles of points indicate the three independent experiments. Bars indicate mean ± s.e.m. *Naip*$^{fl/fl}$ -FTY720 N=10, *Naip*$^{fl/fl}$ +FTY720 N=3, *Naip*$^{\Delta/\Delta}$ -FTY720, N=9, *Naip*$^{\Delta/\Delta}$ +FTY720 N=11, three independent experiments. One-way ANOVA statistical analysis was performed with Tukey's post-test.

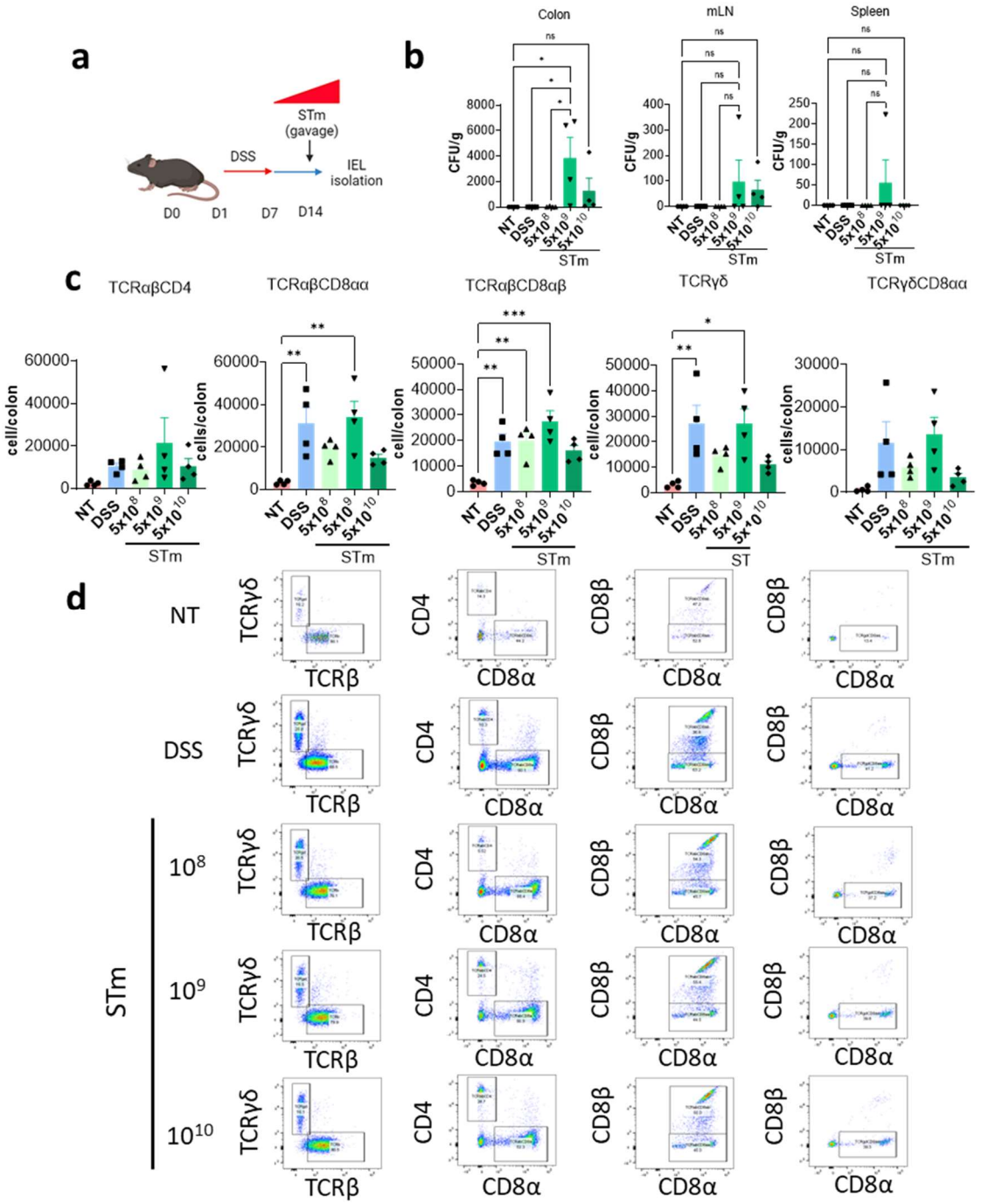

Figure 5.13 - IELs increase doesn't correlate with increased STm load

a – C57BL/6 mice were either not treated (NT) or administered one round of DSS in drinking water for 6 days then returned to normal water for 7 days. On day 13, mice were either left as DSS treatment only, or administered a range of STm$^{\Delta aroA}$ concentrations via oral gavage. 24hrs later mice were sacrificed and colonic IELs isolated and analysed by flow cytometry. Figure created in Biorender. **b** – Pieces of colon, mLNs and spleens were homogenised, plated, and the number of CFUs calculated for each treatment group. **c** – IELs per colon for each IEL subgroup. **d** – Example flow plots for each IEL subgroup. For bar plots (**b-c**), each individual point indicates a separate mouse. Bars indicate mean ± s.e.m. N=4,one independent experiment. One-way ANOVA statistical analysis was performed with Tukey's post-test. *=P<0.05, **=P<0.01, **=P<0.001

5.2.8 IL-15/IL-15R is increased in *Naip*$^{\Delta/\Delta}$ organoids

Multiple PRRs, such as TLR4 and NOD2, act via IL-15 to maintain the IEL compartment (Kaneko *et al.*, 2004; Yu *et al.*, 2006; Jiang *et al.*, 2013; Qiu *et al.*, 2016). As Naips are also a PRR and reside in the IECs, with close proximity to affect the IEL compartment, we investigated the effect of Naip knock-out on IL-15. As IL-15 is trans-presented on the epithelial cell surface by its receptor (Dubois *et al.*, 2002), we assayed normal epithelium and tumour-derived organoids as well as *ex vivo*-derived colonic epithelial cells for IL-15/IL-15R by ELISA. *Naip*$^{fl/fl}$ and *Naip*$^{\Delta/\Delta}$ organoids were either not treated or infected with STm$^{\Delta aroA}$. In both tumour-derived and normal organoids, *Naip*$^{\Delta/\Delta}$ organoids had significantly higher levels of IL-15/IL-15R (fig. 5.14a-b). STm infection appeared to have no effect on IL-15/IL-15R. To test this in vivo, mice were given 3% DSS in the drinking water for 7 days to disrupt the epithelial barrier (Gillis *et al.*, 2018), followed by 7 days of normal water, mice were then infected with STm$^{\Delta aroA}$ and sacrificed 24 hours later. The epithelium was then isolated using dithiothreitol (DTT) and IL-15/IL-15R measured by ELISA. There were no significant differences in IL-15/IL-15R complex between genotype, however, there was a strong trend towards an increase in *Naip*$^{\Delta/\Delta}$ mice (fig. 5.14c). As IL-15 has a role in IEL survival, we hypothesised that this may lead to an increase in IEL numbers in *Naip*$^{\Delta/\Delta}$ mice.

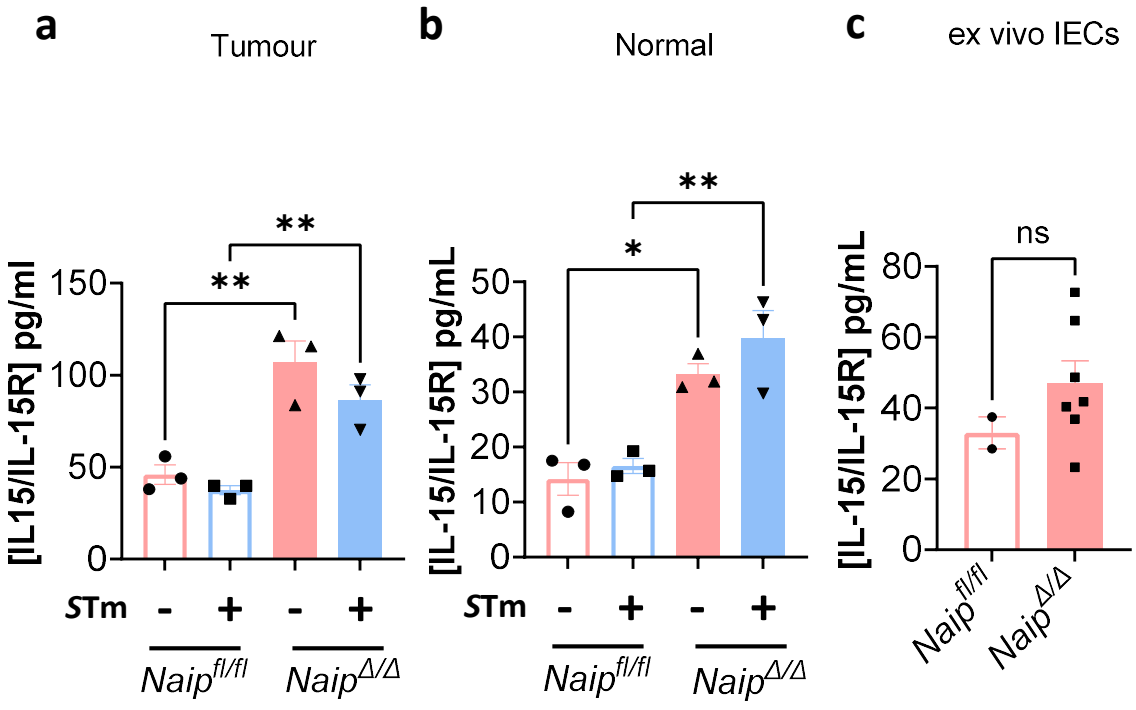

Figure 5.14 – IL-15/IL-15R is increased in Naip$^{Δ/Δ}$ colonic organoids and in mouse colonic epithelial cells

IL-15/IL-15R ELISA was performed on *Naip$^{fl/fl}$* and *Naip$^{Δ/Δ}$* tumour-derived (**a**) and normal (**b**) organoids, and on ex-vivo colonic epithelial cells from *Naip$^{fl/fl}$* and *Naip$^{Δ/Δ}$* mice (**c**). (**a-b**) -Organoids were either not treated or infected with STm^{ΔaroA} for 2hrs, media was then replaced, and gentamycin added to kill any extracellular bacteria. After 24hrs organoids were then collected and lysed for ELISA. Each individual point is the average of two technical repeats and represents a separate well of organoids (i.e. a biological repeat). N=3, one independent experiment. **c** – Mice were treated with DSS (3%) in the drinking water for 7 days, followed by 7 days of normal water, and then infection with STm^{ΔaroA}. 24hr later colons were excised, and epithelial cells extracted and then lysed for ELISA. Each individual point represents an individual mouse and the average of two technical replicates. *Naip$^{fl/fl}$* N=2, *Naip$^{Δ/Δ}$* N=7. One-way ANOVA statistical analysis was performed with Tukey's post-test. * = P<0.05, **=P<0.001.

5.2.9 Co-culture of IEL-like splenocytes with organoids

To attempt to elucidate the mechanism behind the increase in colonic IELs in *Naip*$^{\Delta/\Delta}$ mice following DSS+STm treatment, I devised an in vitro method of monitoring IEL proliferation. It has previously been reported that splenocytes, cultured with retinoic acid (RA), can adopt an IEL-like phenotype (Rogoz *et al.*, 2015). Here, I aimed to co-culture IEL-like splenocytes with *Naip*$^{fl/fl}$ and *Naip*$^{\Delta/\Delta}$ organoids and to determine cell proliferation with CellTrace Blue. Firstly, following RA treatment, CD4 and CD8 T cells were analysed for IEL markers. CCR9 and CD103, which allow the homing of IELs to IECs via recognition of CCL25 and E-cadherin, respectively. We also investigated LPAM1, an integrin which acts as a homing receptor to Peyers patches and mLNs (Marelli-Berg *et al.*, 2008) Only expression of LPAM1 was significantly increased, however there was a strong trend towards increased CCR9, particularly in the CD8s (fig. 5.15-16). Therefore, we concluded that RA treatment of splenocytes does impart of moderate phenotypic change as described by Rogoz *et al.*, particularly in the CD8+ T cells, though further optimisation may be required.

To determine the effect that co-culture with either *Naip*$^{fl/fl}$ or *Naip*$^{\Delta/\Delta}$ organoids would have on proliferation RA-conditioned splenocytes, cells were stained with CellTrace Blue and cultured with the organoids for 48hrs. This was tested with both tumour-derived and normal organoids. To recreate the effect seen in vivo with DSS+STm treatment, some organoids were infected with STm prior to co-culture. As changes had been seen in both eicosanoid production and IL15 presentation in these organoids, to determine whether these were influencing IEL proliferation Ibu and a blocking αIL15 antibody were used in conjunction with the coculture (fig. 5.17b). As CellTrace Blue is dissipated amongst daughter cells when a cell divides, cells were divided between CellTrace-hi cells, which had not divided, and CellTrace-lo cells, which had. To push cells to divide, T cells were stimulated with αCD3 for the coculture. In both tumour-derived and normal organoid co-cultures, very little change was seen in the CellTrace Blue content of CD4 cells. However, in CD8 cells, in all STm infected conditions a reduction in cell proliferation was seen, which is also in keeping with

reduced activation seen chapter 1 and other work conducted in our lab (Copland *et al.*, 2023). In conditions without STm infection, the CellTrace-lo percentage was higher, indicating proliferation, but there were no changes between *Naip*$^{fl/fl}$ and *Naip*$^{\Delta/\Delta}$, nor with the addition of Ibu or αIL15 antibody (fig. 5.17c-d).

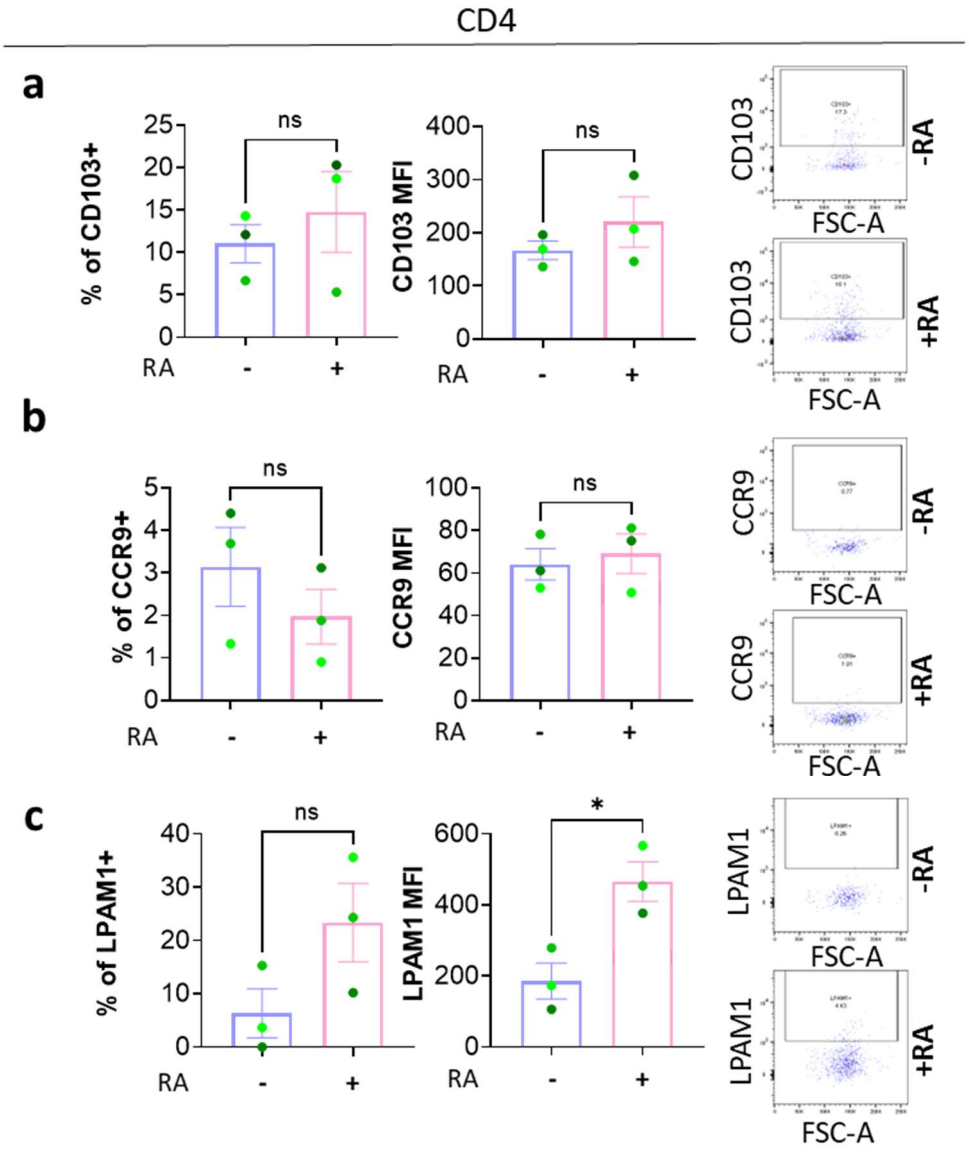

Figure 5.15 - Treatment of CD4 splenocytes with RA induces an IEL-like state

Splenocytes from C57BL/6 mice were isolated and cultured with retinoic acid (RA) to induce an IEL-like state before being analysed by flow cytometry for IEL markers. (**a-c**) CD4+ T cells only. **a** – Percentage of CD4+ T cells expressing CD103 and CD103 MFI of CD4+ cells, alongside example flow plots. **b** - Percentage of CD4+ T cells expressing CCR9 and CCR9 MFI of CD4+ cells, alongside example flow plots. **c** - Percentage of CD4+ T cells expressing LPAM1 and LPAM1 MFI of CD4+ cells, alongside example flow plots. Each individual point represents a separate experiment. Points are colour-coordinated so points across each treatment group which were performed in the same experiment are the same colour. Bars indicate mean ± s.e.m. N=3. Unpaired t-test statistical analysis performed.

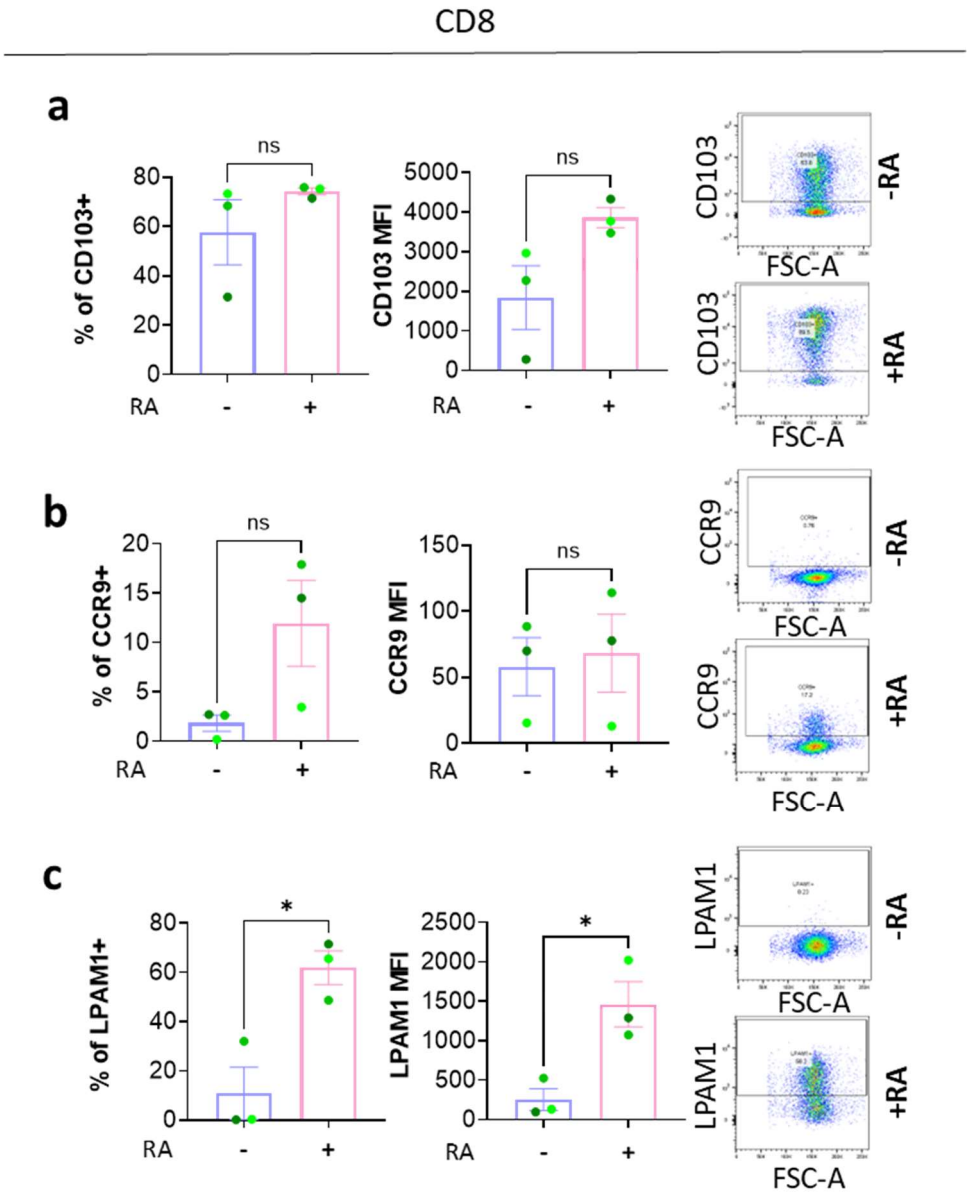

Figure 5.16 - Treatment of CD8 splenocytes with RA induces an IEL-like state

Splenocytes from C57BL6 mice were isolated and cultured with retinoic acid (RA) to induce an IEL-like state before being analysed by flow cytometry for IEL markers. (**a-c**) CD8+ T cells only. **a** – Percentage of CD8+ T cells expressing CD103 and CD103 MFI of CD8+ cells, alongside example flow plots. **b** - Percentage of CD8+ T cells expressing CCR9 and CCR9 MFI of CD8+ cells, alongside example flow plots. **c** - Percentage of CD8+ T cells expressing LPAM1 and LPAM1 MFI of CD8+ cells, alongside example flow plots. Each individual point represents a separate experiment. Points are colour-coordinated so points across each treatment group which were performed in the same experiment are the same colour. Bars indicate mean ± s.e.m. N=3. Unpaired t-test statistical analysis performed. *=P<0.05.

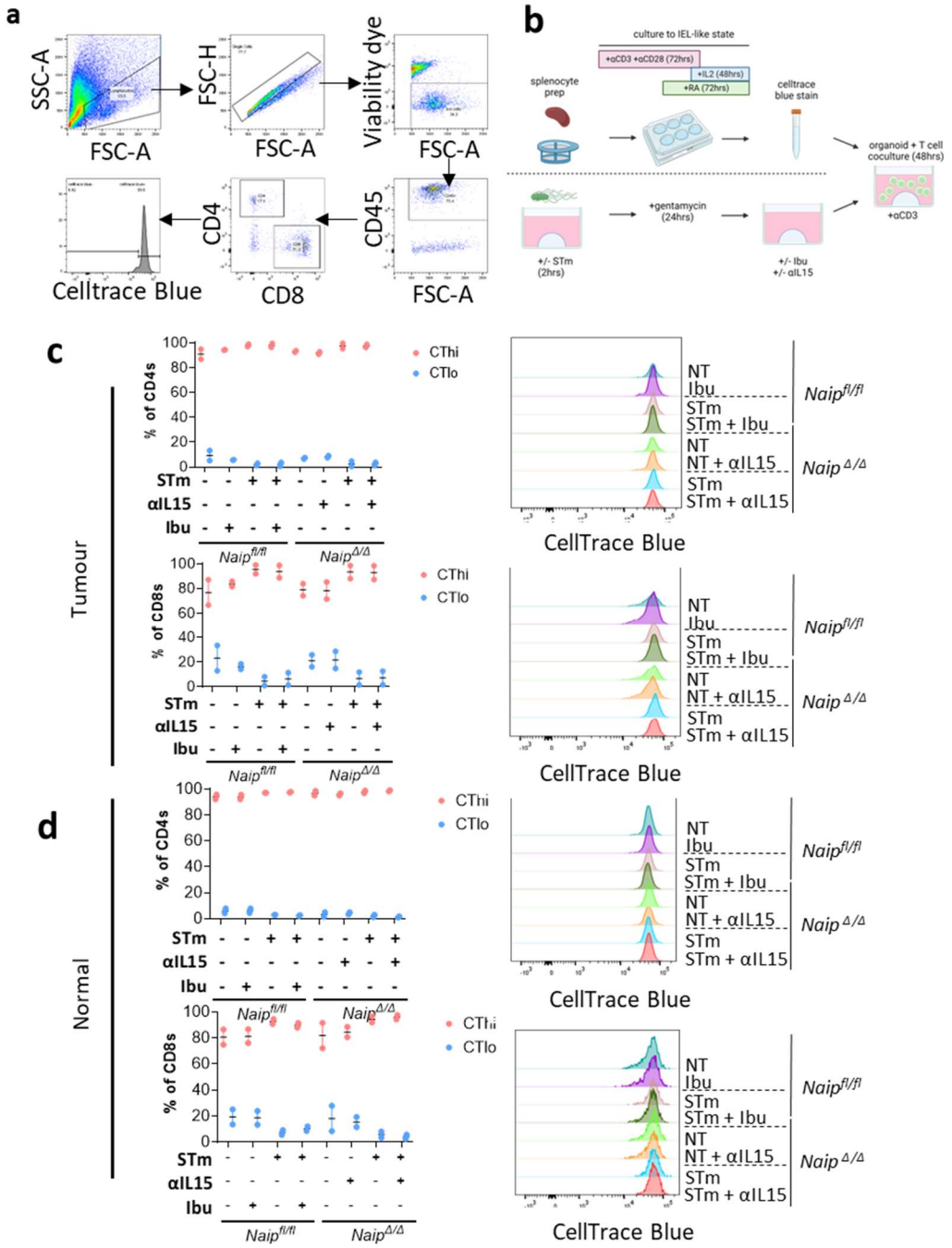

Figure 5.17 - αIL15 and Ibu have no effect on proliferation of IEL-like splenocytes

Splenocytes of C57BL/6 mice were cultured with retinoic acid (RA) to induce an IEL-like state. Cells were stained with CellTrace blue and co-cultured with organoids with αIL15 antibody or Ibu. Prior to co-culture some organoids were infected with STm$^{\Delta aroA}$. After 48hrs cells were analysed by flow. **a** – gating strategy for gating on lymphocytes, single cells, live cells, CD45+, CD4+ or CD8+, and finally on CellTrace Blue high or low. As a cell divides CellTrace Blue is split between cells, therefore CellTrace low cells have divided. **b** – workflow schematic as described above. (**c-d**) – Percentage of CD4 and CD8 cells in the CellTrace high and low fractions for splenocytes co-cultured with tumour-derived organoids (**c**) and normal organoids (**d**). Each individual point indicates the percentage of cells that are high or low for CellTrace from a single well of organoids in independent experiment. Lines indicate mean ± s.e.m. Representative histograms also shown.

5.3 Discussion

IELs play an important role in maintenance of gut health and response to pathogens. Maintenance and function of the IEL compartment is dependent on signalling by PRRs, as exemplified by TLR2 TLR4 and NOD2 at baseline (Kaneko *et al.*, 2004; Ramanan *et al.*, 2014; Qiu *et al.*, 2016), and by TLR9 during STm infection (Li *et al.*, 2017). IELs have also been implicated in development of colitis (Inagaki-Ohara *et al.*, 2004). Loss of PRRs, such as TLR2 have also been shown to increase susceptibility to colitis (Qiu *et al.*, 2016). However, whilst Naips are known to sense STm and *Naip* knockout has proved to protect against DSS-induced colitis (Kofoed and Vance, 2011; Sellin *et al.*, 2015; Rauch *et al.*, 2017), how Naips influence the IEL compartment in these scenarios remained to be established. Here, we found that *Naip*$^{\Delta/\Delta}$ mice, which lacked all Naip isoforms specifically in the IECs, had no significant changes in IELs at baseline or in response to DSS alone, but had increased colonic IELs in response to STm infection. This coincided with increased IL-15/IL-15R expression in *Naip*$^{\Delta/\Delta}$ organoids. However, preliminary co-culture experiments could not pin down IL-15 /IL-15R expression as the driver of increased IEL; these co-culture experiments will require further optimisation. An increase in bacterial burden could also not fully explain the increase in IELs. Whilst we established an effect of *Naip* knockout on the IEL compartment, the mechanism of these changes and the downstream effects of these could not be established.

5.3.1 Increased IELs in response to DSS and DSS+STm

Our findings that *Naip*$^{\Delta/\Delta}$ mice have no changes in baseline levels of IELs is perhaps surprising given the strong increase seen in IL-15/IL-15R in organoids and is in contrast to other PRRs. Knockout of TLR4 has been shown to significantly reduce the development of TCRαβCD8αα IELs, TLR2 knockout reduced CD8αα+, CD8αβ+ and TCRγδ+ IELs at baseline, and MyD88 or NOD2 deficient mice had reduced TCRαβCD8αα and TCRγδ+ IELs (Kaneko *et al.*, 2004; Yu *et al.*, 2006; Jiang *et al.*, 2013; Qiu *et al.*, 2016). TLR2, TLR4 and MyD88 knockouts were also found to have reduced IL-15 expression in the

IECS, with NOD2 knockout shown to have reduced IL-15 in the intestinal macrophages. Previously, *IL15Rα*-/- mice have been shown to have decreased TCRγδCD8αα IELs, specifically Thy1^{lo} cells, and this is restored in mice exclusively expressing IL15Rα in the IECs, via a Villin-driven transgene backcrossed to *IL15Rα*-/- mice (Ma *et al.*, 2009). Although previous data has indicated that STm infection does not increase IL-15 expression in IECs (Hoytema Van Konijnenburg *et al.*, 2017), this hasn't been assessed in the absence of Naips. The stage at which the possible connection between IL-15/IL-15R and IEL numbers became apparent mice were in scarce supply and so the IL-15 ELISA was only carried out as a secondary endpoint to other experiments which all employed DSS+STm treatment. As we only see a trend towards increased IL-15/IL-15R in the isolated *ex vivo* epithelial cells, perhaps the organoids do not fully reflect the *in vivo* conditions. However, the *ex vivo* analysis could only be repeated once with only two *Naip*$^{fl/fl}$ mice (due to limitations in colony breeding and time), so it is possible that if the experiment had been better powered we would have seen significance. Additionally, it will be pertinent to assess the levels of IL-15/IL-15R in isolated IECs from naïve and challenged *Naip*$^{fl/fl}$ and *Naip*$^{\Delta/\Delta}$ mice over different time points.

One reason why *Naip*$^{\Delta/\Delta}$ mice may not mirror the relationship seen between other PRRs, IL-15 and IELs at baseline is that for the TLRs and NOD2 IL-15 expression is driven largely by recognition of the microbiota. Mice with depleted gut microbiota have reduced IEL numbers, mimicking the effect seen in TLR2, TLR4 and NOD2 knockouts (Jiang *et al.*, 2013). However, the remaining IELs have been shown to be more inflammatory, expressing higher IFNγ (Ramanan *et al.*, 2014). When these mice were treated with MDP, a NOD2 agonist, IELs increased (Jiang *et al.*, 2013). As the Naip/NLRC4 is not thought to be activated by commensal bacteria (Zheng, Liwinski and Elinav, 2020), this may explain why *Naip*$^{\Delta/\Delta}$ mice have increased IL-15/IL-15R expression and only slightly reduced IELs at baseline; Naips may have a different baseline function to these other PRRs.

In response to DSS and DSS+STm treatment, we saw IELs increase in both *Naip*$^{fl/fl}$ and *Naip*$^{\Delta/\Delta}$ mice, although this wasn't always significant. This is in contrast to one study, which found decreased TCRγδCD8αα IELs following DSS treatment, although this was in the small intestine and IELs were expressed as a percentage as opposed to total number so could indicate a change in IEL subset distribution (Pai *et al.*, 2014). At this point, we focused our efforts on the colonic IELs, given that DSS primarily affects the colon (Yazbeck *et al.*, 2011; Chassaing *et al.*, 2014) and Naips are enriched in the colon compared to the SI (Allam *et al.*, 2015). *Naip*$^{\Delta/\Delta}$ mice are protected from colitis and show increased repair pathway activation (Allam *et al.*, 2015), so it might be surprising that no significant changes in IEL number between *Naip*$^{fl/fl}$ and *Naip*$^{\Delta/\Delta}$ mice treated with DSS. There was, however, a trend toward higher IEL numbers in the *Naip*$^{\Delta/\Delta}$ mice. It may be that repeating in a larger cohort of mice and assessing at different timepoints (e.g. during or soon after DSS treatment) may tease apart any impact of epithelial Naips loss on IEL-guided intestinal regeneration. Also, this analysis was conducted at a timepoint where colons are already regenerating. Extensive data suggests that TCRγδ+ IELs are protective in colitis (Hu and Edelblum, 2017). Genetic or antibody-mediated deletion of TCRγδ+ cells results in increased disease severity in TNBS and DSS treated mice and in TNF$^{\Delta ARE}$ mice, all of which model colitis (Tsuchiya *et al.*, 2003; Inagaki-Ohara *et al.*, 2004; Kühl *et al.*, 2007). This has been attributed to IL-10 and TGF-β production in TNBS colitis (Inagaki-Ohara *et al.*, 2004). TCRγδ+ IELs have also been shown to produce keratinocyte growth factor (KGF), which stimulates epithelial regeneration, upon treatment with DSS, and mice deficient in the γδ T cell co-stimulatory molecule CD100, which binds plexin B2 on IECs, have decreased KGF production following DSS administration (Boismenu and Havran, 1994; Chen *et al.*, 2002; Meehan *et al.*, 2014).

The most striking difference between IELs in *Naip*$^{fl/fl}$ and *Naip*$^{\Delta/\Delta}$ mice was seen following DSS+STm treatment (fig. 5.3), with TCRαβCD8αα, TCRγδ+ and TCRγδCD8αα subsets significantly increased in *Naip*$^{\Delta/\Delta}$ mice. There was also a strong trend towards increased TCRαβCD8αβ. Notably, the overall number of IELs appeared less in these experiments but we believe this was an error made in the

addition of the counting beads in the initial DSS experiment (fig. 5.2), as this was only repeated once. Our data is consistent with data from other PRR knockout mice; when WT and *TLR9*-/- mice were infected with STm, both had increased IEL numbers over time, but TCRγδ+ IELs increased significantly more in *TLR9*-/- mice (Y. Li *et al.*, 2017). In this study, enhanced IEL-mediated NKG2D-dependent killing contributed to exacerbated epithelial damage in *TLR9*-/- mice (Li *et al.*, 2017). TLR9 signalling was found to dampen NFκB, and in the absence of TLR9 increased NFκB signalling lead to increased NKG2D ligand expression on IECs and increased IL-1β production via the NLRP3 inflammasome, resulting in increased IEL expression of NKG2D (Y. Li *et al.*, 2017). Notably, the strain of STm this study used was not attenuated, unlike the $STm^{\Delta aroA}$ strain we used. This study looked at IELs 7 days post-infection (p.i.), whereas we observed 24hrs p.i.. This highlights that investigating later timepoints may be of interest. However $Naip^{\Delta/\Delta}$ mice experience epithelial barrier collapse at 72 hrs p.i with wild-type STm, so although the strain we are using is attenuated and therefore infection is limited (Felgner *et al.*, 2016), we would have to be mindful of this. (Fattinger *et al.*, 2021). It also suggests it may be useful to investigate NFκB signalling in $Naip^{\Delta/\Delta}$ mice in future, as NFκB also contributes to transcriptional activation of IL-15 (Qiu *et al.*, 2016).

5.3.2 Explaining the increase in IEL

Once we established that $Naip^{\Delta/\Delta}$ mice had increased IELs in comparison to $Naip^{fl/fl}$ following DSS+STm treatment, we next aimed to establish the cause of this increase. We first questioned whether these cells represented newly recruited or actively proliferating resident cells. We used the drug FTY720, which blocks egress from lymph nodes and Peyer's patches (Yanagawa, Masubuchi and Chiba, 1998), to establish if more cells were migrating from lymph nodes along with Ki67 staining to determine if IELs in $Naip^{\Delta/\Delta}$ mice were more proliferative. FTY720 reduced IELs in $Naip^{fl/fl}$ mice, significantly so in the TCRαβCD8αα subset, but in $Naip^{\Delta/\Delta}$ mice levels were only partially affected with overall no significant change but some considerable spread of data points. The fact that the TCRαβCD8αα subset was the most significantly affected by FTY720 treatment may be explained by

the fact it falls into the 'induced' category of IEL, meaning it migrates from the thymus to the lymphoid tissue, before eventually moving to the intestinal epithelium (Olivares-Villagómez and Van Kaer, 2018). Perhaps more surprising is that the TCRγδCD8αα cells are affected, given that they are 'natural' IELs which migrate straight from the thymus following agonist positive selection (Olivares-Villagómez and Van Kaer, 2018). We concluded then that the majority of the increased IELs seen in *Naip*$^{\Delta/\Delta}$ mice is most likely due to increased proliferation. However, Ki67 is at almost 100% expression in both genotypes, making it difficult to distinguish if proliferation is indeed higher. In hindsight, the use of an untreated control would have been useful to compare Ki67 expression at baseline, however we were limited with mouse numbers. Another method of assessing this in future would be to inject mice with bromodeoxyuridine, a thymidine analogue that can be used in DNA synthesis, and observe incorporation into cells (Crane and Bhattacharya, 2013).

We next looked at whether increased bacterial burden could lead to the IEL increase in *Naip*$^{\Delta/\Delta}$ mice. Following STm infection, *Naip*$^{\Delta/\Delta}$ mice have previously been shown to have higher bacterial burden (Rauch *et al.*, 2017; Fattinger *et al.*, 2021). Thus, we wanted to determine if bacterial burden itself directly drives increased *Naip*$^{\Delta/\Delta}$ IELs, or whether it is due to some other factor altered in *Naip*$^{\Delta/\Delta}$ epithelium. STm infection has previously been shown to cause expansion and increased motility of γδ IELs (Davies *et al.*, 2004; Hoytema Van Konijnenburg *et al.*, 2017). However, we could not show significantly increased CFU in *Naip*$^{\Delta/\Delta}$ mice in our model, though there is perhaps a modest trend towards increased CFU (fig. 5.12). It is worth noting that our model does differ from previous models in that we use DSS to disrupt the epithelium and an attenuated STm strain (STm$^{\Delta aroA}$). This may also explain why no CFUs were detected in some samples, possibly indicating that these mice had cleared the infection but not ruling out that the infection may have had some downstream immunological effects. *Naip*$^{\Delta/\Delta}$ mice treated with FTY720 had equivalent STm CFU to *Naip*$^{\Delta/\Delta}$ mice without FTY720, perhaps correlating with sustained IEL numbers. However, comparing *Naip*$^{fl/fl}$ and *Naip*$^{\Delta/\Delta}$, the numbers of IELs do not correlate with STm burden. If greater IEL frequencies was responsible for

reduced STm CFU, then we'd expect to see less CFU in the *Naip*$^{\Delta/\Delta}$ mice. However, this is perhaps balanced by the previous reports that Naip knockouts have reduced expulsion of STm infected cells and thus higher STm burden. Our model differs in that we use an inflammatory trigger to disrupt the epithelium, rather than antibiotics to disrupt the microbiota to enable STm invasion.

We next tried dosing wild-type mice with a range of STm CFUs, but this did not result in the expected CFUs in the tissue. Mice that were infected with $5x10^9$ CFUs had a greater bacterial burden than those infected with both $5x10^8$ and $5x10^{10}$. It is possible that a saturating dose had been reached, preventing further CFUs. However, this does not fully explain why the $5x10^{10}$ treatment group is slightly lower than the $5x10^9$ group, although the difference is not significant. Possibly there was an issue in preparing the $5x10^{10}$ dose of STm, but each dose was generated from the same stock and diluted accordingly so this seems unlikely. Whilst the trend in CFUs is mirrored in the IELs, with the $5x10^9$ CFU treated group having the highest number of IELs, looking at individual mice showed that CFU burden did not correlate with IEL number. However, in the TCRαβCD8αα, TCRαβCD8αβ and TCRγδ subsets the DSS-only treatment group is also significantly increased compared to no treatment. This is similar to our previous results findings (fig. 5.2) which showed a trend towards increased IELs following DSS-treatment, suggesting that only *Naip*$^{\Delta/\Delta}$ mice increase IEL numbers above that seen with DSS alone. Whilst DSS has been used to enhance STm infection before (Gillis *et al.*, 2018), in future, it would be interesting to repeat the STm infection of *Naip*$^{fl/fl}$ and *Naip*$^{\Delta/\Delta}$ mice in the absence of DSS, using the streptomycin depletion model alongside wild-type Salmonella to reflect previous work. Currently we are unable to do this due to license restrictions.

If increased bacterial burden did not explain the increased IEL in *Naip*$^{\Delta/\Delta}$ mice, we next aimed to elucidate the mechanisms *in vitro*. To do this, we used a protocol established by Rogoz *et al.* in which splenocytes are cultured with retinoic acid (RA) to induce them to an IEL-like state. Rogoz *et al.,* established that upon culturing with RA, splenocyte had increased level of CCR9 and CD103, two

important IEL markers (Olivares-Villagómez and Van Kaer, 2018), as well as increased motility in organoids (Rogoz *et al.*, 2015). We also examined LPAM1, an integrin which acts as a homing receptor to the gut, specifically to Peyers patches and mLNs, which is upregulated in Vδ2 T cells during CRC (Marelli-Berg *et al.*, 2008; McCarthy *et al.*, 2013). The protocol required slightly different treatment of CD4 and CD8s, with 3 days of αCD3 and αCD28 for CD4s and 2 days for CD8s. However, as we had not observed any differences in CD4 IELs, we streamlined this and treated all splenocytes for 2 days. This was reflected in a smaller increase in IEL markers in CD4s (fig 4.14) compared to CD8s. If there had been more time to perform these experiments, we would have preferred to separate the CD4s and CD8s. Whilst in CD8s the IEL markers increased in percentage and MFI upon RA treatment, this was only significant in LPAM1. Whilst LPAM1 is not a classical IEL marker, this supports the idea that these cells are more 'gut-like', but perhaps highlights that this is a model and the RA-treated splenocytes are not perfect mimics of IELs. The trend towards increased CCR9 was also strikingly high, supporting the idea that these cells are in fact IEL-like. It should also be noted that there was significant variation between experiments, and as each experiment point is colour-coordinated, it can be observed that 2 out of 3 experiments showed an increase in the markers upon RA stimulation, but this variance prevented any significant changes. As such, experiments using these IEL-like splenocytes should be interpreted with caution. It should also be noted that addition of organoids also seemed to increase some of the IEL markers, suggesting that the IECs could be giving other signals that influence the IEL phenotype, such as TGF-β (Konkel *et al.*, 2011). This makes sense as markers such as CD8αα are known to only emerge upon migration to the gut epithelium (Konkel *et al.*, 2011), and CD8αα would be an interesting marker to check in these RA-treated splenocytes in future.

To see if *Naip*$^{\Delta/\Delta}$ organoids affected IEL proliferation, as we had concluded was occurring in *Naip*$^{\Delta/\Delta}$ mice upon STm infection, we co-cultured these IEL-like splenocytes with tumour-derived and normal organoids with CellTrace Blue staining to determine proliferation levels. To model the *in vivo*

observation *in vitro*, some of these organoids were infected with STm prior to co-culture. As we had previously established that IL-15/IL-15R was increased and eicosanoids altered in *Naip*$^{\Delta/\Delta}$ organoids, we used αIL-15 blocking antibodies and Ibu to see if this altered RA-induced splenocyte proliferation. Other studies have used similar co-culture models but with IELs isolated from mice rather than RA-treated splenocytes (Morikawa *et al.*, 2021), however we chose this RA-induced model as many mice need to be culled to harvest very few IELs. CD4s did not appear to proliferate much, possibly this is due to prioritising CD8s in the culture protocol, as previously mentioned. In CD8s, proliferation was reduced in all STm-treated groups, which is similar to what we have observed in another study on our lab (Copland *et al.*, 2023). As αIL-15 and Ibu had no effect on CD4 or CD8 proliferation we can't conclude whether they had any effect on the IELs *in vivo*, although proliferation with was low in all conditions possibly suggesting further optimisation of the co-culture protocol is needed. We would have hypothesised that we would see increased proliferation in the presence of IL-15, as shown previously (James *et al.*, 2021). Possibly this protocol needs further optimisation to allow for more proliferation.

5.3.3 Cytokine changes in *Naip*$^{\Delta/\Delta}$ mice

Whilst most changes in cytokines in both genotypes following DSS or DSS+STm treatment were not statistically significant, there was an increase in IL17 following DSS treatment in both. This is consistent with previous data that IL17 is increased during colitis (Zenewicz, Antov and Flavell, 2009). There was a very slight trend towards increased TNF in *Naip*$^{\Delta/\Delta}$ mice following DSS+STm treatment; perhaps if this experiment was repeated (it was performed only once) this difference would become more apparent, in keeping with the study from Fattinger *et al.* Interestingly, the +FTY720 treatment group had a trend for reduced TNF, supporting the findings of Fattinger *et al*. who demonstrated that TNFα release by haemopoietic cells drives epithelial barrier collapse in *Naip*$^{\Delta/\Delta}$ mice (Fattinger *et al.*, 2021). However, this was at 72 hrs post infection, whereas we took colon samples 24hrs post infection. Li *et al*. also observed increased epithelial damage in *TLR9*-/- knockouts upon STm infection

when IL1β production was reduced by NLRP3 knockout, and speculated that this may be due to increased TNF release mediated by NFκB activation (Li *et al.*, 2017). Therefore, it would be interesting to observe TNF at a later timepoint and investigate the NFκB activation of the IELs.

5.3.4 Limitations of the models

Limitations in these experiments include batch variation between experiments. This can be seen in the TCRγδCD8αα subset in figure 4.7c, where the individual points (i.e. each mouse) of the three experiments clearly separate. It is also present in CFU analysis and in the treatment of splenocytes with RA, as previously mentioned. There were also clear differences in weight loss upon DSS treatment between experiments. This may be relevant, given that different DSS-only treated experiments (i.e. figure 5.2 and 5.15) gave both non-significant and significant increases in IELs. In future we would repeat this with a streptomycin depletion model and assess how the results compare (Kaiser *et al.*, 2012).

5.3.5 Conclusions

From this chapter, we can conclude that *Naip*$^{\Delta/\Delta}$ mice have increased IELs in response to STm infection. However, whilst IL-15/IL-15R expression is increased in *Naip*$^{\Delta/\Delta}$ organoids, we could not ascribe this difference in IELs to IL-15 expression with the current set of experiments. Despite previous studies finding increased bacterial burden in *Naip*$^{\Delta/\Delta}$ mice following STm infection, we could not confirm this consistently in our own experiments. Equally, increased bacterial burden did not appear to explain the increased IELs seen in *Naip*$^{\Delta/\Delta}$ mice. Questions remain regarding the mechanism and effect of increased IELs in this model, and further work will be needed to determine if IELs are having an effect on the epithelial barrier collapse seen in *Naip*$^{\Delta/\Delta}$ mice 72hrs p.i. with STm (Fattinger *et al.*, 2021).

6 Discussion

6.1 Summary of findings

Overall, this thesis aimed to identify how Naips in the intestinal epithelium influence the immune compartment during inflammatory disease. We identified that mice lacking epithelial Naips have increased IELs in response to STm infection. Despite increased tumorigenesis in *Naip*$^{\Delta/\Delta}$ mice, we identified no statistically significant changes in TILs, however we did observe a strong trend towards increased tumour-infiltrating γδ T cells and changes in immune-modulating markers in tumour-derived *Naip*$^{\Delta/\Delta}$ organoids. Alterations in baseline eicosanoid synthesis were also observed, building on Naips previously known role in PGE_2 synthesis following STm infection. Overall, the main findings from this thesis are as follows:

- *Naip*$^{\Delta/\Delta}$ tumour-derived organoids have altered expression of eicosanoid-related genes, including decreases in *Ptgs1* (COX1), *Ptgs2* (COX2) and some leukotriene-related genes, and increases *Pla2g2a* (PLA_2 group IIA) and *Ptger4* (EP4) and altered production of $PGF_{2\alpha}$ and 17,18-DiHETE.
- Strong trend towards increased γδ T cells, particularly CD4+, in *Naip*$^{\Delta/\Delta}$ tumours compared to *Naip*$^{fl/fl}$ tumours following AOM+DSS treatment.
- Following IFNγ treatment, *Naip*$^{\Delta/\Delta}$ tumour-derived organoids upregulate MHCII significantly more than *Naip*$^{fl/fl}$ but IFNγ signalling pathways remain similar in both genotypes.
- Co-culture of *Naip*$^{\Delta/\Delta}$ tumour-derived organoids with splenocytes results in reduced expression of IFNγ in CD4+ T cells.
- IELs are increased in *Naip*$^{\Delta/\Delta}$ mice compared to *Naip*$^{fl/fl}$ mice following DSS+STm treatment but this cannot be explained by reduced PG expression, increased bacterial burden or IL-15/IL-15R expression.

6.1.1 A possible non-inflammasome role of Naips?

We initially identified that, as well the role for Naips in initiating PGE_2 production upon STm infection identified by Rauch *et al*., mice lacking epithelial Naips also had altered eicosanoid production at baseline (Rauch *et al.*, 2017). This is the first suggestion that Naips may be serving a function in the IECs at steady-state, not just in response to infection. Unpublished data from our lab has found that *Naip*$^{\Delta/\Delta}$ tumour-derived organoids cannot express PGE_2 in response to other stimuli, such as TNFα, lipopolysaccharide and melittin, suggesting a fundamental issue in PG expression in these cells. In combination with transcriptional data described here, which shows downregulation of *Ptgs1* (COX1), *Ptgs2* (COX2) and some leukotriene-related genes, this suggests that Naips could possibly be acting at the transcriptional level to regulate eicosanoids. It is not unprecedented for an NLR protein to act as a transcriptional co-activator/repressor. CIITA, described earlier in this thesis as a transcriptional activator of MHCII, is a member of the NLR family (Jorgovanovic *et al.*, 2020). In addition, NLRC5 has been shown to translocate to the nucleus following IFNγ stimulation to promote MHCI gene transcription (Meissner *et al.*, 2010). NLRP14 has also been shown to regulate nuclear translocation of factors involved in spermatid DNA packaging (Yin *et al.*, 2020). Many NLRs, including NOD1, NOD2, NLRP10, NLRC3, NLRC5, NLRX1 and CIITA have non-inflammasome functions (Zaki *et al.*, 2011; Allen *et al.*, 2012; Wilson *et al.*, 2015; Karki *et al.*, 2016; Koblansky *et al.*, 2016; Tattoli *et al.*, 2016). Naips have already been proposed to have a non-inflammasome dependent role in regulating STAT3 activation during tumorigenesis (Allam *et al.*, 2015). It is therefore plausible that Naips could have non-inflammasome-dependent role in regulating transcription of eicosanoid genes. Preliminary data from the lab also suggests that Naips may contain nuclear localisation sequences, further supporting this idea.

In the second chapter of this thesis, we identified that *Naip*$^{\Delta/\Delta}$ tumour-derived organoids upregulated MHCII in response to IFNγ signalling, whereas *Naip*$^{fl/fl}$ organoids did not. However, IFNγ signalling via STAT1 and Akt/mTOR remained intact. It is possible that this could also represent a non-

inflammasome role for Naips. Many NLRs are reported to regulate NFκB, MAPK, STAT3 and Akt signalling via non-inflammasome pathways (Zhu and Cao, 2017). For example, NLRX1 has been suggested to inhibit MAPK and NFκB signalling, resulting in reduced IL-6 expression and STAT3 phosphorylation (Koblansky *et al.*, 2016). A consequence of this was increased tumorigenesis and expedited recovery from DSS damage in *Nlrx1*-/- mice (Koblansky *et al.*, 2016; Lei and Maloy, 2016; Tattoli *et al.*, 2016). Parallels can be drawn between *Nlrx1*-/-mice and mice lacking epithelial Naips; $Naip^{IEC\Delta/\Delta}$ mice have increased tumorigenesis and are protected from DSS colitis, with increased STAT3 phosphorylation and IL-6 expression (Allam *et al.*, 2015). Interestingly, TLR2/MyD88 signalling via NFκB and MAPK has previously been shown to downregulate MHCII expression induced by IFNγ in macrophages by driving CCAATT/enhancer-binding protein-β expression which subsequently binds to the CIITA promoter, inhibiting its expression (Harding and Boom, 2010). It would therefore be interesting to assess NFκB and MAPK activation in tumour-derived organoids in response to IFNγ, to determine whether Naips affect these pathways and whether this affected MHCII expression. This could also involve transcriptional regulation by Naips themselves, as hypothesised above.

However, one thing to consider is that in normal organoids both $Naip^{fl/fl}$ and $Naip^{\Delta/\Delta}$ upregulated MHCII in response to IFNγ. It is also not unusual for tumours to downregulate MHCII expression to aid immune evasion (Axelrod *et al.*, 2019). The effect we observed in tumour-derived organoids therefore appears to be a tumour-specific effect, and whether this truly reflects a role for Naips in MHCII expression or other tumour-related mechanisms remains to be seen. A study of human patient-derived colorectal cancer organoids identified three possible responses to IFNγ stimulation – strong, weak or no induction of MHCII. The reduction in MHCII was mediated by EZH2 (enhancer of zeste homolog 2) occupancy of the CIITA gene, which would be interesting to assess in our own tumour-derived organoids (Pickles *et al.*, 2023).

6.1.2 The role of eicosanoids in *Naip*$^{\Delta/\Delta}$ phenotypes

As previously summarised, *Naip*$^{\Delta/\Delta}$ organoids were found to have altered eicosanoid production. Eicosanoids have a wide range of roles in gut maintenance and disease as well as in modulating the immune system. Throughout this thesis, we have tested whether these changes in eicosanoids have influenced the phenotypes we have observed using ibuprofen and spiked in PGE_2. However, at no point did PG alterations appear to be a clear-cut source of differences between *Naip*$^{\Delta/\Delta}$ and *Naip*$^{fl/fl}$ organoid phenotypes. Ibuprofen inhibits COX enzymes, and so restricts PG production, thus allowing us to mimic the reduced $PGF_{2\alpha}$ seen in *Naip*$^{\Delta/\Delta}$ organoids. Blocking $PGF_{2\alpha}$ in infected *Naip*$^{fl/fl}$ organoids did partially rescue some of the effects on T cell suppression as CD69 recovered (fig.3.4). However, in these experiments we spiked PGE_2, not $PGF_{2\alpha,}$ into *Naip*$^{\Delta/\Delta}$ organoids in order to rescue any alterations compared to Naip$^{fl/fl}$. Many of these experiments were performed prior to the LC/MS was performed, and so we believed PGE_2 to be reduced in *Naip*$^{\Delta/\Delta}$ organoids based on the ELISA result. However, its possible that if we had used $PGF_{2\alpha}$ we would have seen different results. This would be something to repeat in future. We were also never able to inhibit PG production or administer PGs *in vivo*. Given the complex and multifaceted roles of eicosanoids, assessing these effects *in vivo* would give a more accurate picture of eicosanoids role in *Naip*$^{\Delta/\Delta}$ mice during CRC and colitis. It seems likely that such dramatic changes in the eicosanoid profile must be having some effect during these disease models, however in this project we were unable to identify them.

PGE_2 and Ibu were employed to investigate how alterations in eicosanoids could be affected activation of T cells in response to organoids conditioned supernatant and STm infection (fig 3.4) and expression of markers on epithelial organoids (fig. 4.11). However, this is a fraction of the effects alterations eicosanoids could be having in *Naip*$^{\Delta/\Delta}$ mice and organoids. Eicosanoids have well reported effects in both colitis and CRC that are epithelial intrinsic. At no point have we investigated how alterations in eicosanoids could affect the epithelial cells, and this would be an area of future research. Particularly, it would be interesting to assess receptor expression of the epithelial cells, as

our RNAseq data suggests EP4 expression is increased in *Naip*$^{\Delta/\Delta}$ tumour-derived organoids. Whilst this thesis focused more on the effects on the immune compartment, we only focused on T cells and eicosanoids have been shown to have effects on other cell types with consequences for inflammation. For example, PGE_2 has been shown to support an anti-inflammatory neutrophil phenotype following injury, by inducing LXA_4 expression and neutrophil migration (Loynes *et al.*, 2018). It would therefore be interesting to investigate other cell types during CRC, colitis and STm infection in *Naip*$^{\Delta/\Delta}$ mice in future. This study by Loynes *et al.* also exemplifies how eicosanoids in early stages of inflammation can trigger the production of other eicosanoids involved in resolution of inflammation, termed lipid mediator class switching (Serhan *et al.*, 2015). How this process is affected by the alterations in eicosanoids seen in *Naip*$^{\Delta/\Delta}$ remains to be seen and is an area for future research, particularly since 17,18-DiHETE is derived from eicosapentaenoic acid and therefore related to the class of pro-resolution mediators (Serhan *et al.*, 2015).

6.1.3 The effect of Naips on the TILs and the IEL compartment

Whilst Naips have been shown to limit tumorigenesis (Allam *et al.*, 2015), the role of the immune compartment in this effect had not been studied. Here, we found a trend towards increased γδ T cells and decreased TCRαβCD4 cells in the tumours of *Naip*$^{\Delta/\Delta}$ mice when compared to *Naip*$^{fl/fl}$. How exactly this fits with the increased tumorigenesis seen in *Naip*$^{\Delta/\Delta}$ mice remains unclear, though γδ T cells have been known to have both pro-and anti-tumorigenic effects (Reis *et al.*, 2014). We also observed a suppression of T cell activation when T cells were cultured in *Naip*$^{\Delta/\Delta}$ organoid-conditioned medium. Clearly dissecting the effect of Naips on T cells during CRC will require further in vivo and *ex vivo* functional analysis. How this interacts with another area of active research in our lab, developing *Salmonella* bacterial cancer therapy for CRC, would also be of interest. Currently, our understanding is that STm infection in mice with colorectal tumours can lead to a decrease in tumour size, with STm homing specifically to tumours (Mackie *et al.*, 2021). However, T cells appear to be redundant in this treatment and TILs have a variety of activation defects due to inhibition of the

master metabolic controller c-Myc by STm (Copland *et al.*, 2023). Since Naips recognise STm, further understanding how Naips impact the immune compartment during CRC could be pivotal in understanding the immune response during this treatment and how it could be enhanced. Current work in the lab has investigated expression of human NAIP in patient-derived colonic tumour organoids to compare this to the bacterial cancer therapy response (data not published).

In the final chapter of this thesis, we identified increased IELs in *Naip*$^{\Delta/\Delta}$ mice following STm infection, with no statistically significant reductions in IELs at baseline. Many PRRs have been shown to regulate IELs at baseline, however, in most of these studies knockout of the PRR or MyD88 results in decreased IL-15 trans-presentation and decreased IELs (Kaneko *et al.*, 2004; Yu *et al.*, 2006; Jiang *et al.*, 2013; Qiu *et al.*, 2016), whereas we have observed increased IL-15/IL-15R. These PRRs were in many cases shown to be responding to commensal microbiota in order to maintain IEL numbers, whereas to date no commensal bacterial ligand has been identified for Naips (Man, 2018). The fact that IL-15/IL-15R is increased at baseline supports the idea that Naips could be having a homeostatic function. This increase in IL-15/IL-15R in *Naip*$^{\Delta/\Delta}$ IECs could also be having effects on T cells in other contexts, for example during CRC, but we are yet to investigate that.

As mentioned above, there is currently no suggestion that Naips have a commensal bacterial ligand, however we are yet to establish the composition of the gut microbiome of our *Naip*$^{IEC\Delta/\Delta}$ mice. It is possible that this could be altered and have a knock-on effect on the diseases we investigated, as the gut microbiota is known to affect CRC and colitis. Bacteria such as *Bacteroides fragilis*, *Streptococcus gallolyticus*, *Enterococcus faecalis* and *Escherichia coli* promote CRC through a variety of mechanisms including DNA damage, TLR2/4 activation and promotion of an acidic and hypoxic tumour environment (Rebersek, 2021). Changes in the microbiota has also been demonstrated to result in changes in immune infiltration during CRC, with increased CD8αα γδ T cells in both tumour and healthy tissue following antibiotic treatment (Reis *et al.*, 2022). Dysbiosis is also pathogenic in colitis,

with therapeutic faecal microbiota transplantation shown to reduce permeability of the bowel by promoting short-chain fatty acid production, in particular butyrate, which promotes intestinal integrity (Shen *et al.*, 2018). Further investigating how Naips influence the gut microbiota would therefore be an interesting next step.

How this increase in IELs in *Naip*$^{\Delta/\Delta}$ mice following STm infection arises was not determined during this project. Whilst preliminary co-cultures could not pin down the mechanism, it would be interesting to investigate the effects of IL-15 and eicosanoids *in vivo*. Additionally, the effect this increase in IELs has during STm infection remains to be identified. Infection with wild-type *Salmonella* in mice lacking Naips has been shown to result in epithelial barrier breakdown at 72hrs post infection, via a mechanism involving TNFα release (Fattinger *et al.*, 2021). It is possible that IELs could be playing a role in this process and this would be an area of future research.

6.2 Future work

This thesis has covered a range of topics and work remains to fully understand each of the phenotypes seen in *Naip*$^{\Delta/\Delta}$ mice and organoids and tie these threads together. Whilst some of these future directions would have been outside the remit of this project and indeed are entire projects of their own, others are experiments we did not have time to perform. The latter is particularly relevant for *in vivo* studies, as our *Naip*$^{\Delta/\Delta}$ mice were not ready for use in experiments until later into the project than anticipated.

Firstly, to understand the role Naips play in eicosanoid expression we would repeat the LC/MS analysis on normal organoids, to determine changes in the absence of tumorigenesis, and on ex vivo samples, to establish if these effects persist in mice. It would also be interesting to establish alterations in eicosanoid profiles in ex vivo samples during different disease models, such as AOM+DSS, DSS and STm infection as described in this thesis. Prostaglandins have been shown to have different roles at different stages of diseases such as colitis, therefore we could also perform

LC/MS at different stages of disease. RNAseq could also be performed with a similar analysis on normal organoids. It is likely that these data could also be mined further than the current analysis. Understanding the mechanism of how Naips regulate eicosanoids would be a broad task, but to begin to tackle it we would assess whether Naips could be localising to the nucleus for example by blocking nuclear import, mutating the possible nuclear localisation sequences or cloning the possible nuclear localisation sequence onto a GFP construct. Additionally, we could perform ChIPseq analysis to determine if there are Naip binding sites in the promoters of genes differentially regulated in *Naip*$^{\Delta/\Delta}$, for examples *Ptgs1*. We could also assess whether NAIPs interact with other nuclear proteins by immunoprecipitating FLAG tagged Naips from the nuclear extract and performing mass spectrometry. To determine whether this role of Naips inflammasome independent we could assess whether NLRC4 knockout mice phenocopy the eicosanoid alterations seen in *Naip*$^{\Delta/\Delta}$.

To further understand how the immune response is altered in *Naip*$^{\Delta/\Delta}$ mice, we would perform RNAseq with tumour-derived and normal organoids with IFNγ stimulation, to identify what changes in expression are taking place beyond the markers investigated here. This may also give clues as to the mechanism of altered MHCII upregulation. It would also be interesting to see if the effect of *Naip*$^{\Delta/\Delta}$ tumour-derived organoids persists in other tumours, which could be assessed using immunohistochemistry of in vivo samples. This would be important in determining whether this was an effect mediated by Naips or whether it was a tumour-driven effect. Investigation of IFNγ expression in tumours could also be assessed to determine if increased IFNγ sensitivity would have functional consequences. This could be assessed by flow cytometry, using Brefeldin A, by ELISA.

Whilst preliminary co-culture experiments could not identify the cause of increased IELs following STm infection, further optimisation may be worthwhile, as it would enable the screening of candidates using fewer mice. It would also be pertinent to address this *in vivo*. Mice could be treated with ibuprofen to assess the effect of PGs on IELs and blocking antibodies for IL-15 could be used.

Particularly with PGs, since these can influence such a wide range of cell types in the gut, this may more accurately depict the effects reduced PGs are having on the IEL compartment.

We would also be interested to establish the function of the γδ T cells we found to be enriched in the TILs of *Naip*$^{\Delta/\Delta}$ mice. We would be interested to see if these cells expressed IL-17, which we could assess using Brefeldin A and flow cytometry. We would also use mice lacking γδ T cells crossed with our *Naip*$^{\Delta/\Delta}$ to establish the effect this had on tumour burden and therefore whether the γδ T cells were pro-tumorigenic.

6.3 Final Summary

To conclude, epithelial Naips have the potential to affect the immune compartment in various ways. We have identified alterations in eicosanoids, specifically decreases in $PGF_{2\alpha}$ and increases in 17,18-DiHETE, and increased IL-15/IL-15R expression in mice lacking epithelial Naips, but have not yet deduced the effect this has on immune cells. We have confirmed that NAIPs protect against colon tumorigenesis, and determined that in a tumour setting, Naips may be altering expression of MHCII in response to IFNγ. However, whether this alteration in MHCII results in an altered immune response remain to be elucidated. Finally, we found that mice lacking epithelial Naips have increased IELs in response to STm infection. This was not due to increased bacterial burden and did not appear to due to altered IL-15/IL-15R or eicosanoid expression. Questions therefore remain as to how the changes in eicosanoids, IL-15/IL-15R and MHCII expression affect the immune compartment in mice lacking Naips and what consequences this has for inflammatory disease and infection.

7 References

Abadie, V., Discepolo, V. and Jabri, B. (2012) 'Intraepithelial lymphocytes in celiac disease immunopathology', *Seminars in Immunopathology*, 34(4), pp. 551–566. Available at: https://doi.org/10.1007/s00281-012-0316-x.

de Aberasturi, A.L. and Calvo, A. (2015) 'TMPRSS4: an emerging potential therapeutic target in cancer', *British Journal of Cancer*, 112(1), pp. 4–8. Available at: https://doi.org/10.1038/bjc.2014.403.

Adegboyega, P.A. *et al.* (2004) 'Subepithelial Myofibroblasts Express Cyclooxygenase-2 in Colorectal Tubular Adenomas', *Clinical Cancer Research*, 10(17), pp. 5870–5879. Available at: https://doi.org/10.1158/1078-0432.CCR-0431-03.

Agoff, S.N. *et al.* (2000) 'The role of cyclooxygenase 2 in ulcerative colitis-associated neoplasia', *The American Journal of Pathology*, 157(3), pp. 737–745. Available at: https://doi.org/10.1016/S0002-9440(10)64587-7.

Allam, R. *et al.* (2015) 'Epithelial NAIPs protect against colonic tumorigenesis', *Journal of Experimental Medicine*, 212(3), pp. 369–383. Available at: https://doi.org/10.1084/jem.20140474.

Allen, I.C. *et al.* (2012) 'NLRP12 Suppresses Colon Inflammation and Tumorigenesis through the Negative Regulation of Noncanonical NF-κB Signaling', *Immunity*, 36(5), pp. 742–754. Available at: https://doi.org/10.1016/j.immuni.2012.03.012.

Alspach, E., Lussier, D.M. and Schreiber, R.D. (2019) 'Interferon γ and Its Important Roles in Promoting and Inhibiting Spontaneous and Therapeutic Cancer Immunity', *Cold Spring Harbor Perspectives in Biology*, 11(3), p. a028480. Available at: https://doi.org/10.1101/cshperspect.a028480.

Amicarella, F. *et al.* (2017) 'Dual role of tumour-infiltrating T helper 17 cells in human colorectal cancer', *Gut*, 66(4), pp. 692–704. Available at: https://doi.org/10.1136/gutjnl-2015-310016.

Aristin Revilla, S., Kranenburg, O. and Coffer, P.J. (2022) 'Colorectal Cancer-Infiltrating Regulatory T Cells: Functional Heterogeneity, Metabolic Adaptation, and Therapeutic Targeting', *Frontiers in Immunology*, 13, p. 903564. Available at: https://doi.org/10.3389/fimmu.2022.903564.

Armstrong, T.D. *et al.* (1997) 'Major histocompatibility complex class II-transfected tumor cells present endogenous antigen and are potent inducers of tumor-specific immunity', *Proceedings of the National Academy of Sciences*, 94(13), pp. 6886–6891. Available at: https://doi.org/10.1073/pnas.94.13.6886.

Axelrod, M.L. *et al.* (2019) 'Biological Consequences of MHC-II Expression by Tumor Cells in Cancer', *Clinical Cancer Research*, 25(8), pp. 2392–2402. Available at: https://doi.org/10.1158/1078-0432.CCR-18-3200.

Ayers, M. *et al.* (2017) 'IFN-**γ**–related mRNA profile predicts clinical response to PD-1 blockade', *The Journal of Clinical Investigation*, 127(8), pp. 2930–2940. Available at: https://doi.org/10.1172/JCI91190.

Bai, Z. *et al.* (2022) 'Tumor-Infiltrating Lymphocytes in Colorectal Cancer: The Fundamental Indication and Application on Immunotherapy', *Frontiers in Immunology*, 12. Available at: https://www.frontiersin.org/articles/10.3389/fimmu.2021.808964 (Accessed: 11 October 2023).

Ball, D.P. *et al.* (2020) 'Caspase-1 interdomain linker cleavage is required for pyroptosis', *Life Science Alliance*, 3(3), p. e202000664. Available at: https://doi.org/10.26508/lsa.202000664.

Bamba, H. *et al.* (1999) 'High expression of cyclooxygenase-2 in macrophages of human colonic adenoma', *International Journal of Cancer*, 83(4), pp. 470–475. Available at: https://doi.org/10.1002/(SICI)1097-0215(19991112)83:4<470::AID-IJC6>3.0.CO;2-F.

Banerjee, D.K. *et al.* (2006) 'Expansion of FOXP3high regulatory T cells by human dendritic cells (DCs) in vitro and after injection of cytokine-matured DCs in myeloma patients', *Blood*, 108(8), pp. 2655–2661. Available at: https://doi.org/10.1182/blood-2006-03-011353.

Baratelli, F. *et al.* (2005) 'Prostaglandin E2 Induces FOXP3 Gene Expression and T Regulatory Cell Function in Human CD4+ T Cells1', *The Journal of Immunology*, 175(3), pp. 1483–1490. Available at: https://doi.org/10.4049/jimmunol.175.3.1483.

Barker, N. *et al.* (2009) 'Crypt stem cells as the cells-of-origin of intestinal cancer', *Nature*, 457(7229), pp. 608–611. Available at: https://doi.org/10.1038/nature07602.

Barker, N. *et al.* (2010) 'Lgr5+ve Stem Cells Drive Self-Renewal in the Stomach and Build Long-Lived Gastric Units In Vitro', *Cell Stem Cell*, 6(1), pp. 25–36. Available at: https://doi.org/10.1016/j.stem.2009.11.013.

Baskar, S. *et al.* (1996) 'Rejection of MHC class II-transfected tumor cells requires induction of tumor-encoded B7-1 and/or B7-2 costimulatory molecules.', *The Journal of Immunology*, 156(10), pp. 3821–3827. Available at: https://doi.org/10.4049/jimmunol.156.10.3821.

Bauer, R. and Rauch, I. (2020) 'The NAIP/NLRC4 inflammasome in infection and pathology', *Molecular Aspects of Medicine*, 76, p. 100863. Available at: https://doi.org/10.1016/j.mam.2020.100863.

Bauer, S. *et al.* (1999) 'Activation of NK Cells and T Cells by NKG2D, a Receptor for Stress-Inducible MICA', *Science*, 285(5428), pp. 727–729. Available at: https://doi.org/10.1126/science.285.5428.727.

Bending, D., Paduraru, A., *et al.* (2018) 'A temporally dynamic Foxp3 autoregulatory transcriptional circuit controls the effector Treg programme', *The EMBO Journal*, 37(16), p. e99013. Available at: https://doi.org/10.15252/embj.201899013.

Bending, D., Martín, P.P., *et al.* (2018) 'A timer for analyzing temporally dynamic changes in transcription during differentiation in vivo', *Journal of Cell Biology*, 217(8), pp. 2931–2950. Available at: https://doi.org/10.1083/jcb.201711048.

Berner, V. *et al.* (2007) 'IFN-γ mediates CD4+ T-cell loss and impairs secondary antitumor responses after successful initial immunotherapy', *Nature Medicine*, 13(3), pp. 354–360. Available at: https://doi.org/10.1038/nm1554.

Bertelsen, L.S. *et al.* (2003) 'Salmonella Infection Induces a Hypersecretory Phenotype in Human Intestinal Xenografts by Inducing Cyclooxygenase 2', *Infection and Immunity*, 71(4), pp. 2102–2109. Available at: https://doi.org/10.1128/IAI.71.4.2102-2109.2003.

Blatner, N.R. *et al.* (2012) 'Expression of RORγt Marks a Pathogenic Regulatory T Cell Subset in Human Colon Cancer', *Science Translational Medicine*, 4(164), pp. 164ra159-164ra159. Available at: https://doi.org/10.1126/scitranslmed.3004566.

Blouin, C.M. and Lamaze, C. (2013) 'Interferon Gamma Receptor: The Beginning of the Journey', *Frontiers in Immunology*, 4, p. 267. Available at: https://doi.org/10.3389/fimmu.2013.00267.

Boismenu, R. and Havran, W.L. (1994) 'Modulation of Epithelial Cell Growth by Intraepithelial γδ T Cells', *Science*, 266(5188), pp. 1253–1255. Available at: https://doi.org/10.1126/science.7973709.

Boniface, K. *et al.* (2009) 'Prostaglandin E2 regulates Th17 cell differentiation and function through cyclic AMP and EP2/EP4 receptor signaling', *Journal of Experimental Medicine*, 206(3), pp. 535–548. Available at: https://doi.org/10.1084/jem.20082293.

Bou Nasser Eddine, F. *et al.* (2017) 'CIITA-driven MHC class II expressing tumor cells can efficiently prime naive CD4+ TH cells in vivo and vaccinate the host against parental MHC-II-negative tumor cells', *OncoImmunology*, 6(1), p. e1261777. Available at: https://doi.org/10.1080/2162402X.2016.1261777.

Bowman, C.C. and Bost, K.L. (2004) 'Cyclooxygenase-2-Mediated Prostaglandin E2 Production in Mesenteric Lymph Nodes and in Cultured Macrophages and Dendritic Cells after Infection with Salmonella1', *The Journal of Immunology*, 172(4), pp. 2469–2475. Available at: https://doi.org/10.4049/jimmunol.172.4.2469.

Bowman, C.C. and Bost, K.L. (2009) 'Cyclooxygenase-2 Inhibition Enhances Activation of T Helper Type 1 Responses During Salmonella Infection', *The Open Microbiology Journal*, 3, pp. 23–28. Available at: https://doi.org/10.2174/1874285800903010023.

Braumüller, H. *et al.* (2013) 'T-helper-1-cell cytokines drive cancer into senescence', *Nature*, 494(7437), pp. 361–365. Available at: https://doi.org/10.1038/nature11824.

Braumüller, H. *et al.* (2023) 'The Cytokine Network in Colorectal Cancer: Implications for New Treatment Strategies', *Cells*, 12(1), p. 138. Available at: https://doi.org/10.3390/cells12010138.

Brenner, E. *et al.* (2020) 'Cancer immune control needs senescence induction by interferon-dependent cell cycle regulator pathways in tumours', *Nature Communications*, 11(1), p. 1335. Available at: https://doi.org/10.1038/s41467-020-14987-6.

Brinkman, B.M. *et al.* (2013) 'Gut Microbiota Affects Sensitivity to Acute DSS-induced Colitis Independently of Host Genotype', *Inflammatory Bowel Diseases*, 19(12), pp. 2560–2567. Available at: https://doi.org/10.1097/MIB.0b013e3182a8759a.

Brown, S.L. *et al.* (2007) 'Myd88-dependent positioning of Ptgs2-expressing stromal cells maintains colonic epithelial proliferation during injury', *Journal of Clinical Investigation*, 117(1), pp. 258–269. Available at: https://doi.org/10.1172/JCI29159.

Bruni, D., Angell, H.K. and Galon, J. (2020) 'The immune contexture and Immunoscore in cancer prognosis and therapeutic efficacy', *Nature Reviews Cancer*, 20(11), pp. 662–680. Available at: https://doi.org/10.1038/s41568-020-0285-7.

Burke, J.D. and Young, H.A. (2019) 'IFN-γ: A cytokine at the right time, is in the right place', *Seminars in immunology*, 43, p. 101280. Available at: https://doi.org/10.1016/j.smim.2019.05.002.

Bygdeman, M. (2003) 'Pharmacokinetics of prostaglandins', *Best Practice & Research Clinical Obstetrics & Gynaecology*, 17(5), pp. 707–716. Available at: https://doi.org/10.1016/S1521-6934(03)00043-9.

Cantrell, M.A. and Kuo, C.J. (2015) 'Organoid modeling for cancer precision medicine', *Genome Medicine*, 7(1), p. 32. Available at: https://doi.org/10.1186/s13073-015-0158-y.

Caretto, D. *et al.* (2010) 'Cutting Edge: The Th1 Response Inhibits the Generation of Peripheral Regulatory T Cells', *Journal of immunology (Baltimore, Md. : 1950)*, 184(1), pp. 30–34. Available at: https://doi.org/10.4049/jimmunol.0903412.

Castellone, M.D. *et al.* (2005) 'Prostaglandin E2 Promotes Colon Cancer Cell Growth Through a Gs-Axin-ß-Catenin Signaling Axis', *Science*, 310(5753), pp. 1504–1510. Available at: https://doi.org/10.1126/science.1116221.

Cervantes-Barragan, L. *et al.* (2017) 'Lactobacillus reuteri induces gut intraepithelial CD4+CD8αα+ T cells', *Science*, 357(6353), pp. 806–810. Available at: https://doi.org/10.1126/science.aah5825.

Chapple, K.S. *et al.* (2000) 'Localization of Cyclooxygenase-2 in Human Sporadic Colorectal Adenomas', *The American Journal of Pathology*, 156(2), pp. 545–553.

Chassaing, B. *et al.* (2014) 'Dextran Sulfate Sodium (DSS)-Induced Colitis in Mice', *Current protocols in immunology / edited by John E. Coligan ... [et al.]*, 104, p. Unit-15.25. Available at: https://doi.org/10.1002/0471142735.im1525s104.

Chaudhry, A. *et al.* (2011) 'Interleukin-10 signaling in regulatory T cells is required for suppression of Th17 cell-mediated inflammation', *Immunity*, 34(4), pp. 566–578. Available at: https://doi.org/10.1016/j.immuni.2011.03.018.

Chen, E.P. *et al.* (2014) 'Myeloid Cell COX-2 deletion reduces mammary tumor growth through enhanced cytotoxic T-lymphocyte function', *Carcinogenesis*, 35(8), pp. 1788–1797. Available at: https://doi.org/10.1093/carcin/bgu053.

Chen, G.Y. *et al.* (2011) 'A functional role for Nlrp6 in intestinal inflammation and tumorigenesis', *Journal of Immunology (Baltimore, Md.: 1950)*, 186(12), pp. 7187–7194. Available at: https://doi.org/10.4049/jimmunol.1100412.

Chen, H. *et al.* (2009) 'Effects of leukotriene B4 and prostaglandin E2 on the differentiation of murine Foxp3+ T regulatory cells and Th17 cells', *Prostaglandins, Leukotrienes and Essential Fatty Acids*, 80(4), pp. 195–200. Available at: https://doi.org/10.1016/j.plefa.2009.01.006.

Chen, H.-C. *et al.* (2011) 'Induction of metastatic cancer stem cells from the NK/LAK-resistant floating, but not adherent, subset of the UP-LN1 carcinoma cell line by IFN-γ', *Laboratory Investigation*, 91(10), pp. 1502–1513. Available at: https://doi.org/10.1038/labinvest.2011.91.

Chen, J., Wang, Z. and Yu, S. (2017) 'AIM2 regulates viability and apoptosis in human colorectal cancer cells via the PI3K/Akt pathway', *OncoTargets and therapy*, 10, pp. 811–817. Available at: https://doi.org/10.2147/OTT.S125039.

Chen, Y. *et al.* (2002) 'Protection of the intestinal mucosa by intraepithelial γδ T cells', *Proceedings of the National Academy of Sciences of the United States of America*, 99(22), pp. 14338–14343. Available at: https://doi.org/10.1073/pnas.212290499.

Cheroutre, H. and Lambolez, F. (2008) 'Doubting the TCR Coreceptor Function of CD8αα', *Immunity*, 28(2), pp. 149–159. Available at: https://doi.org/10.1016/j.immuni.2008.01.005.

Cheroutre, H., Lambolez, F. and Mucida, D. (2011) 'The light and dark sides of intestinal intraepithelial lymphocytes', *Nature Reviews Immunology*, 11(7), pp. 445–456. Available at: https://doi.org/10.1038/nri3007.

Cherukuri, D.P. *et al.* (2014) 'Targeted Cox2 gene deletion in intestinal epithelial cells decreases tumorigenesis in female, but not male, Apc Min/+ mice', *Molecular Oncology*, 8(2), pp. 169–177. Available at: https://doi.org/10.1016/j.molonc.2013.10.009.

Chhonker, Y.S. *et al.* (2021) 'Simultaneous Quantitation of Lipid Biomarkers for Inflammatory Bowel Disease Using LC–MS/MS', *Metabolites*, 11(2), p. 106. Available at: https://doi.org/10.3390/metabo11020106.

Chiba, T. *et al.* (2004) 'Intraepithelial CD8+ T-cell-count becomes a prognostic factor after a longer follow-up period in human colorectal carcinoma: possible association with suppression of micrometastasis', *British Journal of Cancer*, 91(9), pp. 1711–1717. Available at: https://doi.org/10.1038/sj.bjc.6602201.

Chiu, C.-L. *et al.* (2022) 'The Role of MARCKS in Metastasis and Treatment Resistance of Solid Tumors', *Cancers*, 14(19), p. 4925. Available at: https://doi.org/10.3390/cancers14194925.

Chizzolini, C. *et al.* (2008) 'Prostaglandin E2 synergistically with interleukin-23 favors human Th17 expansion', *Blood*, 112(9), pp. 3696–3703. Available at: https://doi.org/10.1182/blood-2008-05-155408.

Christou, N. *et al.* (2017) 'E-cadherin: A potential biomarker of colorectal cancer prognosis', *Oncology Letters*, 13(6), pp. 4571–4576. Available at: https://doi.org/10.3892/ol.2017.6063.

Chulada, P.C. *et al.* (2000) 'Genetic Disruption of Ptgs-1, as well as of Ptgs-2, Reduces Intestinal Tumorigenesis in Min Mice', *Cancer Research*, 60(17), pp. 4705–4708.

Cibrián, D. and Sánchez-Madrid, F. (2017) 'CD69: from activation marker to metabolic gatekeeper', *European journal of immunology*, 47(6), pp. 946–953. Available at: https://doi.org/10.1002/eji.201646837.

Cohn, S.M. *et al.* (1997) 'Crypt stem cell survival in the mouse intestinal epithelium is regulated by prostaglandins synthesized through cyclooxygenase-1.', *The Journal of Clinical Investigation*, 99(6), pp. 1367–1379. Available at: https://doi.org/10.1172/JCI119296.

Colgan, S.P. *et al.* (1996) 'IFN-gamma modulates CD1d surface expression on intestinal epithelia', *American Journal of Physiology-Cell Physiology*, 271(1), pp. C276–C283. Available at: https://doi.org/10.1152/ajpcell.1996.271.1.C276.

Copland, A. *et al.* (2023) 'Salmonella cancer therapy metabolically disrupts tumours at the collateral cost of T cell immunity'. bioRxiv, p. 2023.01.12.523780. Available at: https://doi.org/10.1101/2023.01.12.523780.

Corpet, D.E. and Pierre, F. (2003) 'Point: From animal models to prevention of colon cancer. Systematic review of chemoprevention in min mice and choice of the model system', *Cancer Epidemiology, Biomarkers & Prevention*, 12(5), pp. 391–400.

Corvaisier, M. *et al.* (2005) 'Vγ9Vδ2 T Cell Response to Colon Carcinoma Cells1', *The Journal of Immunology*, 175(8), pp. 5481–5488. Available at: https://doi.org/10.4049/jimmunol.175.8.5481.

Cracowski, J.-L. *et al.* (2002) 'Increased urinary F2-isoprostanes in patients with Crohn's disease', *The American Journal of Gastroenterology*, 97(1), pp. 99–103. Available at: https://doi.org/10.1016/S0002-9270(01)03989-2.

Crane, A.M. and Bhattacharya, S.K. (2013) 'The Use of Bromodeoxyuridine Incorporation Assays to Assess Corneal Stem Cell Proliferation', in B. Wright and C.J. Connon (eds) *Corneal Regenerative Medicine: Methods and Protocols*. Totowa, NJ: Humana Press (Methods in Molecular Biology), pp. 65–70. Available at: https://doi.org/10.1007/978-1-62703-432-6_4.

Crowley, S.M. *et al.* (2020) 'Intestinal restriction of Salmonella Typhimurium requires caspase-1 and caspase-11 epithelial intrinsic inflammasomes', *PLOS Pathogens*. Edited by I.E. Brodsky, 16(4), p. e1008498. Available at: https://doi.org/10.1371/journal.ppat.1008498.

Das, G. *et al.* (2003) 'An important regulatory role for CD4+CD8αα T cells in the intestinal epithelial layer in the prevention of inflammatory bowel disease', *Proceedings of the National Academy of Sciences*, 100(9), pp. 5324–5329. Available at: https://doi.org/10.1073/pnas.0831037100.

Dasgupta, S. *et al.* (2021) 'γδ T Cells Control Gut Pathology in a Chronic Inflammatory Model of Colorectal Cancer', *Cellular and Molecular Gastroenterology and Hepatology*, 12(3), pp. 1163-1165.e8. Available at: https://doi.org/10.1016/j.jcmgh.2021.05.002.

Davies, A. *et al.* (2004) 'Infection-Induced Expansion of a MHC Class Ib-Dependent Intestinal Intraepithelial γδ T Cell Subset12', *The Journal of Immunology*, 172(11), pp. 6828–6837. Available at: https://doi.org/10.4049/jimmunol.172.11.6828.

De Simone, V. *et al.* (2013) 'Role of TH17 cytokines in the control of colorectal cancer', *OncoImmunology*, 2(12), p. e26617. Available at: https://doi.org/10.4161/onci.26617.

Deffrennes, V. *et al.* (2001) 'Constitutive Expression of MHC Class II Genes in Melanoma Cell Lines Results from the Transcription of Class II Transactivator Abnormally Initiated from Its B Cell-Specific Promoter1', *The Journal of Immunology*, 167(1), pp. 98–106. Available at: https://doi.org/10.4049/jimmunol.167.1.98.

Dey, I., Lejeune, M. and Chadee, K. (2006) 'Prostaglandin E2 receptor distribution and function in the gastrointestinal tract', *British Journal of Pharmacology*, 149(6), pp. 611–623. Available at: https://doi.org/10.1038/sj.bjp.0706923.

Di Lorenzo, B., Ravens, S. and Silva-Santos, B. (2019) 'High-throughput analysis of the human thymic Vδ1+ T cell receptor repertoire', *Scientific Data*, 6(1), p. 115. Available at: https://doi.org/10.1038/s41597-019-0118-2.

Di Rosa, F., Cossarizza, A. and Hayday, A.C. (2021) 'To Ki or Not to Ki: Re-Evaluating the Use and Potentials of Ki-67 for T Cell Analysis', *Frontiers in Immunology*, 12. Available at: https://www.frontiersin.org/articles/10.3389/fimmu.2021.653974 (Accessed: 13 December 2023).

Diez, E. *et al.* (2000) 'The Neuronal Apoptosis Inhibitory Protein (Naip) Is Expressed in Macrophages and Is Modulated After Phagocytosis and During Intracellular Infection with Legionella pneumophila', *The Journal of Immunology*, 164(3), pp. 1470–1477. Available at: https://doi.org/10.4049/jimmunol.164.3.1470.

Dihlmann, S. *et al.* (2014) 'Lack of Absent in Melanoma 2 (AIM2) expression in tumor cells is closely associated with poor survival in colorectal cancer patients', *International Journal of Cancer*, 135(10), pp. 2387–2396. Available at: https://doi.org/10.1002/ijc.28891.

Di Marco Barros, R. *et al.* (2016) 'Epithelia Use Butyrophilin-like Molecules to Shape Organ-Specific γδ T Cell Compartments', *Cell*, 167(1), pp. 203-218.e17. Available at: https://doi.org/10.1016/j.cell.2016.08.030.

Djenidi, F. *et al.* (2015) 'CD8+CD103+ Tumor–Infiltrating Lymphocytes Are Tumor-Specific Tissue-Resident Memory T Cells and a Prognostic Factor for Survival in Lung Cancer Patients', *The Journal of Immunology*, 194(7), pp. 3475–3486. Available at: https://doi.org/10.4049/jimmunol.1402711.

Dolcetti, R. *et al.* (1999) 'High Prevalence of Activated Intraepithelial Cytotoxic T Lymphocytes and Increased Neoplastic Cell Apoptosis in Colorectal Carcinomas with Microsatellite Instability', *The American Journal of Pathology*, 154(6), pp. 1805–1813. Available at: https://doi.org/10.1016/S0002-9440(10)65436-3.

Dubois, S. *et al.* (2002) 'IL-15Rα Recycles and Presents IL-15 In trans to Neighboring Cells', *Immunity*, 17(5), pp. 537–547. Available at: https://doi.org/10.1016/S1074-7613(02)00429-6.

Dumauthioz, N., Labiano, S. and Romero, P. (2018) 'Tumor Resident Memory T Cells: New Players in Immune Surveillance and Therapy', *Frontiers in Immunology*, 9, p. 2076. Available at: https://doi.org/10.3389/fimmu.2018.02076.

Durinck, S. *et al.* (2009) 'Mapping identifiers for the integration of genomic datasets with the R/Bioconductor package biomaRt', *Nature Protocols*, 4(8), pp. 1184–1191. Available at: https://doi.org/10.1038/nprot.2009.97.

Eberhart, C.E. *et al.* (1994) 'Up-regulation of cyclooxygenase 2 gene expression in human colorectal adenomas and adenocarcinomas', *Gastroenterology*, 107(4), pp. 1183–1188. Available at: https://doi.org/10.1016/0016-5085(94)90246-1.

Eckmann, L. *et al.* (1997) 'Role of intestinal epithelial cells in the host secretory response to infection by invasive bacteria. Bacterial entry induces epithelial prostaglandin h synthase-2 expression and prostaglandin E2 and F2alpha production.', *Journal of Clinical Investigation*, 100(2), pp. 296–309.

Edelblum, K.L. *et al.* (2012) 'Dynamic migration of γδ intraepithelial lymphocytes requires occludin', *Proceedings of the National Academy of Sciences*, 109(18), pp. 7097–7102. Available at: https://doi.org/10.1073/pnas.1112519109.

Endo, T. *et al.* (2004) 'Expression of IAP family proteins in colon cancers from patients with different age groups', *Cancer Immunology, Immunotherapy*, 53(9), pp. 770–776. Available at: https://doi.org/10.1007/s00262-004-0534-8.

English, K. *et al.* (2009) 'Cell contact, prostaglandin E2 and transforming growth factor beta 1 play non-redundant roles in human mesenchymal stem cell induction of CD4+CD25Highforkhead box P3+ regulatory T cells', *Clinical and Experimental Immunology*, 156(1), pp. 149–160. Available at: https://doi.org/10.1111/j.1365-2249.2009.03874.x.

Ettersperger, J. *et al.* (2016) 'Interleukin-15-Dependent T-Cell-like Innate Intraepithelial Lymphocytes Develop in the Intestine and Transform into Lymphomas in Celiac Disease', *Immunity*, 45(3), pp. 610–625. Available at: https://doi.org/10.1016/j.immuni.2016.07.018.

Fabre, J. *et al.* (2016) 'Targeting the Tumor Microenvironment: The Protumor Effects of IL-17 Related to Cancer Type', *International Journal of Molecular Sciences*, 17(9), p. 1433. Available at: https://doi.org/10.3390/ijms17091433.

Fabricius, D. *et al.* (2009) 'Prostaglandin E2 Inhibits IFN-α Secretion and Th1 Costimulation by Human Plasmacytoid Dendritic Cells via E-Prostanoid 2 and E-Prostanoid 4 Receptor Engagement', *The Journal of Immunology*, 184(2), pp. 677–684. Available at: https://doi.org/10.4049/jimmunol.0902028.

Fang, P. *et al.* (2018) 'Immune cell subset differentiation and tissue inflammation', *Journal of Hematology & Oncology*, 11(1), p. 97. Available at: https://doi.org/10.1186/s13045-018-0637-x.

Fattinger, S.A. *et al.* (2021) 'Epithelium-autonomous NAIP/NLRC4 prevents TNF-driven inflammatory destruction of the gut epithelial barrier in Salmonella -infected mice', *Mucosal Immunology*, pp. 1–15. Available at: https://doi.org/10.1038/s41385-021-00381-y.

Felgner, S. *et al.* (2016) 'aroA-Deficient Salmonella enterica Serovar Typhimurium Is More Than a Metabolically Attenuated Mutant', *mBio*, 7(5). Available at: https://doi.org/10.1128/mBio.01220-16.

Ferrer, R. and Moreno, J.J. (2010) 'Role of eicosanoids on intestinal epithelial homeostasis', *Biochemical Pharmacology*, 80(4), pp. 431–438. Available at: https://doi.org/10.1016/j.bcp.2010.04.033.

Fina, D. *et al.* (2008) 'Regulation of Gut Inflammation and Th17 Cell Response by Interleukin-21', *Gastroenterology*, 134(4), pp. 1038-1048.e2. Available at: https://doi.org/10.1053/j.gastro.2008.01.041.

Fischer, M.A., Golovchenko, N.B. and Edelblum, K.L. (2020) 'γδ T cell migration: Separating trafficking from surveillance behaviors at barrier surfaces', *Immunological Reviews*, 298(1), pp. 165–180. Available at: https://doi.org/10.1111/imr.12915.

Forero, A. *et al.* (2016) 'Expression of the MHC Class II Pathway in Triple-Negative Breast Cancer Tumor Cells Is Associated with a Good Prognosis and Infiltrating Lymphocytes', *Cancer Immunology Research*, 4(5), pp. 390–399. Available at: https://doi.org/10.1158/2326-6066.CIR-15-0243.

Franchi, L. *et al.* (2006) 'Cytosolic flagellin requires Ipaf for activation of caspase-1 and interleukin 1β in salmonella-infected macrophages', *Nature Immunology*, 7(6), pp. 576–582. Available at: https://doi.org/10.1038/ni1346.

Fuchs, A. *et al.* (2013) 'Intraepithelial type 1 innate lymphoid cells are a unique subset of cytokine responsive interferon-γ-producing cells', *Immunity*, 38(4), pp. 769–781. Available at: https://doi.org/10.1016/j.immuni.2013.02.010.

Fujii, M. *et al.* (2015) 'Efficient genetic engineering of human intestinal organoids using electroporation', *Nature Protocols*, 10(10), pp. 1474–1485. Available at: https://doi.org/10.1038/nprot.2015.088.

Fukata, M. *et al.* (2006) 'Cox-2 Is Regulated by Toll-Like Receptor-4 (TLR4) Signaling: Role in Proliferation and Apoptosis in the Intestine', *Gastroenterology*, 131(3), pp. 862–877. Available at: https://doi.org/10.1053/j.gastro.2006.06.017.

Fukata, M. *et al.* (2007) 'Toll-like receptor-4 promotes the development of colitis-associated colorectal tumors', *Gastroenterology*, 133(6), pp. 1869–1881. Available at: https://doi.org/10.1053/j.gastro.2007.09.008.

Galon, J., Fridman, W.-H. and Pagès, F. (2007) 'The Adaptive Immunologic Microenvironment in Colorectal Cancer: A Novel Perspective', *Cancer Research*, 67(5), pp. 1883–1886. Available at: https://doi.org/10.1158/0008-5472.CAN-06-4806.

Gandhi, A.S. *et al.* (2017) 'Quantitative analysis of lipids: a higher-throughput LC–MS/MS-based method and its comparison to ELISA', *Future Science OA*, 3(1), p. FSO157. Available at: https://doi.org/10.4155/fsoa-2016-0067.

Gangadharan, D. and Cheroutre, H. (2004) 'The CD8 isoform CD8αα is not a functional homologue of the TCR co-receptor CD8αβ', *Current Opinion in Immunology*, 16(3), pp. 264–270. Available at: https://doi.org/10.1016/j.coi.2004.03.015.

Garcia-Peñarrubia, P., Bankhurst, A.D. and Koster, F.T. (1989) 'Prostaglandins from human T suppressor/cytotoxic cells modulate natural killer antibacterial activity.', *Journal of Experimental Medicine*, 170(2), pp. 601–606. Available at: https://doi.org/10.1084/jem.170.2.601.

Garcillán, B. *et al.* (2015) 'gd T lymphocytes in the diagnosis of human T cell receptor immunodeficiencies', *Frontiers in Immunology*, 6. Available at: https://www.frontiersin.org/articles/10.3389/fimmu.2015.00020 (Accessed: 1 October 2023).

Garrity-Park, M.M. *et al.* (2009) 'MHC Class II alleles in ulcerative colitis-associated colorectal cancer', *Gut*, 58(9), pp. 1226–1233. Available at: https://doi.org/10.1136/gut.2008.166686.

Geng, J. and Raghavan, M. (2019) 'CD8αα homodimers function as a coreceptor for KIR3DL1', *Proceedings of the National Academy of Sciences*, 116(36), pp. 17951–17956. Available at: https://doi.org/10.1073/pnas.1905943116.

Gentles, A.J. *et al.* (2015) 'The prognostic landscape of genes and infiltrating immune cells across human cancers', *Nature Medicine*, 21(8), pp. 938–945. Available at: https://doi.org/10.1038/nm.3909.

Gillis, C.C. *et al.* (2018) 'Dysbiosis-associated change in host metabolism generates lactate to support Salmonella growth', *Cell host & microbe*, 23(1), pp. 54-64.e6. Available at: https://doi.org/10.1016/j.chom.2017.11.006.

Girardin, A. *et al.* (2013) 'Inflammatory and regulatory T cells contribute to a unique immune microenvironment in tumor tissue of colorectal cancer patients', *International Journal of Cancer*, 132(8), pp. 1842–1850. Available at: https://doi.org/10.1002/ijc.27855.

Gober, H.-J. *et al.* (2003) 'Human T Cell Receptor γδ Cells Recognize Endogenous Mevalonate Metabolites in Tumor Cells', *Journal of Experimental Medicine*, 197(2), pp. 163–168. Available at: https://doi.org/10.1084/jem.20021500.

Golstein, P. and Griffiths, G.M. (2018) 'An early history of T cell-mediated cytotoxicity', *Nature Reviews Immunology*, 18(8), pp. 527–535. Available at: https://doi.org/10.1038/s41577-018-0009-3.

Gouvello, S.L. *et al.* (2008) 'High prevalence of Foxp3 and IL17 in MMR-proficient colorectal carcinomas', *Gut*, 57(6), pp. 772–779. Available at: https://doi.org/10.1136/gut.2007.123794.

Griffith, B.D. *et al.* (2022) 'MHC Class II Expression Influences the Composition and Distribution of Immune Cells in the Metastatic Colorectal Cancer Microenvironment', *Cancers*, 14(17), p. 4092. Available at: https://doi.org/10.3390/cancers14174092.

Grivennikov, S.I. *et al.* (2012) 'Adenoma-linked barrier defects and microbial products drive IL-23/IL-17-mediated tumour growth', *Nature*, 491(7423), pp. 254–258. Available at: https://doi.org/10.1038/nature11465.

Gulig, P.A. and Doyle, T.J. (1993) 'The Salmonella typhimurium virulence plasmid increases the growth rate of salmonellae in mice.', *Infection and Immunity*, 61(2), pp. 504–511.

Guy-Grand, D. *et al.* (1996) 'Complexity of the mouse gut T cell immune system: Identification of two distinct natural killer T cell intraepithelial lineages', *European Journal of Immunology*, 26(9), pp. 2248–2256. Available at: https://doi.org/10.1002/eji.1830260942.

Guy-Grand, D. *et al.* (1998) 'Small bowel enteropathy: role of intraepithelial lymphocytes and of cytokines (IL-12, IFN-γ, TNF) in the induction of epithelial cell death and renewal', *European Journal of Immunology*, 28(2), pp. 730–744. Available at: https://doi.org/10.1002/(SICI)1521-4141(199802)28:02<730::AID-IMMU730>3.0.CO;2-U.

Haas, J.D. *et al.* (2012) 'Development of Interleukin-17-Producing γδ T Cells Is Restricted to a Functional Embryonic Wave', *Immunity*, 37(1), pp. 48–59. Available at: https://doi.org/10.1016/j.immuni.2012.06.003.

Halter, F. *et al.* (2001) 'Cyclooxygenase 2—implications on maintenance of gastric mucosal integrity and ulcer healing: controversial issues and perspectives', *Gut*, 49(3), pp. 443–453. Available at: https://doi.org/10.1136/gut.49.3.443.

Hao, Q. and Tang, H. (2018) 'Interferon-γ and Smac mimetics synergize to induce apoptosis of lung cancer cells in a TNFα-independent manner', *Cancer Cell International*, 18(1), p. 84. Available at: https://doi.org/10.1186/s12935-018-0579-y.

Hao, X. *et al.* (1999) 'Early expression of cyclo-oxygenase-2 during sporadic colorectal carcinogenesis', *The Journal of Pathology*, 187(3), pp. 295–301. Available at: https://doi.org/10.1002/(SICI)1096-9896(199902)187:3<295::AID-PATH254>3.0.CO;2-Y.

Harding, C.V. and Boom, W.H. (2010) 'Regulation of antigen presentation by Mycobacterium tuberculosis: a role for Toll-like receptors', *Nature Reviews Microbiology*, 8(4), pp. 296–307. Available at: https://doi.org/10.1038/nrmicro2321.

Harris, S.G. *et al.* (2002) 'Prostaglandins as modulators of immunity', *Trends in Immunology*, 23(3), pp. 144–150. Available at: https://doi.org/10.1016/S1471-4906(01)02154-8.

Hausmann, A. *et al.* (2020) 'Intestinal epithelial NAIP/NLRC4 restricts systemic dissemination of the adapted pathogen Salmonella Typhimurium due to site-specific bacterial PAMP expression', *Mucosal Immunology*, 13(3), pp. 530–544. Available at: https://doi.org/10.1038/s41385-019-0247-0.

He, K. *et al.* (2023) 'Gasdermin D licenses MHCII induction to maintain food tolerance in small intestine', *Cell*, 186(14), pp. 3033-3048.e20. Available at: https://doi.org/10.1016/j.cell.2023.05.027.

Heo, K. and Lee, S. (2020) 'TSPAN8 as a Novel Emerging Therapeutic Target in Cancer for Monoclonal Antibody Therapy', *Biomolecules*, 10(3), p. 388. Available at: https://doi.org/10.3390/biom10030388.

Hernandez, Y. *et al.* (2010) 'The role of prostaglandin E2 (PGE 2) in toll-like receptor 4 (TLR4)-mediated colitis-associated neoplasia', *BMC Gastroenterology*, 10, p. 82. Available at: https://doi.org/10.1186/1471-230X-10-82.

Hilvering, B. *et al.* (2018) 'Synergistic activation of pro-inflammatory type-2 CD8+ T lymphocytes by lipid mediators in severe eosinophilic asthma', *Mucosal Immunology*, 11(5), pp. 1408–1419. Available at: https://doi.org/10.1038/s41385-018-0049-9.

Hoiseth, S.K. and Stocker, B. a. D. (1981) 'Aromatic-dependent Salmonella typhimurium are non-virulent and effective as live vaccines', *Nature*, 291(5812), pp. 238–239. Available at: https://doi.org/10.1038/291238a0.

Hong, L., Webb, T.J. and Wilkes, D.S. (2007) 'Dendritic Cell – T Cell Interactions: CD8αα Expressed on Dendritic Cells Regulates T Cell Proliferation', *Immunology letters*, 108(2), pp. 174–178. Available at: https://doi.org/10.1016/j.imlet.2006.12.003.

Houchen, C.W., Stenson, W.F. and Cohn, S.M. (2000) 'Disruption of cyclooxygenase-1 gene results in an impaired response to radiation injury', *American Journal of Physiology. Gastrointestinal and Liver Physiology*, 279(5), pp. G858-865. Available at: https://doi.org/10.1152/ajpgi.2000.279.5.G858.

Housseau, F. *et al.* (2016) 'Redundant Innate and Adaptive Sources of IL17 Production Drive Colon Tumorigenesis', *Cancer Research*, 76(8), pp. 2115–2124. Available at: https://doi.org/10.1158/0008-5472.CAN-15-0749.

Hoytema Van Konijnenburg, D.P. *et al.* (2017) 'Intestinal Epithelial and Intraepithelial T Cell Crosstalk Mediates a Dynamic Response to Infection', *Cell*, 171(4), pp. 783-794.e13. Available at: https://doi.org/10.1016/j.cell.2017.08.046.

Hu, B. *et al.* (2010) 'Inflammation-induced tumorigenesis in the colon is regulated by caspase-1 and NLRC4', *Proceedings of the National Academy of Sciences*, 107(50), pp. 21635–21640. Available at: https://doi.org/10.1073/pnas.1016814108.

Hu, B. *et al.* (2013) 'Microbiota-induced activation of epithelial IL-6 signaling links inflammasome-driven inflammation with transmissible cancer', *Proceedings of the National Academy of Sciences of*

the United States of America, 110(24), pp. 9862–9867. Available at: https://doi.org/10.1073/pnas.1307575110.

Hu, M.D. and Edelblum, K.L. (2017) 'Sentinels at the frontline: the role of intraepithelial lymphocytes in inflammatory bowel disease', *Current pharmacology reports*, 3(6), pp. 321–334. Available at: https://doi.org/10.1007/s40495-017-0105-2.

Hu, M.D., Jia, L. and Edelblum, K.L. (2018) 'Policing the intestinal epithelial barrier: Innate immune functions of intraepithelial lymphocytes', *Current pathobiology reports*, 6(1), pp. 35–46.

Hu, W. *et al.* (2019) 'Prognostic significance of resident CD103+CD8+T cells in human colorectal cancer tissues', *Acta Histochemica*, 121(5), pp. 657–663. Available at: https://doi.org/10.1016/j.acthis.2019.05.009.

Hull, M.A. *et al.* (1999) 'Cyclooxygenase 2 is up-regulated and localized to macrophages in the intestine of Min mice', *British Journal of Cancer*, 79(9–10), pp. 1399–1405. Available at: https://doi.org/10.1038/sj.bjc.6690224.

Hult, L.T.O. *et al.* (2011) 'EP Receptor Expression in Human Intestinal Epithelium and Localization Relative to the Stem Cell Zone of the Crypts', *PLOS ONE*, 6(10), p. e26816. Available at: https://doi.org/10.1371/journal.pone.0026816.

Inagaki-Ohara, K. *et al.* (2004) 'Mucosal T Cells Bearing TCRγδ Play a Protective Role in Intestinal Inflammation1', *The Journal of Immunology*, 173(2), pp. 1390–1398. Available at: https://doi.org/10.4049/jimmunol.173.2.1390.

Ishikawa, T. and Herschman, H.R. (2010) 'Tumor formation in a mouse model of colitis-associated colon cancer does not require COX-1 or COX-2 expression', *Carcinogenesis*, 31(4), pp. 729–736. Available at: https://doi.org/10.1093/carcin/bgq002.

Ishikawa, T., Oshima, M. and Herschman, H.R. (2011) 'Cox-2 deletion in myeloid and endothelial cells, but not in epithelial cells, exacerbates murine colitis.', *Carcinogenesis*, 32(3), pp. 417–426. Available at: https://doi.org/10.1093/carcin/bgq268.

Ismail, A.S., Behrendt, C.L. and Hooper, L.V. (2009) 'Reciprocal Interactions between Commensal Bacteria and γδ Intraepithelial Lymphocytes during Mucosal Injury1', *The Journal of Immunology*, 182(5), pp. 3047–3054. Available at: https://doi.org/10.4049/jimmunol.0802705.

Jabri, B. and Abadie, V. (2015) 'IL-15 functions as a danger signal to regulate tissue-resident T cells and tissue destruction', *Nature reviews. Immunology*, 15(12), pp. 771–783. Available at: https://doi.org/10.1038/nri3919.

Jabri, B. and Sollid, L.M. (2017) 'T Cells in Celiac Disease', *The Journal of Immunology*, 198(8), pp. 3005–3014. Available at: https://doi.org/10.4049/jimmunol.1601693.

Jaffar, Z. *et al.* (2011) 'Prostaglandin I2 Promotes the Development of IL-17–Producing γδ T Cells That Associate with the Epithelium during Allergic Lung Inflammation', *The Journal of Immunology*, 187(10), pp. 5380–5391. Available at: https://doi.org/10.4049/jimmunol.1101261.

Jakubowska, K. *et al.* (2017) 'Stromal and intraepithelial tumor-infiltrating lymphocytes in colorectal carcinoma', *Oncology Letters*, 14(6), pp. 6421–6432. Available at: https://doi.org/10.3892/ol.2017.7013.

James, O.J. *et al.* (2020) 'Comprehensive proteomics analyses identify PIM kinases as key regulators of IL-15 driven activation of intestinal intraepithelial lymphocytes', *bioRxiv*, p. 2020.03.27.011338. Available at: https://doi.org/10.1101/2020.03.27.011338.

James, O.J. *et al.* (2021) 'IL-15 and PIM kinases direct the metabolic programming of intestinal intraepithelial lymphocytes', *Nature Communications*, 12, p. 4290. Available at: https://doi.org/10.1038/s41467-021-24473-2.

Jenner, R.G. *et al.* (2009) 'The transcription factors T-bet and GATA-3 control alternative pathways of T-cell differentiation through a shared set of target genes', *Proceedings of the National Academy of Sciences*, 106(42), pp. 17876–17881. Available at: https://doi.org/10.1073/pnas.0909357106.

Jiang, G.-L. *et al.* (2007) 'The prevention of colitis by E Prostanoid receptor 4 agonist through enhancement of epithelium survival and regeneration', *The Journal of Pharmacology and Experimental Therapeutics*, 320(1), pp. 22–28. Available at: https://doi.org/10.1124/jpet.106.111146.

Jiang, W. *et al.* (2013) 'Recognition of gut microbiota by NOD2 is essential for the homeostasis of intestinal intraepithelial lymphocytes', *Journal of Experimental Medicine*, 210(11), pp. 2465–2476. Available at: https://doi.org/10.1084/jem.20122490.

Johansson-Lindbom, B. *et al.* (2003) 'Selective Generation of Gut Tropic T Cells in Gut-associated Lymphoid Tissue (GALT)', *The Journal of Experimental Medicine*, 198(6), pp. 963–969. Available at: https://doi.org/10.1084/jem.20031244.

Johnson, D.B. *et al.* (2016) 'Melanoma-specific MHC-II expression represents a tumour-autonomous phenotype and predicts response to anti-PD-1/PD-L1 therapy', *Nature Communications*, 7(1), p. 10582. Available at: https://doi.org/10.1038/ncomms10582.

Jorgovanovic, D. *et al.* (2020) 'Roles of IFN-γ in tumor progression and regression: a review', *Biomarker Research*, 8(1), p. 49. Available at: https://doi.org/10.1186/s40364-020-00228-x.

Kabashima, K. *et al.* (2002) 'The prostaglandin receptor EP4 suppresses colitis, mucosal damage and CD4 cell activation in the gut', *The Journal of Clinical Investigation*, 109(7), pp. 883–893. Available at: https://doi.org/10.1172/JCI14459.

Kaer, L.V. *et al.* (2013) 'In Vitro Induction of Regulatory CD4+CD8α+ T Cells by TGF-β, IL-7 and IFN-γ', *PLOS ONE*, 8(7), p. e67821. Available at: https://doi.org/10.1371/journal.pone.0067821.

Kaiser, P. *et al.* (2012) 'The streptomycin mouse model for Salmonella diarrhea: functional analysis of the microbiota, the pathogen's virulence factors, and the host's mucosal immune response', *Immunological Reviews*, 245(1), pp. 56–83. Available at: https://doi.org/10.1111/j.1600-065X.2011.01070.x.

Kammertoens, T. *et al.* (2017) 'Tumour ischaemia by interferon-γ resembles physiological blood vessel regression', *Nature*, 545(7652), pp. 98–102. Available at: https://doi.org/10.1038/nature22311.

Kaneko, M. *et al.* (2004) 'Development of TCRab CD8aa Intestinal Intraepithelial Lymphocytes Is Promoted by Interleukin-15-Producing Epithelial Cells Constitutively Stimulated by Gram-Negative Bacteria via TLR4', 27(6).

Karki, R. *et al.* (2016) 'NLRC3 is an inhibitory sensor of PI3K-mTOR pathways in cancer', *Nature*, 540(7634), pp. 583–587. Available at: https://doi.org/10.1038/nature20597.

Karki, R. *et al.* (2017) 'NLRC3 regulates cellular proliferation and apoptosis to attenuate the development of colorectal cancer', *Cell Cycle*, 16(13), pp. 1243–1251. Available at: https://doi.org/10.1080/15384101.2017.1317414.

Kathania, M. *et al.* (2016) 'Itch inhibits IL-17-mediated colon inflammation and tumorigenesis by ROR-γt ubiquitination', *Nature Immunology*, 17(8), pp. 997–1004. Available at: https://doi.org/10.1038/ni.3488.

Kawahara, K. *et al.* (2015) 'Prostaglandin E2-induced inflammation: Relevance of prostaglandin E receptors', *Biochimica et Biophysica Acta (BBA) - Molecular and Cell Biology of Lipids*, 1851(4), pp. 414–421. Available at: https://doi.org/10.1016/j.bbalip.2014.07.008.

Kawajiri, H. *et al.* (2002) 'Arachidonic and Linoleic Acid Metabolism in Mouse Intestinal Tissue: Evidence for Novel Lipoxygenase Activity', *Archives of Biochemistry and Biophysics*, 398(1), pp. 51–60. Available at: https://doi.org/10.1006/abbi.2001.2685.

Kennedy, M.K. *et al.* (2000) 'Reversible Defects in Natural Killer and Memory Cd8 T Cell Lineages in Interleukin 15–Deficient Mice', *The Journal of Experimental Medicine*, 191(5), pp. 771–780.

Khan, I. *et al.* (2022) 'Differential Susceptibility of the Gut Microbiota to DSS Treatment Interferes in the Conserved Microbiome Association in Mouse Models of Colitis and Is Related to the Initial Gut Microbiota Difference', *Advanced Gut & Microbiome Research*, 2022, p. e7813278. Available at: https://doi.org/10.1155/2022/7813278.

Khayrullina, T. *et al.* (2008) 'In Vitro Differentiation of Dendritic Cells in the Presence of Prostaglandin E2 Alters the IL-12/IL-23 Balance and Promotes Differentiation of Th17 Cells', *Journal of immunology (Baltimore, Md. : 1950)*, 181(1), pp. 721–735.

Knodler, L.A. *et al.* (2014) 'Noncanonical Inflammasome Activation of Caspase-4/Caspase-11 Mediates Epithelial Defenses against Enteric Bacterial Pathogens', *Cell Host & Microbe*, 16(2), pp. 249–256. Available at: https://doi.org/10.1016/j.chom.2014.07.002.

Ko, S.C. *et al.* (2002) 'Paracrine cyclooxygenase-2-mediated signalling by macrophages promotes tumorigenic progression of intestinal epithelial cells', *Oncogene*, 21(47), pp. 7175–7186. Available at: https://doi.org/10.1038/sj.onc.1205869.

Kober, O.I. *et al.* (2014) 'γδ T-cell-deficient mice show alterations in mucin expression, glycosylation, and goblet cells but maintain an intact mucus layer', *American Journal of Physiology - Gastrointestinal and Liver Physiology*, 306(7), pp. G582–G593. Available at: https://doi.org/10.1152/ajpgi.00218.2013.

Koblansky, A.A. *et al.* (2016) 'The Innate Immune Receptor NLRX1 Functions as a Tumor Suppressor by Reducing Colon Tumorigenesis and Key Tumor-Promoting Signals', *Cell Reports*, 14(11), pp. 2562–2575. Available at: https://doi.org/10.1016/j.celrep.2016.02.064.

Kofoed, E.M. and Vance, R.E. (2011) 'Innate immune recognition of bacterial ligands by NAIPs determines inflammasome specificity', *Nature*, 477(7366), pp. 592–595. Available at: https://doi.org/10.1038/nature10394.

Kohno, H. *et al.* (2005) 'Suppression of colitis-related mouse colon carcinogenesis by a COX-2 inhibitor and PPAR ligands', *BMC cancer*, 5, p. 46. Available at: https://doi.org/10.1186/1471-2407-5-46.

Kolde, R. (2019) 'pheatmap: Pretty Heatmaps'. Available at: https://cran.r-project.org/web/packages/pheatmap/index.html (Accessed: 18 October 2023).

Konkel, J.E. *et al.* (2011) 'Control of the development of CD8αα+ intestinal intraepithelial lymphocytes by TGF-β', *Nature Immunology*, 12(4), pp. 312–319. Available at: https://doi.org/10.1038/ni.1997.

Kortmann, J., Brubaker, S.W. and Monack, D.M. (2015) 'Cutting Edge: Inflammasome Activation in Primary Human Macrophages Is Dependent on Flagellin', *The Journal of Immunology*, 195(3), pp. 815–819. Available at: https://doi.org/10.4049/jimmunol.1403100.

Kühl, A.A. *et al.* (2007) 'Aggravation of intestinal inflammation by depletion/deficiency of γδ T cells in different types of IBD animal models', *Journal of Leukocyte Biology*, 81(1), pp. 168–175. Available at: https://doi.org/10.1189/jlb.1105696.

Lambolez, F. and Rocha, B. (2001) 'A Molecular Gut Reaction', *Science*, 294(5548), pp. 1848–1849. Available at: https://doi.org/10.1126/science.1067117.

Lee, J. *et al.* (2012) 'Role of Mouse Peptidoglycan Recognition Protein PGLYRP2 in the Innate Immune Response to Salmonella enterica Serovar Typhimurium Infection In Vivo', *Infection and Immunity*, 80(8), pp. 2645–2654. Available at: https://doi.org/10.1128/IAI.00168-12.

Lee, J.-J. *et al.* (2002) 'The Role of PGE2 in the Differentiation of Dendritic Cells: How Do Dendritic Cells Influence T-Cell Polarization and Chemokine Receptor Expression?', *Stem Cells*, 20(5), pp. 448–459. Available at: https://doi.org/10.1634/stemcells.20-5-448.

Lee, S.H., Kwon, J. eun and Cho, M.-L. (2018) 'Immunological pathogenesis of inflammatory bowel disease', *Intestinal Research*, 16(1), pp. 26–42. Available at: https://doi.org/10.5217/ir.2018.16.1.26.

Lei, A. and Maloy, K.J. (2016) 'Colon Cancer in the Land of NOD: NLRX1 as an Intrinsic Tumor Suppressor', *Trends in Immunology*, 37(9), pp. 569–570. Available at: https://doi.org/10.1016/j.it.2016.07.004.

Leishman, A.J. *et al.* (2001) 'T Cell Responses Modulated Through Interaction Between CD8αα and the Nonclassical MHC Class I Molecule, TL', *Science*, 294(5548), pp. 1936–1939. Available at: https://doi.org/10.1126/science.1063564.

Leishman, A.J. *et al.* (2002) 'Precursors of Functional MHC Class I- or Class II-Restricted CD8αα+ T Cells Are Positively Selected in the Thymus by Agonist Self-Peptides', *Immunity*, 16(3), pp. 355–364. Available at: https://doi.org/10.1016/S1074-7613(02)00284-4.

Leoz, M.L. *et al.* (2015) 'The genetic basis of familial adenomatous polyposis and its implications for clinical practice and risk management', *The Application of Clinical Genetics*, 8, pp. 95–107. Available at: https://doi.org/10.2147/TACG.S51484.

Li, H. *et al.* (2011) 'Cyclooxygenase-2 Regulates Th17 Cell Differentiation during Allergic Lung Inflammation', *American Journal of Respiratory and Critical Care Medicine*, 184(1), pp. 37–49. Available at: https://doi.org/10.1164/rccm.201010-1637OC.

Li, H. *et al.* (2017) 'Prostaglandin E2 restrains human Treg cell differentiation via E prostanoid receptor 2-protein kinase A signaling', *Immunology Letters*, 191, pp. 63–72. Available at: https://doi.org/10.1016/j.imlet.2017.09.009.

Li, M. *et al.* (2018) 'Initial gut microbiota structure affects sensitivity to DSS-induced colitis in a mouse model', *Science China Life Sciences*, 61(7), pp. 762–769. Available at: https://doi.org/10.1007/s11427-017-9097-0.

Li, X. *et al.* (2020) 'Tim-3 suppresses the killing effect of Vγ9Vδ2 T cells on colon cancer cells by reducing perforin and granzyme B expression', *Experimental Cell Research*, 386(1), p. 111719. Available at: https://doi.org/10.1016/j.yexcr.2019.111719.

Li, Y. *et al.* (2017) 'TLR9 Regulates the NF-κB–NLRP3–IL-1β Pathway Negatively in Salmonella-Induced NKG2D-Mediated Intestinal Inflammation', *The Journal of Immunology*, 199(2), pp. 761–773. Available at: https://doi.org/10.4049/jimmunol.1601416.

Li, Z. *et al.* (2012) 'Small Intestinal Intraepithelial Lymphocytes Expressing CD8 and T Cell Receptor γδ Are Involved in Bacterial Clearance during Salmonella enterica Serovar Typhimurium Infection', *Infection and Immunity*, 80(2), pp. 565–574. Available at: https://doi.org/10.1128/IAI.05078-11.

Ling, K.L. *et al.* (2007) 'Increased frequency of regulatory T cells in peripheral blood and tumour infiltrating lymphocytes in colorectal cancer patients', *Cancer Immunity*, 7(1), p. 7. Available at: https://doi.org/10.1158/1424-9634.DCL-7.7.1.

Lo Presti, E. *et al.* (2019) 'Characterization of γδ T Cells in Intestinal Mucosa From Patients With Early-Onset or Long-Standing Inflammatory Bowel Disease and Their Correlation With Clinical Status', *Journal of Crohn's and Colitis*, 13(7), pp. 873–883. Available at: https://doi.org/10.1093/ecco-jcc/jjz015.

Lo Presti, E. *et al.* (2020) 'Analysis of colon-infiltrating γδ T cells in chronic inflammatory bowel disease and in colitis-associated cancer', *Journal of Leukocyte Biology*, 108(2), pp. 749–760. Available at: https://doi.org/10.1002/JLB.5MA0320-201RR.

Lo, U.-G. *et al.* (2019) 'Interferon-induced IFIT5 promotes epithelial-to-mesenchymal transition leading to renal cancer invasion', *American Journal of Clinical and Experimental Urology*, 7(1), pp. 31–45.

Lodolce, J.P. *et al.* (1998) 'IL-15 Receptor Maintains Lymphoid Homeostasis by Supporting Lymphocyte Homing and Proliferation', *Immunity*, 9(5), pp. 669–676. Available at: https://doi.org/10.1016/S1074-7613(00)80664-0.

Loi, S. *et al.* (2016) 'RAS/MAPK Activation Is Associated with Reduced Tumor-Infiltrating Lymphocytes in Triple-Negative Breast Cancer: Therapeutic Cooperation Between MEK and PD-1/PD-L1 Immune

Checkpoint Inhibitors', *Clinical Cancer Research*, 22(6), pp. 1499–1509. Available at: https://doi.org/10.1158/1078-0432.CCR-15-1125.

Lone, A.M. and Taskén, K. (2013) 'Proinflammatory and Immunoregulatory Roles of Eicosanoids in T Cells', *Frontiers in Immunology*, 4, p. 130. Available at: https://doi.org/10.3389/fimmu.2013.00130.

Love, M.I., Huber, W. and Anders, S. (2014) 'Moderated estimation of fold change and dispersion for RNA-seq data with DESeq2', *Genome Biology*, 15(12), p. 550. Available at: https://doi.org/10.1186/s13059-014-0550-8.

Loynes, C.A. *et al.* (2018) 'PGE2 production at sites of tissue injury promotes an anti-inflammatory neutrophil phenotype and determines the outcome of inflammation resolution in vivo', *Science Advances*, 4(9), p. eaar8320. Available at: https://doi.org/10.1126/sciadv.aar8320.

Lu, Y. *et al.* (2009) 'Responsiveness of Stromal Fibroblasts to IFN-γ Blocks Tumor Growth via Angiostasis1', *The Journal of Immunology*, 183(10), pp. 6413–6421. Available at: https://doi.org/10.4049/jimmunol.0901073.

Luster, A.D. and Tager, A.M. (2004) 'T-cell trafficking in asthma: lipid mediators grease the way', *Nature Reviews Immunology*, 4(9), pp. 711–724. Available at: https://doi.org/10.1038/nri1438.

Ma, H., Qiu, Y. and Yang, H. (2021) 'Intestinal intraepithelial lymphocytes: Maintainers of intestinal immune tolerance and regulators of intestinal immunity', *Journal of Leukocyte Biology*, 109(2), pp. 339–347. Available at: https://doi.org/10.1002/JLB.3RU0220-111.

Ma, L.J. *et al.* (2009) 'Trans-presentation of IL-15 by intestinal epithelial cells drives development of CD8αα IELs', *Journal of immunology (Baltimore, Md. : 1950)*, 183(2), pp. 1044–1054. Available at: https://doi.org/10.4049/jimmunol.0900420.

Ma, R. *et al.* (2020) 'Immune Effects of γδ T Cells in Colorectal Cancer: A Review', *Frontiers in Immunology*, 11, p. 1600. Available at: https://doi.org/10.3389/fimmu.2020.01600.

Maccalli, C. *et al.* (2003) 'NKG2D engagement of colorectal cancer-specific T cells strengthens TCR-mediated antigen stimulation and elicits TCR independent anti-tumor activity', *European Journal of Immunology*, 33(7), pp. 2033–2043. Available at: https://doi.org/10.1002/eji.200323909.

Macho-Fernandez, E. and Brigl, M. (2015) 'The Extended Family of CD1d-Restricted NKT Cells: Sifting through a Mixed Bag of TCRs, Antigens, and Functions', *Frontiers in Immunology*, 6. Available at: https://www.frontiersin.org/articles/10.3389/fimmu.2015.00362 (Accessed: 16 October 2023).

Mackie, G.M. *et al.* (2021) 'Bacterial cancer therapy in autochthonous colorectal cancer affects tumor growth and metabolic landscape', *JCI Insight*, 6(23). Available at: https://doi.org/10.1172/jci.insight.139900.

Maeurer, M.J. *et al.* (1996) 'Human intestinal Vdelta1+ lymphocytes recognize tumor cells of epithelial origin.', *Journal of Experimental Medicine*, 183(4), pp. 1681–1696. Available at: https://doi.org/10.1084/jem.183.4.1681.

Mamantopoulos, M. *et al.* (2017) 'Nlrp6- and ASC-Dependent Inflammasomes Do Not Shape the Commensal Gut Microbiota Composition', *Immunity*, 47(2), pp. 339-348.e4. Available at: https://doi.org/10.1016/j.immuni.2017.07.011.

Man, S.M. *et al.* (2015) 'Critical role for the DNA sensor AIM2 in stem-cell proliferation and cancer', *Cell*, 162(1), pp. 45–58. Available at: https://doi.org/10.1016/j.cell.2015.06.001.

Man, S.M. (2018) 'Inflammasomes in the gastrointestinal tract: infection, cancer and gut microbiota homeostasis', *Nature Reviews Gastroenterology & Hepatology*, 15(12), pp. 721–737. Available at: https://doi.org/10.1038/s41575-018-0054-1.

Marchiori, C. *et al.* (2019) 'Epithelial CD80 promotes immune surveillance of colonic preneoplastic lesions and its expression is increased by oxidative stress through STAT3 in colon cancer cells', *Journal of Experimental & Clinical Cancer Research*, 38(1), p. 190. Available at: https://doi.org/10.1186/s13046-019-1205-0.

Marelli-Berg, F. *et al.* (2008) 'The highway code of T cell trafficking', *The Journal of Pathology*, 214(2), pp. 179–189. Available at: https://doi.org/10.1002/path.2269.

Martens, M. *et al.* (2021) 'WikiPathways: connecting communities', *Nucleic Acids Research*, 49(D1), pp. D613–D621. Available at: https://doi.org/10.1093/nar/gkaa1024.

Martinet, L. *et al.* (2010) 'PGE2 inhibits natural killer and γδ T cell cytotoxicity triggered by NKR and TCR through a cAMP-mediated PKA type I-dependent signaling', *Biochemical Pharmacology*, 80(6), pp. 838–845. Available at: https://doi.org/10.1016/j.bcp.2010.05.002.

Martins, I. *et al.* (2007) 'Pathologic expression of MHC class II is driven by mitogen-activated protein kinases', *European Journal of Immunology*, 37(3), pp. 788–797. Available at: https://doi.org/10.1002/eji.200636620.

Maseda, D., Johnson, E.M., *et al.* (2018) 'mPGES1-Dependent Prostaglandin E2 (PGE2) Controls Antigen-Specific Th17 and Th1 Responses by Regulating T Autocrine and Paracrine PGE2 Production', *The Journal of Immunology*, 200(2), pp. 725–736. Available at: https://doi.org/10.4049/jimmunol.1601808.

Maseda, D., Banerjee, A., *et al.* (2018) 'mPGES-1-Mediated Production of PGE2 and EP4 Receptor Sensing Regulate T Cell Colonic Inflammation', *Frontiers in Immunology*, 9. Available at: https://www.frontiersin.org/articles/10.3389/fimmu.2018.02954 (Accessed: 9 October 2023).

Maseda, D., Ricciotti, E. and Crofford, L.J. (2019) 'Prostaglandin regulation of T cell biology', *Pharmacological Research*, 149, p. 104456. Available at: https://doi.org/10.1016/j.phrs.2019.104456.

Maslowski, K.M. *et al.* (2019) 'Attenuated Salmonella typhimurium cancer therapy has direct effects on the tumor epithelium in colorectal cancer', *bioRxiv*, p. 741686. Available at: https://doi.org/10.1101/741686.

Matsuda, S., Kudoh, S. and Katayama, S. (2001) 'Enhanced Formation of Azoxymethane-induced Colorectal Adenocarcinoma in γδ T Lymphocyte-deficient Mice', *Japanese Journal of Cancer Research*, 92(8), pp. 880–885. Available at: https://doi.org/10.1111/j.1349-7006.2001.tb01176.x.

McCarthy, N.E. *et al.* (2013) 'Proinflammatory Vδ2+ T Cells Populate the Human Intestinal Mucosa and Enhance IFN-γ Production by Colonic αβ T Cells', *The Journal of Immunology*, 191(5), pp. 2752–2763. Available at: https://doi.org/10.4049/jimmunol.1202959.

McVay, L.D. *et al.* (1997) 'Changes in human mucosal gamma delta T cell repertoire and function associated with the disease process in inflammatory bowel disease.', *Molecular Medicine*, 3(3), pp. 183–203.

Meazza, R. *et al.* (2003) 'Tumor rejection by gene transfer of the MHC class II transactivator in murine mammary adenocarcinoma cells', *European Journal of Immunology*, 33(5), pp. 1183–1192. Available at: https://doi.org/10.1002/eji.200323712.

Meehan, T.F. *et al.* (2014) 'Protection against colitis by CD100 dependent modulation of intraepithelial γδ T lymphocyte function', *Mucosal immunology*, 7(1), pp. 134–142. Available at: https://doi.org/10.1038/mi.2013.32.

Meissner, T.B. *et al.* (2010) 'NLR family member NLRC5 is a transcriptional regulator of MHC class I genes', *Proceedings of the National Academy of Sciences*, 107(31), pp. 13794–13799. Available at: https://doi.org/10.1073/pnas.1008684107.

Melandri, D. *et al.* (2018) 'The γδ T cell receptor combines innate with adaptive immunity by utilizing spatially distinct regions for agonist-selection and antigen responsiveness', *Nature immunology*, 19(12), pp. 1352–1365. Available at: https://doi.org/10.1038/s41590-018-0253-5.

Melgar, S. *et al.* (2006) 'Local production of chemokines and prostaglandin E2 in the acute, chronic and recovery phase of murine experimental colitis', *Cytokine*, 35(5–6), pp. 275–283. Available at: https://doi.org/10.1016/j.cyto.2006.09.007.

Melgar, S., Karlsson, A. and Michaëlsson, E. (2005) 'Acute colitis induced by dextran sulfate sodium progresses to chronicity in C57BL/6 but not in BALB/c mice: correlation between symptoms and inflammation', *American Journal of Physiology-Gastrointestinal and Liver Physiology*, 288(6), pp. G1328–G1338. Available at: https://doi.org/10.1152/ajpgi.00467.2004.

Meraviglia, S. *et al.* (2017) 'Distinctive features of tumor-infiltrating γδ T lymphocytes in human colorectal cancer', *OncoImmunology*, 6(10), p. e1347742. Available at: https://doi.org/10.1080/2162402X.2017.1347742.

Miao, E.A. *et al.* (2006) 'Cytoplasmic flagellin activates caspase-1 and secretion of interleukin 1β via Ipaf', *Nature Immunology*, 7(6), pp. 569–575. Available at: https://doi.org/10.1038/ni1344.

Miao, E.A. *et al.* (2010) 'Innate immune detection of the type III secretion apparatus through the NLRC4 inflammasome', *Proceedings of the National Academy of Sciences*, 107(7), pp. 3076–3080. Available at: https://doi.org/10.1073/pnas.0913087107.

Mikulak, J. *et al.* (2019) 'NKp46-expressing human gut-resident intraepithelial V**δ**1 T cell subpopulation exhibits high antitumor activity against colorectal cancer', *JCI Insight*, 4(24). Available at: https://doi.org/10.1172/jci.insight.125884.

Mitson-Salazar, A. *et al.* (2016) 'Hematopoietic prostaglandin D synthase defines a proeosinophilic pathogenic effector human TH2 cell subpopulation with enhanced function', *Journal of Allergy and Clinical Immunology*, 137(3), pp. 907-918.e9. Available at: https://doi.org/10.1016/j.jaci.2015.08.007.

Miyazaki, Y. *et al.* (2021) 'Urinary 8-iso PGF2α and 2,3-dinor-8-iso PGF2α can be indexes of colitis-associated colorectal cancer in mice', *PLOS ONE*, 16(1), p. e0245292. Available at: https://doi.org/10.1371/journal.pone.0245292.

Miyoshi, H. *et al.* (2017) 'Prostaglandin E2 promotes intestinal repair through an adaptive cellular response of the epithelium', *The EMBO Journal*, 36(1), pp. 5–24. Available at: https://doi.org/10.15252/embj.201694660.

Molofsky, A.B. *et al.* (2006) 'Cytosolic recognition of flagellin by mouse macrophages restricts Legionella pneumophila infection', *Journal of Experimental Medicine*, 203(4), pp. 1093–1104. Available at: https://doi.org/10.1084/jem.20051659.

Moltke, J. von *et al.* (2012) 'Rapid induction of inflammatory lipid mediators by the inflammasome in vivo', *Nature*, 490(7418), pp. 107–111. Available at: https://doi.org/10.1038/nature11351.

Monteleone, G. *et al.* (2005) 'Interleukin-21 enhances T-helper cell type I signaling and interferon-γ production in Crohn's disease', *Gastroenterology*, 128(3), pp. 687–694. Available at: https://doi.org/10.1053/j.gastro.2004.12.042.

Montrose, D.C. *et al.* (2010) 'cPLA2 Is protective against COX inhibitor-induced intestinal damage', *Toxicological Sciences*, 117(1), pp. 122–132. Available at: https://doi.org/10.1093/toxsci/kfq184.

Montrose, D.C. *et al.* (2015) 'The Role of PGE2 in Intestinal Inflammation and Tumorigenesis', *Prostaglandins & other lipid mediators*, 0, pp. 26–36. Available at: https://doi.org/10.1016/j.prostaglandins.2014.10.002.

Montufar-Solis, D., Garza, T. and Klein, J.R. (2007) 'T-cell activation in the intestinal mucosa', *Immunological Reviews*, 215(1), pp. 189–201. Available at: https://doi.org/10.1111/j.1600-065X.2006.00471.x.

Moon, C.M. *et al.* (2014) 'Nonsteroidal anti-inflammatory drugs suppress cancer stem cells via inhibiting PTGS2 (cyclooxygenase 2) and NOTCH/HES1 and activating PPARG in colorectal cancer', *International Journal of Cancer*, 134(3), pp. 519–529. Available at: https://doi.org/10.1002/ijc.28381.

Moreno, J.J. (2017) 'Eicosanoid receptors: Targets for the treatment of disrupted intestinal epithelial homeostasis', *European Journal of Pharmacology*, 796, pp. 7–19. Available at: https://doi.org/10.1016/j.ejphar.2016.12.004.

Morgan, J.E. *et al.* (2015) 'The class II transactivator (CIITA) is regulated by post-translational modification cross-talk between ERK1/2 phosphorylation, mono-ubiquitination and Lys63 ubiquitination', *Bioscience Reports*, 35(4), p. e00233. Available at: https://doi.org/10.1042/BSR20150091.

Morikawa, R. *et al.* (2021) 'Intraepithelial Lymphocytes Suppress Intestinal Tumor Growth by Cell-to-Cell Contact via CD103/E-Cadherin Signal', *Cellular and Molecular Gastroenterology and Hepatology*, 11(5), pp. 1483–1503. Available at: https://doi.org/10.1016/j.jcmgh.2021.01.014.

Mortara, L. *et al.* (2006) 'CIITA-Induced MHC Class II Expression in Mammary Adenocarcinoma Leads to a Th1 Polarization of the Tumor Microenvironment, Tumor Rejection, and Specific Antitumor Memory', *Clinical Cancer Research*, 12(11), pp. 3435–3443. Available at: https://doi.org/10.1158/1078-0432.CCR-06-0165.

Mucida, D. *et al.* (2013) 'Transcriptional reprogramming of mature CD4+ helper T cells generates distinct MHC class II–restricted cytotoxic T lymphocytes', *Nature Immunology*, 14(3), pp. 281–289. Available at: https://doi.org/10.1038/ni.2523.

Müller, E. *et al.* (2017) 'Toll-Like Receptor Ligands and Interferon-γ Synergize for Induction of Antitumor M1 Macrophages', *Frontiers in Immunology*, 8, p. 1383. Available at: https://doi.org/10.3389/fimmu.2017.01383.

Munder, M. *et al.* (1998) 'Murine Macrophages Secrete Interferon γ upon Combined Stimulation with Interleukin (IL)-12 and IL-18: A Novel Pathway of Autocrine Macrophage Activation', *Journal of Experimental Medicine*, 187(12), pp. 2103–2108. Available at: https://doi.org/10.1084/jem.187.12.2103.

Muzaki, A.R.B.M. *et al.* (2017) 'Long-Lived Innate IL-17–Producing γ/δ T Cells Modulate Antimicrobial Epithelial Host Defense in the Colon', *The Journal of Immunology*, 199(10), pp. 3691–3699. Available at: https://doi.org/10.4049/jimmunol.1701053.

Napolitani, G. *et al.* (2009) 'Prostaglandin E2 enhances Th17 responses via modulation of IL-17 and IFN-γ production by memory CD4+ T cells', *European Journal of Immunology*, 39(5), pp. 1301–1312. Available at: https://doi.org/10.1002/eji.200838969.

Ni, C. *et al.* (2013) 'IFN-γ selectively exerts pro-apoptotic effects on tumor-initiating label-retaining colon cancer cells', *Cancer Letters*, 336(1), pp. 174–184. Available at: https://doi.org/10.1016/j.canlet.2013.04.029.

Normand, S. *et al.* (2011) 'Nod-like receptor pyrin domain-containing protein 6 (NLRP6) controls epithelial self-renewal and colorectal carcinogenesis upon injury', *Proceedings of the National Academy of Sciences of the United States of America*, 108(23), pp. 9601–9606. Available at: https://doi.org/10.1073/pnas.1100981108.

Ogino, S. *et al.* (2008) 'Cyclooxygenase-2 Expression is an Independent Predictor of Poor Prognosis in Colon Cancer', *Clinical cancer research : an official journal of the American Association for Cancer Research*, 14(24), pp. 8221–8227. Available at: https://doi.org/10.1158/1078-0432.CCR-08-1841.

Olalekan, S.A. *et al.* (2015) 'B cells expressing IFN-γ suppress Treg-cell differentiation and promote autoimmune experimental arthritis', *European journal of immunology*, 45(4), pp. 988–998. Available at: https://doi.org/10.1002/eji.201445036.

Olguín, J.E. *et al.* (2020) 'Relevance of Regulatory T Cells during Colorectal Cancer Development', *Cancers*, 12(7), p. 1888. Available at: https://doi.org/10.3390/cancers12071888.

Olivares-Villagómez, D. and Kaer, L.V. (2018) 'Intestinal Intraepithelial Lymphocytes: Sentinels of the Mucosal Barrier', *Trends in Immunology*, 39(4), pp. 264–275. Available at: https://doi.org/10.1016/j.it.2017.11.003.

Olszak, T. *et al.* (2014) 'Protective mucosal immunity mediated by epithelial CD1d and IL-10', *Nature*, 509(7501), pp. 497–502. Available at: https://doi.org/10.1038/nature13150.

Ostrand-Rosenberg, S., Thakur, A. and Clements, V. (1990) 'Rejection of mouse sarcoma cells after transfection of MHC class II genes.', *The Journal of Immunology*, 144(10), pp. 4068–4071. Available at: https://doi.org/10.4049/jimmunol.144.10.4068.

Pai, M.-H. *et al.* (2014) 'Glutamine modulates acute dextran sulphate sodium-induced changes in small-intestinal intraepithelial γδ-T-lymphocyte expression in mice', *British Journal of Nutrition*, 111(6), pp. 1032–1039. Available at: https://doi.org/10.1017/S0007114513003425.

Pai, R. *et al.* (2002) 'Prostaglandin E 2 transactivates EGF receptor: A novel mechanism for promoting colon cancer growth and gastrointestinal hypertrophy', *Nature Medicine*, 8(3), pp. 289–293. Available at: https://doi.org/10.1038/nm0302-289.

Pan, J. *et al.* (2004) 'Interferon-γ is an autocrine mediator for dendritic cell maturation', *Immunology Letters*, 94(1), pp. 141–151. Available at: https://doi.org/10.1016/j.imlet.2004.05.003.

Pandey, A., Shen, C. and Man, S.M. (2019) 'Inflammasomes in Colitis and Colorectal Cancer: Mechanism of Action and Therapies', *The Yale Journal of Biology and Medicine*, 92(3), pp. 481–498.

Park, I.A. *et al.* (2017) 'Expression of the MHC class II in triple-negative breast cancer is associated with tumor-infiltrating lymphocytes and interferon signaling', *PLOS ONE*, 12(8), p. e0182786. Available at: https://doi.org/10.1371/journal.pone.0182786.

Park, J.M. *et al.* (2007) 'Hematopoietic prostaglandin D synthase suppresses intestinal adenomas in ApcMin/+ mice', *Cancer Research*, 67(3), pp. 881–889. Available at: https://doi.org/10.1158/0008-5472.CAN-05-3767.

Pastille, E. *et al.* (2014) 'Transient Ablation of Regulatory T cells Improves Antitumor Immunity in Colitis-Associated Colon Cancer', *Cancer Research*, 74(16), pp. 4258–4269. Available at: https://doi.org/10.1158/0008-5472.CAN-13-3065.

Paul, S. *et al.* (2019) 'Natural killer T cell activation increases iNOS+CD206- M1 macrophage and controls the growth of solid tumor', *Journal for Immunotherapy of Cancer*, 7, p. 208. Available at: https://doi.org/10.1186/s40425-019-0697-7.

Peng, X. *et al.* (2017) 'COX-1/PGE 2 /EP4 alleviates mucosal injury by upregulating β-arr1-mediated Akt signaling in colitis', *Scientific Reports*, 7(1), pp. 1–12. Available at: https://doi.org/10.1038/s41598-017-01169-6.

Pettipher, R., Hansel, T.T. and Armer, R. (2007) 'Antagonism of the prostaglandin D2 receptors DP1 and CRTH2 as an approach to treat allergic diseases', *Nature Reviews Drug Discovery*, 6(4), pp. 313–325. Available at: https://doi.org/10.1038/nrd2266.

Phillips, S.M. *et al.* (2004) 'Tumour-infiltrating lymphocytes in colorectal cancer with microsatellite instability are activated and cytotoxic', *British Journal of Surgery*, 91(4), pp. 469–475. Available at: https://doi.org/10.1002/bjs.4472.

Pickles, O.J. *et al.* (2023) 'MHC Class II is Induced by IFNγ and Follows Three Distinct Patterns of Expression in Colorectal Cancer Organoids', *Cancer Research Communications*, 3(8), pp. 1501–1513. Available at: https://doi.org/10.1158/2767-9764.CRC-23-0091.

Platanias, L.C. (2005) 'Mechanisms of type-I- and type-II-interferon-mediated signalling', *Nature Reviews Immunology*, 5(5), pp. 375–386. Available at: https://doi.org/10.1038/nri1604.

Polese, B. *et al.* (2021) 'Prostaglandin E2 amplifies IL-17 production by γδ T cells during barrier inflammation', *Cell Reports*, 36(4), p. 109456. Available at: https://doi.org/10.1016/j.celrep.2021.109456.

Price, A.E. *et al.* (2012) 'Marking and Quantifying IL-17A-Producing Cells In Vivo', *PLOS ONE*, 7(6), p. e39750. Available at: https://doi.org/10.1371/journal.pone.0039750.

Pyke, R.M. *et al.* (2018) 'Evolutionary pressure against MHC class II binding cancer mutations', *Cell*, 175(2), pp. 416-428.e13. Available at: https://doi.org/10.1016/j.cell.2018.08.048.

Qian, J. *et al.* (2018) 'The IFN-γ/PD-L1 axis between T cells and tumor microenvironment: hints for glioma anti-PD-1/PD-L1 therapy', *Journal of Neuroinflammation*, 15(1), p. 290. Available at: https://doi.org/10.1186/s12974-018-1330-2.

Qiu, W. *et al.* (2010) 'Chemoprevention by nonsteroidal anti-inflammatory drugs eliminates oncogenic intestinal stem cells via SMAC-dependent apoptosis', *Proceedings of the National Academy of Sciences of the United States of America*, 107(46), pp. 20027–20032. Available at: https://doi.org/10.1073/pnas.1010430107.

Qiu, Y. *et al.* (2016) 'TLR2-Dependent Signaling for IL-15 Production Is Essential for the Homeostasis of Intestinal Intraepithelial Lymphocytes', *Mediators of Inflammation*, 2016, p. 4281865. Available at: https://doi.org/10.1155/2016/4281865.

Qualtrough, D. *et al.* (2007) 'Prostaglandin F2α stimulates motility and invasion in colorectal tumor cells', *International Journal of Cancer*, 121(4), pp. 734–740. Available at: https://doi.org/10.1002/ijc.22755.

Quinn, E. *et al.* (2003) 'CD103+ intraepithelial lymphocytes—a unique population in microsatellite unstable sporadic colorectal cancer', *European Journal of Cancer*, 39(4), pp. 469–475. Available at: https://doi.org/10.1016/S0959-8049(02)00633-0.

Raab, Y. *et al.* (1995) 'Mucosal synthesis and release of prostaglandin E2 from activated eosinophils and macrophages in ulcerative colitis', *The American Journal of Gastroenterology*, 90(4), pp. 614–620.

Ramanan, D. *et al.* (2014) 'Bacterial sensor Nod2 prevents small intestinal inflammation by restricting the expansion of the commensal Bacteroides vulgatus', *Immunity*, 41(2), pp. 311–324. Available at: https://doi.org/10.1016/j.immuni.2014.06.015.

Rauch, I. *et al.* (2017) 'NAIP-NLRC4 Inflammasomes Coordinate Intestinal Epithelial Cell Expulsion with Eicosanoid and IL-18 Release via Activation of Caspase-1 and -8', *Immunity*, 46(4), pp. 649–659. Available at: https://doi.org/10.1016/j.immuni.2017.03.016.

Ravichandran, G. *et al.* (2019) 'Interferon-γ-dependent immune responses contribute to the pathogenesis of sclerosing cholangitis in mice', *Journal of Hepatology*, 71(4), pp. 773–782. Available at: https://doi.org/10.1016/j.jhep.2019.05.023.

Razi, S. *et al.* (2019) 'IL-17 and colorectal cancer: From carcinogenesis to treatment', *Cytokine*, 116, pp. 7–12. Available at: https://doi.org/10.1016/j.cyto.2018.12.021.

Rebersek, M. (2021) 'Gut microbiome and its role in colorectal cancer', *BMC Cancer*, 21(1), p. 1325. Available at: https://doi.org/10.1186/s12885-021-09054-2.

Refaeli, Y. *et al.* (2002) 'Interferon γ Is Required for Activation-induced Death of T Lymphocytes', *The Journal of Experimental Medicine*, 196(7), pp. 999–1005. Available at: https://doi.org/10.1084/jem.20020666.

Reis, B.S. *et al.* (2014) 'Transcription factor T-bet regulates intraepithelial lymphocyte functional maturation', *Immunity*, 41(2), pp. 244–256. Available at: https://doi.org/10.1016/j.immuni.2014.06.017.

Reis, B.S. *et al.* (2022) 'TCR-Vγδ usage distinguishes protumor from antitumor intestinal γδ T cell subsets', *Science*, 377(6603), pp. 276–284. Available at: https://doi.org/10.1126/science.abj8695.

Rentschler, M. *et al.* (2022) 'Cytokine-Induced Senescence in the Tumor Microenvironment and Its Effects on Anti-Tumor Immune Responses', *Cancers*, 14(6), p. 1364. Available at: https://doi.org/10.3390/cancers14061364.

Ribot, J.C. *et al.* (2009) 'CD27 is a thymic determinant of the balance between interferon-γ- and interleukin 17–producing γδ T cell subsets', *Nature Immunology*, 10(4), pp. 427–436. Available at: https://doi.org/10.1038/ni.1717.

Rochman, Y., Spolski, R. and Leonard, W.J. (2009) 'New insights into the regulation of T cells by γc family cytokines', *Nature reviews. Immunology*, 9(7), p. 480. Available at: https://doi.org/10.1038/nri2580.

Rodig, S.J. *et al.* (2018) 'MHC proteins confer differential sensitivity to CTLA-4 and PD-1 blockade in untreated metastatic melanoma', *Science Translational Medicine*, 10(450), p. eaar3342. Available at: https://doi.org/10.1126/scitranslmed.aar3342.

Roemer, M.G.M. *et al.* (2018) 'Major Histocompatibility Complex Class II and Programmed Death Ligand 1 Expression Predict Outcome After Programmed Death 1 Blockade in Classic Hodgkin Lymphoma', *Journal of Clinical Oncology*, 36(10), pp. 942–950. Available at: https://doi.org/10.1200/JCO.2017.77.3994.

Rogoz, A. *et al.* (2015) 'A 3-D enteroid-based model to study T-cell and epithelial cell interaction', *Journal of immunological methods*, 421, pp. 89–95. Available at: https://doi.org/10.1016/j.jim.2015.03.014.

Roulis, M. *et al.* (2020) 'Paracrine orchestration of intestinal tumorigenesis by a mesenchymal niche', *Nature* [Preprint]. Available at: https://doi.org/10.1038/s41586-020-2166-3.

Ruiz, V.M.R. *et al.* (2017) 'Broad detection of bacterial type III secretion system and flagellin proteins by the human NAIP/NLRC4 inflammasome', *Proceedings of the National Academy of Sciences*, 114(50), pp. 13242–13247. Available at: https://doi.org/10.1073/pnas.1710433114.

Russell, J.H. and Ley, T.J. (2002) 'Lymphocyte-Mediated Cytotoxicity', *Annual Review of Immunology*, 20(1), pp. 323–370. Available at: https://doi.org/10.1146/annurev.immunol.20.100201.131730.

Russell, M.S. *et al.* (2009) 'IFN-γ Expressed by T Cells Regulates the Persistence of Antigen Presentation by Limiting the Survival of Dendritic Cells1', *The Journal of Immunology*, 183(12), pp. 7710–7718. Available at: https://doi.org/10.4049/jimmunol.0901274.

Rutter, M.D. *et al.* (2006) 'Thirty-Year Analysis of a Colonoscopic Surveillance Program for Neoplasia in Ulcerative Colitis', *Gastroenterology*, 130(4), pp. 1030–1038. Available at: https://doi.org/10.1053/j.gastro.2005.12.035.

Sasahara, T. *et al.* (1994) 'Unique Properties of a Cytotoxic CD4+CD8+ Intraepithelial T-Cell Line Established from the Mouse Intestinal Epithelium', *Microbiology and Immunology*, 38(3), pp. 191–199. Available at: https://doi.org/10.1111/j.1348-0421.1994.tb01764.x.

Sato, T. *et al.* (2009) 'Single Lgr5 stem cells build crypt-villus structures in vitro without a mesenchymal niche', *Nature*, 459(7244), pp. 262–265. Available at: https://doi.org/10.1038/nature07935.

Satoh, A. *et al.* (2004) 'Epigenetic inactivation of class II transactivator (CIITA) is associated with the absence of interferon-γ-induced HLA-DR expression in colorectal and gastric cancer cells', *Oncogene*, 23(55), pp. 8876–8886. Available at: https://doi.org/10.1038/sj.onc.1208144.

Scarfe, L., Mackie, G.M. and Maslowski, K.M. (2021) 'Inflammasome-independent functions of NAIPs and NLRs in the intestinal epithelium', *Biochemical Society Transactions*, 49(6), pp. 2601–2610. Available at: https://doi.org/10.1042/BST20210365.

Schmidleithner, L. *et al.* (2019) 'Enzymatic Activity of HPGD in Treg Cells Suppresses Tconv Cells to Maintain Adipose Tissue Homeostasis and Prevent Metabolic Dysfunction', *Immunity*, 50(5), pp. 1232-1248.e14. Available at: https://doi.org/10.1016/j.immuni.2019.03.014.

Schön, M.P. *et al.* (1999) 'Mucosal T Lymphocyte Numbers Are Selectively Reduced in Integrin αE (CD103)-Deficient Mice1', *The Journal of Immunology*, 162(11), pp. 6641–6649. Available at: https://doi.org/10.4049/jimmunol.162.11.6641.

Sconocchia, G. *et al.* (2014) 'HLA Class II Antigen Expression in Colorectal Carcinoma Tumors as a Favorable Prognostic Marker', *Neoplasia (New York, N.Y.)*, 16(1), pp. 31–42.

Sellin, M.E. *et al.* (2014) 'Epithelium-Intrinsic NAIP/NLRC4 Inflammasome Drives Infected Enterocyte Expulsion to Restrict Salmonella Replication in the Intestinal Mucosa', *Cell Host & Microbe*, 16(2), pp. 237–248. Available at: https://doi.org/10.1016/j.chom.2014.07.001.

Sellin, M.E. *et al.* (2015) 'Inflammasomes of the intestinal epithelium', *Trends in Immunology*, 36(8), pp. 442–450. Available at: https://doi.org/10.1016/j.it.2015.06.002.

Seno, H. *et al.* (2002) 'Cyclooxygenase 2- and Prostaglandin E2 Receptor EP2-dependent Angiogenesis in ApcΔ716 Mouse Intestinal Polyps', *Cancer Research*, 62(2), pp. 506–511.

Serhan, C.N. *et al.* (2015) 'Lipid Mediators in the Resolution of Inflammation', *Cold Spring Harbor Perspectives in Biology*, 7(2), p. a016311. Available at: https://doi.org/10.1101/cshperspect.a016311.

Shattuck-Brandt, R.L. *et al.* (2000) 'Cyclooxygenase 2 expression is increased in the stroma of colon carcinomas from IL–10−/− mice', *Gastroenterology*, 118(2), pp. 337–345. Available at: https://doi.org/10.1016/S0016-5085(00)70216-2.

Sheehan, K.M. *et al.* (1999) 'The Relationship Between Cyclooxygenase-2 Expression and Colorectal Cancer', *JAMA*, 282(13), pp. 1254–1257. Available at: https://doi.org/10.1001/jama.282.13.1254.

Sheibanie, A.F. *et al.* (2007) 'The proinflammatory effect of prostaglandin E2 in experimental inflammatory bowel disease is mediated through the IL-23-->IL-17 axis', *Journal of Immunology (Baltimore, Md.: 1950)*, 178(12), pp. 8138–8147. Available at: https://doi.org/10.4049/jimmunol.178.12.8138.

Shen, Z.-H. *et al.* (2018) 'Relationship between intestinal microbiota and ulcerative colitis: Mechanisms and clinical application of probiotics and fecal microbiota transplantation', *World Journal of Gastroenterology*, 24(1), pp. 5–14. Available at: https://doi.org/10.3748/wjg.v24.i1.5.

Sheng, H. *et al.* (1998) 'Modulation of Apoptosis and Bcl-2 Expression by Prostaglandin E2 in Human Colon Cancer Cells', *Cancer Research*, 58(2), pp. 362–366.

Sheng, H. *et al.* (2001) 'Prostaglandin E2 Increases Growth and Motility of Colorectal Carcinoma Cells', *Journal of Biological Chemistry*, 276(21), pp. 18075–18081. Available at: https://doi.org/10.1074/jbc.M009689200.

Sheng, K.-C. *et al.* (2013) 'Enhanced Dendritic Cell-Mediated Antigen-Specific CD4+ T Cell Responses: IFN-Gamma Aids TLR Stimulation', *Journal of Drug Delivery*, 2013, p. e516749. Available at: https://doi.org/10.1155/2013/516749.

Sheppe, A.E.F. *et al.* (2018) 'PGE2 Augments Inflammasome Activation and M1 Polarization in Macrophages Infected With Salmonella Typhimurium and Yersinia enterocolitica', *Frontiers in Microbiology*, 9. Available at: https://www.frontiersin.org/articles/10.3389/fmicb.2018.02447 (Accessed: 2 October 2023).

Shi, J. *et al.* (2015) 'Cleavage of GSDMD by inflammatory caspases determines pyroptotic cell death', *Nature*, 526(7575), pp. 660–665. Available at: https://doi.org/10.1038/nature15514.

Singer, I.I. *et al.* (1998) 'Cyclooxygenase 2 is induced in colonic epithelial cells in inflammatory bowel disease', *Gastroenterology*, 115(2), pp. 297–306. Available at: https://doi.org/10.1016/s0016-5085(98)70196-9.

Smyth, E.M. *et al.* (2009) 'Prostanoids in health and disease', *Journal of Lipid Research*, 50(Supplement), pp. S423–S428. Available at: https://doi.org/10.1194/jlr.R800094-JLR200.

Song, M. *et al.* (2019) 'Low-Dose IFNγ Induces Tumor Cell Stemness in Tumor Microenvironment of Non–Small Cell Lung Cancer', *Cancer Research*, 79(14), pp. 3737–3748. Available at: https://doi.org/10.1158/0008-5472.CAN-19-0596.

Specht, C. *et al.* (2001) 'Prostaglandins, but not tumor-derived IL-10, shut down concomitant tumor-specific CTL responses during murine plasmacytoma progression', *International Journal of Cancer*, 91(5), pp. 705–712. Available at: https://doi.org/10.1002/1097-0215(200002)9999:9999<::AID-IJC1066>3.0.CO;2-J.

Sreeramkumar, V., Fresno, M. and Cuesta, N. (2012a) 'Prostaglandin E2 and T cells: friends or foes?', *Immunology and Cell Biology*, 90(6), pp. 579–586. Available at: https://doi.org/10.1038/icb.2011.75.

Sreeramkumar, V., Fresno, M. and Cuesta, N. (2012b) 'Prostaglandin E2 and T cells: friends or foes?', *Immunology and Cell Biology*, 90(6), pp. 579–586. Available at: https://doi.org/10.1038/icb.2011.75.

Steimle, V. *et al.* (1994) 'Regulation of MHC Class II Expression by Interferon-γ Mediated by the Transactivator Gene CIITA', *Science*, 265(5168), pp. 106–109. Available at: https://doi.org/10.1126/science.8016643.

Stephens, M. (2017) 'False discovery rates: a new deal', *Biostatistics*, 18(2), pp. 275–294. Available at: https://doi.org/10.1093/biostatistics/kxw041.

Sujino, T. *et al.* (2016) 'Tissue adaptation of regulatory and intraepithelial CD4+ T cells controls gut inflammation', *Science*, 352(6293), pp. 1581–1586. Available at: https://doi.org/10.1126/science.aaf3892.

Suzuki, H. *et al.* (1997) 'Abnormal Development of Intestinal Intraepithelial Lymphocytes and Peripheral Natural Killer Cells in Mice Lacking the IL-2 Receptor β Chain', *The Journal of Experimental Medicine*, 185(3), pp. 499–506.

Suzuki, T. *et al.* (2020) 'Gut γδ T cells as guardians, disruptors, and instigators of cancer', *Immunological Reviews*, 298(1), pp. 198–217. Available at: https://doi.org/10.1111/imr.12916.

Szabo, S.J. *et al.* (2002) 'Distinct Effects of T-bet in TH1 Lineage Commitment and IFN-γ Production in CD4 and CD8 T Cells', *Science*, 295(5553), pp. 338–342. Available at: https://doi.org/10.1126/science.1065543.

Szeponik, L. *et al.* (2020) 'Regulatory T cells specifically suppress conventional CD8αβ T cells in intestinal tumors of APCMin/+ mice', *Cancer Immunology, Immunotherapy*, 69(7), pp. 1279–1292. Available at: https://doi.org/10.1007/s00262-020-02540-9.

Tager, A.M. *et al.* (2003) 'Leukotriene B4 receptor BLT1 mediates early effector T cell recruitment', *Nature Immunology*, 4(10), pp. 982–990. Available at: https://doi.org/10.1038/ni970.

Takahashi, Y. *et al.* (2002) 'Augmentation of allergic inflammation in prostanoid IP receptor deficient mice', *British Journal of Pharmacology*, 137(3), pp. 315–322. Available at: https://doi.org/10.1038/sj.bjp.0704872.

Talhouni, S. *et al.* (2023) 'Activated tissue resident memory T-cells (CD8+CD103+CD39+) uniquely predict survival in left sided "immune-hot" colorectal cancers', *Frontiers in Immunology*, 14. Available at: https://www.frontiersin.org/articles/10.3389/fimmu.2023.1057292 (Accessed: 4 October 2023).

Tanaka, K.-I. *et al.* (2009) 'Inhibition of both COX-1 and COX-2 and resulting decrease in the level of prostaglandins E2 is responsible for non-steroidal anti-inflammatory drug (NSAID)-dependent exacerbation of colitis', *European Journal of Pharmacology*, 603(1–3), pp. 120–132. Available at: https://doi.org/10.1016/j.ejphar.2008.11.058.

Tang, C. *et al.* (2018) 'Suppression of IL-17F, but not of IL-17A, provides protection against colitis by inducing Treg cells through modification of the intestinal microbiota', *Nature Immunology*, 19(7), pp. 755–765. Available at: https://doi.org/10.1038/s41590-018-0134-y.

Tariq, K. and Ghias, K. (2016) 'Colorectal cancer carcinogenesis: a review of mechanisms', *Cancer Biology & Medicine*, 13(1), pp. 120–135. Available at: https://doi.org/10.28092/j.issn.2095-3941.2015.0103.

Tattoli, I. *et al.* (2016) 'NLRX1 Acts as an Epithelial-Intrinsic Tumor Suppressor through the Modulation of TNF-Mediated Proliferation', *Cell Reports*, 14(11), pp. 2576–2586. Available at: https://doi.org/10.1016/j.celrep.2016.02.065.

Tawfik, D. *et al.* (2019) 'TRAIL-Receptor 4 Modulates γδ T Cell-Cytotoxicity Toward Cancer Cells', *Frontiers in Immunology*, 10. Available at: https://www.frontiersin.org/articles/10.3389/fimmu.2019.02044 (Accessed: 1 October 2023).

Tessner, T.G. *et al.* (2004) 'Prostaglandin E2 reduces radiation-induced epithelial apoptosis through a mechanism involving AKT activation and bax translocation', *Journal of Clinical Investigation*, 114(11), pp. 1676–1685. Available at: https://doi.org/10.1172/JCI200422218.

Thelemann, C. *et al.* (2014) 'Interferon-γ Induces Expression of MHC Class II on Intestinal Epithelial Cells and Protects Mice from Colitis', *PLOS ONE*, 9(1), p. e86844. Available at: https://doi.org/10.1371/journal.pone.0086844.

Todaro, M. *et al.* (2009) 'Efficient Killing of Human Colon Cancer Stem Cells by γδ T Lymphocytes1', *The Journal of Immunology*, 182(11), pp. 7287–7296. Available at: https://doi.org/10.4049/jimmunol.0804288.

Trapecar, M. *et al.* (2017) 'An Optimized and Validated Method for Isolation and Characterization of Lymphocytes from HIV+ Human Gut Biopsies', *AIDS Research and Human Retroviruses*, 33(S1), p. S-31. Available at: https://doi.org/10.1089/aid.2017.0208.

Tsuchiya, T. *et al.* (2003) 'Role of γδT Cells in the Inflammatory Response of Experimental Colitis Mice 1', *The Journal of Immunology*, 171(10), pp. 5507–5513. Available at: https://doi.org/10.4049/jimmunol.171.10.5507.

Tsujii, M. and DuBois, R.N. (1995) 'Alterations in cellular adhesion and apoptosis in epithelial cells overexpressing prostaglandin endoperoxide synthase 2', *Cell*, 83(3), pp. 493–501. Available at: https://doi.org/10.1016/0092-8674(95)90127-2.

Tu, M. *et al.* (2020) 'ω-3 Polyunsaturated Fatty Acids on Colonic Inflammation and Colon Cancer: Roles of Lipid-Metabolizing Enzymes Involved', *Nutrients*, 12(11), p. 3301. Available at: https://doi.org/10.3390/nu12113301.

Uchiya, K. and Nikai, T. (2004) 'Salmonella enterica Serovar Typhimurium Infection Induces Cyclooxygenase 2 Expression in Macrophages: Involvement of Salmonella Pathogenicity Island 2', *Infection and Immunity*, 72(12), pp. 6860–6869. Available at: https://doi.org/10.1128/IAI.72.12.6860-6869.2004.

Van Der Kraak, L.A. *et al.* (2021) 'Genetic and commensal induction of IL-18 drive intestinal epithelial MHCII via IFNγ', *Mucosal Immunology*, 14(5), pp. 1100–1112. Available at: https://doi.org/10.1038/s41385-021-00419-1.

Van Opdenbosch, N. *et al.* (2017) 'Caspase-1 Engagement and TLR-Induced c-FLIP Expression Suppress ASC/Caspase-8-Dependent Apoptosis by Inflammasome Sensors NLRP1b and NLRC4', *Cell Reports*, 21(12), pp. 3427–3444. Available at: https://doi.org/10.1016/j.celrep.2017.11.088.

Varesano, S., Zocchi, M.R. and Poggi, A. (2018) 'Zoledronate Triggers Vδ2 T Cells to Destroy and Kill Spheroids of Colon Carcinoma: Quantitative Image Analysis of Three-Dimensional Cultures', *Frontiers in Immunology*, 9. Available at: https://www.frontiersin.org/articles/10.3389/fimmu.2018.00998 (Accessed: 11 October 2023).

Ventayol, P.S. *et al.* (2021) 'Bacterial detection by NAIP/NLRC4 elicits prompt contractions of intestinal epithelial cell layers', *Proceedings of the National Academy of Sciences*, 118(16). Available at: https://doi.org/10.1073/pnas.2013963118.

Voabil, P. *et al.* (2021) 'An ex vivo tumor fragment platform to dissect response to PD-1 blockade in cancer', *Nature Medicine*, 27(7), pp. 1250–1261. Available at: https://doi.org/10.1038/s41591-021-01398-3.

Wakita, D. *et al.* (2010) 'Tumor-infiltrating IL-17-producing γδ T cells support the progression of tumor by promoting angiogenesis', *European Journal of Immunology*, 40(7), pp. 1927–1937. Available at: https://doi.org/10.1002/eji.200940157.

Waldmann, T.A. (2006) 'The biology of interleukin-2 and interleukin-15: implications for cancer therapy and vaccine design', *Nature Reviews Immunology*, 6(8), pp. 595–601. Available at: https://doi.org/10.1038/nri1901.

Wang, D. *et al.* (2005) 'Prostaglandin E2 Enhances Intestinal Adenoma Growth via Activation of the Ras-Mitogen-Activated Protein Kinase Cascade', *Cancer Research*, 65(5), pp. 1822–1829. Available at: https://doi.org/10.1158/0008-5472.CAN-04-3671.

Wang, D. *et al.* (2015) 'Prostaglandin E2 Promotes Colorectal Cancer Stem Cell Expansion and Metastasis in Mice', *Gastroenterology*, 149(7), pp. 1884-1895.e4. Available at: https://doi.org/10.1053/j.gastro.2015.07.064.

Wang, D. and DuBois, R.N. (2010a) 'Eicosanoids and cancer', *Nature Reviews Cancer*, 10(3), pp. 181–193. Available at: https://doi.org/10.1038/nrc2809.

Wang, D. and DuBois, R.N. (2010b) 'The Role of COX-2 in Intestinal Inflammation and Colorectal Cancer', *Oncogene*, 29(6), pp. 781–788. Available at: https://doi.org/10.1038/onc.2009.421.

Wang, D. and DuBois, R.N. (2013) 'The Role of Anti-Inflammatory Drugs in Colorectal Cancer', *Annual Review of Medicine*, 64(1), pp. 131–144. Available at: https://doi.org/10.1146/annurev-med-112211-154330.

Wang, D. and DuBois, R.N. (2014) 'PPARδ and PGE2 signaling pathways communicate and connect inflammation to colorectal cancer', *Inflammation and cell signaling*, 1(6). Available at: https://www.ncbi.nlm.nih.gov/pmc/articles/PMC4539244/ (Accessed: 6 June 2020).

Wang, W. *et al.* (2019) 'CD8+ T cells regulate tumor ferroptosis during cancer immunotherapy', *Nature*, 569(7755), pp. 270–274. Available at: https://doi.org/10.1038/s41586-019-1170-y.

Wang, Z.-Q. *et al.* (2016) 'CD103 and Intratumoral Immune Response in Breast Cancer', *Clinical Cancer Research*, 22(24), pp. 6290–6297. Available at: https://doi.org/10.1158/1078-0432.CCR-16-0732.

Warabi, M., Kitagawa, M. and Hirokawa, K. (2000) 'Loss of MHC class II expression is associated with a decrease of tumor-infiltrating T cells and an increase of metastatic potential of colorectal cancer: immunohistological and histopathological analyses as compared with normal colonic mucosa and adenomas', *Pathology, Research and Practice*, 196(12), pp. 807–815. Available at: https://doi.org/10.1016/S0344-0338(00)80080-1.

Watanabe, K. *et al.* (1999) 'Role of the Prostaglandin E Receptor Subtype EP1 in Colon Carcinogenesis', *Cancer Research*, 59(20), pp. 5093–5096.

Watchmaker, P.B. *et al.* (2009) 'Independent Regulation of Chemokine Responsiveness and Cytolytic Function versus CD8+ T Cell Expansion by Dendritic Cells', *The Journal of Immunology*, 184(2), pp. 591–597. Available at: https://doi.org/10.4049/jimmunol.0902062.

Webb, J.R. *et al.* (2014) 'Tumor-Infiltrating Lymphocytes Expressing the Tissue Resident Memory Marker CD103 Are Associated with Increased Survival in High-Grade Serous Ovarian Cancer', *Clinical Cancer Research*, 20(2), pp. 434–444. Available at: https://doi.org/10.1158/1078-0432.CCR-13-1877.

Whitmire, J.K., Tan, J.T. and Whitton, J.L. (2005) 'Interferon-γ acts directly on CD8+ T cells to increase their abundance during virus infection', *The Journal of Experimental Medicine*, 201(7), pp. 1053–1059. Available at: https://doi.org/10.1084/jem.20041463.

Wickham, H. *et al.* (2019) 'Welcome to the Tidyverse', *Journal of Open Source Software*, 4(43), p. 1686. Available at: https://doi.org/10.21105/joss.01686.

Wiercińska–Drapało, A., Flisiak, R. and Prokopowicz, D. (1999) 'Effects of ulcerative colitis activity on plasma and mucosal prostaglandin E2 concentration', *Prostaglandins & Other Lipid Mediators*, 58(2), pp. 159–165. Available at: https://doi.org/10.1016/S0090-6980(99)00032-5.

Williams, T.M. *et al.* (2015) 'The NLRP1 Inflammasome Attenuates Colitis and Colitis-Associated Tumorigenesis', *Journal of immunology (Baltimore, Md. : 1950)*, 194(7), pp. 3369–3380. Available at: https://doi.org/10.4049/jimmunol.1402098.

Wilson, J.E. *et al.* (2015) 'Inflammasome-independent role of AIM2 in suppressing colon tumorigenesis by interfering with DNA-PK–dependent Akt activation', *Nature medicine*, 21(8), pp. 906–913. Available at: https://doi.org/10.1038/nm.3908.

Winsor, N. *et al.* (2019) 'Canonical and noncanonical inflammasomes in intestinal epithelial cells', *Cellular Microbiology*, 21(11), p. e13079. Available at: https://doi.org/10.1111/cmi.13079.

Wirtz, S. and Neurath, M.F. (2007) 'Mouse models of inflammatory bowel disease', *Advanced Drug Delivery Reviews*, 59(11), pp. 1073–1083. Available at: https://doi.org/10.1016/j.addr.2007.07.003.

Wu, P. *et al.* (2014) 'γδT17 Cells Promote the Accumulation and Expansion of Myeloid-Derived Suppressor Cells in Human Colorectal Cancer', *Immunity*, 40(5), pp. 785–800. Available at: https://doi.org/10.1016/j.immuni.2014.03.013.

Wu, S. *et al.* (2009) 'A human colonic commensal promotes colon tumorigenesis via activation of T helper type 17 T cell responses', *Nature Medicine*, 15(9), pp. 1016–1022. Available at: https://doi.org/10.1038/nm.2015.

Xin, L. *et al.* (2014) 'Committed Th1 CD4+ T cell differentiation blocks pregnancy induced Foxp3 expression with antigen specific fetal loss', *Journal of immunology (Baltimore, Md. : 1950)*, 192(7), pp. 2970–2974. Available at: https://doi.org/10.4049/jimmunol.1302678.

Xue, L., Barrow, A. and Pettipher, R. (2009) 'Interaction between prostaglandin D2 and chemoattractant receptor-homologous molecule expressed on Th2 cells mediates cytokine production by Th2 lymphocytes in response to activated mast cells', *Clinical and Experimental Immunology*, 156(1), pp. 126–133. Available at: https://doi.org/10.1111/j.1365-2249.2008.03871.x.

Yanagawa, Y., Masubuchi, Y. and Chiba, K. (1998) 'FTY720, a novel immunosuppressant, induces sequestration of circulating mature lymphocytes by acceleration of lymphocyte homing in rats, III. Increase in frequency of CD62L-positive T cells in Peyer's patches by FTY720-induced lymphocyte homing.', *Immunology*, 95(4), pp. 591–594.

Yang, J. *et al.* (2013) 'Human NAIP and mouse NAIP1 recognize bacterial type III secretion needle protein for inflammasome activation', *Proceedings of the National Academy of Sciences*, 110(35), pp. 14408–14413. Available at: https://doi.org/10.1073/pnas.1306376110.

Yao, C. *et al.* (2009) 'Prostaglandin E 2 –EP4 signaling promotes immune inflammation through T H 1 cell differentiation and T H 17 cell expansion', *Nature Medicine*, 15(6), pp. 633–640. Available at: https://doi.org/10.1038/nm.1968.

Yao, C. *et al.* (2013) 'Prostaglandin E 2 promotes Th1 differentiation via synergistic amplification of IL-12 signalling by cAMP and PI3-kinase', *Nature Communications*, 4(1), p. 1685. Available at: https://doi.org/10.1038/ncomms2684.

Yazbeck, R. *et al.* (2011) 'Biochemical and histological changes in the small intestine of mice with dextran sulfate sodium colitis', *Journal of Cellular Physiology*, 226(12), pp. 3219–3224. Available at: https://doi.org/10.1002/jcp.22682.

Yin, Y. *et al.* (2020) 'A noncanonical role of NOD-like receptor NLRP14 in PGCLC differentiation and spermatogenesis', *Proceedings of the National Academy of Sciences of the United States of America*, 117(36), pp. 22237–22248. Available at: https://doi.org/10.1073/pnas.2005533117.

Yu, G. *et al.* (2012) 'clusterProfiler: an R Package for Comparing Biological Themes Among Gene Clusters', *OMICS: A Journal of Integrative Biology*, 16(5), pp. 284–287. Available at: https://doi.org/10.1089/omi.2011.0118.

Yu, P. and Fu, Y.-X. (2006) 'Tumor-infiltrating T lymphocytes: friends or foes?', *Laboratory Investigation*, 86(3), pp. 231–245. Available at: https://doi.org/10.1038/labinvest.3700389.

Yu, Q. *et al.* (2006) 'MyD88-Dependent Signaling for IL-15 Production Plays an Important Role in Maintenance of CD8αα TCRαβ and TCRγδ Intestinal Intraepithelial Lymphocytes1', *The Journal of Immunology*, 176(10), pp. 6180–6185. Available at: https://doi.org/10.4049/jimmunol.176.10.6180.

Yuki, K. *et al.* (2020) 'Organoid Models of Tumor Immunology', *Trends in Immunology*, 41(8), pp. 652–664. Available at: https://doi.org/10.1016/j.it.2020.06.010.

Zaki, Md.H. *et al.* (2010) 'IL-18 production downstream of the Nlrp3 inflammasome confers protection against colorectal tumor formation', *Journal of immunology (Baltimore, Md. : 1950)*, 185(8), pp. 4912–4920. Available at: https://doi.org/10.4049/jimmunol.1002046.

Zaki, Md.H. *et al.* (2011) 'The NOD-Like Receptor NLRP12 Attenuates Colon Inflammation and Tumorigenesis', *Cancer Cell*, 20(5), pp. 649–660. Available at: https://doi.org/10.1016/j.ccr.2011.10.022.

Zanin, N. *et al.* (2021) 'Interferon Receptor Trafficking and Signaling: Journey to the Cross Roads', *Frontiers in Immunology*, 11. Available at: https://www.frontiersin.org/articles/10.3389/fimmu.2020.615603 (Accessed: 5 October 2023).

Zenewicz, L.A., Antov, A. and Flavell, R.A. (2009) 'CD4 T-cell differentiation and inflammatory bowel disease', *Trends in Molecular Medicine*, 15(5), pp. 199–207. Available at: https://doi.org/10.1016/j.molmed.2009.03.002.

Zhang, L. *et al.* (2017) 'Serum polyunsaturated fatty acid metabolites as useful tool for screening potential biomarker of colorectal cancer', *Prostaglandins, Leukotrienes and Essential Fatty Acids*, 120, pp. 25–31. Available at: https://doi.org/10.1016/j.plefa.2017.04.003.

Zhao, D. *et al.* (2015) 'WNT5A transforms intestinal CD8αα+ IELs into an unconventional phenotype with pro-inflammatory features', *BMC Gastroenterology*, 15(1), p. 173. Available at: https://doi.org/10.1186/s12876-015-0402-3.

Zhao, Y. *et al.* (2011) 'The NLRC4 inflammasome receptors for bacterial flagellin and type III secretion apparatus', *Nature*, 477(7366), pp. 596–600. Available at: https://doi.org/10.1038/nature10510.

Zheng, D., Liwinski, T. and Elinav, E. (2020) 'Inflammasome activation and regulation: toward a better understanding of complex mechanisms', *Cell Discovery*, 6(1), pp. 1–22. Available at: https://doi.org/10.1038/s41421-020-0167-x.

Zheng, Z. *et al.* (2023) 'T Cells in Colorectal Cancer: Unravelling the Function of Different T Cell Subsets in the Tumor Microenvironment', *International Journal of Molecular Sciences*, 24(14), p. 11673. Available at: https://doi.org/10.3390/ijms241411673.

Zhi, L. *et al.* (2011) 'FTY720 blocks egress of T cells in part by abrogation of their adhesion on the lymph node sinus', *Journal of immunology (Baltimore, Md. : 1950)*, 187(5), pp. 2244–2251. Available at: https://doi.org/10.4049/jimmunol.1100670.

Zhou, F. (2009) 'Molecular Mechanisms of IFN-γ to Up-Regulate MHC Class I Antigen Processing and Presentation', *International Reviews of Immunology*, 28(3–4), pp. 239–260. Available at: https://doi.org/10.1080/08830180902978120.

Zhou, W. *et al.* (2016) 'Prostaglandin I2 Suppresses Proinflammatory Chemokine Expression, CD4 T Cell Activation, and STAT6-Independent Allergic Lung Inflammation', *The Journal of Immunology*, 197(5), pp. 1577–1586. Available at: https://doi.org/10.4049/jimmunol.1501063.

Zhu, H. and Cao, X. (2017) 'NLR members in inflammation-associated carcinogenesis', *Cellular and Molecular Immunology*, 14(5), pp. 403–405. Available at: https://doi.org/10.1038/cmi.2017.14.

Zhu, R. *et al.* (2019) 'TSPAN8 promotes cancer cell stemness via activation of sonic Hedgehog signaling', *Nature Communications*, 10(1), p. 2863. Available at: https://doi.org/10.1038/s41467-019-10739-3.

Zocchi, M.R. *et al.* (2017) 'Zoledronate can induce colorectal cancer microenvironment expressing BTN3A1 to stimulate effector γδ T cells with antitumor activity', *OncoImmunology*, 6(3), p. e1278099. Available at: https://doi.org/10.1080/2162402X.2016.1278099.

8 Appendix – RNA sequencing scripts

8.1 Differential gene analysis and PCA plot

```
library(biomaRt)

library(DOSE)

library(clusterProfiler)

library(org.Mm.eg.db)

library(DESeq2)

library(tidyverse)

cts <- as.matrix(read.table("rna.txt")) #count matrix prepared for DESeq2

coldata <- read.csv("coldata.csv") #coldata provides sample information

dds <- DESeqDataSetFromMatrix(countData=cts,colData=coldata,design=~condition) #this combines the sample info and count matrix and aligns count data to correct sample in an object called dds

keep <- rowSums(counts(dds))>=10 #tells it to remove low count genes/keep higher count genes

dds <-dds[keep,] #out of dds keep only the higher count genes (as described above)

dds$condition <- relevel(dds$condition, ref = "WT_T")#sets WT tumour as reference level to which expression changes are compared

dds <- DESeq(dds) #run DESeq to get log fold change
```

8.1.1 PCA plot

```
rld=rlog(dds,blind=F) #rlog function normalisation of library and plotting of PCA

rld.sub <- rld[ , rld$condition %in% c("KO_T", "WT_T") ] # compare WT and KO tumour conditions with the normalised data so can do pca

write.csv(assay(rld.sub),file="tumouronlytesting.csv") #this is a file of regularized log2 transformed data that is best for PCA and heatmap analysis

norm=log2(counts(dds, normalized=T)+1)# show log2 normalised counts as interested in individual genes

write.csv(norm, file="log2normalisedcounts.csv")#this is a file of log2 normalised counts for each gene

pdf("PCAtumouronly.pdf") #makes a pdf file with this name

plotPCA(rld.sub, "condition")#PCA plotted based on the condition ie KO or WT

dev.off()

pcaData=plotPCA(rld.sub, intgroup="condition", ntop=500, returnData=TRUE)#plots PCA

write.csv(pcaData,file="tumouronly.csv")#writes PCA data so you could plot in prism and modify yourself
```

8.1.2 Contrasting genotypes and generating differentially expressed gene list

```
res=lfcShrink(dds, contrast=c("condition","KO_T","WT_T"), type="ashr")#shrinks log2 fold change differences

res=res[order(res$padj),]#orders results by padj value
```

res=subset(res,padj<0.05) #takes genes with padj less than 0.05

write.csv(res, file="tumouronlyDEG.csv")#writes file of DEGs

#find external gene names from bioMart and add names to DEG list:

df=as.data.frame(res)

ensembl_ids=rownames(df)

mart=useMart(biomart="ensembl",dataset="mmusculus_gene_ensembl") #get gene names from *mus musculus* genome

x=getBM(mart=mart,
values=ensembl_ids,filter=c("ensembl_gene_id"),attributes=c("ensembl_gene_id","external_gene_name")) #list of *mus musculus* genes in an object called x

df2=read.csv("tumouronlyDEG.csv", header=T) #read the DEG list and make it an object called df2

colnames(df2)[1]="ensembl_gene_id"

m=merge(df2,x,by="ensembl_gene_id") #merge the DEG list (df2) with the list of genes names from the *mus musculus* genome (object x)

m2=m[,c(1,7,2:6)]

write.csv(m2, file="tumouronlynamedDEG.csv")#named csv of DEGs with actual gene names

8.1.3 KEGG pathway analysis

m2 <- read.csv("tumouronlynamedDEG.csv") #read the list of DEGs with ensembl gene names

e=m2[,2]

mart <- useDataset("mmusculus_gene_ensembl", useMart("ensembl"))

genes <- getBM(

filters="ensembl_gene_id",

attributes=c("ensembl_gene_id", "entrezgene_id"),

values=e,

mart=mart)

gen2=genes[!is.na(genes[,2]),]

kk=enrichKEGG(gene=gen2[,2], minGSSize=20, organism='mmu', pvalueCutoff=0.05) #plots top20 KEGG pathways that are DEGs

pdf("tumouronlyKEGG.pdf", height=6, width=8)

dotplot(kk, orderBy="Count", font.size=6, showCategory=20) #prepares dotplot showing top20 pathways, change showCategory for fewer or more

dev.off()

y=setReadable(kk, OrgDb=org.Mm.eg.db, keyType="ENTREZID") #makes a readable table of KEGG pathways

write.csv(y, file="tumouronlyKEGGnamed.csv") #writes table of genes in each pathway for all KEGG pathways enriched

8.2 Heatmap analysis

```
library(pheatmap)

counts <- read.csv("tumouronlytesting.csv", row.names = 1) # read the RNAseq result summary file

results <- read.csv("tumouronlynamedDEG.csv", row.names = 2) #has ensembl, gene names and fold change

results$sig <- ifelse(results$padj <= 0.05, "yes", "no")

sigresults <- subset(results, padj <=0.05) #only keep significant DEGs

sigall <- merge(counts, sigresults, by = 0 )

sigall2 <- sigall[,2:7]

rownames(sigall2) <- sigall[,9]

eicosanoidgenes <- read.csv("eicosanoidgenes.csv", row.names = 1) #list of eicosanoid only genes

eicosanoidtumour <- merge(sigall2, eicosanoidgenes, by = 0)#merge to keep only significantly changed
eicosanoid related genes

rownames(eicosanoidtumour) <- eicosanoidtumour[,1]

eicosanoidtumour <- eicosanoidtumour[,2:7]

library(pheatmap)

pheatmap(eicosanoidtumour) #makes heatmap from 'eicosanoidtumour' which contained significant DEGs
which also came up as eicosanoid-related gene
```

8.3 Volcano plots

```
library(ggplot2)

tumourdegs <- read.csv("tumouronlynamedDEG.csv") #Read in tumour-specific DEGs

ggplot(tumourdegs, aes(x=log2FoldChange, y=-log10(padj)))+ geom_point() + #The basic scatter plot: x is
"log2FoldChange", y is "pvalue"

 theme_minimal()+ # Add more simple "theme"

 geom_vline(xintercept=c(-2, 2), col="red") +

 geom_hline(yintercept=-log10(0.05), col="red")# Add vertical lines for log2FoldChange thresholds (interect x
axis), and one horizontal line for the p-value threshold

#The significantly differentially expressed genes are the ones found in the upper-left and upper-right corners.

# Add a column to the data frame to specify if they are UP- or DOWN- regulated (log2FoldChange respectively
positive or negative)

# add a column of NAs

tumourdegs$diffexpressed <- "NO"

# if log2Foldchange > 2 and pvalue < 0.05, set as "UP"

tumourdegs$diffexpressed[tumourdegs$log2FoldChange > 2 & tumourdegs$padj < 0.05] <- "UP"
```

```
# if log2Foldchange < -2 and pvalue < 0.05, set as "DOWN"

tumourdegs$diffexpressed[tumourdegs$log2FoldChange < -2 & tumourdegs$padj < 0.05] <- "DOWN"

# Re-plot but this time color the points with "diffexpressed"

ggplot(tumourdegs, aes(x=log2FoldChange, y=-log10(padj), col=diffexpressed)) + geom_point() +
theme_minimal()+

  geom_vline(xintercept=c(-2, 2), col="red") +

  geom_hline(yintercept=-log10(0.05), col="red")+ # Add lines as before

  scale_color_manual(values=c("blue", "black", "red")) ## Change point color 1. by default, it is assigned to the
categories in an alphabetical order):

# to automate a bit: create a named vector: the values are the colours to be used, the names are the categories
they will be assigned to:

mycolours <- c("blue", "black", "red")

names(mycolours) <- c("DOWN", "NO", "UP")

ggplot(tumourdegs, aes(x=log2FoldChange, y=-log10(padj), col=diffexpressed)) + geom_point() +
theme_minimal()+

  geom_vline(xintercept=c(-2, 2), col="red") +

  geom_hline(yintercept=-log10(0.05), col="red")+

  scale_color_manual(values=c("blue", "black", "red"))+

    scale_colour_manual(values = mycolours)

# Now write down the name of genes beside the points.

# Create a new column "degslabel" that will contain the name of genes differentially expressed (NA in case they
are not)

library(ggrepel)

tumourdegs$degslabel <- ifelse(log2FoldChange>2&-log10>75 | log2FoldChange>-2&-log10>75,
as.character(rownames(gene_names)), tumourdegs$gene_names, NA)

ggplot(tumourdegs, aes(x=log2FoldChange, y=-log10(padj), col=diffexpressed, label = degslabel)) +

  geom_vline(xintercept=c(-2, 2), col="red") +

  geom_hline(yintercept=-log10(0.05), col="red")+

  scale_color_manual(values=c("blue", "black", "red"))+ scale_colour_manual(values = mycolours)+

  geom_text_repel(max.overlaps = 200, max.iter = 2500, max.time = 2, (label =ifelse(log2FoldChange>2&-
log10>75 | log2FoldChange>-2&-log10>75, as.character(rownames(gene_names)))))+

  geom_text() +

  labs(title= "Differentially expressed genes in WT vs KO tumour")+

  coord_cartesian(clip = "off")

ggplot(tumourdegs, aes(x=log2FoldChange, y=-log10(padj), col=diffexpressed, label = degslabel)) +

  geom_point() +
```

```
  theme_minimal()+
  geom_text_repel(max.overlaps = 200, max.iter = 2500, max.time = 2, (label =ifelse(log2FoldChange>2&-
log10>75 | log2FoldChange>-2&-log10>75, as.character(rownames(gene_names))))+
  geom_vline(xintercept=c(-2, 2), col="red") +
  geom_hline(yintercept=-log10(0.05), col="red")+
  scale_color_manual(values=c("blue", "black", "red"))+
  scale_colour_manual(values = mycolours)+
  labs(title= "Differentially expressed genes in WT vs KO tumour")+
  coord_cartesian(clip = "off"))
# Finally, the labels were organised using the "ggrepel" package and the geom_text_repel() function
# load library
# plot adding up all layers
ggplot(tumourdegs, aes(x=log2FoldChange, y=-log10(padj), col=diffexpressed, label=degslabel)) +
  geom_point() +
  theme_minimal() +
  geom_text_repel(max.overlaps = 200, max.iter = 2500, max.time = 2, (label =ifelse(log2FoldChange>2&-
log10>75 | log2FoldChange>-2&-log10>75, as.character(rownames(gene_names))))
              +
                scale_color_manual(values=c("blue", "black", "red")) +
                geom_vline(xintercept=c(-2, 2), col="red") +
                geom_hline(yintercept=-log10(0.05), col="red") +
                labs(title= "Differentially expressed genes in WT vs KO tumour")+
                coord_cartesian(clip = "off"))
write.csv=(tumourdegs, file="tumour_degs_labelled.csv") ##makes file with new columns from workflow
```